

SELECTIVE SYNTHESIS OF AROMATIC AND SATURATED ORGANOBORON
COMPOUNDS

By

Timothy Michael Shannon

A DISSERTATION

Submitted to
Michigan State University
in partial fulfillment of the requirements
for the degree of

Chemistry – Doctor of Philosophy

2019

ABSTRACT

SELECTIVE SYNTHESIS OF AROMATIC AND SATURATED ORGANOBORON COMPOUNDS

By

Timothy Michael Shannon

C-H borylation (CHB) is a method to functionalize C-H bonds. The development of CHB has taken many years but is getting to the point of well-established chemistry. The directed CHB is possible for a variety of differing substrates and differing locations of direction. A new method for ortho directed CHB of esters amides and ketones was developed through the use of pyridine based monodentate ligands.

Using 4-cyano-2-methoxypyridine as a ligand iridium catalyzed CHB of esters ketones and amides were performed. The mechanism of CHB in this process likely operates through a different rate-determining step than the other C-H borylation methods used as it was found that the kinetic isotope effect data did not clearly support C-H activation as rate-determining.

The development of sp^3 C-H borylation is not as advanced as sp^2 CHB; a 2-step process to generate the same products could be equally desirable. Utilizing a borylation-hydrogenation process the selectivity that have already been developed for sp^2 C-H borylation can be used to generate the sp^3 carbon boron bond at the desired location. This process has been developed and limitations of it have been investigated.

Philip Lucasse
and
Kristin Shannon

ACKNOWLEDGMENTS

Thank you Dr. Milton R Smith III for your time and patience. I came to graduate school hoping to learn how to identify a chemical problem and figure out a possible solution. Without a doubt you helped to teach me that. While we fundamentally think about things differently, your scientific approach is amazing and I am thankful and beyond grateful to have worked with you.

Dr. Malezcka, special thanks for all of the years of guidance and for stepping into the role of 2nd reader in the last few weeks. Dr. Odom and Dr. Jackson, I will always be thankful for the indepth questions while serving on my committee.

Graduate school would not hve been survivable without the great pears that I worked with along the way: Dr. Sean, Don, Dr. Buddhadeb, Dr. Behnaz, Dr. Dimity, Dr. Olivia, Dr. Yu-ling, PoJen, Alex, Ryan, Seokjoo, Mona, Reza, Dr. Suzi, Dr. Aaron, Dr. Hao Li, Dr. Ruwi , Jonathan, Fang Yi, and Pepe. Thank you for always being there to have a conversation about crazy ideas inside or outside of our group meetings.

Drs. Tanner, Corey, Travis, Matt, Kristen, Josh, Dan, Hammed, Brennan, Kelly, and Tyler being able to chat about ideas, chemistry, our advisors, or students made for a great time.

Dr. Staples, Dr. Holmes thanks you for your guidance and mentoring throughout my time at MSU. Dr. Azadnia, and Dr. Vassilou, ti was great to work with you as TA for several semesters.

My friends and family that are not in chemistry I made a promise to myself to not let graduate school change our relationships in negative way. I cnot say with any

confidence that I fulfilled that promise, and I am beyond appreciative for all of your support even when I missed life events or was not available as much as I wished.

Dr. Kristin... There is nothing I write on paper that would do justice to all the support you have shown me. Finding you at MSU made the 10 to 14 hour days, weekends, stress induced migranes, and failiures all worthwhile. There is no amount of joy I get from chemistry, science experiments or teaching that will ever compare to the joy I get to spend every day of the rest of my life with you. I love you and thank you for always being there for me.

TABLE OF CONTENTS

LIST OF TABLES	viii
LIST OF FIGURES	ix
LIST OF SCHEMES	xvi
KEY TO ABBREVIATIONS	xviii
Chapter 1. Formation of Carbon-Boron Bonds.....	1
1.1 Importance of Boron Containing Compounds in Synthetic Chemistry.....	1
1.2 C-H functionalization.....	3
1.3 Early C-H Borylation.....	6
1.4 Mechanistic Investigations into Iridium Catalyzed C-H borylation.....	9
1.5 Selectivity of CHB.....	12
1.6 Ortho-Directed C-H borylation.....	13
1.7 Meta-Directed CHB.....	18
1.8 Para-Directed C-H Borylation.....	20
1.9 Aliphatic C-B Bond Formation.....	22
1.10 sp^3 C-H borylation.....	23
1.11 Conclusions and Future Work.....	26
Chapter 2. Hydrogenation of Aromatic and Heteroaromatic Organoboronic Esters and Organosilicon Compounds	27
2.1 A Brief History of Hydrogenation Chemistry.....	27
2.2 Hydrogenation of Borylated Olefins.....	30
2.3 Hydrogenation of Borylated Arenes.....	32
2.4 Additives for Hydrogenation of Borylated 6-Membered Heterocycles.....	33
2.5 Additives Free Hydrogenation of Borylated 6-Membered Heterocycles.....	39
2.6 Hydrogenation of Borylated 5-Membered Heterocycles.....	42
2.7 Hydrogenation of Borylated Arenes.....	44
2.8 Silylated heterocycles.....	45
2.9 Chiral Resolution of a reduced borylated piperidine.....	48
2.10 Hydrogenation Conclusion.....	50
Chapter 3. Pyridine Ligands for ortho-Directed C-H Borylation.....	51
3.1 Chelate Directed ortho C-H Borylation.....	51
3.2 Hemi-Labile Ligand Systems.....	52
3.3 L-X type Ligand Systems for Chelate Directed ortho-Borylation.....	55
3.4 Monodentate Ligand Systems.....	57
3.5 Further Challenges in Chelate Directed ortho-Borylation.....	60
3.6 Pyridine Ligand Screens for ortho Selectivity.....	61
3.7 Investigation into Substrate Scope.....	68
3.8 Insights into mechanism of pyridine ligated iridium systems for ortho borylation.....	73

3.9 Selectivity Dependence on Concentration of the Catalyst.....	78
3.10 Combined Mechanism for Pyridine Ligated Iridium CHB.....	80
3.11 Pyridine Ligands for ortho CHB Conclusions	81
Chapter 4. Experimental.....	82
4.1 General Considerations.....	82
4.2 Experimental Information for Chapter 2.....	83
4.3 Experimental information for Chapter 3.....	114
APPENDICES.....	137
APPENDIX A: NMR Spectra.....	138
APPENDIX B: Crystal Structure Data	270
REFERENCES.....	273

LIST OF TABLES

Table 1. Heterogeneous catalyst screen for hydrogenation of 2a	35
Table 2. Solvent Screen for the Hydrogenation of 2a	36
Table 3. Bronsted acid additives for the hydrogenation of 2a by rhodium on carbon	37
Table 4. Lewis Acid Screen for the Rhodium on carbon hydrogenation of 2a	38
Table 5. Hydrogenation of 6-membered heterocycles ^{a,b}	40
Table 6. Heterogeneous Hydrogenation of 5-membered Heterocycles	43
Table 7. Hydrogenation of borylated arenes ^{a,b}	45
Table 8. Hydrogenation of silylated heterocycles.....	46
Table 9. Screen of pyridine ligands for ortho borylation of methyl benzoate with one equivalent of diboron	63
Table 10. Screen of pyridine ligands for ortho-borylation of methyl benzoate with half an equivalent of diboron	65
Table 11. Ligand Screen for ortho-Borylation of Cyclopropyl Phenylketone.....	66
Table 12. Electronic effects of 4-substituted-2-methoxypyridines for ortho-borylation of cyclopropyl phenylketone.....	67
Table 13. ortho C-H borylation of aryl esters and amides using a monodentate pyridine ligand.....	69
Table 14. ortho C-H borylation of aryl ketones using a monodentate pyridine ligand	70
Table 15. ortho-borylation on complex substrates.....	72
Table 16. Pyridine to iridium ratio impact on reactivity.....	73
Table 17. Underlying data for Figure 16	135
Table 18. Underlying data for Figure 17	136
Table B1 Crystal data for compound 2e	271
Table B2 Crystal structure data for 2za	272

LIST OF FIGURES

Figure 1. Transformations of C-B bonds	2
Figure 2. Proposed Relay-directed ortho CHB transition state	13
Figure 3. Electrostatic directed ortho CHB transition state	14
Figure 4. Hydrogen bonding directed ortho CHB of aniline ³²	15
Figure 5. Chelate directed ortho CHB	17
Figure 6. Thioether directed ortho CHB	17
Figure 7. Hydrogen bond-directed meta-borylation	18
Figure 8. Imine directed meta borylation.....	19
Figure 9. Ion pairing interactions for meta-directed CHB.....	20
Figure 10. Directed para borylation of aryl esters	22
Figure 11. Homogeneous hydrogenation catalysts. ⁹⁻¹²	29
Figure 12. Hydrogenation of 2a yielding borylated and deborylated product.....	34
Figure 13. Crystal Structure of Compound 2e	41
Figure 14. ¹ H NMR signal from the TMS group on 2u	47
Figure 15. Crystal Structure of Compound 2za	50
Figure 16. C-H Activation in Chelate Directed ortho-Borylation	51
Figure 17. General catalytic cycle for chelate directed ortho-borylation	52
Figure 18. Selectivity vs concentration of catalyst in iridium catalyzed ortho borylation of methyl benzoate.	78
Figure 19. Selectivity of ortho-Borylation of Methyl Benzoate With no Added Ligand. 79	
Figure 20. 400 MHz ¹ H-NMR of pinacol in D ₂ O.....	87
Figure 21. gCOSY of compound 21	95
Figure 22. NOE between protons on 21 showing cis stereochemistry 3.9ppm irradiated. 96	

Figure 23. NOE between protons on 2l showing cis stereochemistry 3.7ppm irradiated.	97
Figure 24. NOE between the major species of 2q showing cis stereochemistry	100
Figure 25. NOE between the major species of 2r showing cis stereochemistry	102
Figure 26. NOE between the major species of 2s showing cis stereochemistry.....	104
Figure 27. NOE between the major species of 2t showing cis stereochemistry.....	106
Figure 28. gHMQC for assignments of 3ba an 3bb	131
Figure 29. gHMBCAD for assignments of 3ba an 3bb	132
Figure 30. gCOSY for assignments of 3ba an 3bb	133
Figure A1. 500 MHz ¹ H NMR of 2b in D ₂ O	139
Figure A2. 500 MHz ¹ H NMR of 2b in D ₂ O from 3.9 to 1.0 ppm.....	140
Figure A3. 125 MHz ¹³ C NMR of 2b in D ₂ O.....	141
Figure A4. 125 MHz ¹³ C NMR of 2b in D ₂ O from 85 to 15 ppm.....	142
Figure A5. 500 MHz ¹ H NMR of 2c in D ₂ O	143
Figure A6. 500 MHz ¹ H NMR of 2c in D ₂ O from 3.6 to 0.6 ppm	144
Figure A7. 125 MHz ¹³ C NMR of 2c in D ₂ O	145
Figure A8. 125 MHz ¹³ C NMR of 2c in D ₂ O from 85 to 15 ppm	146
Figure A9. 160 MHz ¹¹ B NMR of 2c in D ₂ O	147
Figure A10. 500 MHz ¹ H NMR of 2d' in CDCl ₃	148
Figure A11. 160 MHz ¹¹ B NMR of 2d' in D ₂ O.....	149
Figure A12. 500 MHz ¹ H NMR of 2d in D ₂ O.....	150
Figure A13. 125 MHz ¹³ C NMR of 2d in D ₂ O.....	151
Figure A14. 125 MHz ¹³ C NMR of 2d in D ₂ O from 60 to 15 ppm.....	152
Figure A15. 160 MHz ¹¹ B NMR of 2d in D ₂ O.....	153
Figure A16. 500 MHz ¹ H NMR of 2e' in CDCl ₃	154
Figure A17. 125 MHz ¹³ C NMR of 2e' in CDCl ₃	155

Figure A18. 160 MHz ^{11}B NMR of 2e' in CDCl_3	156
Figure A19. 500 MHz ^1H NMR of 2e in D_2O	157
Figure A20. 500 MHz ^1H NMR of 2e in D_2O from 3.8 to 1.0 ppm	158
Figure A21. 125 MHz ^{13}C NMR of 2e in D_2O	159
Figure A22. 160 MHz ^{11}B NMR of 2e in D_2O	160
Figure A23. 500 MHz ^1H NMR of 2f in CDCl_3	161
Figure A24. 160 MHz ^{11}B NMR of 2f in CDCl_3	162
Figure A25. 500 MHz ^1H NMR of 2g' in CDCl_3	163
Figure A26. 500 MHz ^1H NMR of 2g in CDCl_3	164
Figure A27. 500 MHz ^1H NMR of 2g in CDCl_3 from 4.0 to 0.9 ppm.....	165
Figure A28. 125 MHz ^{13}C NMR of 2g in CDCl_3	166
Figure A29. 125 MHz ^{13}C NMR of 2g in CDCl_3 from 85 to 15 ppm.....	167
Figure A30. 160 MHz ^{11}B NMR of 2g in CDCl_3	168
Figure A31. 500 MHz ^1H NMR of 2h in CDCl_3	169
Figure A32. 160 MHz ^{11}B NMR of 2h in CDCl_3	170
Figure A33. 500 MHz ^1H NMR of 2i in C_6D_6	171
Figure A34. 500 MHz ^1H NMR of 2i in C_6D_6 from 2.3ppm to 0.9ppm	172
Figure A35. 500 MHz ^1H NMR of 2i in C_6D_6 from 4.1ppm to 3.5ppm	173
Figure A36. 125 MHz ^{13}C NMR of 2i in C_6D_6	174
Figure A37. 125 MHz ^{13}C NMR of 2i in C_6D_6 from 43ppm to 18 ppm.....	175
Figure A38. 160 MHz ^{11}B NMR of 2i in C_6D_6	176
Figure A39. 500 MHz ^1H NMR of 2o in CDCl_3	177
Figure A40. 125 MHz ^{13}C NMR of 2o in CDCl_3	178
Figure A41. 160 MHz ^{11}B NMR of 2o in CDCl_3	179
Figure A42. 500 MHz ^1H NMR of 2p in D_2O	180

Figure A43. 160 MHz ^{11}B NMR of 2p in D_2O	181
Figure A44. 500 MHz ^1H NMR of 2q in CDCl_3	182
Figure A45. 500 MHz ^1H NMR of 2q in CDCl_3	183
Figure A46. 125 MHz ^{13}C NMR of 2q in CDCl_3	184
Figure A47. 125 MHz ^{13}C NMR of 2q in CDCl_3 from 44 to 22 ppm	185
Figure A48. 470 MHz ^{19}F NMR of 2q in CDCl_3	186
Figure A49. 500 MHz ^1H NMR of 2r in C_6D_6	187
Figure A50. 125 MHz ^{13}C NMR of 2r in C_6D_6	188
Figure A51. 160 MHz ^{11}B NMR of 2r in C_6D_6	189
Figure A52. 500 MHz ^1H NMR of 2s in C_6D_6	190
Figure A53. 500 MHz ^1H NMR of 2s in C_6D_6 from 2.5 to 0.4 ppm.....	191
Figure A54. 125 MHz ^{13}C NMR of 2s in C_6D_6	192
Figure A55. 160 MHz ^{11}B NMR of 2s in C_6D_6	193
Figure A56. 500 MHz ^1H NMR of 2t in C_6D_6	194
Figure A57. 500 MHz ^1H NMR of 2t in C_6D_6 from 3.6 to 0.7 ppm.....	195
Figure A58. 500 MHz ^1H NMR of 2t in C_6D_6 from 3.45 to 2.5 ppm.....	196
Figure A59. 125 MHz ^{13}C NMR of 2t in CDCl_3	197
Figure A60. 160 MHz ^{11}B NMR of 2t in CDCl_3	198
Figure A61. 500 MHz ^1H NMR of 2u in CDCl_3	199
Figure A62. 500 MHz ^1H NMR of 2u in CDCl_3 from 3.8 to 0.0 ppm.....	200
Figure A63. 125 MHz ^{13}C NMR of 2u in CDCl_3	201
Figure A64. 125 MHz ^{13}C NMR of 2u in D_2O from 60 to 18 ppm.....	202
Figure A65. 500 MHz ^1H NMR of 2v in D_2O	203
Figure A66. 500 MHz ^1H NMR of 2v in D_2O from 4.4 to -0.2ppm.....	204
Figure A67. 125 MHz ^{13}C NMR of 2v in D_2O	205

Figure A68. 470 MHz ^{19}F NMR of 2v in D_2O	206
Figure A69. 500 MHz ^1H NMR of 2w in C_6D_6	207
Figure A70. 125 MHz ^{13}C NMR of 2w in C_6D_6	208
Figure A71. 500 MHz ^1H NMR of 2x in CDCl_3	209
Figure A72. 125 MHz ^{13}C NMR of 2x in CDCl_3	210
Figure A73. 500 MHz ^1H NMR of 2y in C_6D_6	211
Figure A74. 125 MHz ^{13}C NMR of 2y in CDCl_3	212
Figure A75. 99 MHz ^{29}Si NMR of 2y in CDCl_3	213
Figure A76. 500 MHz ^1H NMR of 2za in C_6D_6	214
Figure A77. 500 MHz ^1H NMR of 2za in C_6D_6 from 3.0 to 0.3 ppm	215
Figure A78. 125 MHz ^{13}C NMR of 2za in C_6D_6	216
Figure A79. 125 MHz ^{13}C NMR of 2za in C_6D_6 from 36 to 6 ppm	217
Figure A80. 160 MHz ^{11}B NMR of 2za in C_6D_6	218
Figure A81. 500 MHz ^1H NMR of 2zb in C_6D_6	219
Figure A82. 500 MHz ^1H NMR of 2zb in C_6D_6	220
Figure A83. 125 MHz ^{13}C NMR of 2zb in C_6D_6	221
Figure A84. 125 MHz ^{13}C NMR of 2zb in C_6D_6 from 85 to 5 ppm	222
Figure A85. 160 MHz ^{11}B NMR of 2zb in C_6D_6	223
Figure A86. 500 MHz ^1H NMR of 3z in CDCl_3	224
Figure A87. 500 MHz ^1H NMR of 3z in CDCl_3 from 9.0 to 6.5 ppm	225
Figure A88. 500 MHz ^1H NMR of 3aa in CDCl_3	226
Figure A89. 500 MHz ^1H NMR of 3aa in CDCl_3 from 9.0 to 6.5 ppm	227
Figure A90. 160 MHz ^{11}B NMR of 3aa in CDCl_3	228
Figure A91. 500 MHz ^1H NMR of 3ab' in CDCl_3	229
Figure A92. 500 MHz ^1H NMR of 3ab' in CDCl_3 from 9.0 to 6.5 ppm	230

Figure A93. 125 MHz ^{13}C NMR of 3ab' in CDCl_3	231
Figure A94. 125 MHz ^{13}C NMR of 3ab' in CDCl_3 from 150 to 110 ppm.....	232
Figure A95. 470 MHz ^{19}F NMR of 3ab' in CDCl_3	233
Figure A96. 500 MHz ^1H NMR of 3ab in CDCl_3	234
Figure A97. 500 MHz ^1H NMR of 3ab in CDCl_3 from 8.4 to 7.0 ppm	235
Figure A98. 125 MHz ^{13}C NMR of 3ab in CDCl_3	236
Figure A99. 125 MHz ^{13}C NMR of 3ab in CDCl_3 from 168 to 108 ppm	237
Figure A100. 470 MHz ^{19}F NMR of 3ab in CDCl_3	238
Figure A101. 160 MHz ^{11}B NMR of 3ab in CDCl_3	239
Figure A102. 500 MHz ^1H NMR of 3ac in CDCl_3	240
Figure A103. 500 MHz ^1H NMR of 3ac in CDCl_3 from 7.9 to 7.2 ppm.....	241
Figure A104. 500 MHz ^1H NMR of 3ad in CDCl_3	242
Figure A105. 160 MHz ^{11}B NMR of 3ad in CDCl_3	243
Figure A106. 500 MHz ^1H NMR of 3ae in CDCl_3	244
Figure A107. 500 MHz ^1H NMR of 3ae in CDCl_3 from 8.0 to 7.35 ppm.....	245
Figure A108. 125 MHz ^{13}C NMR of 3ae in CDCl_3	246
Figure A109. 160 MHz ^{11}B NMR of 3ae in CDCl_3	247
Figure A110. 500 MHz ^1H NMR of 3af in CDCl_3	248
Figure A111. 500 MHz ^1H NMR of 3af in CDCl_3 from 7.85 to 7.40 ppm	249
Figure A112. 125 MHz ^{13}C NMR of 3af in CDCl_3	250
Figure A113. 160 MHz ^{11}B NMR of 3af in CDCl_3	251
Figure A114. 500 MHz ^1H NMR of 3ah in CDCl_3	252
Figure A115. 500 MHz ^1H NMR of 3ah in CDCl_3 from 7.50 to 7.00 ppm	253
Figure A116. 125 MHz ^{13}C NMR of 3ah in CDCl_3	254
Figure A117. 470 MHz ^{19}F NMR of 3ah in CDCl_3	255

Figure A118. 160 MHz ^{11}B NMR of 3ah in CDCl_3	256
Figure A119. 500 MHz ^1H NMR of 3ai in CDCl_3	257
Figure A120. 500 MHz ^1H NMR of 3ao in CDCl_3	258
Figure A121. 500 MHz ^1H NMR of 3ao in CDCl_3 from 9.0 to 6.8 ppm.....	259
Figure A122. 125 MHz ^{13}C NMR of 3ao in CDCl_3	260
Figure A123. 470 MHz ^{19}F NMR of 3ao in CDCl_3	261
Figure A124. 160 MHz ^{11}B NMR of 3ao in CDCl_3	262
Figure A125. 500 MHz ^1H NMR of 3az in CDCl_3	263
Figure A126. 500 MHz ^1H NMR of 3az in CDCl_3 from 9.0 to 6.5 ppm.....	264
Figure A127. 125 MHz ^{13}C NMR of 3az in CDCl_3	265
Figure A128. 500 MHz ^1H NMR of 3ba and 3bb in CDCl_3	266
Figure A129. 500 MHz ^1H NMR of 3ba and 3bb in CDCl_3 between 2.0ppm and 1.0ppm	267
Figure A130. 500 MHz ^1H NMR of 3ba and 3bb in CDCl_3 between 8.0ppm and 6.4ppm	268
Figure A131. 125 MHz ^{13}C NMR of 3ba and 3bb in CDCl_3	269

LIST OF SCHEMES

Scheme 1. Chiral hydroboration/oxidation of 2,3-dihydrofuran ³	1
Scheme 2. First cross coupling of an aryl boronic acid with an aryl halide ⁵	2
Scheme 3. Lithiation-borylation chemistry.....	3
Scheme 4. Carbonylation of 1-diphenylmethanimine using octacarbonyldicobalt ¹⁷	4
Scheme 5. ortho Carbon-hydrogen bond activation by nickelocene ¹⁹	5
Scheme 6. Ruthenium C-H bond activation equilibrium reported by Chatt and Davidson ²⁰	5
Scheme 7. Iridium complex oxidative addition to cyclohexane ²¹	6
Scheme 8. First thermal catalytic C-H silylation ²²	6
Scheme 9. First isolated thermal catalytic CHB ²³	7
Scheme 10. Comparison between Rhodium and Iridium precatalysts for CHB.....	8
Scheme 11. Iridium catalyzed borylation of iodobenzene.....	9
Scheme 12. Proposed mechanism of iridium CHB ^{25,27-29}	12
Scheme 13. Enantioselective CHB through relay silyl-directed borylation	14
Scheme 14. Hydrogen bond directed ortho diborylation ³³	16
Scheme 15. Steric directed para-borylation of bulky monosubstituted arenes.....	21
Scheme 16. Aluminum/iridium co-catalysts for para-directed CHB of esters and pyridines	21
Scheme 17. Octane CHB using a rhodium catalyst	24
Scheme 18. CHB of saturated cyclic ethers.....	24
Scheme 19. Pyridine directed triborylation of primary C-H bonds	25
Scheme 20. Palladium catalyzed sp ³ CHB directed by amides ⁵⁵	25
Scheme 21. First enantioselective CHB of a sp ³ carbon.....	26
Scheme 22. Platinum oxide catalyst for hydrogenation. ³	27

Scheme 23. Hydrogenation of Fluorinated Arenes. ¹³	29
Scheme 24. First reported hydrogenation of a borylated olefin ²³	30
Scheme 25. First reported hydrogenation of a vinyl boronic ester. ²⁴	31
Scheme 26. Hydrogenation of n-Boc-2-pyrrolyl-boronic acid. ³¹	32
Scheme 27. Homogeneous hydrogenation of fluorinated aryl boronic esters. ¹³	33
Scheme 28. sp ³ CHB of tetrahydrofuran. ³⁷	42
Scheme 29. Chiral resolution of 2b through chiral amide formation	49
Scheme 30. Lassaletta Hemi-Labile ortho-Directed Borylation. ⁴	53
Scheme 31. Picolylamine for ortho-Directed CHB of Benzylamines and Benzylphosphines. ¹⁵	54
Scheme 32. ortho-Borylation of Aryl-DMG Using Phosphine-Silane Based Ligands. ¹⁹ .	55
Scheme 33. ortho-Borylation of Aryl-DMG Using Nitrogen-Boron Based Ligands. ⁷	56
Scheme 34. Supported Phosphine Catalysts for ortho CHB.....	58
Scheme 35. Homogeneous ortho CHB with Excess Ligand.....	59
Scheme 36. Homogeneous electron poor monodentate phosphine ligand for ortho CHB	59
Scheme 37. Intermolecular Kinetic Isotope Effects of CHB on Cyclopropyl Phenylketone	74
Scheme 38. Intramolecular kinetic isotope effects of CHB on cyclopropyl phenylketone	75
Scheme 39. sp ³ CHB of Electron Rich 4-N,N-dimethyl-2-methoxypyridine.....	75
Scheme 40. Competition reactions for ortho CHB of ketones vs esters	76
Scheme 41. Competition reaction between methyl benzoate and N,N-dimethylbenzamide	76
Scheme 42. Competition of electronically different methyl benzoates	77
Scheme 43. Proposed catalytic cycle of py' ligand ortho borylation.....	80

KEY TO ABBREVIATIONS

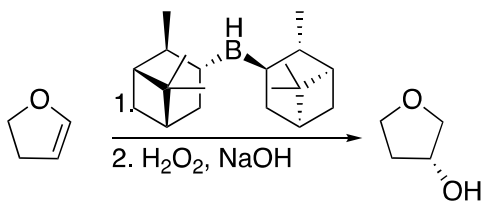
B ₂ pin ₂	Bis(pinacolato)diboron
HBpin	Pinacolborane
Boc	<i>tert</i> -butyloxycarbonyl
CHB	C-H Borylation
Cp	Cyclopentadienyl
Cp*	Pentamethylcyclopentadienyl
COD	Cyclooctadiene
Ind	Indenyl
dtbpy	4,4'-di- <i>tert</i> -butylbipyridine
NMR	Nuclear magnetic resonance
TMS	Trimethylsilyl
gHMBC	gradient Heteronuclear Multiple Bond Coherence

Chapter 1. Formation of Carbon-Boron Bonds

1.1 Importance of Boron Containing Compounds in Synthetic Chemistry.

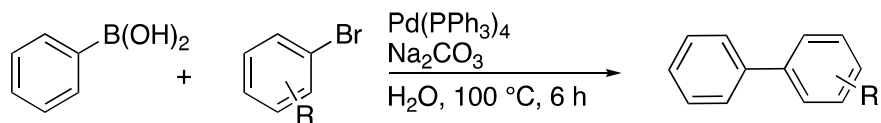
Carbon-boron bonds have a diverse and rich chemistry of chemical transformations. As such organoboron compounds have been heavily utilized in organic chemistry. One of the first transformations that was utilized to a large extent was the use of boranes to produce anti-Markovnikov alcohols via one pot hydroboration/oxidation chemistry.¹ By using chiral boranes, chiral alcohols were synthesized.² This chemistry was mainly pioneered by H.C. Brown, who won a Nobel prize for his development of this chemistry.

Scheme 1. Chiral hydroboration/oxidation of 2,3-dihydrofuran³



In 1979, the first catalytic cross coupling of an organoboron compound with an organohalide to generate a carbon-carbon bond was reported by Miyaura, Yamada and Suzuki.⁴ While the first few reactions demonstrated the ability of alkenyl boronic esters to transform from a C-B bond into a C-C bond further papers demonstrated the power that could be developed by using aryl carbon-boron bonds to generate carbon-carbon bonds via palladium coupling.⁵ Since then, the Suzuki coupling has become one of the most widely utilized reactions for synthesis of carbon-carbon bonds.⁶

Scheme 2. First cross coupling of an aryl boronic acid with an aryl halide⁵



Carbon-boron bonds can be transformed into carbon-nitrogen bonds through the use of a Chan-Lam coupling.⁷ Transformations converting carbon-boron bonds into carbon bonded to chlorine,^{8,9} bromine,^{8,9} iodide,⁸ and finally fluorine¹⁰ have also been reported. This expansion of transformations of organoboron compounds continued and now includes the likes of cyanation,¹¹ trifluoromethylation,^{12,13} thiolations,¹⁴ stereospecific conversions to carbon-carbon bonds,¹⁵ and others.

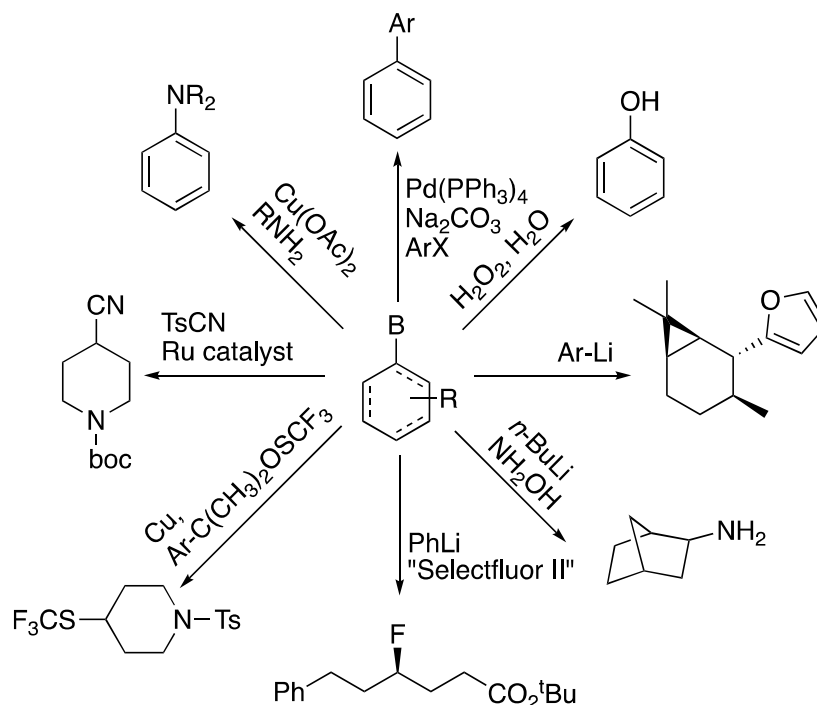
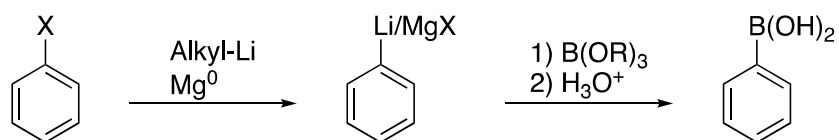


Figure 1. Transformations of C-B bonds

The variety of transformations, especially in the development in aryl functionalizations resulted in research into synthesis of carbon-boron bonds.¹⁶ While carbon-boron bonds could be generated through lithiation or a Grignard reagent followed by quenching with a borate these boronic acid synthesis generated large quantities of salt waste. Another challenge of stoichiometric metalation chemistry is that they tend to require cryogenic temperatures. This can be a challenge in scaled up processes.

Scheme 3. Lithiation-borylation chemistry



A step forward was by the report of the Miyaura coupling, which used a palladium catalyst to convert a carbon-bromine or carbon-iodide bond into a carbon-boron bond. All of this was incredibly helpful to the chemical industry and the use of carbon boron bonds continued to expand in discovery chemistry. However, this did little to limit the amount of salt waste generated. As such, further development of methods into C-H functionalization/borylation were needed.

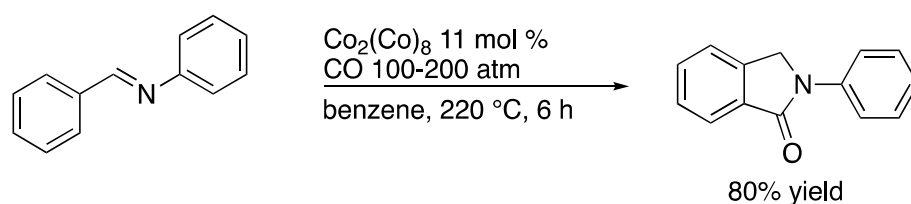
1.2 C-H functionalization

Carbon-hydrogen bonds are pervasive in chemicals. As such for atom economical synthesis, a direct functionalization of these bonds is necessary. As discussed in the previous section the transformations of carbon boron bonds are incredibly useful. As such, the catalytic synthesis of carbon-boron bonds through carbon-hydrogen borylation (CHB)

would be incredibly useful. Through CHB the direct transformation of any C-H bond into a large range of functionalities could be accomplished through a two-step process.

Murahashi reported in 1955 a carbonylation of Schiff bases to generate phthalimide. This resulted from a reaction of dicobaltoctacarbonyl under 100-200 atm of carbon monoxide at 220-230 °C.¹⁷ While the mechanism was unknown, a Friedel-Crafts type mechanism could have been possible with hydride transfer to rearomatize the arene and form the product. This possibility is why this reaction is not considered the first metal mediated C-H activation.

Scheme 4. Carbonylation of 1-diphenylmethanimine using octacarbonyldicobalt¹⁷

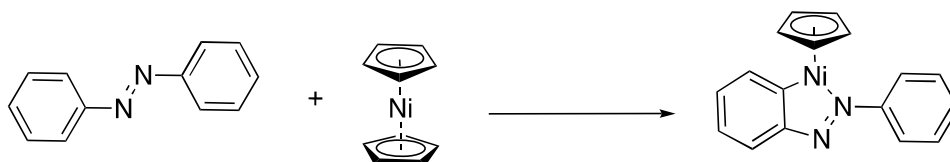


In 1962 Chatt and Watson showed that metal complexes of osmium, and ruthenium reacted with sodium naphthalide to produce a C-H functionalization of the naphthlene shown in scheme 5.¹⁸ They did not report the structure of the metal hydride complex discussed but said investigations were still ongoing. This was the first mention of what turned out to be C-H activation.

This was followed by the activation of azobenzene by Kleiman and Dubeck with nickelocene which resulted in a C-H activation of one of the $\text{C}(\text{sp}^2)\text{-H}$ bonds.¹⁹ This was the first isolated complex with a formal C-H activation. However, the metal hydride was

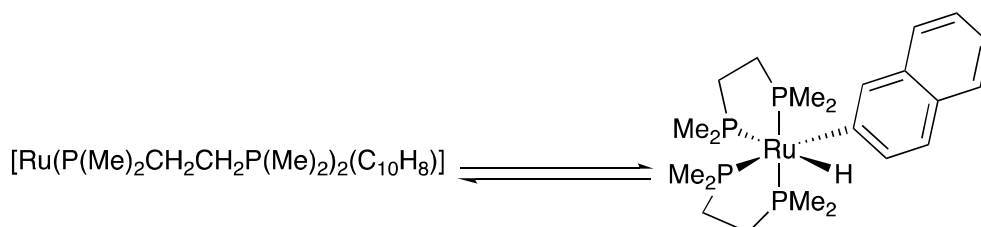
not observed or isolated. As a result, the definitive evidence of metal activated C-H cleavage occurring was not shown.

Scheme 5. ortho Carbon-hydrogen bond activation by nickelocene¹⁹



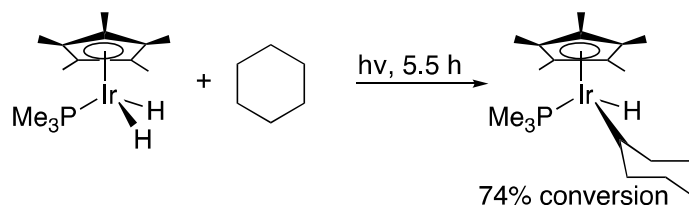
The first definitive metal hydride formation from the reaction of a metal complex and a C-H bond was reported by Chatt and Davidson in 1965 when they showed that a ruthenium(0) complex with two dmpe ligands on it would have an equilibrium between a coordinated naphthalene and a C-H activated metal hydride and naphthalyl lignd.²⁰ They also showed that in the absence of naphthalene, C-H activation from the methyl on the dimethylphosphinoethane (dmpe) occurred and was also reversible.

Scheme 6. Ruthenium C-H bond activation equilibrium reported by Chatt and Davidson²⁰



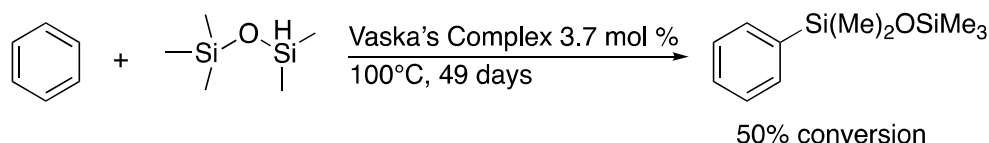
One of the first reported intermolecular C-H activations of non-activated carbon-hydrogen bonds was demonstrated by Bergman in 1982.²¹ They showed that a $\text{Cp}^*\text{Ir}(\text{PMe}_3)\text{H}_2$ catalyst would undergo UV light mediated oxidative addition of unactivated hydrocarbons such as cyclohexane, isopentane and an aromatic compound benzene. This result demonstrated that intermolecular C-H activation was possible with unactivated C-H bonds.

Scheme 7. Iridium complex oxidative addition to cyclohexane²¹



C-H silylation, which has many similarities to CHB was first reported by Curtis and co-workers in 1982, when they showed that when heated at 100 °C for 49 days in a closed container, Vaska's complex catalyzed the hydrosilylation of benzene with $(\text{CH}_3)_3\text{SiOSi}(\text{CH}_3)_2\text{H}$.²² The reaction proceeded with a 50% conversion to $\text{Ph-Si}(\text{CH}_3)_2\text{OSi}(\text{CH}_3)_3$ and disilylated unidentified isomers. They calculated that there were 13.4 turnovers per catalyst.

Scheme 8. First thermal catalytic C-H silylation²²



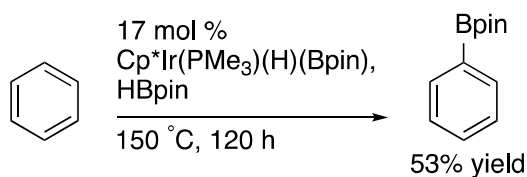
1.3 Early C-H Borylation

In 1995, Hartwig and co-workers reported the first CHB of using an iron complex with UV light to activate the reaction.²¹ They were able to demonstrate the potential for transforming C-H bonds of sp^2 carbons into carbon-boron bonds. This UV-based functionalization was further expanded with the switch to a tungsten catalyst, which resulted in better yields, that was also able to functionalize alkyl C-H bonds.²² However, neither of these two systems were catalytic. The metal complexes that underwent the stoichiometric transformations could be regenerated through a multi-step recovery

process. The failure of these complexes to turnover and provide catalysis was a major drawback from their use. A metal boryl complex that could result in C-H functionalization catalytically would be a major improvement.

While today there are many UV-Vis reactors that utilize flow chemistry, in 1999 that was not well established. As such a reaction that operated through thermal energy was desired. In 1999 Iverson and Smith published the first thermal catalytic CHB reaction.²³ This opened the door to a lot of chemistry to convert a carbon-hydrogen bond into a carbon-boron bond. This first CHB reaction used an iridium Cp* chair complex with excess borane run in neat benzene. The reaction used was analogous to the complex (Cp*Ir(PMe₃)H₂) used by Bergman for the first intermolecular C-H activation.²¹ Shown in Scheme 9 this reaction generated a little over 3 turnovers.

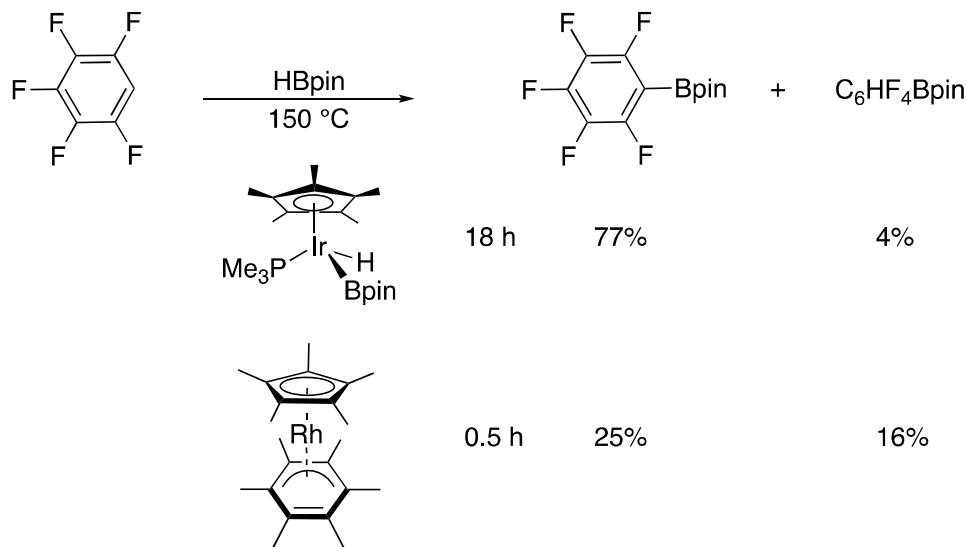
Scheme 9. First isolated thermal catalytic CHB²³



Further development of CHB quickly followed. In 2000 Hartwig reported a rhodium catalyst for borylation of alkanes and benzene in high yields at 150 °C (Scheme 19).⁵¹ Cho, Iverson and Smith used similar iridium chair structures with phosphine ligands to look into the CHB of various arenes.²⁴ What they found was that the CHB of arenes was largely sterically driven. The iridium catalyst was also more selective for C-H activation over C-F activation with only 4% of C-F bond activation. While the rhodium catalyst, Cp*Rh(η^4 -C₆Me₆), resulted in 16% of C-F bond activation. The rhodium catalyst

that was first developed by Hartwig and co-workers for the borylation of alkanes was a much faster catalyst but this showed early indications that iridium would be a more selective catalyst.

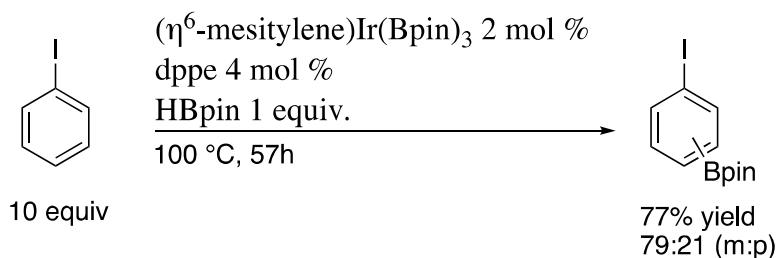
Scheme 10. Comparison between Rhodium and Iridium precatalysts for CHB



In 2002, Maleczka, Smith and co-workers demonstrated that using (Ind)Ir(COD) and (η^6 -mesitylene)Ir(Bpin)₃ as precatalysts with combination of bisphosphine ligands resulted in a very selective catalyst for steric control of the product formation. This was the first report of bidentate ligands for CHB. An important finding from this paper was the selectivity for the meta position on 1,3 disubstituted arenes. Of particular note was the borylation of iodobenzene. Using (η^6 -mesitylene)Ir(Bpin)₃ as a precatalyst and di(phenyl)phosphine ethane as a ligand they were able to borylate iodobenzene in 77% yield with a 79:21 meta to para selectivity. This was important as it illustrated the incredible halogen tolerance of the system. They showed how this system could be

combined with Suzuki couplings in the first one pot borylation-suzuki coupling to make complex molecules or even synthesis of polymers of aryl compounds.²⁷

Scheme 11. Iridium catalyzed borylation of iodobenzene



In 2002 Ishiyama, Hartwig, Miyuara and co-workers reported use of 4,4'-di-*tert*-butyl 2,2'-bipyridine(dtbpy) with $[\text{Ir}(\text{Cl})\text{COD}]_2$ for CHB of arenes. They found that this combination of precatalyst and ligand worked incredibly efficiently at room temperature or 80 °C with high turnovers.²⁵ They followed this with an investigation into precatalysts and different bipyridines to help determine the best combination of iridium precatalysts and ligands.²⁶ They found that the best combination of ligands and precatalysts were electron rich bipyridines with $[\text{Ir}(\text{OMe})\text{COD}]_2$.

1.4 Mechanistic Investigations into Iridium Catalyzed C-H borylation

Maleczka and Smith first started the process of determining the reaction mechanism of iridium catalyzed CHB in 2002.²⁷ They looked into two possible mechanisms; one operating via an iridium (I/III) cycle and the other through a (III/V) cycle. To investigate this, they isolated two different iridium complexes. First was $\text{Ir}(\text{III})(\text{PMe}_3)_3(\text{Bpin})_3$ and the other was $\text{Ir}(\text{I})(\text{Bpin})(\text{PMe}_3)_4$. Using these metal complexes they performed the CHB of iodobenzene. The differences in reactivity between the two

catalysts was telling. It was found that the Ir(I)(Bpin)(PMe₃)₄ failed to make any C₆H₄IBpin product while the Ir(III)(PMe₃)₃(Bpin)₃ yielded 54% of the borylated iodobenzene. This was consistent with the previous reaction (Scheme 11) showing that the iridium CHB would tolerate iodide in the reaction. This experiment suggested that an iridium (I/III) cycle would likely not have tolerance for iodides. As such they proposed that the iridium CHB operated through an iridium (III/V) cycle.

In 2002, submitted shortly after the Maleczka and Smith paper²⁷, Ishiyama, Hartwig and co-workers reported the isolation of an iridium (III) trisboryl bipyridine complex by using cyclohexene to trap it in a six coordinate 18-electron complex.²⁵ Upon loss of cyclooctene this complex was a potential intermediate in the CHB mechanism. Using this complex, they showed that it could transfer all three boryl ligands to benzene in minutes.

Sakaki computed the transition states for the CHB using iridium trisboryl catalyst. They were able to calculate the transition states for a variety of different possibilities and concluded that the most likely mechanism was through an Ir(III/V) species. Their results also supported the proposed mechanism by Maleczka and Smith. They also calculated the rate determining step to be C-H functionalization with an activation barrier just under 25 kcal/mol.

In 2005, Hartwig and co-workers reported the mechanistic study of iridium catalyzed CHB, using dtbpy as a ligand.²⁸ They isolated a trisboryl(dtbpy)Ir(COE) complex that they used for the study along with performing in-situ generated reactions. They found that iridium CHB was first order in arene concentration and zero order in boron concentration. They also found that increased COE concentration acted as an

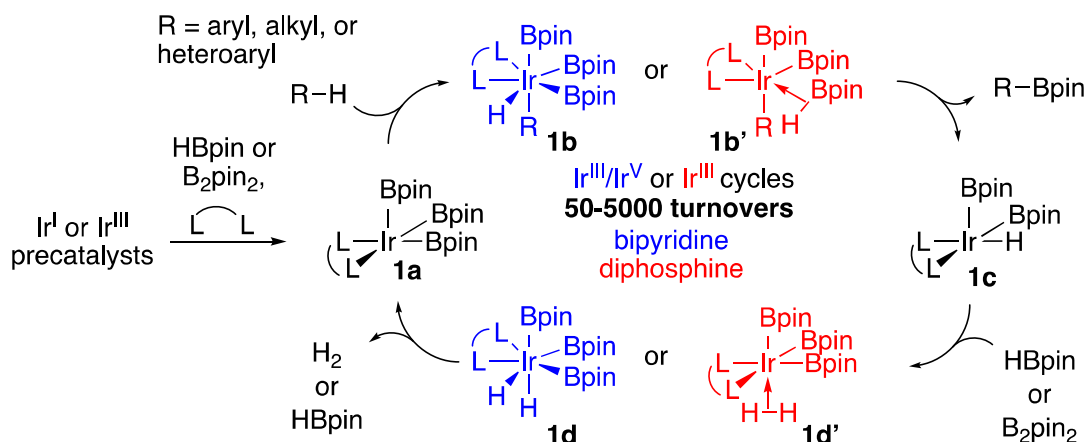
inhibitor to the reaction. From this data they were able to state that the rate-determining step was C-H activation, which was similar to the computational results of Sakaki. They also determined from their data that the iridium CHB system likely operated through an iridium III/V cycle, which supported the results of the experiments performed by Maleczka, Smith, and co-workers.

In 2015 Maleczka, Smith, and co-workers investigated at the mechanism of CHB using phosphine ligands.²⁹ Using phosphine ligands they were able to isolate and identify several different hydride intermediates in the CHB catalytic reaction cycle. They were able to identify 4 different iridium hydride states of the catalyst and show their interconversion through additions of HBpin or H₂. They then demonstrated that each of the hydride species that contained an iridium-boryl bond were competent for CHB. They also showed that under catalytically relevant conditions the different hydride species would all potentially be operational for differing CHB catalytic cycles.

From these previous papers a general catalytic cycle can be proposed depending on the nature of the ligand as shown in Scheme 12. From the precatalyst of [Ir(OMe)cod]₂ with a bidentate nitrogen-based ligand and boron source an iridium(III)trisboryl complex is formed (**1a**). Oxidative addition of an aryl or heteroaryl C-H bond results in a 7-coordinate iridium (V) species shown as **1b**. This complex undergoes reductive elimination to generate an iridium hydride species **1c**. Oxidative addition of either B₂pin₂ or HBpin results in a 7-coordinate, iridium(V) complex **1d**. Reductive elimination of either HBpin or H₂ respectively, based on the boron source, results in regeneration of the resting state of the catalyst (**1a**).

When a bidentate phosphorus-base ligand is used the catalyst undergoes a similar process, however, the generation of **1b'** results in an iridium (III) species, instead of an iridium (V) intermediate, due to the η^2 coordination of a pinacolborane. **1b'** then follows a similar path through the rest of the catalytic cycle through reductive elimination to generate **1c**. With bisphosphines addition of pinacol borane results in a η^2 -binding of hydrogen to make **1d'**. Reductive elimination results in regeneration of **1a**.

Scheme 12. Proposed mechanism of iridium CHB^{25,27-29}



1.5 Selectivity of CHB

Without a specific interaction that results in a directed borylation, CHB reactions are mostly directed by steric interactions. Maleczka, Smith and co-workers first noted the selectivity of substituted arenes in 2000 when they were comparing the reaction of iridium and rhodium complexes for CHB.²⁴ This was followed by observations from Hartwig^{25,26} and publication in a 2002 science paper by Maleczka Smith and co-workers where they described the selective meta borylation of 1,3 disubstituted benzenes.²⁴ Up to that point in chemistry most aromatic functionalizations operated through either

electrophilic or nucleophilic conditions. With CHB the electronics had a much less impact on the selectivity of the catalyst.

1.6 Ortho-Directed C-H borylation

Through the years there have been several methods of generating ortho-selective CHB. The different methods have been proposed to accomplish this through generating a silicon-iridium covalent bond to the iridium center,³⁰ an “outer-sphere” type interaction with the ligands on the iridium catalyst through a hydrogen bond interaction,^{31–33} electrostatic interactions,³⁴ or a chelating interaction with an open coordination site on the iridium center.³⁵

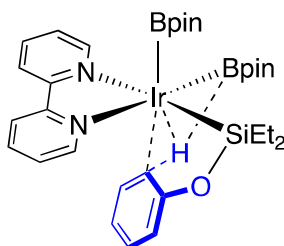
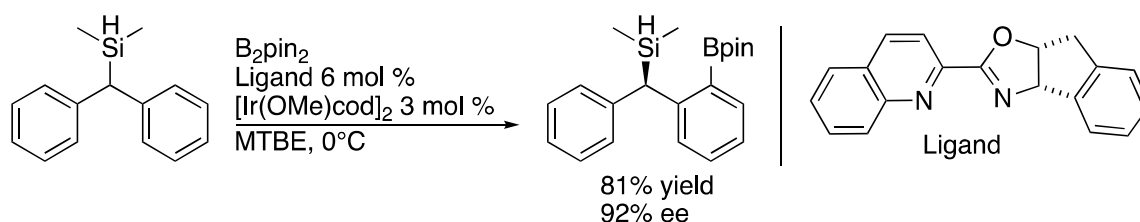


Figure 2. Proposed Relay-directed ortho CHB transition state

First reported by Hartwig and coworkers,³⁰ relay directed borylation covalently binds the substrate to the homogeneous iridium catalyst by first undergoing a Si-H oxidative addition to the iridium center (Figure 2). Reductive elimination of HBpin, the catalyst shown in Figure 2 is generated. This directs the C-H activation at the ortho position relative to the silyl group. The relay directed C-H borylation was expanded to generate chiral centers through CHB differentiation of substituents.³⁶ By hydrosilylation of benzophenone compounds followed by use of a chiral ligand on the catalyst to

generate the C-B bond formation on the aromatic ring (Scheme 13). Relay direction provides incredible control of the selectivity of borylation, however, this is a substrate-controlled direction method that requires an auxiliary to be added to the substrate. Because of this it is limited to phenols, ketones, or substrates with benzylic positions that can undergo addition of a silane or generation of a benzylic silane through synthesis.

Scheme 13. Enantioselective CHB through relay silyl-directed borylation



A second type of ortho direction used in CHB is an electrostatic interaction between the substrate and the bidentate ligand. This direction method was reported by Maleczka and Smith and co-workers for phenols³⁷ and anilines.³⁸

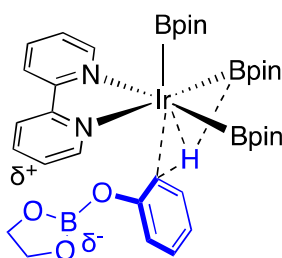


Figure 3. Electrostatic directed ortho CHB transition state

Starting from a phenol or an aniline treatment with the boron source used for CHB generates a borate protecting group. The substrate that is generated has electron density on the borate that interacts with a partial positive charge on the bipyridine ligand.

This electrostatic interaction directs borylation to the ortho position of the phenol or aniline. This interaction may seem weak but, as the authors note, a 2.7 kcal/mol difference at 25 °C is needed to generate 99:1 selectivity.³⁷ The majority of the substrate scope contained para substitutions. However, when moving from a pinacol boronate to an ethylene glycol boronate the authors found that the interaction was enhanced and the selectivity was greatly improved. The limitations of this system are similar, but fewer, than the limitations of the relay directed ortho borylation by Hartwig. Both systems require the substrate to react with something that before the directing effect occurs. Both systems result in this protecting or directing group to be sacrificed after the reaction is complete. However, the boron directed system allows for use of the same reagent as will be used to replace the C-H bond., This new type of interaction shows promise and indicates that other electron rich type systems might be possible to interact with a bidentate ligand to generate selective borylations.

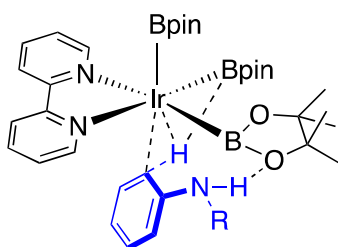
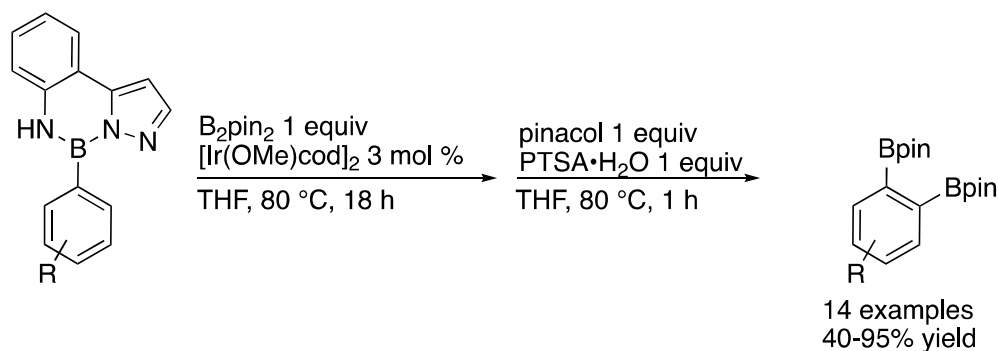


Figure 4. Hydrogen bonding directed ortho CHB of aniline³²

There have been two distinct types of directed ortho borylation in the literature generated by a hydrogen bond interaction between the substrate and the catalyst. In both cases they take advantage of the oxygen atoms on the boryl ligands to act as the hydrogen bond acceptor. In one method reported by Maleczka, Smith, and co-workers anilines,

protected by either a Boc group³² or a boronate,³⁹ can result in a hydrogen bond interaction that generates ortho selectivity. The limitation to this chemistry is that it requires that the aniline not be fully substituted. Also during the course of their investigations it was discovered that 2-substituted anilines did not borylate effectively at the ortho position due to a steric interaction between the substitution and the protecting group of the aniline resulting in the N-H bond angling away from the open ortho position on the ring.

Scheme 14. Hydrogen bond directed ortho diborylation³³



Another type of ortho borylation using a hydrogen bond interaction was reported by Suginome and co-workers where they used a pyrazolylaniline as the protecting group on a boron (Scheme 14).³³ The resulting borylation of these compounds was ortho diborylated substrates with differing boron substructures that can undergo orthogonal chemistry or be converted to the Bpin as shown in Scheme 14. In the absence of ligand, $[\text{Ir}(\text{OMe})\text{cod}]_2$ catalyzed the CHB in high yield and high selectivity.

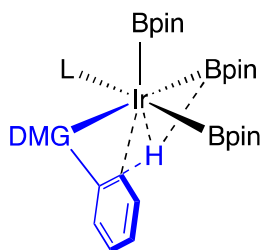


Figure 5. Chelate directed ortho CHB

Chelate-directed CHB will be discussed in more detail in Chapter 3. As shown in Figure 5, chelate directed CHB operates through opening up an extra coordination site on the iridium catalyst. In this extra site a directing group, containing a lone electron pair, coordinates to the iridium center and promotes C-H activation to proceed ortho to the directing group. This chelate directed borylation has been the most widely used method for ortho borylation and as such there are more differing methods for this process than other types of ortho borylation.

Kanai and co-workers demonstrated that a Lewis acid could be used to direct CHB. They followed methods that were developed first in meta directed CHB to put a Lewis acid off of the side of a bipyridine. This allowed a thioether to coordinate to the Lewis acid, in this case a boronic ester, and direct the CHB to the ortho position.

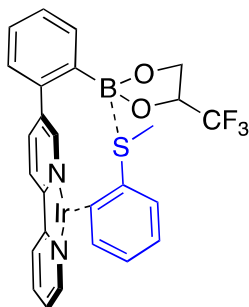


Figure 6. Thioether directed ortho CHB

1.7 Meta-Directed CHB

There have been three reported methods of directed meta borylation. This is defined as borylation that is not controlled by steric effects but on mono or sparsely substituted arenes or heteroarenes where a specific interaction dictates the CHB result at the meta position. The first example of this was reported by Kanai and co-workers.⁴⁰ He found that by attaching a urea moiety off of the side of a bipyridine ligand the selectivity of the borylation for aryl and heteroaryl compounds with functional groups that contained an adjacent carbonyl such as esters, ketones, amides, phosphates and others could be controlled. It was found that by switching the solvent from hexane to *p*-xylene the selectivity was able to be increased from 8.3:1 *m:p* to 17:1.

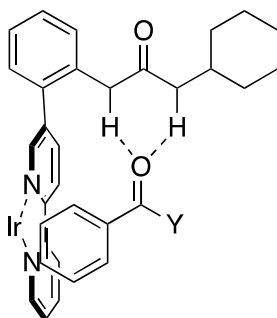


Figure 7. Hydrogen bond-directed meta-borylation

The second example of meta borylation was published by Chattopadhyay and Bisht.⁴¹ They showed that generation of imines in-situ from aldehydes could result in formal borylation of aldehydes upon workup. The borylation was selective for the meta position upon use of methyl amine as the nitrogen for the imine source. Using bulkier amines resulted in poorer selectivity. By reducing the steric hindrance around the imine center they proposed that the imine would coordinate to the open p-orbital of the boronic

ester on the catalyst and that would result in greater meta-direction. This reaction proceeded better with more electron donating ligands. 3,4,7,8-Tetramethyl-1,10-phenanthroline (TMP) resulted in the greatest amount of meta-directed CHB of benzaldehyde at 97:3 *m:(o+p)* ratio when methyl amine was used to form the imines. No heteroaromatics were reported for meta directed borylation using this method.

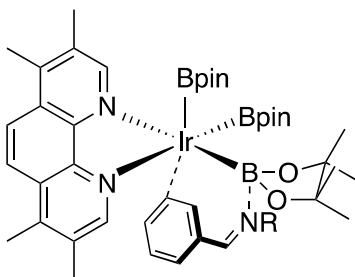


Figure 8. Imine directed meta borylation

The final method for meta directed borylation was developed by Phipps and co-workers.⁴² Phipps used ion pairing to direct the borylation. Using a sulfate ion dangling off of a bipyridine the interaction with benzyl ammonium tosylate ions created a directed borylation that resulted in meta borylation. Phipps followed this up with two other papers on meta-directed borylation of tethered amines⁴³ and of tethered ammonium salts.⁴⁴ While this is similar to the electrostatic interaction there is formally a full charge on each ligand and substrate, while the borylation by Maleczka, Smith and co-workers was partial build-up of electron density.

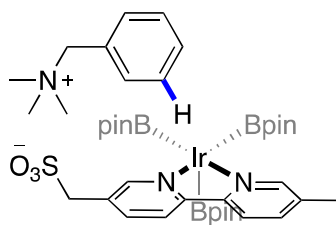


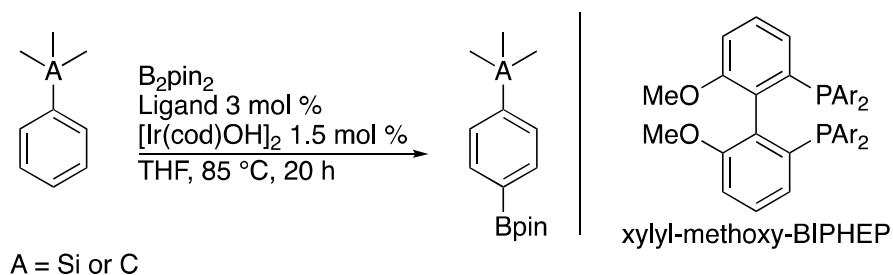
Figure 9. Ion pairing interactions for meta-directed CHB

As of yet, nobody has flipped the ion pair such that the positive charge is on the ligand and the negative charge on the substrate. While a negatively charged substrate might result in difficult interactions with the iridium, other lone pair type interactions with a positively charged ion might be a potential for directed borylation.

1.8 Para-Directed C-H Borylation

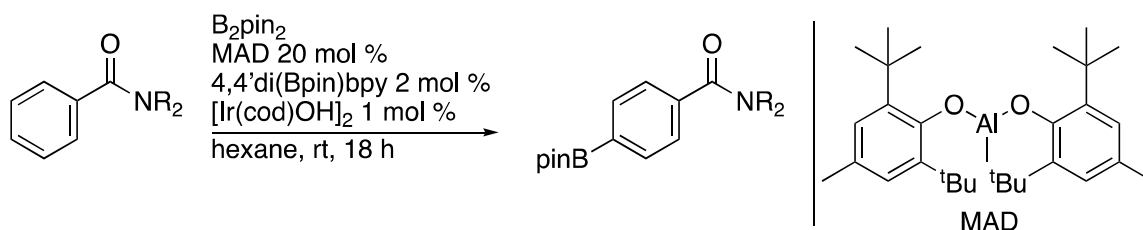
There have been three methods of para-directed borylation reported. The first method is the use of steric interactions between the substrate and the ligand to generate para selectivity. In 2015 Itami and co-workers demonstrated that by using a xylyl-methoxy-BIPHEP ligand they could achieve 9:1 para:meta selectivity with 94% yield in hexane.⁴⁵ They found that para selectivity could be obtained for a variety of arenes with quaternary carbons and silanes as substituents. When they switched to an isopropyl group the selectivity dropped to 58:42 and when they tested the borylation of ethylbenzene using the catalyst the selectivity reverted to a near statistical distribution of 31:68 para:meta.

Scheme 15. Steric directed para-borylation of bulky monosubstituted arenes



In 2017, Nakao and co-workers demonstrated how to use cooperative catalysis in CHB reactions.⁴⁶ Use of a large aluminum complex acts as a Lewis acid and blocks half of the substrate. Using dtbpy as a ligand, the CHB was directed to the para position. CHB of pyridines, amides, and phosphonates with examples more than 20:1 para selective. The solvent choice was important as use of a polar solvent would result in lower interaction between substrate and the aluminate co-catalyst. This use of a co-catalyst is a unique technique for CHB and was a creative way to solve the challenge of para selectivity for a wider range of substrates than Itami and co-workers.

Scheme 16. Aluminum/iridium co-catalysts for para-directed CHB of esters and pyridines



Shortly after the report by Nakao and co-workers, Chattopadhyay and co-workers published a para-directed CHB utilizing an L-shaped ligand to interact with the

substrate.⁴⁷ They designed a ligand similar in concept to that used by Kanai for meta-directed borylation by adding 2-quinone as side chain to a bipyridine ligand. What they found was that through the addition of potassium *tert*-butoxide they were able to generate up to 33:1 para-selective borylation of ethyl esters. This was demonstrated on ethyl benzoates as well as on esters on pyridines. 5-membered rings resulted in C2-borylation selectively and failed to show differences from other bipyridine-based borylation.⁴⁸

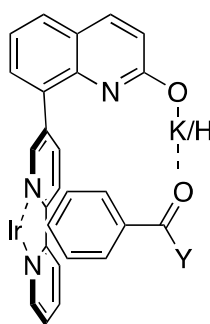


Figure 10. Directed para borylation of aryl esters

1.9 Aliphatic C-B Bond Formation

There have been a few different routes to synthesizing sp^3 -carbon-boron bonds. One route that has been around for quite some time is by the use of hydroboration of alkenes.³ When an alkyl halide is used as a starting material generation of a lithium or Grignard reagent followed by quenching the product with a borate can be used.⁴⁹ When an activated substrate is around lithiation and quenching with a borate is an established route.⁴⁹ All of these methods have been used to generate chiral sp^3 -carbon-boron bonds. Like all chemistry they both have drawbacks to general use. Selectivity of hydroboration is mainly sterically driven but has some electronic components. However, when there is

not a significant difference in steric size between different sides of an olefin selectivity can be problematic.

As mentioned earlier Grignard reagents and lithiation chemistry can have issues with chemoselectivity and some functional groups are not tolerated in these processes. Use of this metalation/borylation process is dependent on the selectivity for halogenations. Without a halogen present lithiation needs to be at the most acidic position or directed in order to be effective.

A different route to synthesizing aliphatic carbon boron bonds was demonstrated by Ito and co-workers. They demonstrated that through dearomative borylation they could enantioselectively borylate the 3-position of piperidines.⁵⁰

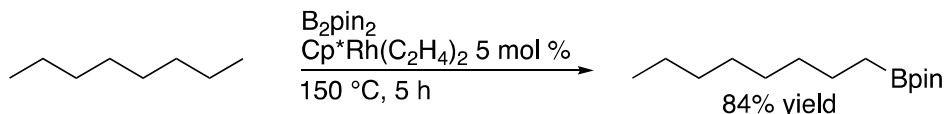
1.10 sp^3 C-H borylation

One of the more enticing routes to sp^3 C-B bonds is metal catalyzed CHB. Since 1999, there have been a few different reactions that have been developed for this transformation. However, each of them has specific limitations that prevent it from becoming a general reaction for use.

The first example of a transition metal catalyzed CHB of an sp^3 carbon-hydrogen bond was, a photocatalytic example using a rhenium complex to catalyzed CHB of octane by Hartwig and co-workers. They found when irradiating a solution of $CpRe(CO)_3$ they were able to borylate alkanes at the terminal position selectively.⁵¹ They further studied the CHB of alkane when they found that by using $RhCp^*(C_2H_4)_2$ as a precatalyst with B_2pin_2 as a boron source resulted in borylation of the primary carbon of n-octane in 84% yield over 5 hours at 150 °C.⁵² This was performed without the use of photocatalytic

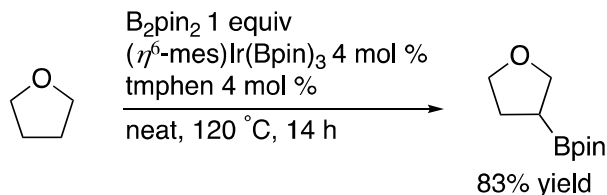
process. These were incredible reactions as they were selective for the primary carbon-hydrogen bond in the presence of all of the other secondary C-H bonds.

Scheme 17. Octane CHB using a rhodium catalyst



Years later, Hartwig and co-workers expanded the use of CHB on sp^3 centers with the selective CHB of cyclic ethers. The CHB of cyclic ethers was selective for borylation at the 3-position. This reaction was counter to many different C-H functionalizations of cyclic ethers prior to that which functionalized the 2-position. However, the CHB resulted in a very similar selectivity to the products generated by hydroboration of an alkene in a similar position. This represented the first use of iridium for CHB on an sp^3 center.⁵³

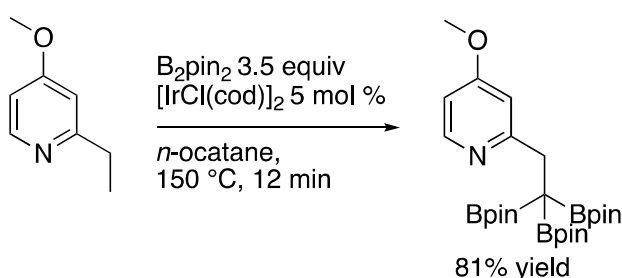
Scheme 18. CHB of saturated cyclic ethers



Sato and Michigami used a pyridyl directing group to triborylate a primary sp^3 C-H center. They did this with using 3.5 equivalents of B_2pin_2 , or 1.2 equivalents of B_2pin_2

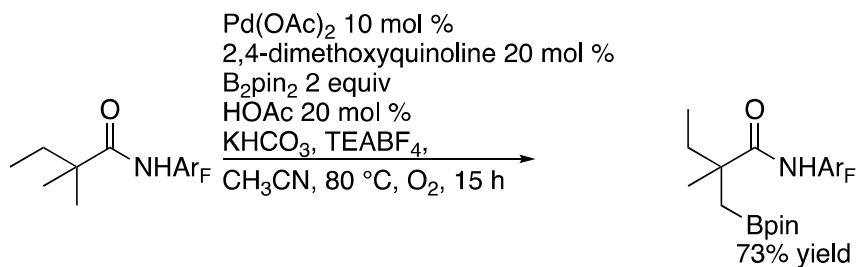
for every borylation. The reaction they ran was quite hot at 150 °C, similar to the octane borylation by Hartwig, however the reaction was complete in only 12 minutes when the 4-position contains an ether off of it. The triborylation was a very unique result that was not repeated with a different system until years later when Chirik and coworkers performed it with a nickel catalyst.⁵⁴

Scheme 19. Pyridine directed triborylation of primary C-H bonds



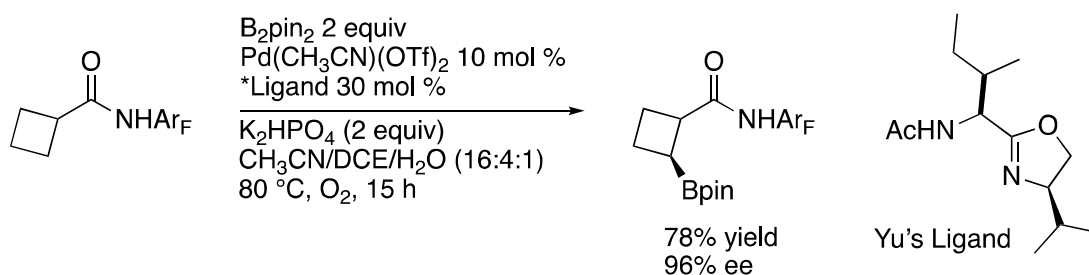
The directed ortho borylation of saturated cyclic centers was reported by Yu and co-workers. Using an electron deficient amide system shown in Scheme 20.⁵⁵ Yu borylated primary and secondary sp^3 centers as well as aromatic compounds. They did this through the use of a palladium catalyst and a catalytic cycle that was significantly different than that of iridium CHB. The result was the ability to direct borylation selectively using a quinoline based ligand on the palladium.

Scheme 20. Palladium catalyzed sp^3 CHB directed by amides⁵⁵



Yu and co-workers followed that work with a report of the enantioselective borylation of sp^3 centers. They used a very similar catalyst as their work in 2016 but with a chiral ligand as shown in Scheme 21.⁵⁶ This was the first example of an enantioselective CHB reaction.

Scheme 21. First enantioselective CHB of a sp^3 carbon



1.11 Conclusions and Future Work

Carbon-boron bonds are important intermediates in synthetic chemistry. They have the ability to be transformed through a variety of different methods. The synthesis of carbon-boron bonds has become incredibly selective with methods developed for every position on arenes. The advancement of CHB into aliphatic CHB represents the next major area of research and selective synthesis of borylated saturated cyclic compounds is an important future step. Enantioselective CHB has been demonstrated and future work will continue to push for more selective routes to install boron on saturated substrates.

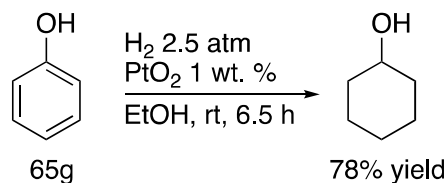
Chapter 2. Hydrogenation of Aromatic and Heteroaromatic Organoboronic Esters and Organosilicon Compounds

2.1 A Brief History of Hydrogenation Chemistry

Heterogeneous hydrogenation has been a staple in synthetic chemistry dating back to when Sabatier and Senderens made important discoveries in 1897.⁵⁷ In the first report by Senderens and Sabatier, ethylene was reduced with a dispersed nickel catalyst. Further experimentation by Senderens and Sabatier found that a nickel catalyst could hydrogenate aromatic compounds such as phenol and aniline.⁵⁸ For these advancements in reduction chemistry Sabatier won the Nobel prize in 1912. Since that time, heterogeneous hydrogenation has expanded to a variety of different metals and catalysts.

Voorhees and Adams found that the reports in the literature of platinum metal for hydrogenations generated mixed results.⁵⁹ Consequently, they sought a repeatable synthesis of a platinum catalyst for hydrogenation. They synthesized platinum oxide by fusion of chloroplatinic acid with sodium nitrate at 320 °C. This platinum oxide was then used to hydrogenate ketones, aldehydes, and esters to alcohols, as well as hydrogenation of phenol to cyclohexanol.⁵⁹ It became known as Adam's catalyst and it is often used with addition of glacial acetic acid.

Scheme 22. Platinum oxide catalyst for hydrogenation.⁵⁹



In 1925 and 1927 Raney was issued two different patents for the development of a porous nickel catalyst. First, Raney synthesized a silicone/nickel alloy and then treated it with sodium hydroxide.⁶⁰ The resulting nickel was the most active catalyst for hydrogenation of seed oil under high pressure and temperature at that time. Raney followed that by making a 1:1 nickel/aluminum alloy that he treated with sodium hydroxide to generate the nickel catalyst.⁶¹ This nickel/aluminum starting material was found to be incredibly active and up to five times as active of a catalyst as was available for hydrogenation at that time. This porous nickel catalyst became known as Raney nickel.

The use of rhodium as a hydrogenation catalyst was first reported by Beeck in 1945. He illustrated that the rhodium was the fastest of the metals he tested for hydrogenation of ethylene.⁶² The first example found in the literature of hydrogenation chemistry utilizing rhodium on carbon was reported in 1952 by Dunworth and Noord looked at the reactivity of rhodium on carbon.⁶³ Dunworth and Noord found that rhodium on carbon was an effective catalyst for the hydrogenation of olefins, carbonyls, aldehydes, nitro groups and quinones with addition of acid.

Freifender and co-workers looked at the reactivity of different supports of rhodium in hydrogenation chemistry. They found that rhodium was more active and less prone to poisoning when hydrogenating pyridine on a carbon based support than an alumina-based support.⁶⁴ These reports and many others also showed the chemoselectivity of rhodium tolerated esters, ethers, alcohols and amines.

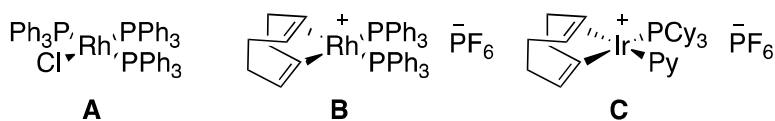
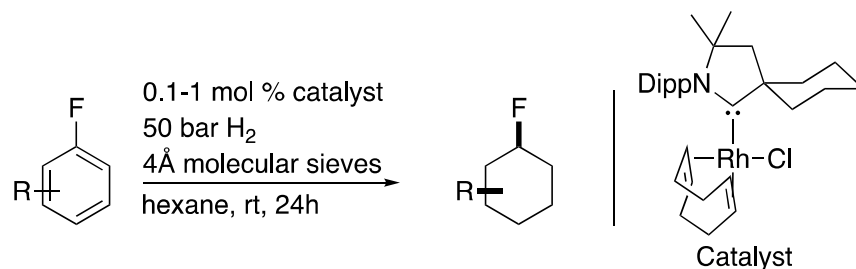


Figure 11. Homogeneous hydrogenation catalysts.⁶⁵⁻⁶⁸

Homogeneous hydrogenations took off with the development of metal complexes that catalyzed reduction of alkenes. Wilkinson developed a tris(triphenylphosphine)rhodium (I)chloride for the use as a hydrogenation catalyst (Figure 11 **A**).⁶⁵ It operated by dissociation of a triphenylphosphine to open up a coordination site and allow for hydrogenation to occur. This work was advanced by Osborn and Schrock.⁶⁶ They synthesized the cationic rhodium complex **B** shown in Figure 11. This Osborn and Schrock catalyst was able to selectively hydrogenate dienes to mono-alkenes and generated more turnovers than Wilkinson's catalyst.⁶⁷ Taking the cationic complex formation further, Crabtree and co-workers develop an iridium-based catalyst for hydrogenation of tri and tetrasubstituted alkenes. While tetrasubstituted alkenes were able to be reduced using Crabtree's catalyst, **C** in Figure 11, Wilkinson's and Osborn's catalysts were unable to reduce highly substituted alkenes.⁶⁸

Scheme 23. Hydrogenation of Fluorinated Arenes.⁶⁹



More recently, homogeneous hydrogenations have been extended to asymmetric hydrogenations of heteroaromatic compounds such as pyridines⁷⁰, indoles⁷¹⁻⁷³, pyrroles,⁷⁴ furans,^{75,76} and others.⁷⁷

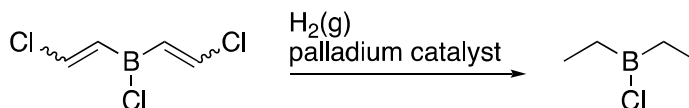
Homogeneous hydrogenation has typically struggled with non-heterocyclic hydrogenations. Illustrated by Scheme 23, one of the most recent developments was the hydrogenation of fluorinated benzenes to generate fluorinated cyclohexanes by Glorius and co-workers.⁶⁹ This process, while using a homogeneous precatalyst, was reported to likely be a heterogeneous catalyst. Using this same system, Glorius also reported the first hydrogenation of arylboronic esters.⁶⁹

Previously there existed only a single other report of fluorine being maintained through the hydrogenation of an arene.⁷⁸ In the hydrogenation of fluorobenzene by Blum and co-workers it was reported to result in only 39 % fluorocyclohexane with the rest being defluorinated compound.

2.2 Hydrogenation of Borylated Olefins

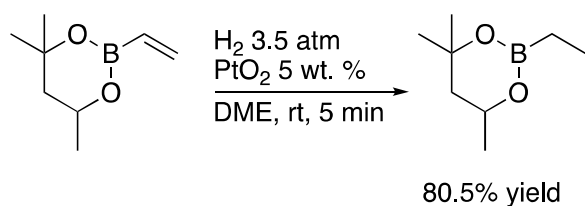
The hydrogenation of borylated olefins has been reported in literature since 1965 when Clark and co-workers patented a process of synthesizing diethyl chloroborane from chlorodivinyborane.⁷⁹ The hydrogenation occurred over palladium on carbon using hydrogen gas as the hydrogen source. The loss of hydrochloric acid during the reaction gave the desired product (Scheme 24).

Scheme 24. First reported hydrogenation of a borylated olefin⁷⁹



Quickly following that patent, 2-vinyl-4,4,6-trimethyl-1,3,2-dioxaborinane was reported to be hydrogenated over a platinum catalyst by Woods and coworkers.⁸⁰ This first report of a oxaborinane being hydrogenated paved the way for hydrogenation of other boronic esters.

Scheme 25. First reported hydrogenation of a vinyl boronic ester.⁸⁰



The first asymmetric hydrogenation of a vinyl boronic ester was performed by Morgan and Morken in 2003.⁸¹ The hydrogenation of 1,2-bis(4,4,5,5-tetramethyl-1,3,2-dioxaborolan-2-yl)styrene yielded the saturated compound in 85% yield with 93% e.e. This was a big step in organoboron chemistry because it illustrated how to create a borylated stereocenter without the use of asymmetric hydroboration. Since the report by Morken, several examples of asymmetric hydrogenation have been performed by Andersson⁸², Pfaltz⁸³, and others to yield enantiopure organoboron compounds.

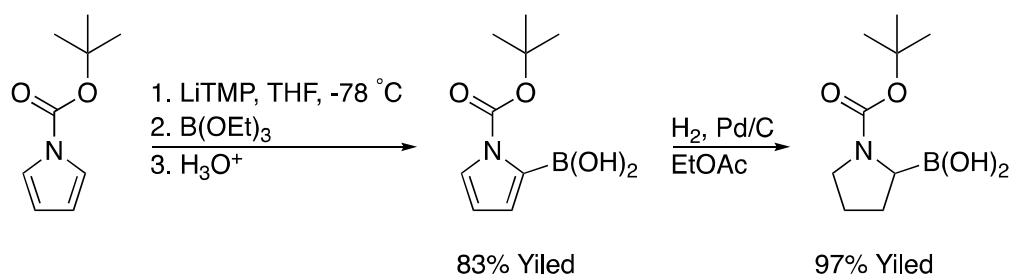
Hydrogenation of borylated olefins extended to other protecting groups on boron as well. In 2007, Molander and co-workers reported the hydrogenation of a vinyl potassium trifluoroborate salt in methanol with palladium on carbon.⁸⁴ Hydrogenation of vinyl MIDA boronate was performed by Burke in 2010 with hydrogenation of an alkynyl MIDA boronate.⁸⁵ In 2010 Suiginome and co-workers hydrogenated a diamionaphthalene boronic ester (Bdan) on an olefin with palladium on carbon.⁸⁶ Overall a wide variety of boron containing olefins have been shown to be stable in

alcoholic, or polar solvents for hydrogenation using palladium on carbon, platinum metal, and a variety of rhodium and iridium homogeneous catalysts.

2.3 Hydrogenation of Borylated Arenes

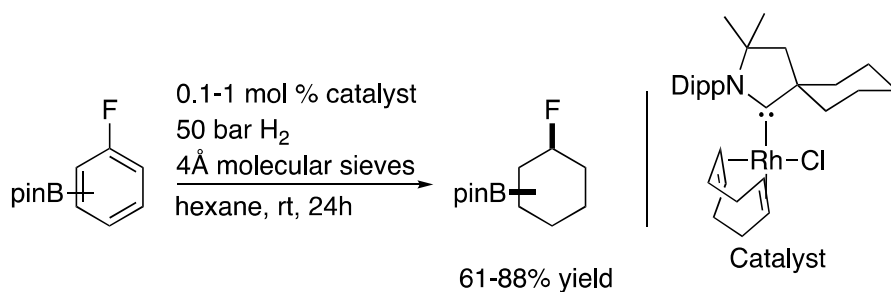
Arenes and heteroarenes are a bigger challenge for hydrogenation than that of olefins. The challenges are varied but the large barrier required to breaking the aromaticity is the largest challenge. As such, there have been a few examples reported in literature where aromatic or heteroaromatic organoboron compound has been hydrogenated. The first was in 1993 by Kelly and co-workers where *n*-Bocpyrrole was subjected to a lithiation/borylation to yield the boronic acid at the 2-position. They followed this by hydrogenating the pyrrole to the pyrrolidine using palladium on carbon. They were able to isolate the product in 97% yield.⁸⁷

Scheme 26. Hydrogenation of *n*-Boc-2-pyrrolyl-boronic acid.⁸⁷



The next example, was recently reported by Glorius and co-workers when they showed the hydrogenation of borylated fluorobenzenes could be performed using a homogeneous catalyst.⁶⁹ They reported three examples of arylboronic esters being reduced to the cyclohexanes.

Scheme 27. Homogeneous hydrogenation of fluorinated aryl boronic esters.⁶⁹



These two examples showed that a general method for the hydrogenation of borylated arenes and heteroarenes could be made. As discussed in Chapter 1, the methods for producing saturated cyclic organoboron compounds are limited to hydroboration or sp^3 CHB. The recent advances in sp^3 CHB are important; however, a simpler route to synthesizing these compounds would be extremely helpful. It would be beneficial to utilize the past 19 years of thermal catalytic CHB research to generate selectivities for the saturated cyclic compounds that are currently challenging to make.

2.4 Additives for Hydrogenation of Borylated 6-Membered Heterocycles.

Many hydrogenations of heteroaromatics are performed with the use of an acid additive. One major concern was that the borylated heteroaromatic compounds would deborylate during the hydrogenation. To screen for conditions that would limit deborylation a sample substrate of 3-(4,4,5,5-tetramethyl-1,3,2-dioxaborolan-2-yl)pyridine (**2a**) was used. The reduction of **2a** was attempted using hydrochloric acid as an additive and the hydrogenation was attempted over a variety of metal catalysts. Upon workup the product distribution was determined by analyzing the ¹H-NMR spectra. An example spectrum is shown below in Figure 12.

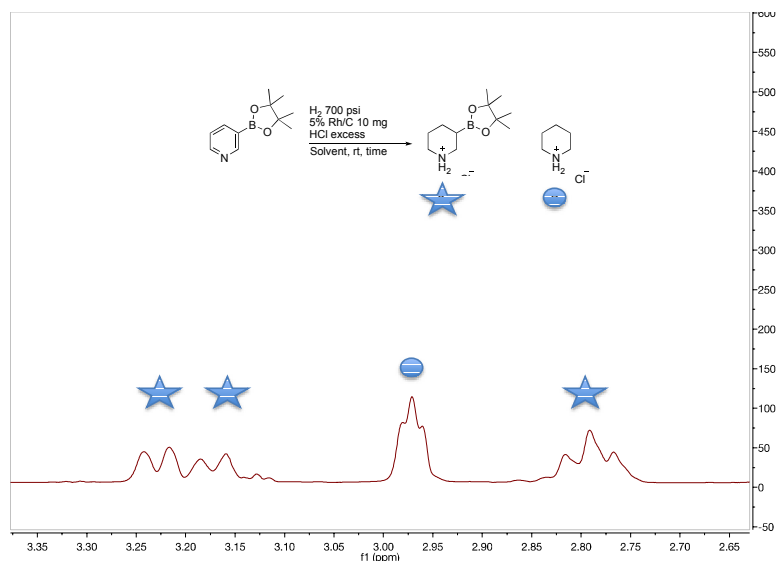
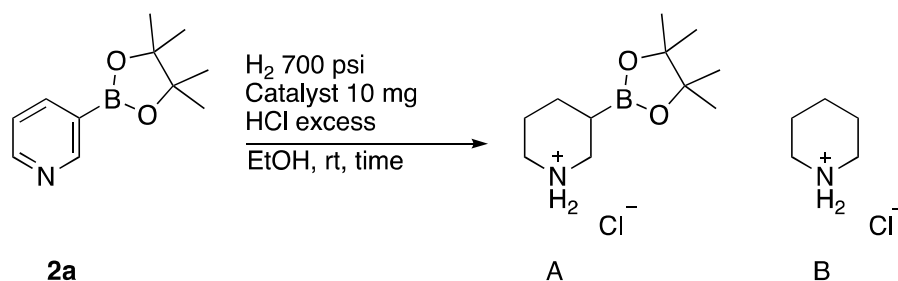


Figure 12. Hydrogenation of **2a** yielding borylated and deborylated product

The catalyst screen results were summarized in Table 1. It was found that 5% rhodium on carbon performed the best. It resulted in the least amount of deborylated product and it was faster than the other catalysts. Rhodium on alumina also had comparable deborylation to product formation but the reaction was slower. Palladium on carbon failed to hydrogenate the **2a**. Platinum oxide showed slower hydrogenation and an increased rate of deborylation as compared to that of the rhodium catalysts. Rhodium on carbon is the catalyst that tends to have the most functional group tolerance while at the same time operates at the lowest temperature of the metals on solid supports. Catalysts available on more exotic support systems or metal alloys were not tested for the hydrogenation of borylated compounds. Raney nickel was not tested under these conditions as an attempt to use Raney nickel with a borylated arene resulted in complete

deborylation; while the use of rhodium on carbon does not result in deborylation under similar conditions.

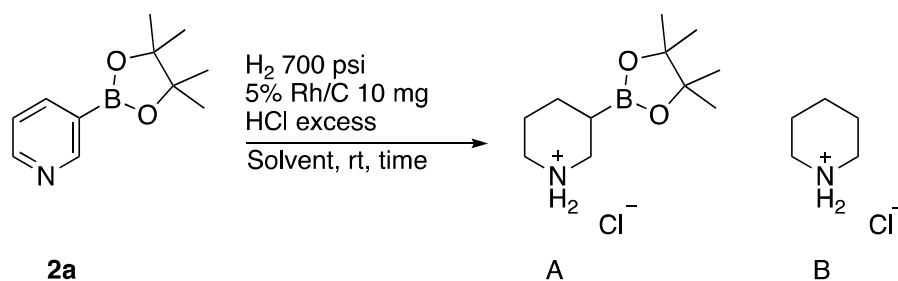
Table 1. Heterogeneous catalyst screen for hydrogenation of **2a**



Entry	Catalyst	Product A (%) ^a	Product B (%)	Starting Material
1	5% Rh/C ^b	72	28	0
2	5% Rh/Al ₂ O ₃	50	15	35
3	PtO ₂	32	32	36
4	10% Pd/C	0	0	100
5	10% Pt/C	24	38	38

a) 3-(4,4,5,5-tetramethyl-1,3,2-dioxaborolan-2-yl)pyridine (0.25 mmol), hydrochloric acid (1 mmol), hydrogen gas (700 psi), ethanol (2 mL), catalyst (10 mg), rt, 2 hours. Conversion % based on ¹H-NMR **b)** 1 hour

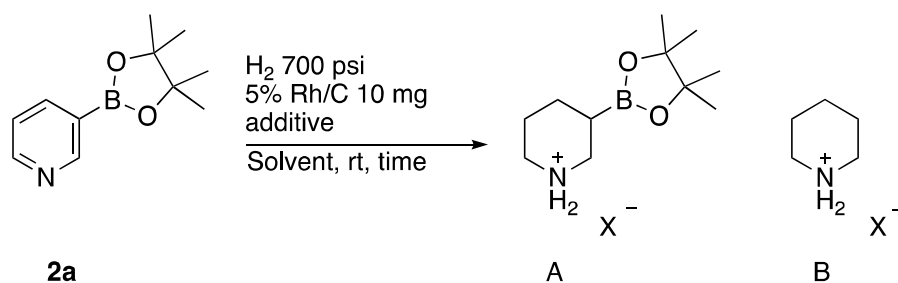
After determining that rhodium on carbon was the best option for a catalyst, a solvent screen was run. It was found that by switching from a potentially nucleophilic solvent such as ethanol to a non-nucleophilic polar solvent, dioxane, no reduction of the deborylation occurred. In fact, the deborylation that occurred in dioxane was actually greater than the amount of deborylation that occurred in ethanol. DCM showed complete deborylation over 36 hours and THF also showed more deborylation than ethanol as well. These results were summarized in Table 2.

Table 2. Solvent Screen for the Hydrogenation of **2a**

Entry	Solvent	Time (hours)	Product A (%) ^a	Product B (%) ^a	2a
1	Ethanol ^b	16	75	25	0
2	Dichloromethane	4	0	0	100
3	Dichloromethane	36	0	100	0
4	Dioxane	7	47	53	0
5	Tetrahydrofuran	7	65	35	0
6	Methanol	2	75	25	0

a) 3-(4,4,5,5-tetramethyl-1,3,2-dioxaborolan-2-yl)pyridine (0.25 mmol), hydrochloric acid (1 mmol), hydrogen gas (700 psi), solvent (2 mL), 5% Rh/C (10 mg), rt. Conversion % based on ¹H-NMR

The amount of deborylation was not found to be significantly different between reactions that proceeded for 16 hours or reactions that were stopped after 1 hour. This was observed when comparing the use of rhodium on carbon in ethanol in Table 2 to that same use in Table 1. Between hours 1 and 16 the compound is fully hydrogenated in the ethanol run of Table 2. However, there is no increased deborylation during the extra time. This implies that the saturated compound is stable under these conditions to deborylation. The deborylation that is occurring must therefore happen while the organoboron compound is either still aromatic or during the process of reduction.

Table 3. Bronsted acid additives for the hydrogenation of **2a** by rhodium on carbon

Entry	Additive (1 equivalent)	Time (hours)	Product A (%) ^a	Product B (%) ^a	2a (%)
1	HCl ^b	16	75	25	0
2	HCl (dry)	1	72	28	0
3	HCl + 1 mL H ₂ O	1	71	28	1
4	MeSO ₃ H	2	63	37	0
5	NH ₄ Cl	24	0	70	30
6	PO ₄ H ₃	2	58	42	0
7	2,6-dichloropyridine	36	38	62	0
8	Sulfuric Acid	2	39	61	0
9	Triflic acid	2	52	48	0

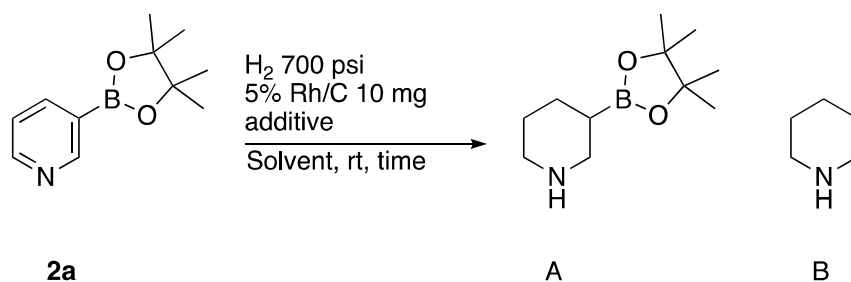
a) Conversion percentages determined by ¹H-NMR. 3-(4,4,5,5-tetramethyl-1,3,2-dioxaborolan-2-yl)pyridine (0.25 mmol), Additive (0.25 mmol), Hydrogen gas (700 psi), Ethanol (2 mL), 5% Rh/C (10 mg), rt.

The reaction was tested with the addition of 1 mL of H₂O in an effort to determine if a failure to properly dry the solvent was a cause of deborylation. The deborylation was very similar to that of using dry solvent.

Other acids with less nucleophilic conjugate bases were tested as well. Methanesulfonic acid resulted in a 2:1 ratio between desired product and that of the deborylated reduced product. Phosphoric acid, sulfuric acid, and triflic acid all saw significantly greater quantities of deborylation than that of hydrochloric acid. Entry 7 was

an attempt to generate hydrochloric acid in-situ. The dichloropyridine would generate 2 equivalents of hydrochloric acid over time instead of being added all at once. However this process resulted in more deborylation compared to simple addition of hydrochloric acid.

Table 4. Lewis Acid Screen for the Rhodium on carbon hydrogenation of **2a**



Entry	Additive (1 equiv)	Product A ^{a,b} (%)	Product B ^{a,b} (%)	2a ^{a,b}
1	Cerium (III) chloride	0	100	0
2	Magnesium chloride	0	30	70
3	Copper sulfate	20	18	62
4	Potassium Iodide	16	42	42
5	Zinc chloride	0	15	85
6	Iron powder (rusted)	0	15	85
7	Magnesium sulfate	0	17	83
8	Trimethyl borate	0	11	89
9	3Å molecular sieves (activated)	0	19	81

a) Conversion percentages determined by GCMS comparing piperidine to starting material. Pyridine was not seen by GC/MS. b) 3-(4,4,5,5-tetramethyl-1,3,2-dioxaborolan-2-yl)pyridine (0.1 mmol), Additive (0.1 mmol), Hydrogen gas (700 psi), Ethanol (1 mL), 5% Rh/C (10 mg), rt.

An attempt was made to hydrogenate **2a** in the presence of a Lewis acid to help facilitate the isolation of the product away from that of the deborylated side product.

However, these were largely unsuccessful. The results are summarized in Table 4, which show that only copper sulfate and potassium iodide resulted in any hydrogenated product. As these reactions were run in ethanol, a few of the compounds likely reacted with the solvent. Overall the Lewis acids that did show some reduction were slow and also showed equal or greater amounts of deborylation.

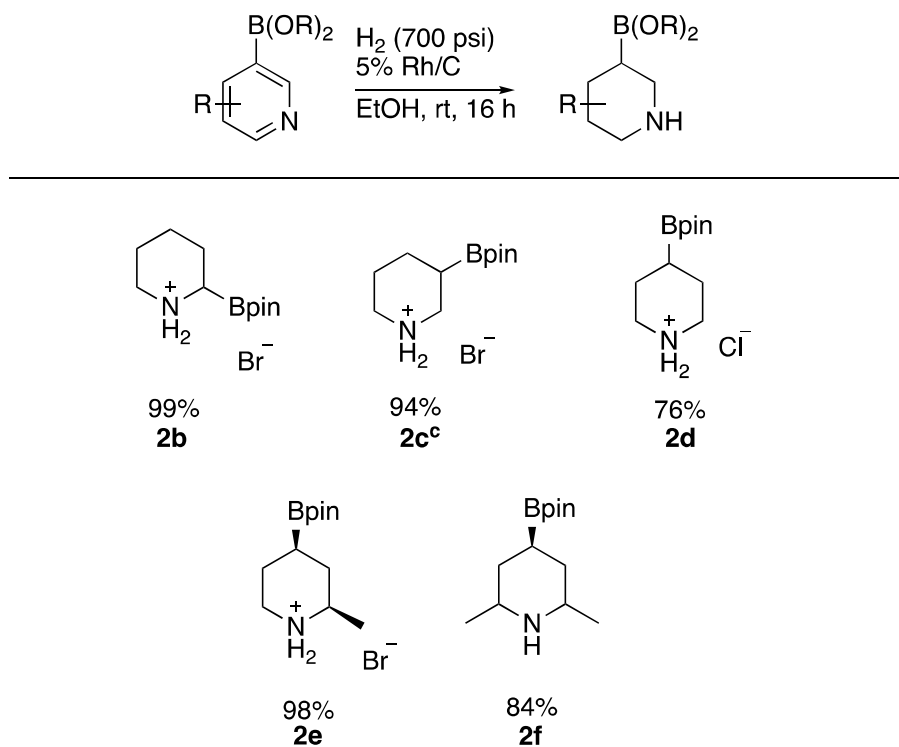
Based on these screens, the best conditions for hydrogenation of pyridines or other heterocycles were determined to be with 5% rhodium on carbon in ethanol with hydrochloric acid as an additive. Rhodium on carbon was the quickest and most tolerated catalyst and should be used for all substrates due to its affinity to hydrogenate a wide variety of arenes and heteroarenes. These conditions were used in an attempt to hydrogenate a variety of differing pyridines, however, isolations proved to be difficult. To start with the hydrogenation of **2a** under conditions labeled above was attempted and after filtration of the rhodium on carbon through Celite and removal of solvents a sticky residue remained. Selective crystallization was unsuccessful. Attempts were made to isolate amides or carbamates by reaction with chloroformates or acid chlorides. However, in those attempts more deborylation occurred.

2.5 Additives Free Hydrogenation of Borylated 6-Membered Heterocycles.

Some six-membered heterocycle substrates tested hydrogenated without the addition of acid. For the most part they fell into one of two classes of compounds. Either they contained steric bulk around the nitrogen or they contained a halogen in the molecule that was eliminated during the hydrogenation to generate an acid that facilitated

the hydrogenation reaction. The hydrogenation under these conditions did not result in any observable deborylation. Table 5 summarizes the results of these hydrogenations.

Table 5. Hydrogenation of 6-membered heterocycles^{a,b}



a) standard conditions 0.5 mmol substrate, 25 mg 5% Rh/C, H₂ (700 psi), EtOH (5 mL), rt, 16 h b) relative stereochemistry shown c) Isolated as a mixture with deborylated product

Starting from 2-Br-6-Bpin-pyridine compound **2b** was synthesized in 99% yield. This was a surprise as elimination is possible from the two positions of heteroaromatics. No deborylation was observed in this reaction. Compound **2b** is incredibly useful as two-substituted piperidines are a common motif in pharmaceutical chemistry. Overall the formation of **2b**, **2c**, and **2d** are important as this provides a clean and quick method for the formation of borylated piperidine in any position desired. Each of them started from

the heteroaryl halides. Compound **2c** was unable to be separated from a mixture of deborylated product.

Other methods for synthesizing borylated piperidines are limited. Borylation at the two position has been synthesized through the use of pyridyl directed CHB,^{88,89} and lithiation/borylation of boc-piperidine.⁹⁰ The 3-borylated piperidine is accessible through some very nice chemistry by Ito and coworkers using a broylative reduction of pyridines to generate the partially saturated piperidine.⁹¹ The 4-borylated piperidine is also available through Miyaura borylation.⁹² The relative stereochemistry generated from this type of transformation follows that of other reductions of pyridines by rhodium on carbon, as illustrated by compound **2e**.

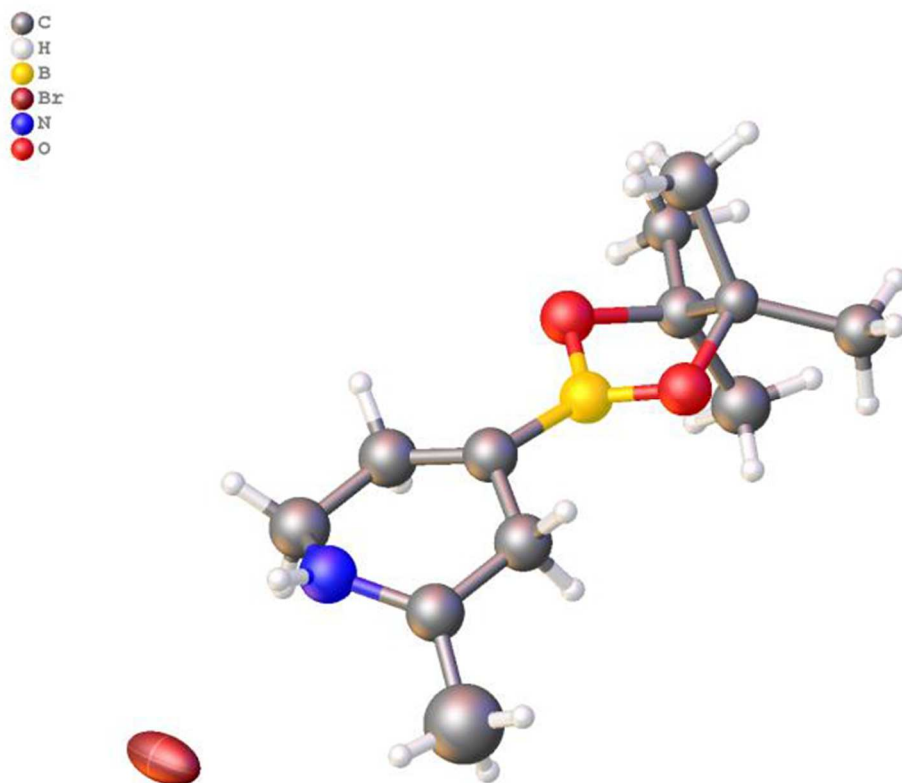


Figure 13. Crystal Structure of Compound **2e**

Compounds **2f** is important in that it does not contain a halogen that eliminated during the hydrogenation. **2f** has steric bulk near the nitrogen that helps to prevent poisoning of the catalyst through the hydrogenation.

2.6 Hydrogenation of Borylated 5-Membered Heterocycles

Furans, indoles, pyrroles and thiophenes all have well developed CHB chemistry. They have been well studied and various papers have included methods of borylating those 5-membered heterocycles at different positions of sp^2 carbon centers. The CHB of these reduced heterocycles has not been reported except for tetrahydrofuran.⁹³ Unfortunately the CHB of tetrahydrofurans mimics the selectivity from a similar hydroboration of the 2,3 dihydrofurans.⁹⁴ Shown in Scheme 28, this selectivity means that there is limited use of those methods for generating the desired product. The use of CHB on a furan or benzofuran results in borylation at the 2-position. Upon hydrogenation this results in complementary selectivity to that of hydroboration of sp^3 CHB.

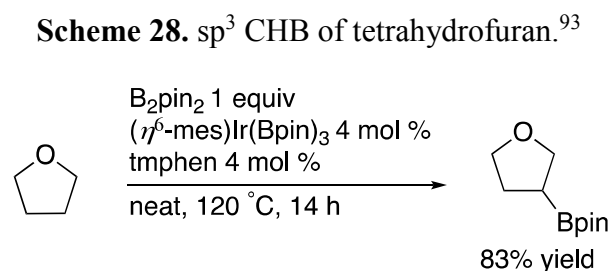
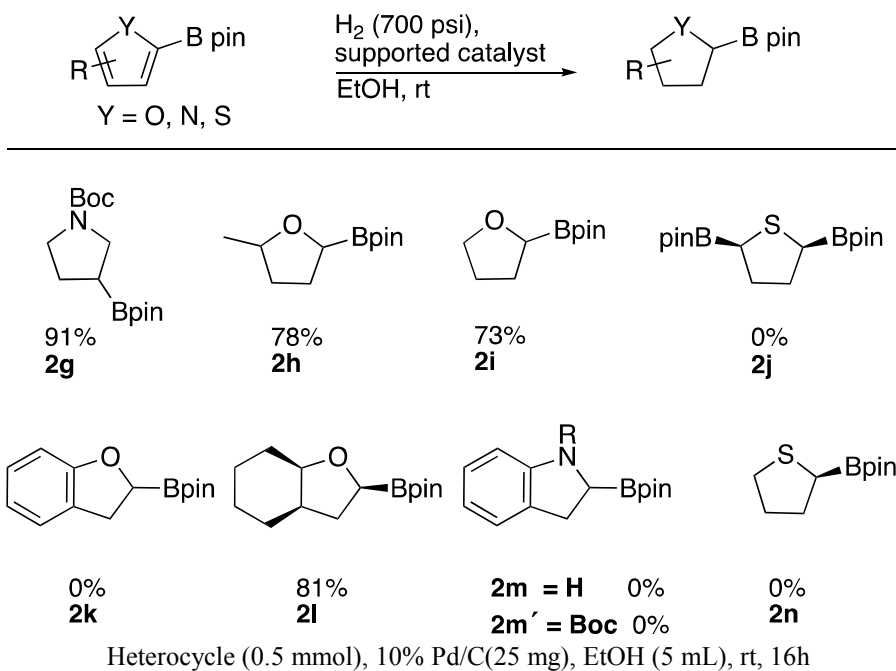


Table 6. Heterogeneous Hydrogenation of 5-membered Heterocycles

Unfortunately, but not unexpectedly, thiophene was unable to be hydrogenated. Both sulfur containing compounds **2j** and **2n** were unable to be formed through hydrogenation. This is not unexpected as the hydrogenation of thiophenes have been a challenge in the literature and thiophene is known to be a poison to catalysts. This is also the case with unsubstituted indoles and pyrroles. Addition of acid to the hydrogenation of borylated pyrroles resulted in polymerization and deborylation of the pyrrole. The 2-position of N-Boc-pyrrole had previously been borylated via lithiation/borylation and hydrogenated to yield the borylated N-Boc-pyrrolidine but using CHB of N-Boc-pyrrole the 3-boryl pyrrolidine was able to be generated. An interesting study was **2m** and **2m'** as the borylation at the 2 position on indole resulted in the reaction failing to generate the saturated cyclic product either protected by a Boc group or without protection. With **2m'** addition of acid resulted in deborylation either prior to or concurrently with hydrogenation. This was slightly surprising. Addition of acid to the reaction mixture

resulted in deborylation. The MIDA boronate of N-methylindole failed to hydrogenate likely due to insolubility in compatible solvents.

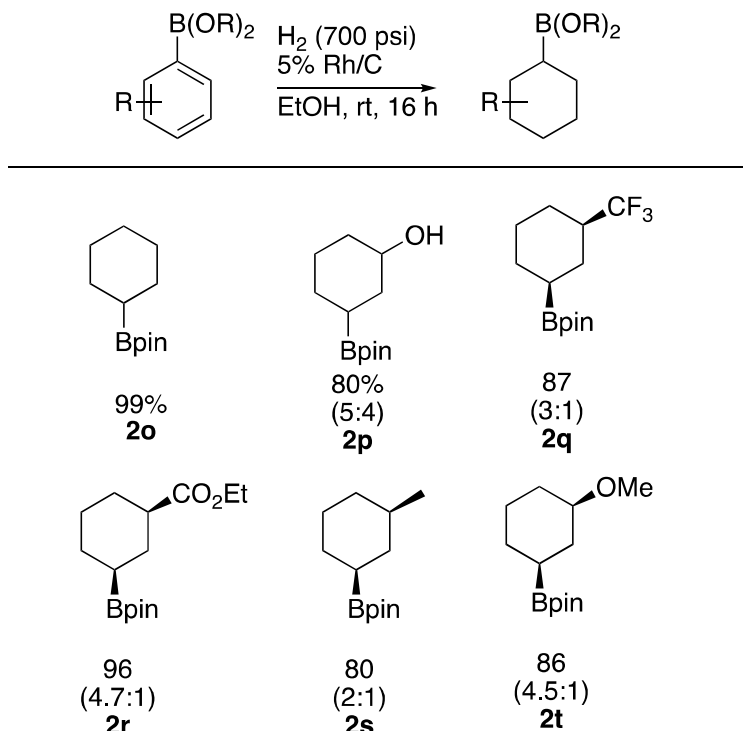
2-Bpin-benzofuran also failed to generate **2k** when palladium on carbon was used for hydrogenation. The use of rhodium on carbon resulted the complete reduction of the compound to generate the 2-borylated octahydrobenzofuran. This was noted by stopping the hydrogenation early and seeing that no build up of 2,3-dihydro-2-Bpin-benzofuran was observed. Without any build up of the 2,3 dihydrobenzofuran this likely means that when rhodium on carbon is used the hydrogenation of the arene occurs first, followed by the hydrogenation of the furan. The hydrogenation of 6 benzene rings are slower than that of heterocycles even when in a fuse system. The hydrogenation of the 5 membered ring were occurring first there would be a build up of that 2,3 dihydrobenzofurn. As there is not, the hydrogenation therefore likely begins with the hydrogenation of the benzene ring.

2.7 Hydrogenation of Borylated Arenes

Using rhodium on carbon the hydrogenation of borylated arenes was demonstrated. The result was generation of borylated cyclohexanes. Unlike the heteroarenes, the arenes resulted in a mixture of cis and trans products. Functional groups such as methoxide, esters or alcohols survived hydrogenation. The diastereoselectivity was determined by 1D-NOE experiments. A positive NOE was seen between the proton on the geminal position on the substituent and that of the geminal position to the boron. This indicated a cis relationship between all of the major isomers. More electron rich substituents such as esters and methoxides that could have interactions with the rhodium

surface resulted in greater selectivity for the cis isomer. The results for the hydrogenations of borylated arenes are summarized in Table 7.

Table 7. Hydrogenation of borylated arenes^{a,b}



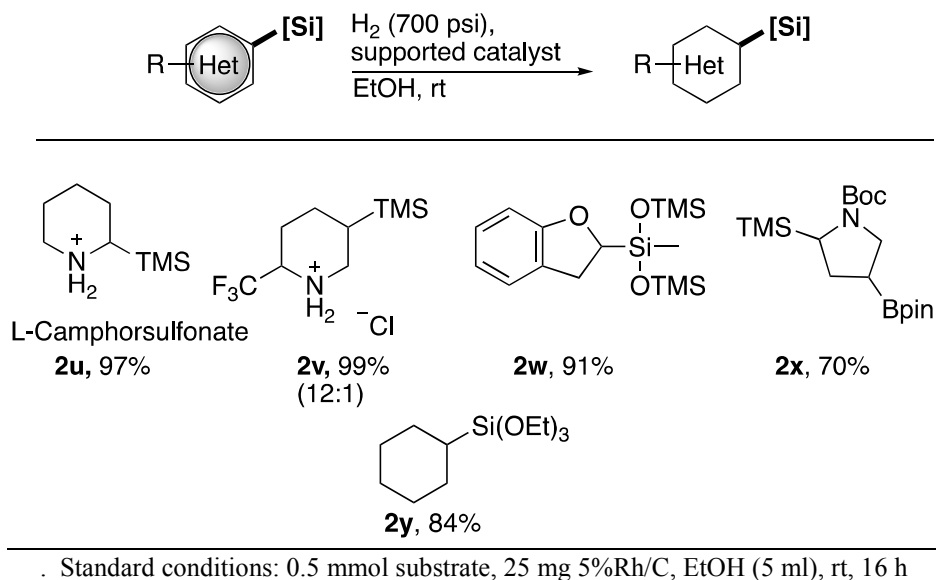
a) Relative stereochemistry shown. b) Substrate (0.5 mmol), 5% Rh/C (25 mg), H₂ (700 psi), EtOH (5 ml), rt, 16 h

2.8 Silylated heterocycles

Similar to borylated compounds, carbon-silicon bonds are very versatile in their synthetic transformations. Going a step beyond boron, they are more often used in materials chemistry as silicone polymers show incredible thermal and chemical resistance. This variety in uses makes the research into development of new organosilicon compounds important. It was found that using the same methods of silylation via lithiation or C-H silylation followed by hydrogenation new compounds containing carbon-silicon bonds could be generated. Similar to organoboron compounds, hydrogenation of silylated compound were previously restricted to that of olefins and

arenes. Hydrogenation of a silylated heteroarene had not been accomplished. Applying the methodology developed in reduction of the organoboron compounds, the reduction of organosilicon heterocycles was achieved.

Table 8. Hydrogenation of silylated heterocycles



The hydrogenation of **2u** resulted in seeing double the normal number of carbons. At first this was thought to be because of de-silylation, however upon looking at the proton NMR the silane peak was split into 2 different silicone resonances. This leads to the conclusion that the diastereomeric peaks are visible.

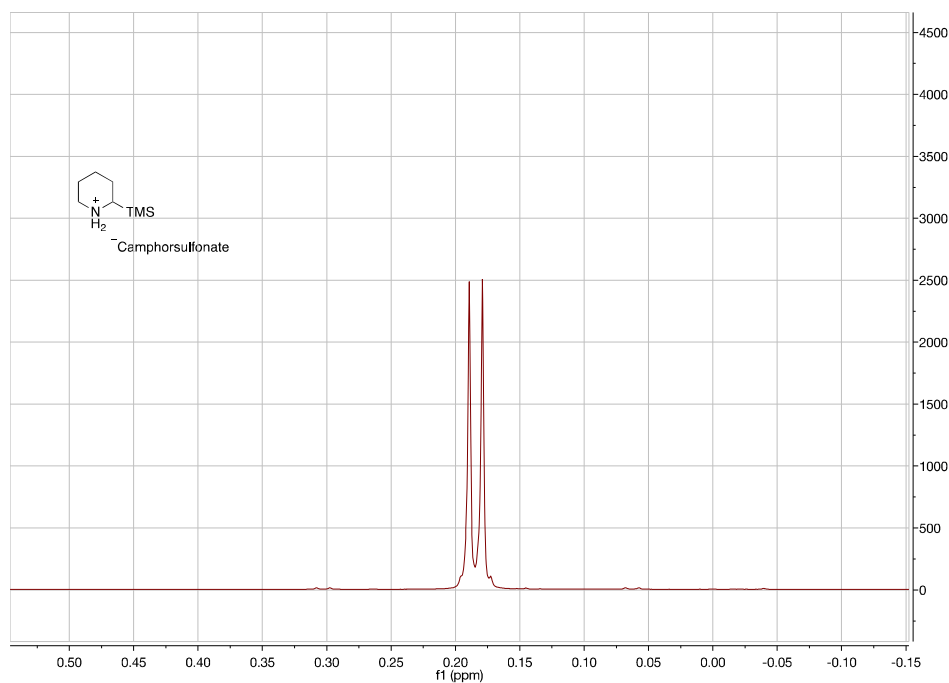


Figure 14. ^1H NMR signal from the TMS group on **2u**

The hydrogenation of **2v** resulted in a 12:1 selectivity between *cis* and *trans*. This was the only heteroaromatic that showed mixtures of relative stereochemistry. The spectrum of **2v** also showed the differences by NMR of the axial and equatorial positions of the substituents. The size of a TMS group and that of a CF_3 group were found to be similar. As such there is little difference in energy between which substituent is in the axial position and which substituent is in the equatorial position. Compound **2w** illustrates that when a borylated compound failed to hydrogenate the possibility exists for complex synthesis using a silyl group instead. While compound **2k** was unable to be synthesized by hydrogenation and only the fully hydrogenated compound could be seen the reduction of the 2,3 bond was possible when silylated. The reaction was clean and the reduction of the 2,3 bond to generate **2w** was performed by palladium on carbon to prevent reduction of the benzene ring.

Compound **2x** shows the possibility for divergent synthesis. Generating a compound with cis-relative stereochemistry that could be used for multiple functionalizations using orthogonal chemistry. One handle being the boronic ester and the other being the silane multiple variations can be synthesized using a scaffold containing these two substituents.

While silylated arenes had been hydrogenated before, the hydrogenation of a trialkoxysilylarene or heteroarene had not been demonstrated. By hydrogenating the triethoxyphenylsilane in ethanol formation of silicone polymers, based on ^{29}Si -NMR, were made. However, when the solvent was switched to hexane only one product was formed by silicon NMR carbon and proton NMR is also consistent with the previously reported synthesis of **2y** via hydrosilylation. The importance that the formation of **2y** shows is that the process of hydrogenation over rhodium on carbon can generate the siloxy-cyclohexane compound. This could then be used in more advanced materials synthesis.

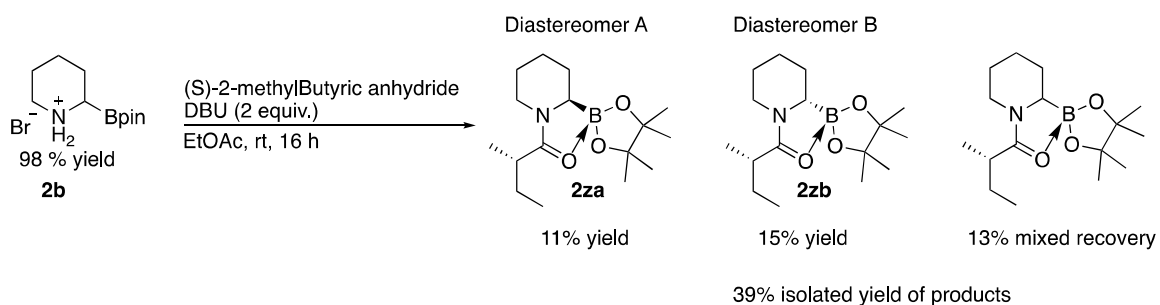
2.9 Chiral Resolution of a reduced borylated piperidine

The resolution of a saturated borylated compound was performed as a way to illustrate how this work could be used to generate enantiopure compounds. There were several failed attempts at the isolation of an enantioenriched compound by crystallization of chiral salts. It was found that the use of chiral carboxylic acids such as tartaric acid were not able to result in a chiral resolution. The attempts then moved on to the use of menthyl chloroformate. However, the products were unable to be separated by column

chromatography. The other issue with the menthol carbamate that was formed was that it was hard to visualize by GCMS.

From there, the attempts turned to the use of (S)-2-methylbutyric anhydride to form a chiral amide. These products could be separated via column chromatography and different peaks with the appropriate mass were observed by GCMS. As shown in Scheme 29, 2-borylated piperidine could be separated into its enantiomeric components using this route. The crystal structure of isomer A was found to be the (S,R) isomer shown in Figure 15.

Scheme 29. Chiral resolution of **2b** through chiral amide formation



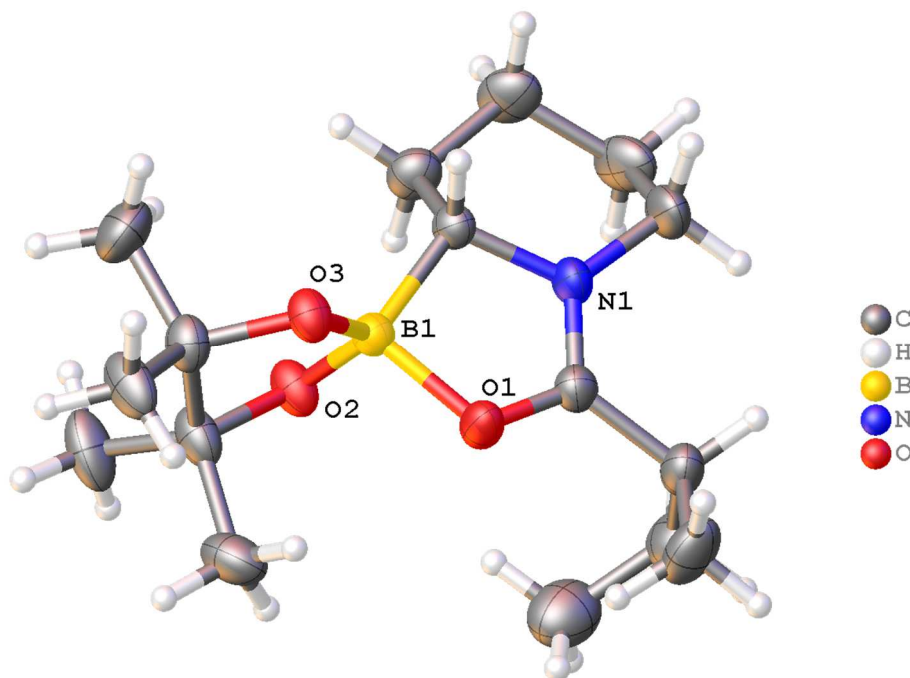


Figure 15. Crystal Structure of Compound **2za**

2.10 Hydrogenation Conclusion

A two-step process for synthesis of saturated cyclic borylated and silylated compounds was developed. The use of rhodium on carbon limits the amount of deborylation that occurs during the hydrogenation process. Utilizing chiral amide formation, chiral resolution of the saturate cyclic organoboron piperidine was shown to be a viable route to enantiopure organoboron compounds. Further research into the use of asymmetric hydrogenation catalysts for asymmetric reduction of heteroaromatic organoboron compounds is necessary to continue to develop important chiral intermediates for synthesis.

Chapter 3. Pyridine Ligands for ortho-Directed C-H Borylation

3.1 Chelate Directed ortho C-H Borylation

One of the most well studied methods of directed C-H borylation is the chelate directed borylation using directed metalation group (DMG) such as ketones, esters, amides, carbonates, carbamates, imines, pyridyl...etc. The chelate direction method utilizes a generated open coordination site on the active catalyst to coordinate a Lewis base to the metal center. The proximity and ring size of the transition state favors the C-H activation occurring at the ortho position relative to the directing group from the substrate. Dissociation of the borylated product turns over the catalyst

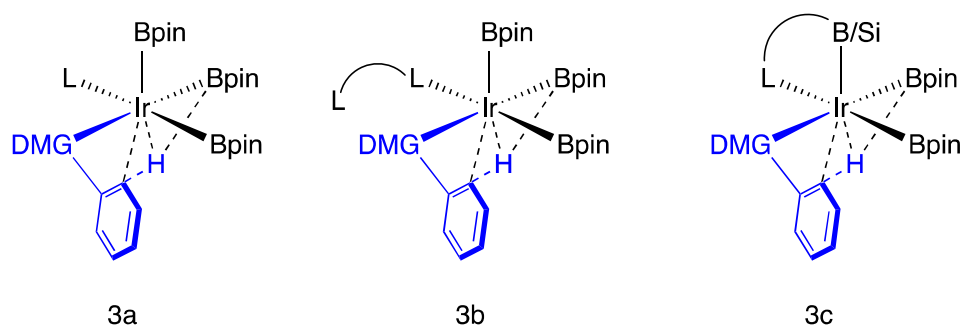


Figure 16. C-H Activation in Chelate Directed ortho-Borylation

There are three general methods for generating an open coordination site on Ir(III) complexes for chelate-directed CHB. First, by the use of a monodentate ligand with only one coordinated ligand on each metal center when the catalyst is active **3a**.⁹⁵⁻⁹⁷ Second is through the use of a hemi-labile bidentate ligand where one of the binding sites of a ligand will oscillate on and off to allow for the substrate chelation and CHB **3b**.^{98,99} The third method is through the use of an L type and X type bidentate ligand **3c**.^{100,101} All of these methods result in a 14/16-electron iridium (III/V) catalytic cycle (Figure 17). This is

different than the iridium (III/V) 16/18 electron cycle when using L,L-type bidentate ligands which tend to favor steric based selectivity.^{102,103} When isolated from excess ligands the spatially open iridium (III) 14/16 electron catalytic system has been found to be incredibly active.^{95,104–107}

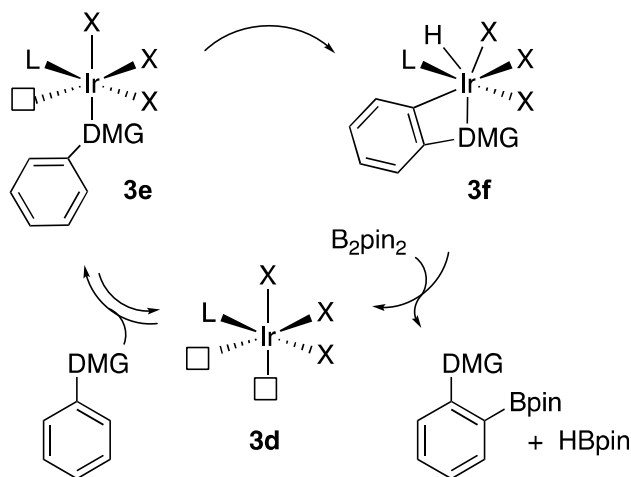


Figure 17. General catalytic cycle for chelate directed ortho-borylation

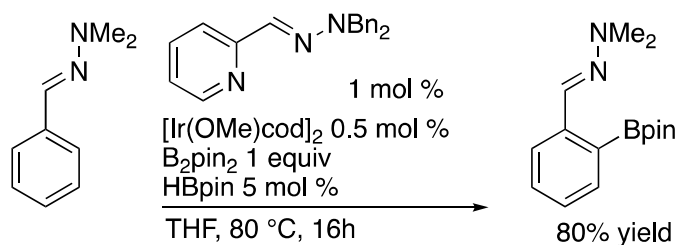
The active catalyst for ortho borylation contains 3 x-type ligands that have been reported as either boryl or silyl groups. With one L-type ligand in on the catalyst when the reaction begins this generates the 14 electron 4-coordinate iridium (III) shown as **3d**. The catalyst coordinates a substrate through a DMG to generate **3e**. Oxidative addition of the C-H bond generates complex **3f**, which is a heptacoordinate iridium (V) complex. Reductive elimination of the catalyst followed by oxidative addition of B_2pin_2 and reductive elimination of HBpin regenerates **3d**.

3.2 Hemi-Labile Ligand Systems

Lassaletta and co-workers generated a method of chelate directed borylation using a pyridyl-imine bidentate catalyst system that is proposed to dissociate the imine arm of

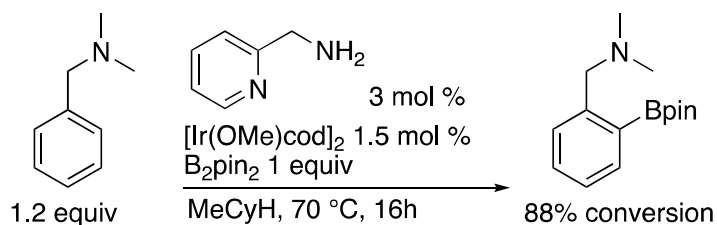
the catalyst before borylation.⁹⁸ This was used to preform the CHB using pyridyl, quinolyl, and imine directing groups. Ortho-borylation is achieved in high yields at 80 °C in a 1:1 ratio of boron source to substrate. Lassaletta further developed this catalyst system to include the borylation of hydrazones that could be generated from various aryl aldehydes.¹⁰⁸ Lassaletta demonstrated how a ligand system could be used to help stabilize the catalyst in a resting state and yet still allow it to provide the ortho selectivity desired.

Scheme 30. Lassaletta Hemi-Labile ortho-Directed Borylation.⁹⁸



Clark and co-workers used pyridin-2-ylmethanamine as a ligand to ortho-borylate benzylic amines (Scheme 31).¹⁰⁹ Clark further explored this work by investigating the bite angle of the amine-pyridine combination. What they found was that the smaller bite angle of a 2-aminopyridine was a better catalyst for ortho-borylation of benzylic amines.¹¹⁰ They further expanded this work to include ortho-borylation of benzylic phosphines with using the benzylphosphines as their own ligand.¹¹¹

Scheme 31. Picolyamine for ortho-Directed CHB of Benzylamines and Benzylphosphines.¹⁰⁹



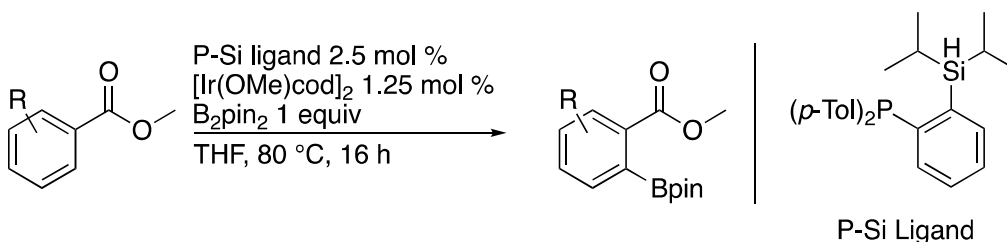
All of these catalysts systems had the drawback of requiring substrates with strong donors as the directing group. This is because the substrate needs to out compete the pendent side of the ligand for coordination to the catalyst. Without a strong donor it is much more likely that the reactant dissociates from the catalyst before the borylation at the ortho position can occur. This would likely lead to a loss of selectivity for weaker donating directing groups such as ketones, esters or amides. This is also likely why there has yet to be a publication using these ligands for the ortho borylation of one of these substrates.

More recently, Chattopadhyay and co-worker used 8-aminoquinoline for borylation ortho to pre-generated imines.¹¹² They directly compared their ligand to Lassaletta and co-worker's ligand to show that while the Lassaletta ligand generated good selectivity, 8-aminoquinoline used as a ligand generated a more active catalyst. Chattopadhyay borylated the ortho position on imines generated in-situ from aldehydes and isolated the aldehydes upon working up the reaction. The amines used for in-situ generation of imines were methyl, isopropyl and *tert*-butyl. Interestingly, only the *tert*-butyl group resulted in ortho borylation in significant quantities in comparison to the other sites. Chattopadhyay argued that this is because the excess bulk was needed to generate an open coordination site.

3.3 L-X type Ligand Systems for Chelate Directed ortho-Borylation

Smith, Maleczka and co-workers developed a system for ortho-borylation¹¹³ that took advantage of a use of the necessity for iridium to be iridium (III) as the resting state of the catalyst. They used an L-X type bidentate ligand such that one phosphine and one silyl group were attached to the catalyst center. The use of an X-type ligand resulted in only two boryl ligands being on the iridium center as well as the one X-type ligand resulting in a 14-electron iridium (III) tetra coordinate complex with two open coordination sites. This catalyst design was inspired by Hartwig and coworkers use of silane-directed ortho borylation,¹¹⁴ but by including the silane on the ligand the selectivity became catalyst controlled and not substrate controlled. This P-Si ligand was used for ortho-borylation using directing groups of esters, amides, methoxides, carbamates and pyridines. By changing from a phosphine-silane to a quinoline-silane ligand the reactivity for ortho-borylation was significantly increased.

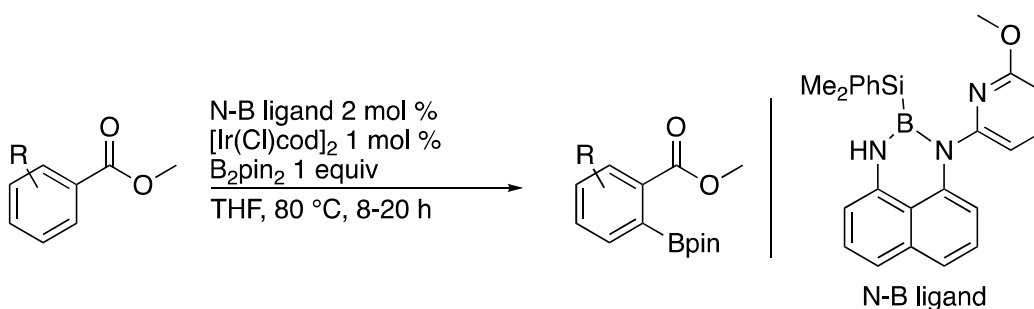
Scheme 32. ortho-Borylation of Aryl-DMG Using Phosphine-Silane Based Ligands.¹¹³



In an effort to improve upon this type of L-X type bidentate system, Yu and co-workers exchanged the silyl group for a boryl group.¹¹⁵ The reasoning behind this exchange was that a boryl group could be more electron donating than a silyl group on a

metal. Thus if an N,B-bidentate ligand could be used, they envisioned a catalyst that would be more reactive than the quinoline-silyl ligand used by Smith, Maleczka and co-workers. They synthesized a ligand dimer that contained a boron-boron bond that would be broken apart upon oxidative addition to the metal. However Yu and co-workers found that this resulted in a catalyst system that contained two N,B bidentate ligands on it. This resulted in a system that generated steric-influenced borylation.¹¹⁵

Scheme 33. ortho-Borylation of Aryl-DMG Using Nitrogen-Boron Based Ligands.¹⁰¹



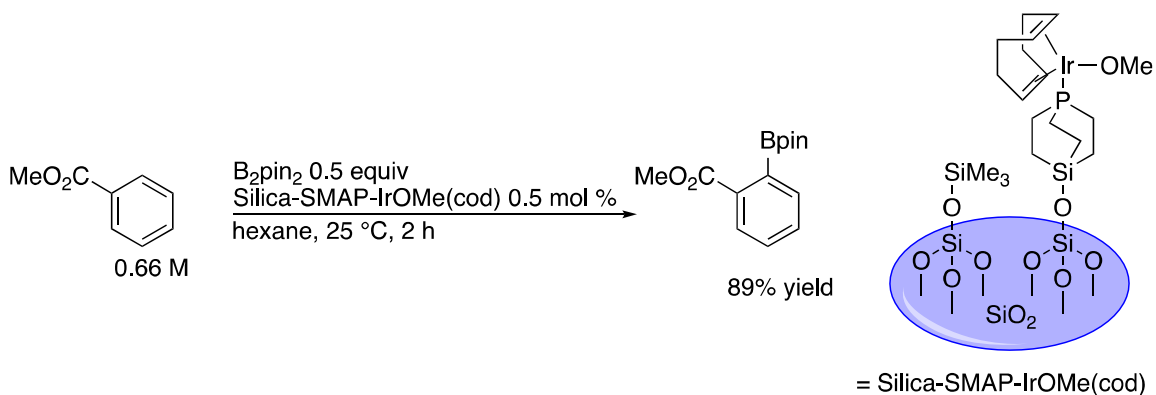
In an attempt to generate a catalyst system with only one bidentate ligand on it Yu and co-workers synthesized a ligand that contained a boron-silyl bond (Scheme 33).¹⁰¹ Using this ligand resulted in a catalyst that performed ortho-borylation of esters, ketones, carbamates, amines, imines, and pyridyl groups. However, this catalyst did not operate under conditions that were an improvement from Maleczka, Smith, and co-workers. There were a few potential reasons for the lowered reactivity of the catalyst used by Yu and co-workers. The first possibility was that the silyl group was still bound to the metal resulting in a less electron rich catalyst that slowed the reaction. The second reason is that the bite angle of the ligand is more acute than that of the quinoline silyl ligand generated. This could result in less orbital overlap and less electron donation to the

metal. The last possibility is that the general premise that any boryl ligand will be a better donor than any silyl ligand is inherently false. A real possibility exists that the diazaboryl ligands are worse donors than that of the dioxaboryl ligands. However, that would run counter to previous calculations on boryl donor strength by Marder and co-workers.¹¹⁶ However, the computation energy levels calculated by Marder are not all that different from each other and Yu's ligand is very different than that of the ligands computed. As such there could still be a question to which ligand is more donating.

3.4 Monodentate Ligand Systems

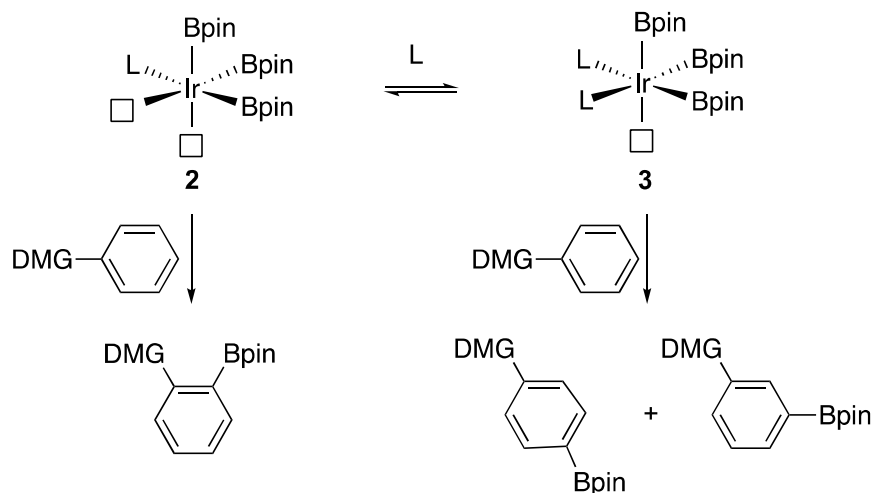
Discussion to this point has focused on bidentate ligands for ortho-directed borylation. However, 14-electron iridium (III) catalysts that contain two open coordination sites could be generated with monodentate ligands. There are two general methods for generating these types of catalysts. The first method is through isolating a metal center on a solid support.^{95,104-107} The second is through use of stoichiometric, steric or electronic factors that result in coordination of only one ligand per metal center.^{96,97}

Scheme 34. Supported Phosphine Catalysts for ortho CHB



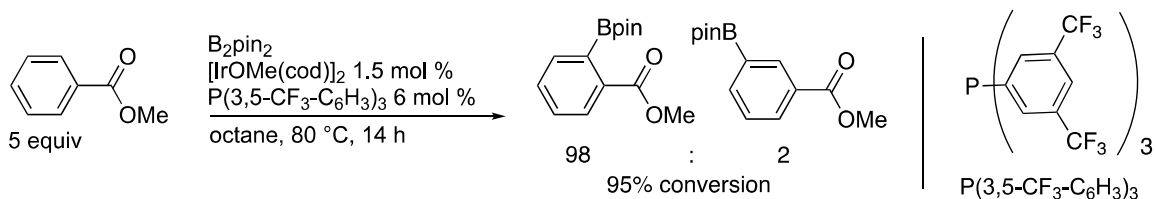
Sawamura and co-workers first used a caged monodentate phosphine ligand bound to silica (Silica-SMAP) to isolate the iridium catalyst sites on one phosphine ligand.⁹⁵ The surface of the silica was passivated with trimethylsilyl groups to prevent the surface hydroxyl groups from interfering in the catalysis. The resulting catalyst system was incredibly active, functioning well at low temperatures and low catalyst loading. Silica-SMAP has been used for the ortho borylation of phenol derivatives,¹⁰⁴ sp³ centers using rhodium¹⁰⁵ as well as esters,¹⁶ amides,⁹⁵ and even produced ortho-borylation of aryl chlorides.⁹⁵ These CHB's were at room temperature or slightly above. The isolated catalyst resulted in a very controlled reaction environment. The caged nature of the phosphine resulted in minimal steric bulk around the catalyst that results in a highly active catalyst. The problem with silica-SMAP is that the ligand is very challenging to synthesize.

Scheme 35. Homogeneous ortho CHB with Excess Ligand



Shortly after silica-SMAP was reported a new method for ortho-directed CHB was developed by Ishiyama, Miyaura and co-workers. They took advantage of the inability of electron poor ligands to stay bound to a catalyst. They generated an open coordination site using large electron poor monophosphines⁹⁶ and triphenylarsine.⁹⁷ Shown in Scheme 35, the electron-poor and sterically bulky nature of these systems lends itself to generate equilibrium between proposed intermediates **2** and **3**. Intermediate **2** is a 14-electron complex with two open coordination sites due to the loss of a ligand that allows for ortho CHB. Intermediate **3** contains two monodentate ligands and is a 16-electron Iridium (III) complex that results in sterically driven borylation.

Scheme 36. Homogeneous electron poor monodentate phosphine ligand for ortho CHB



This was the first method to generate ortho borylated aryl esters² and ketones³ using easily purchasable ligands. However, this ligand required higher reaction temperatures, 80-120 °C, and had greater limitations in substrate scope than silica-SMAP. Another issue with this system developed was the need for excess substrate in an order of 5:1 to boron source in order to prevent diborylation. However, these were the first homogeneous ligand system for ortho-CHB of esters and ketones.

3.5 Further Challenges in Chelate Directed ortho-Borylation

Overall, these methods for directed ortho CHB generated desired product; however, there were issues of selectivity, availability or reactivity depending on the catalyst. After observing how bipyridine systems worked better for steric directed CHB compared to bis-phosphine systems Dmitry Shabahov set out to determine if monodentate pyridine systems could work better than the corresponding phosphine system reported by Ishyama, Miyuara and co-workers. From his preliminary results it was apparent that by changing the sterics or electronics of the pyridine ligands, ortho-borylation could be accomplished.

The benefit of using pyridines as ligands for ortho-borylation was the vast number of different commercially available pyridines. This allowed for the fine-tuning of the catalyst system to control the equilibrium between **2** and **3** from Scheme 35. The use of a sterically encumbered pyridine should generate a weaker bond to the metal and shift the equilibrium towards **2**. However, using a pyridine with too much bulk around the nitrogen could result in a slower catalyst by either steric hinderance of substraight-catalyst inerctions or inhibition of ligation.

The other route to take is the use of electronic poor pyridines. This is similar to the use of triphenylarsine. It results in a lower ability for the ligands to have multiple monodentate ligands on a single metal center due to the lower bond strength to the metal center. This would also result an electronically poor catalyst.

The last controllable variable was the amount of ligand added. By using just one equivalent of pyridine per iridium, a greater amount of complex **2** could be formed. This was supported from literature when Ishiyama, Miyuara and co-workers.⁹⁶ They used a 2:1 ratio of pyridine to iridium metal. This combination favored formation of complex **3**. The result was borylation of methyl benzoate in 7% yield at 80 °C over 16 hours. The selectivity was poor, 1:4:2 ortho:meta:para. This result, rather than discouraging, caused us to think carefully about using more electronically poor and sterically encumbered ligands.

3.6 Pyridine Ligand Screens for ortho Selectivity

A ligand screen was performed to test a variety of monodentate pyridine ligands against ortho-borylation of esters. GC/FID was used to determine the ratios between ortho CHB to meta+para CHB. The results of this screen are illustrated in Table 9. The initial ligand screen was performed under catalytically relevant conditions. It was found with a 1:1 ratio of B₂pin₂ to methyl benzoate that a combination of a 2-methoxypyridine worked quite well as a ligand for ortho-borylation. One challenge that was shown was that use of **3g** resulted in 20% diborylation based on methyl benzoate. Other ligands that worked well were electron-poor pyridines such as **3o** and **3s**. However, these

trifluoromethylated compounds were more expensive and more challenging to modify than a 2-methoxypyridine.

While it was apparent that the electronics play a large role as shown by the trifluoromethyl pyridines **3j**, **3o**, and **3s** if the steric bulk near the nitrogen of the pyridine is too great (**3j**) then the borylation significantly slowed.

One concern about the use of 2-methoxypyridine as a ligand was that it could be borylated during the CHB reaction. To this end, other substitutions were added to the 2-methoxypyridine scaffold. A trifluoromethyl group in the 5-position (**3t**) resulted in high conversions, a reduction in the amount of diborylation, and improved selectivity. However, the overall yield was not as high as **3g** and **3t** is much more expensive than **3g**.

Table 9. Screen of pyridine ligands for ortho borylation of methyl benzoate with one equivalent of diboron

		yield(di) (o:[m+p]) ^{a,b,c}	
 3g 74.2 (20.3) (11.8:1)	 3h 5.8 (10:1)	 3i 20.6 (0.75:1)	 3j 7.9 (1.6:1)
 3k 13.3 (0.5:1)	 3l 33.5 (3.3:1)	 3m 13.8 (1.0:1)	 3n 46.6 (0.5:1)
 3o 43.8 (4) (3.0:1)	 3p 13.9 (2.7:1)	 3q 12.7 (4.7:1)	 3r 17.8 (7.2:1)
	 3s 41.4 (6.1) (52.6:1)	 3t 59.4 (12.3) (30.4:1)	 3u 71.7 (22.3) (14.3:1)

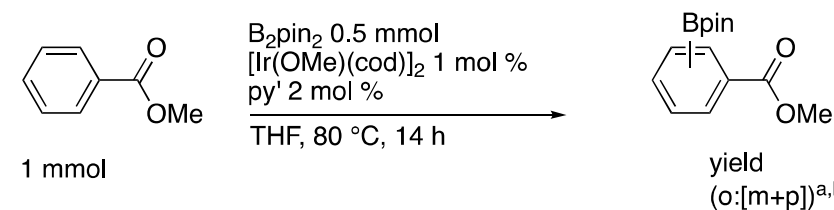
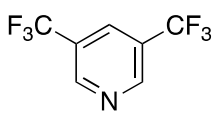
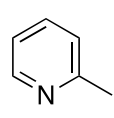
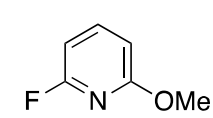
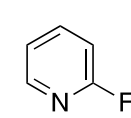
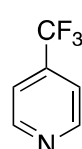
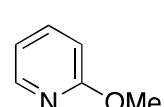
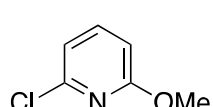
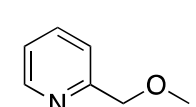
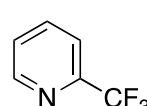
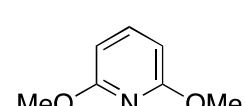
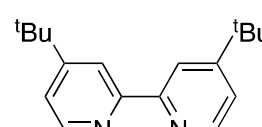
a) All numbers are GC/FID conversions compared to a naphthalene internal standard b) Reaction conditions: methyl benzoate (136 mg, 1 mmol), [Ir(OMe)cod]₂ (6.6 mg, 0.01 mmol), py' (0.02 mmol), B₂pin₂ (254 mg, 1 mmol), THF (2 mL) 80 °C 14 h. c) diborylation reported as combined diborylated isomers.

From this initial ligand screen a major concern that arose was the significant amount of diborylation. This was shown to be an issue with nearly every ligand that resulted in high conversions and reported in Table 9 as the combined diborylated isomers. When diborylation, that was not di-ortho, it is impossible to know which CHB location was first. To determine how the selectivity was impacted with no diborylation, a second

ligand screen was performed with a 0.5:1 B₂pin₂ to substrate ratio. This resulted in less boron for the use in diborylation of the substrate.

With the lower amount of boron in solution, the yields and selectivities were all reduced. Some of the ligands selectivities changed more significantly than others. The trifluoromethylated pyridines, which had great ortho selectivity at a 1:1 ratio of B₂pin₂ to substrate, performed worse when there was less B₂pin₂ present. This gave a stronger argument for the use of 2-methoxypyridine as the backbone of further optimization. The other important finding of the ligand screen in Table 10 was the complete lack of any substrate to exceed 50% yield. This caused us to believe that the catalyst system was incapable of using pinacolborane as the boron source. Follow-up studies attempting borylation with only pinacolborane confirmed that pinacolborane was not a viable boron source for use in this catalyst system.

Table 10. Screen of pyridine ligands for ortho-borylation of methyl benzoate with half an equivalent of diboron

		yield (o:[m+p]) ^{a,b}	
 3s 28.1 (7.5:1)	 3i 5.2 (0.5:1)	 3r 10 (4.8:1)	 3h 7 (3.1:1)
 3o 19.7 (2.4:1)	 3g 24.8 (6.5:1)	 3p 4.8 (2.74:1)	 3v 3.7 (0.33:1)
 3j 3.2 (1.2:1)	No Ligand 2.7 (0.82:1)	 3q 10.2 (4.7:1)	 3w 70 (<1:99)

a) All numbers are GC/FID conversions compared to a naphthalene internal standard . b) Reaction conditions: methyl benzoate (136 mg, 1 mmol), [Ir(OMe)cod]₂ (6.6 mg, 0.01 mmol), py' (0.02 mmol), B₂pin₂ (127 mg, 0.5 mmol), THF (1.5 mL) 80 °C 14 h

3v was significant in that moving the methoxy group further from the pyridine resulted in a complete loss of reactivity and a change in selectivity. This indicated that the methoxy group from **3g** is either hemilabile or not binding to the iridium center during the reaction. When **3v** is used the methoxy group has a greater chance of binding to the iridium center due to the larger bite angle of the pendant ligand. This appears to shut the reaction down and adds evidence that the active catalyst contains only one L-type ligand

bound to the metal. A control experiment was tested without a ligand and resulted in very little CHB.

To see if the same selectivity holds up with a different substrate Dmitry Shababshov ran the same ligands used in Table 10 against cyclopropyl phenyl ketone as a substrate. The results from this screen followed a lot of the same trends as seen in the ligand screen of the esters. From this screen there are two significant results worth mentioning that were different. First, the result of using no ligand had 22% conversion and nearly perfect selectivity for the ortho borylated product. The second was that across the whole ligand subset the conversions were higher against the ketone substrate than the ester substrate. The only ligand that faired worse than not using a ligand was **3v** that showed catalyst inhibition.

Table 11. Ligand Screen for ortho-Borylation of Cyclopropyl Phenylketone

 3s 36 (63:1)	 3i 28 (8:1)	 3j 22 (13:1)	 3v 12 (3:1)	
No Ligand 22 (>99:1)	 3o 28 (7:1)	 3g 48 (27:1)	 3h 24 (11:1)	 3w 96 (<1:99)

a) All reactions performed by Dmitry Shabashov b) All numbers are GC/FID conversions. c) Reaction conditions: cyclopropyl phenylketone (1 mmol), [Ir(OMe)cod]₂ (6.6 mg, 0.01 mmol), py' (0.02 mmol), B₂pin₂ (127 mg, 0.5 mmol), THF (1.5 mL) 80°C 14 h

From the result of these ligand screens Dmitry Shabashov tested two different electronic variations of 2-methoxypyridine as the ligand. The first was 2-methoxy-4-cyanopyridine (**3y**) and the second was 2-methoxy-4-(dimethylamino)pyridine (**3x**). Compound **3y** was found to have much higher selectivity as well as a greater yield than that of **3x**. This result was counter to conventional thought on CHB's because **3y** is more electron poor than **3x**.

Table 12. Electronic effects of 4-substituted-2-methoxypyridines for ortho-borylation of cyclopropyl phenylketone

entry	ligand	time	ortho:(meta+para)	% yield ^{a,b}
1	 3x	17 h	29:1	45
2	 3y	11 h	>99:1	87

- a) Reactions performed by Dmitry Shabashov. b) Isolated yields relative to B₂pin₂
 c) B₂pin₂ (508 mg, 2 mmol), cyclopropyl phenylketone (380 mg, 2.6 mmol), THF(3 mL), [Ir(OMe)cod]₂ (13.2 mg, 0.02 mmol)

3.7 Investigation into Substrate Scope

After it was found that the **3x** worked best as a ligand for ortho-borylation of cyclopropyl phenylketone, a variety of other substrates were tested to determine the functional tolerance and the selectivity for the catalyst system. It was found to have a fairly wide functional group tolerance as shown in Tables 13 and Table 14. Table 13 illustrate that this system was selective for esters, amides, and ketones. Benzamide, not shown, was not viable for CHB under this catalyst-ligand system. Halogen tolerance was demonstrated for fluorides, chlorides, and bromides.

Under the conditions used for CHB in Tables 13 and 14 it was found that the diborylation of the substrate was observed when methyl esters were used, entries 1 and 5, as shown in in Table 13. Diborylation could be mitigated by changing the methyl ester to a *tert*-butyl ester as shown in entries 1 vs 4. After the initial borylation of the substrate an increased interaction from a *tert*-butyl ester and the pinacol group likely reduces the ability for the second ortho CHB. When the ester substrates contain a substitution at the ortho position such as entries 8 and 9 in Table 13 the borylation is still viable at the 6-position on the substrate.

Table 13. ortho C-H borylation of aryl esters and amides using a monodentate pyridine ligand

R = OMe, O-t-Bu, NMe₂ Y = CF₃, F, Me, Br, NMe₂
E = CH, N

entry	substrate	product	yield (%) ^a	entry	substrate	product	yield (%)
1			55 ^{b,c}	8			46 ^{b,g}
2			77	9			71
3			72 ^d	10 ^h			65
4			83	11 ^h			73
5			65 ^{b,c}	12 ^h			
6			21 ^e				61 13:13m = 1.9:1
			37 ^e				15
7			51 ^f	13			84

a) Arene (1 mmol), B₂pin₂ (1.2 mmol), [Ir(OMe)(cod)]₂ (0.01 mmol), py' (0.02 mmol), THF (2 mL) at 70 °C, for 16 h yields reported are isolated yields relative to arene b) B₂pin₂ (1.0 mmol) c) <5% of diborylated product observed by but not isolated. d) 19:1 ratio of 2 to 6 borylated isomers by ¹⁹F-NMR. e) Isolated yields from the same reaction. 29% starting material also recovered. f) Arene (1 mmol), B₂pin₂ (2.2 mmol), [Ir(Cl)(cod)]₂ (0.01 mmol), py' (0.02 mmol), THF (1.5 mL), 28 h g) other isomers were present in the crude reaction mixture in low quantities but only the major product was isolated. h) Performed by Dmitry Shabashov

Table 14. ortho C-H borylation of aryl ketones using a monodentate pyridine ligand

entry	substrate ^a	product	yield ^b (%), time	entry	substrate	product	yield ^{b,d} (%), time
1			87, 11 h	5 ^c			62, 8 h 13e:13f = 1.5:1
2			71, 14 h				
3			68, 5 h	6 ^c			61, 6 h 13g:13h = 1.9:1
4			45, 16 h	7			94, 16 h

a) The reactions were carried out using Arene (1.3 mmol), B₂pin₂ (1.0 mmol), [Ir(μ-Cl)(cod)]₂ (0.01 mmol), py^r (0.02 mmol), THF (1.5 mL) at 70 °C. b) Isolated yields shown are relative to B₂pin₂. c) B₂pin₂ (0.75 mmol) d) All reactions in Table 14 performed by Dmitry Shabashov

Ketone substrates shown in Table 14 showed some interesting selectivity. The CHB of substituted benzophenones occurred more often on the substituted phenyl group regardless of electronic influences of the substrate. Phthalimides and other constrained 5-membered rings with ketones such as fluoren-9-one were not viable for ortho CHB under these conditions (not shown). This is likely a geometric argument as the distance from the ketone lone pair electrons to the ortho C-H bond is different when it is tied back than when it is free.

More complex substrates were tested for ortho CHB that contained multiple potential sites for CHB (Table 15). In entry 1 there are multiple potential directing groups such as methoxides as well as cyclic ethers. However, the selectivity is perfect for the borylation ortho to the ketone. For entry 2 the borylation occurs selectively, however,

significant reduction of the ester was also observed during the reaction. The mechanism of the reduction is not known at this time, but potential formation of an N-B bond²² on the secondary nitrogen could provide a Lewis acid for coordination and a potential reduction pathway for the ester. Entry 3 shows the ortho-borylation on fenofibrate. The borylation is not completely selective and the product was isolated as a mixture of isomers in a 5:1 ratio. The assignments were accomplished through gHMBC and gCOSY NMR experiments. The assignment of **3ba** was based on a resonance between the ipso carbon on the chlorine to the singlet of the proton adjacent to the boron. The other isomer **3bb** was the minor isomer and contained a correlation between the ipso carbon of the ether and a smaller singlet in the aromatic range.

Table 15. ortho-Borylation on complex substrates

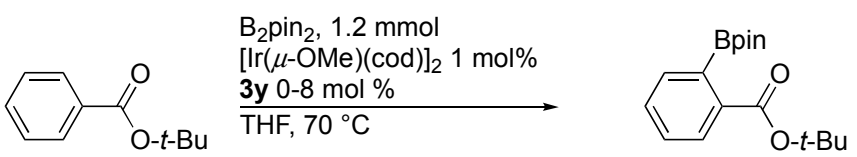
entry	Substrate	Product	Yield(%)
	<p>1.0-1.3 mmol Y = Cl, OR, NHR, alkyl</p>		
1 ^d	<p>1.3 mmol 3ay 105^a</p>		
2	<p>1.0 mmol 3az 38^b</p>		
3	<p>1.0 mmol</p> <p>3ba</p> <p>3bb</p> <p>15c+15d 55^c 15c:15d (5:1)</p>		

a) Arene (1.3 mmol), B₂pin₂ (1.0 mmol), [Ir(Cl)(cod)]₂ (0.01 mmol). **3y** (0.02 mmol), THF (1.5 mL) 70 °c, 11 h. b) Arene (1.0 mmol), B₂pin₂ (0.6 mmol), [Ir(OMe)(cod)]₂ (0.01 mmol). **3y** (0.02 mmol), THF (2.0 mL) 85 °c, 16 h c) Arene (1.0 mmol), B₂pin₂ (0.9 mmol), [Ir(OMe)(cod)]₂ (0.01 mmol). **3y** (0.02 mmol), THF(2.0 mL) 85 °c, 16 h d) performed by Dmitry Shabashov

3.8 Insights into mechanism of pyridine ligated iridium systems for ortho borylation

An investigation into the mechanism of the ortho borylation was performed. Initially an investigation into the ligand to metal ratio was performed using *tert*-butyl benzoate as a substrate. The results were summarized in Table 16. As Expected, the borylation failed to significantly proceed without a ligand; yielding only 7% conversion after 7h. Increasing the ligand to half an equivalent was found to accelerate ortho CHB. When the amount of ligand to iridium reached 1:1 the reaction was found to be nearly complete after 7 hours. Moving beyond 1:1 ligand:iridium resulted in a decrease in catalytic activity. When 4 equivalents of ligand were added, the result was a complete inhibition of the ortho-CHB of *tert*-butyl benzoate over a span of 4 hours. This suggests that an increase in the ligand concentration could result in multiple ligations of the catalyst and a species that could be completely inactive.

Table 16. Pyridine to iridium ratio impact on reactivity



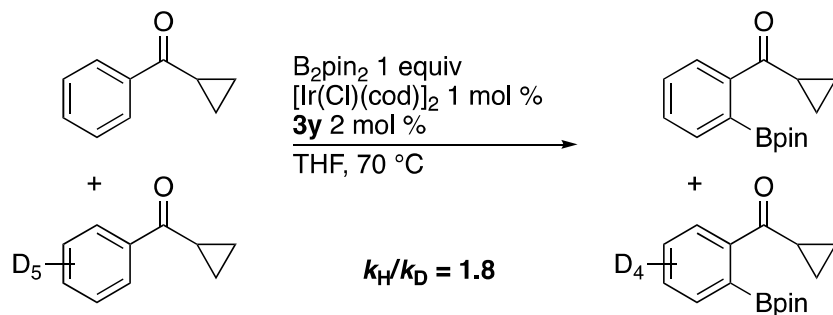
1.0 mmol

[3y]:[Ir]	% conversion ^a		
	3h	5h	7h
0:1	2	5	7
0.5:1	54	71	76
1:1	65	82	90
2:1	<1	5	47
4:1	<1	<1	<1

a) Conversions determined by GC/FID relative to the ester

To determine the rate-determining step, Dmitry Shabashov performed a kinetic isotope effect (KIE) study. He made the deuterated versions of cyclopropyl phenylketone for the study. He found that the intermolecular KIE was 1.8 (Scheme 37).

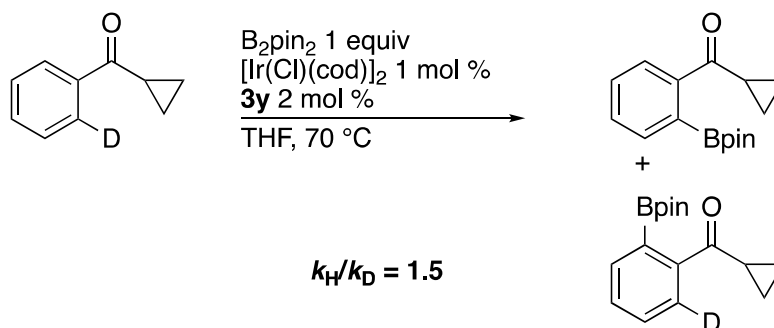
Scheme 37. Intermolecular Kinetic Isotope Effects of CHB on Cyclopropyl Phenylketone



Reaction performed by Dmitry Shabashov

The intramolecular KIE was found to be 1.5 (Scheme 38). These KIE values are inconsistent with C-H activation being the rate-determining step. Previously it has been shown that KIE values of 3.5 to 6.7 indicate C-H bond cleavage being the rate-determining step.¹¹⁸ As a result of this discrepancy, it is quite possible that this CHB system is the first CHB with a definitively different rate-determining step in its mechanism. While other C-H functionalization techniques such as C-H silylation or arylation have different catalyst systems in place that proceed through differing mechanisms this is less common in CHB.

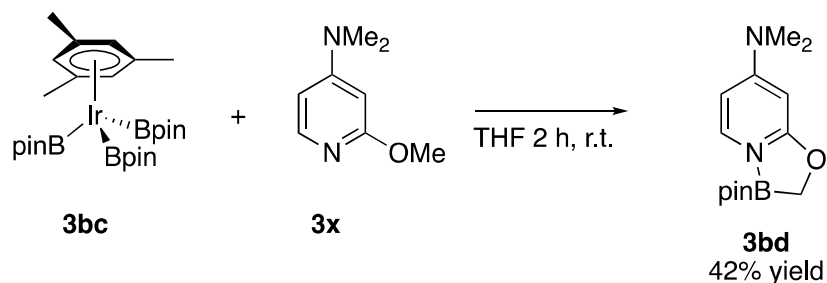
Scheme 38. Intramolecular kinetic isotope effects of CHB on cyclopropyl phenylketone



Reaction performed by Dmitry Shabashov

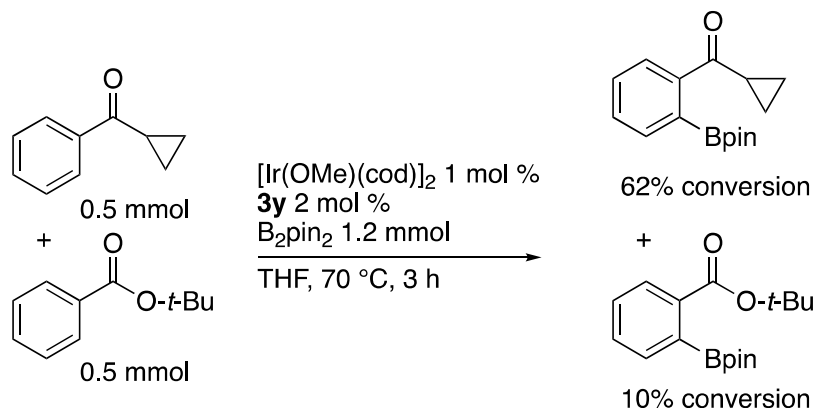
An effort was made by Dmitry Shabashov to isolate important catalytic intermediates. Mixing trisboryl iridium(III)mesitylene with the monodentate pyridine ligands resulted in different outcomes (Scheme 39). When mixed with 4-(*N,N'*-dimethyl)-2-methoxypyridine, the only product observed was that of the C-H borylation on the primary center of the methoxy group. However, when Shabashov, using 4-cyano-2-methoxypyridine, attempted this same experiment no intermolecular borylation of the ligand was observed. This result illustrated why the electron poorer pyridine was the better ligand for ortho CHB.

Scheme 39. sp^3 CHB of Electron Rich 4-*N,N*-dimethyl-2-methoxypyridine



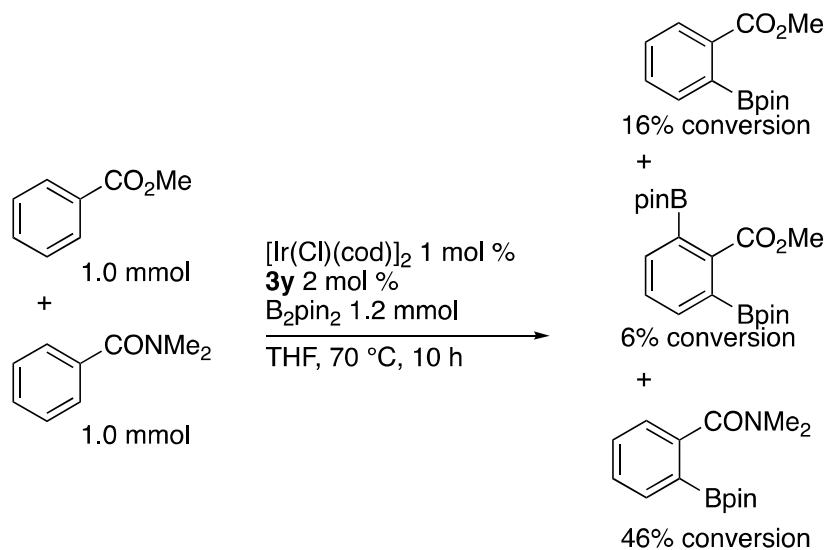
Performed by Dmitry Shabashov

Scheme 40. Competition reactions for ortho CHB of ketones vs esters



Several intermolecular competition reactions were performed to determine which substrates performed better for ortho-CHB. It was found that in an intermolecular competition reaction between tert-butyl benzoate and cyclopropyl phenylketone the ketone was borylated 62% compared to only 10% borylation for the ester in 3 hours.

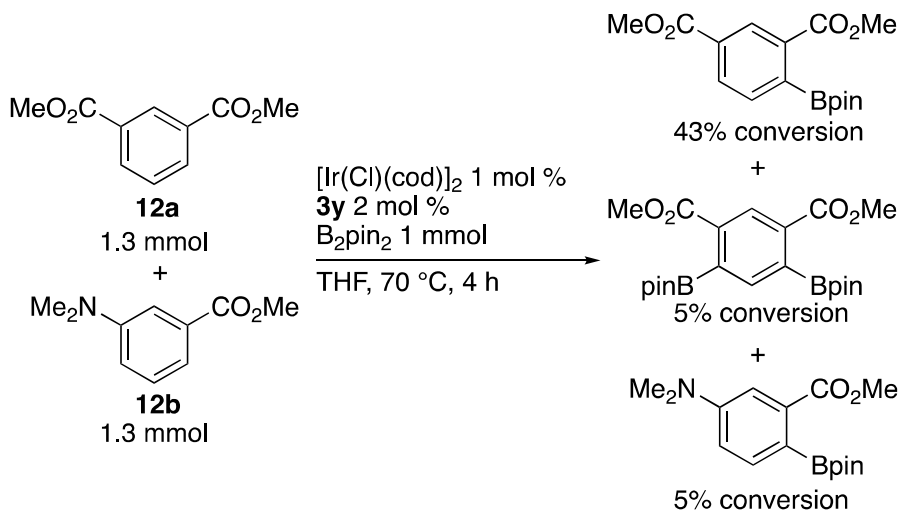
Scheme 41. Competition reaction between methyl benzoate and N,N-dimethylbenzamide



Performed by Dmitry Shabashov

Dimitry Shabashov tested the reaction of the methyl benzoate vs. N,N-dimethylbenzamide. It was found that the combined borylation of the methyl ester was 28% while the borylation of the carbamate was 46% over 10 hours.

Scheme 42. Competition of electronically different methyl benzoates

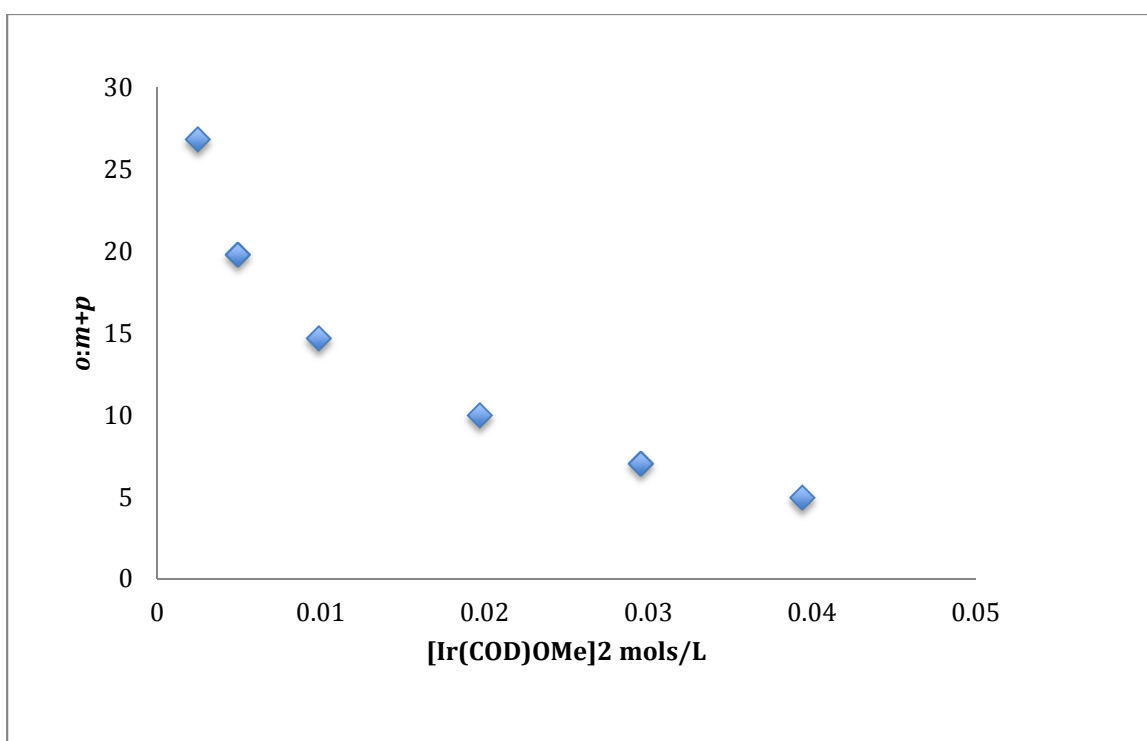


Performed by Dmitry Shabashov

Lastly, in order to determine the better functionalization to have on the substrate an intermolecular reaction was performed comparing dimethyl isophthalate to methyl 3-(dimethylamino)benzoate. The dimethylisophthalate was found to perform better than the methyl 3-(dimethylamino)benzoate. This test determined if an electron poorer or electron richer ring system would be a better substrate for ortho CHB using pyridine ligands. Similar to other CHBs electron-poor substrates reacted faster for ortho CHB.

3.9 Selectivity Dependence on Concentration of the Catalyst

While investigating the mechanism of ortho borylation an interesting observation was made. The selectivity of the reaction for ortho borylation was directly related to the catalyst concentration. When lower loadings of catalyst were used, the reaction proceeded with much greater ortho selectivity (Figure 18).

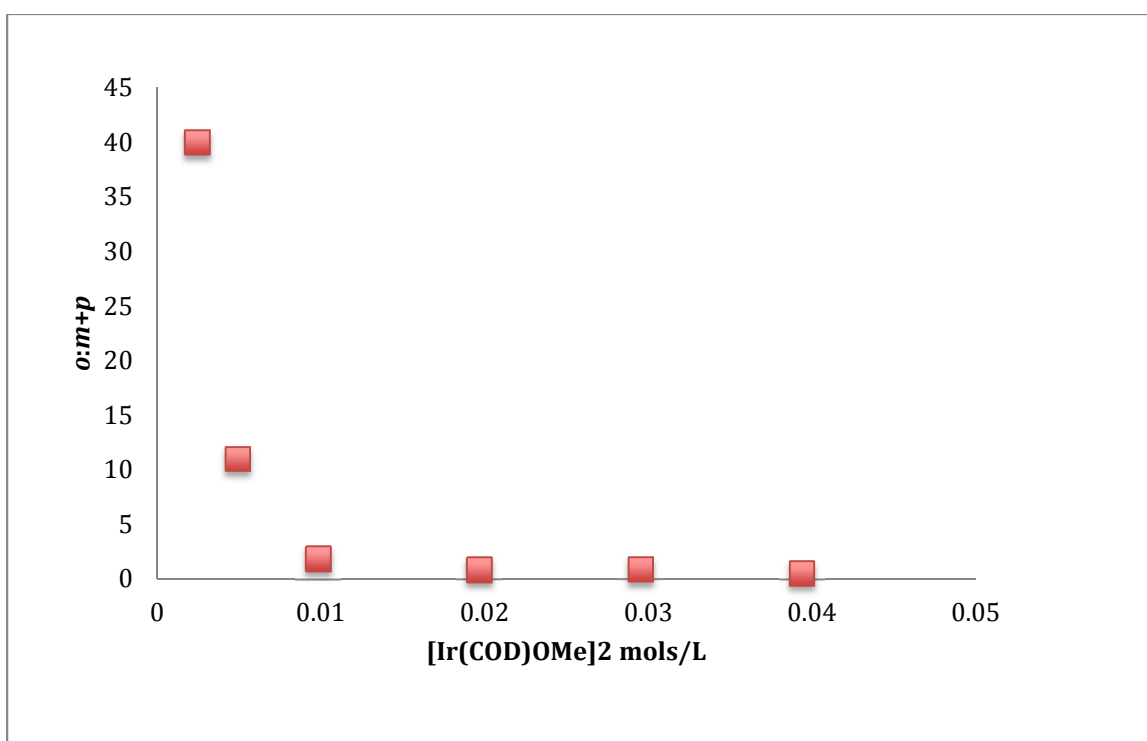


a) Reaction conditions: methyl benzoate (0.2 mmol), [L]/[Ir] (1:1), B₂pin₂ (0.2 mmol), 80 °C, 16 hours.

Figure 18. Selectivity vs concentration of catalyst in iridium catalyzed ortho borylation of methyl benzoate.

This behavior was seen for both the systems with ligand included as well as when just the precatalyst was used without ligand (Figure 19). However, in comparing figure

18 to figure 19, the resulting reaction with 4-cyano-2-methoxy pyridine had less of a change in selectivity than that of the pre-catalyst without ligand. This indicates that the ligand stabilized the ability to perform ortho-borylation even as the catalyst concentrations increase. While it is possible that the increased ortho selectivity is simply due to the equilibrium of a mono-ligated catalyst (**3be**) and a di-ligated catalyst (**3bh**) the exact cause of this selectivity has yet to be determined.

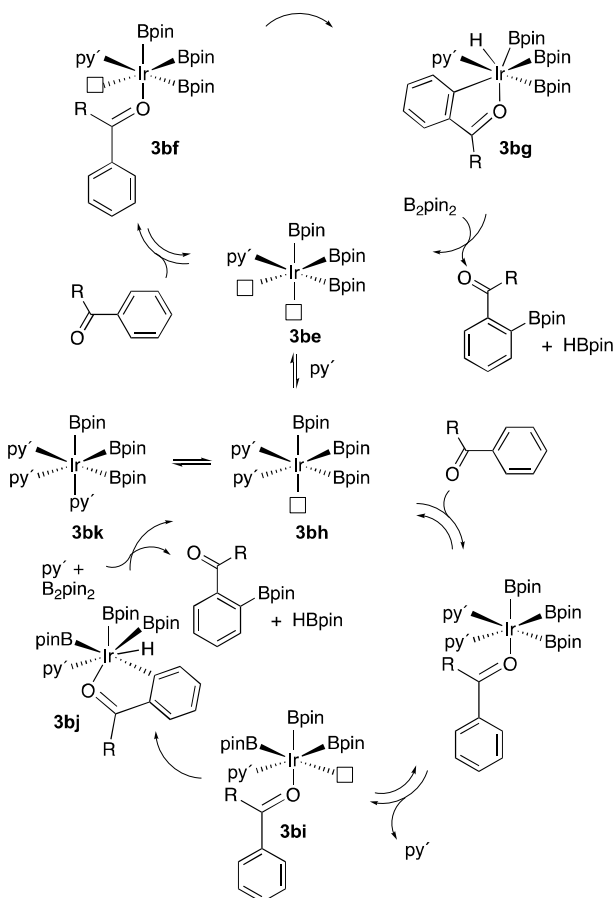


a) Methyl benzoate (0.2 mmol), [Ir(OMe)cod]₂ (0.0025M-0.04M), B₂pin₂ (0.2 mmol), THF(0.4 mL), 80 °C, 16 hours.

Figure 19. Selectivity of ortho-Borylation of Methyl Benzoate With no Added Ligand

3.10 Combined Mechanism for Pyridine Ligated Iridium CHB

Scheme 43. Proposed catalytic cycle of py' ligand ortho borylation



The mechanism of the CHB is likely that of a monoligated iridium (III/V) cycle operating with a 14 or 16 electron intermediates as shown in Scheme 43. With additional pyridine the catalyst can be di-ligated to form **3bh**. However, loss of a pyridine is needed either before the C-H functionalization step or before coordination of the substrate to the metal center. The addition of excess pyridine can result in the catalyst being shut down

through a trispyridyl complex such as **3bk**. All attempts to synthesize **3bk** as of yet have been unsuccessful.

The KIE data from the intramolecular and intermolecular experiments indicate that C-H bond cleavage is likely not the rate-determining step. As of yet the observation of a metal complex with an arene and a hydride on it has not been observed. Initial computational analysis performed by Milton R Smith III and HangYao Wang agrees that the C-H cleavage is likely not the rate-determining step. However, further computational studies, supported with experiments, are needed to help support this initial hypothesis and investigate the rate-determining step.

The off-cycle reactions generating meta and para borylation can be limited with a reduction of the catalyst loading. This suggests that a possible aggregation or nanoparticle formation of iridium is leading to the side products and further increases in selectivity could be generated through isolating the catalyst on a solid support.

3.11 Pyridine Ligands for ortho CHB Conclusions

A method for the ortho-borylation of C-H bonds on aryl esters, ketones and amides has been developed utilizing a variety of commercially available ligands. The tuneability of these ligands has been demonstrated based on electronic and steric factors. The reaction mechanism has been probed, however, further questions regarding the mechanism remain an area for future research.

Chapter 4. Experimental

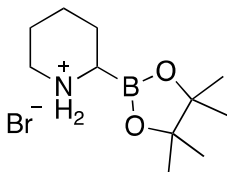
4.1 General Considerations

Tetrahydrofuran was distilled from sodium benzophenone ketyl. All other solvents were used as received unless specifically stated. All commercially available materials were used as received unless otherwise stated. All arenes and heteroarenes were purchased unless specifically stated. ^1H and ^{13}C NMR spectra were recorded on a Varian VXR-500 or Varian Unity-500-Plus spectrometers (499.74 and 125.67 MHz, respectively) and referenced to residual solvent signals. ^{11}B spectra were recorded on Varian VXR-500 operating at 160.41 MHz.

Crystal Structures were obtained on a Bruker APEX-II CCD x-ray diffractometer at 173 K during the acquisition. Olex2 was used to solve the structures using ShelXS for the structure solution program with direct methods used for the solution method. The refinement was done using least squares minimization method.

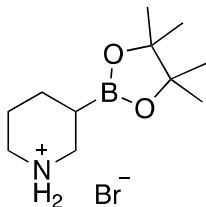
GC-FID was taken on an Agilent 7890A GC. High resolution mass spectra (HRMS) was obtained at the Michigan State University Mass Spectroscopy Service Center.

4.2 Experimental Information for Chapter 2



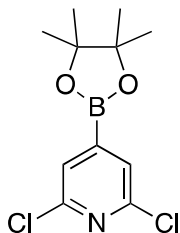
2-(4,4,5,5-tetramethyl-1,3,2-dioxaborolan-2-yl)piperidin-1-ium bromide(2b):

2-Bromo-6-(4,4,5,5-tetramethyl-1,3,2-dioxaborolan-2-yl)pyridine (142 mg, 0.5 mmol), 5% Rh/C (25 mg), and a stir bar were loaded into a 300 mL pressure vessel. Ethanol (5 mL) was added and the reactor was sealed and pressurized with hydrogen gas (700 psi). After 16 hours the reactor was opened and filtered through Celite and washed with methanol (3 X 5 mL) the solvent was removed under vacuum to yield a white solid (143 mg, 98% yield) with a m.p. of 198-199°C. ¹H NMR (500 MHz, D₂O) δ 3.37 – 3.21 (m, 1H), 2.89 (td, *J* = 12.5, 3.2 Hz, 1H), 2.70 (dd, *J* = 12.6, 3.2 Hz, 1H), 1.91 (dtd, *J* = 17.4, 4.7, 4.2, 2.2 Hz, 1H), 1.88 – 1.70 (m, 2H), 1.70 – 1.56 (m, 2H), 1.56 – 1.37 (m, 1H), 1.17 (s, 12 H). ¹³C NMR (126 MHz, D₂O) δ 75.55, 44.52, 24.28, 23.65, 22.53, 22.04. ¹¹B NMR (160 MHz, D₂O) δ 28.42. HRMS (ESI) *m/z* calcd. for C₁₁H₂₃B₁N₁O₂ [M-Br]⁺ 212.1822 found. 212.1819 There are 3 identifiable impurities that appear in the NMR spectrum. Ethanol had a quartet at 3.63 and a triplet at 1.15 which corresponds to 2.5% of the spectrum based on their integration. Piperidinium bromide has one distinguishable peak as a triplet at 2.9 that corresponds to 6.75% of the spectrum. Lastly, acetone has a singlet at 2.17 that corresponds to 1.1% of the spectrum. Three other impurity peaks are unidentified at 3.25 ppm (t), 2.29 ppm (t) as well as 1.28 ppm (s) which may be a pinacol boronate but is not confirmed.



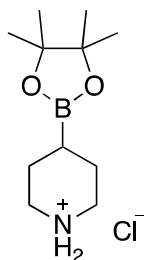
3-(4,4,5,5-tetramethyl-1,3,2-dioxaborolan-2-yl)piperidin-1-ium bromide(2c):

3-Bromo-5-(4,4,5,5-tetramethyl-1,3,2-dioxaborolan-2-yl)pyridine (142 mg, 0.5 mmol), 5% Rh/C (25 mg), and a stir bar were loaded into a 300 mL pressure vessel. Ethanol (5 mL) was added and the reactor was sealed and pressurized with hydrogen gas (700 psi). After 16 hours the reactor was opened and filtered through Celite and washed with methanol (3 X 5 mL) the solvent was removed under vacuum to yield a white solid (134 mg, 94% yield) with a m.p. of 154-156°C. ¹H NMR (500 MHz, D₂O) δ 3.43 – 3.31 (m, 2H), 3.00 – 2.89 (m, 2H), 1.91 – 1.82 (m, 2H), 1.79 – 1.69 (m, 1H), 1.69 – 1.58 (m, 1H), 1.53 – 1.31 (m, 1H), 1.18 (s, 12H). ¹³C NMR (126 MHz, D₂O) δ 75.55, 45.90, 44.43, 44.26, 23.63, 23.42, 22.79, 22.10, 21.37. ¹¹B NMR (160 MHz, D₂O) δ 30.84. HRMS (ESI) m/z calcd. for C₁₁H₂₃B₁N₁O₂ [M-Br]⁺ 212.1822 Found, 212.1826. This compound was isolated as a mixture of the product **2c** with the deborylated piperdinium bromide in a 4:1 ratio based on the integration of the most downfield peaks for the compounds. The distinguishable signal for the piperdinium bromide was a multiplet from 3.02 – 2.96 which correspond to the 4 hydrogens adjacent to the nitrogen. There was also a significant boronate singlet at 1.26 ppm that correlated to an 8:1 ratio of **2c** pinacol vs boronate pinacol.



2,6-dichloro-4-(4,4,5,5-tetramethyl-1,3,2-dioxaborolan-2-yl)pyridine(2d')¹¹⁹:

In a nitrogen filled glove box a Schlenk flask (25 mL) was loaded with bis(1,5-cyclooctadiene)di- μ -methoxydiiridium(I) (9.9 mg, 0.015 mmol), di-*tert*-butyl bipyridine (8 mg, 0.03 mmol) and pinacol borane (1.778g, 14 mmol). The flask was loaded with a stir bar and 2,6-dichloropyridine (1.47g, 10 mmol). The flask was capped with a septa, removed from the glove box and the solution was stirred for 14 hours at room temperature. After 14 hours the reaction was opened and the solvent removed by rotatory evaporation. Purification via a short silica plug (dichloromethane) and evaporation of solvent yielded a white solid (2.158g, 79% yield). All data matched reported literature spectra.¹¹⁹ ¹H NMR (500 MHz, CDCl₃) δ 7.58 (s, 2H) 1.34 (s, 12H) ¹¹B NMR (160 MHz, CDCl₃) δ 29.45. A small water impurity peak was observed in the spectra at 1.56 ppm.



4-(4,4,5,5-tetramethyl-1,3,2-dioxaborolan-2-yl)piperidin-1-ium chloride(2d):

2,6-Dichloro-4-(4,4,5,5-tetramethyl-1,3,2-dioxaborolan-2-yl)pyridine (137 mg, 0.5 mmol), 5% Rh/C (25 mg), and a stir bar were loaded into a 300 mL pressure vessel. Ethanol (5 mL) was added and the reactor was sealed and pressurized with hydrogen gas

(700 psi). After 16 hours the reactor was opened and filtered through Celite and washed with methanol (3 X 5 mL) the solvent was removed under vacuum to yield a white solid (94 mg, 76% yield) with a m.p. of 149-150.5°C. In water or deuterium oxide the pinacol would hydrolyze off leaving 4-boronopiperidin-1-ium chloride. Characterization based on the mixture of **2d** and the hydrolyzed biproduct. ¹H NMR (500 MHz, D₂O) δ 3.19 (ddt, *J* = 24.0, 12.8, 3.7 Hz, 2H), 2.93 – 2.73 (m, 2H), 1.77 (dt, *J* = 14.9, 3.7 Hz, 2H), 1.52 (ddq, *J* = 15.0, 7.1, 3.9 Hz, 2H), 1.12 (s, 7H) 1.05(s, 6H) ¹³C NMR (126 MHz, D₂O) δ 87.46, 46.99,, 26.10, 25.65. ¹¹B NMR (160 MHz, D₂O) δ 31.54. HRMS (ESI) *m/z* calcd. for C₁₁H₂₃B₁N₁O₂ [M-Cl]⁺ 212.1822 Found. 212.1832. In water or deuterium oxide a slow conversion from one singlet peak at 1.05 converts to 1.12. This is a hydrolysis from the pinacol ester to the boronic acid. The impurity peak at 3.13 representing the deborylated piperdinium chloride remained unchanged at 5 % of the sample when the number of protons is taken into account. Shown below is a spectrum of pinacol taken in D₂O that has 1 signal at 1.12 ppm.

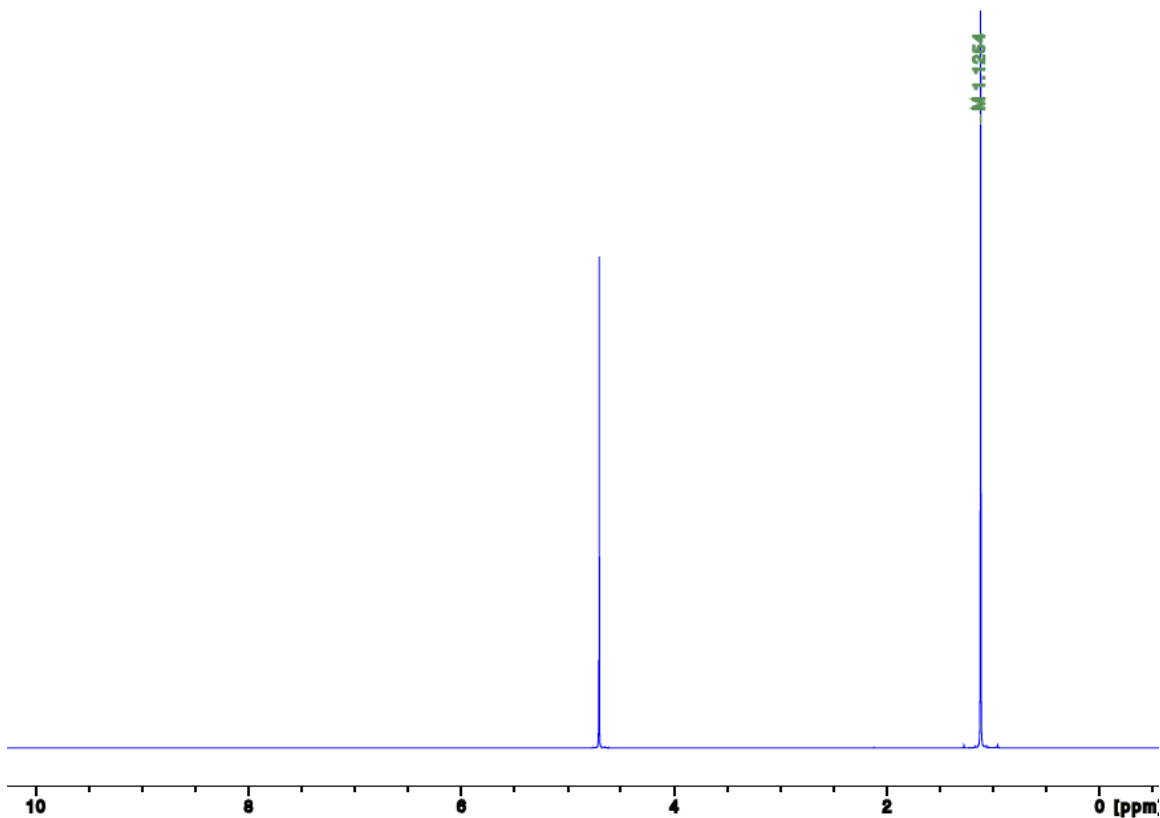
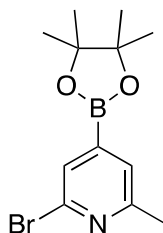


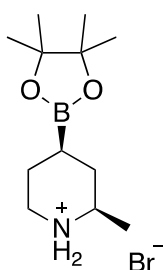
Figure 20. 400 MHz ^1H -NMR of pinacol in D_2O



2-bromo-6-methyl-4-(4,4,5,5-tetramethyl-1,3,2-dioxaborolan-2-yl)pyridine²(2e'):

In a nitrogen filled glove box a Schlenk flask (25 mL) was loaded with Bis(1,5-cyclooctadiene)di- μ -methoxydiiridium(I) (36 mg, 0.055 mmol), di-*tert*-butyl bipyridine (32 mg, 0.12 mmol), pinacol borane (1.90 g, 15 mmol) and tetrahydrofuran (10 mL). The flask was loaded with a stir bar and 2-bromo-6-methylpyridine (1.70 g, 10 mmol). The flask was closed up, removed from the glove box, connected to a Schlenk line and placed in an oil bath. The reaction solution was stirred for 24 hours at 70 °C.

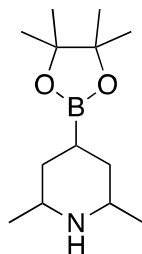
After 24 hours the reaction flask was opened and the solvent removed by rotary evaporation. Purification via a short silica plug (dichloromethane) and evaporation of solvent yielded a tan solid (2.55g, 86% yield) ^1H NMR (500 MHz, CDCl_3) δ 7.62 (s, 1H), 7.43 (s, 1H), 2.52 (s, 3H), 1.33 (s, 12H). ^{13}C NMR (126 MHz, CDCl_3) δ 159.41, 141.42, 129.93, 127.05, 84.76, 24.82, 23.96. ^{11}B NMR (160 MHz, CDCl_3) δ 29.76. Characterization data matched literature precedent.¹²⁰



Cis-2-methyl-4-(4,4,5,5-tetramethyl-1,3,2-dioxaborolan-2-yl)piperidin-1-ium bromide(2e):

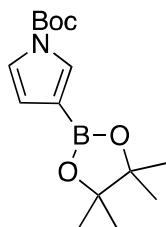
2-Bromo-6-methyl-4-(4,4,5,5-tetramethyl-1,3,2-dioxaborolan-2-yl)pyridine (85mg, 0.3 mmol), 5% Rh/ Al_2O_3 (25 mg), and a stir bar were loaded into the pressure vessel. Ethanol (5 mL) was added and the reactor was sealed and pressurized with hydrogen gas (700 psi). After 16 hours the reactor was opened and filtered through Celite and washed with methanol (3 X 5 mL) the solvent was removed under vacuum to yield a tan solid (86 mg, 98% yield) with a m.p. of 209-211 °C. ^1H NMR (500 MHz, D_2O) δ 3.23 (ddd, J = 12.7, 4.2, 2.2 Hz, 1H), 2.99 (dq, J = 12.9, 6.1, 2.7 Hz, 1H), 2.77 (td, J = 13.0, 3.3 Hz, 1H), 1.87 – 1.67 (m, 2H), 1.38 (dtd, J = 14.5, 13.2, 4.1 Hz, 1H), 1.26 – 1.15 (m, 1H), 1.10 (d, J = 2.1 Hz, 3H), 1.03 (s, 12H). ^{13}C NMR (126 MHz, D_2O) δ 75.54, 53.35, 45.09, 31.70, 23.64, 23.58, 23.15, 18.70. ^{11}B NMR (160 MHz, D_2O) δ 30.77. HRMS (ESI) m/z calcd. for $\text{C}_{12}\text{H}_{25}\text{B}_1\text{N}_1\text{O}_2$ $[\text{M}-\text{Br}]^+$ 226.1978; Found. 226.1986. A crystal structure was

obtained for this compound. Two impurities in the spectra were found and identified. Ethanol has a quartet at 3.65, and a triplet at 1.15 and integrates to 5% of the spectra. Acetone was found with a singlet at 2.20 which integrates to <1% in comparison to **2e**.



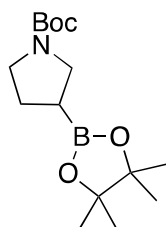
2,6-dimethyl-4-(4,4,5,5-tetramethyl-1,3,2-dioxaborolan-2-yl)piperidine(2f):

2,6-Dimethyl-4-(4,4,5,5-tetramethyl-1,3,2-dioxaborolan-2-yl)pyridine (117 mg, 0.5 mmol), 5 % Rh/Al₂O₃ (50 mg), and a stir bar were loaded into the pressure vessel. Ethanol (5 mL) was added and the reactor was sealed and pressurized with hydrogen gas (700 psi). After 16 hours the reactor was opened and filtered through Celite and washed with methanol (3 X 5 mL) the solvent was removed under vacuum to yield yellow solid (100 mg, 85% yield). The compound was isolated as an incomplete hydrogenation of starting material. ¹H NMR (500 MHz, CDCl₃) δ 2.68 – 2.58 (m, 2H), 1.67 (d, *J* = 3.4 Hz, 2H), 1.35 (s, 1H), 1.23 (d, *J* = 6.2 Hz, 12H), 1.05 (d, *J* = 6.3 Hz, 6H), 0.96 (td, *J* = 12.9, 10.6 Hz, 2H). ¹¹B NMR (160 MHz, CDCl₃) δ 33.87. HRMS (ESI) *m/z* calcd. for C₁₃H₂₇B₁N₁O₂ [M+H]⁺ 240.2135; Found. 240.2131. 2,6-Dimethyl-4-(4,4,5,5-tetramethyl-1,3,2-dioxaborolan-2-yl)pyridine starting material peaks were found in the spectra at 7.30, 2.51, and 1.35 which integrate to 9.9 % of the isolated mixture. The Proton for the N-H peak was not observed.



***tert*-butyl 3-(4,4,5,5-tetramethyl-1,3,2-dioxaborolan-2-yl)-1*H*-pyrrole-1-carboxylate (2g')**

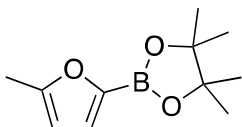
In a nitrogen filled glove box a round bottom flask (50 mL) was loaded with bis(1,5-cyclooctadiene)di- μ -methoxydiiridium(I) (19.6 mg, 0.03 mmol, 0.5 mol %), di-*tert*-butyl bipyridine (15.8 mg, 0.058 mmol, 1 mol %), bis(pinacolato)diboron (1.58 g, 6.22 mmol), tetrahydrofuran (10 mL) and a stir bar. To this mixture was added N-Boc-pyrrole (1.67 mL, 10 mmol). The mixture was placed in an oil bath and the mixture was stirred for 16 hours at 55 °C. The reaction mixture was cooled, the THF was removed via rotary evaporation and the residue was passed through a silica plug (DCM) to yield a white solid (2.13g, 73% yield). ¹H-NMR matched reported data.¹²¹



***tert*-butyl 3-(4,4,5,5-tetramethyl-1,3,2-dioxaborolan-2-yl)pyrrolidine-1-carboxylate (2g)**

tert-Butyl 3-(4,4,5,5-tetramethyl-1,3,2-dioxaborolan-2-yl)-1*H*-pyrrole-1-carboxylate (142 mg, 0.5 mmol), 10 % Pd/C (15 mg), and a stir bar were loaded into a 300 mL pressure vessel. Ethanol (5 mL) was added and the reactor was sealed and

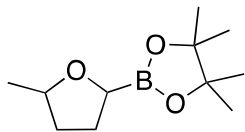
pressurized with hydrogen gas (700 psi). After 16 hours the reactor was opened and the reaction mixture was filtered through Celite and washed with methanol (3 X 5 mL). The solvent was removed under vacuum to yield a clear oil (131 mg, 91% yield). ¹H NMR (500 MHz, CDCl₃, ppm) δ 3.49 (dt, *J* = 19.4, 9.7 Hz, 2H), 3.30 - 3.06 (m, 2H), 2.05 - 1.93 (m, 1H), 1.86 - 1.70 (m, 1H), 1.62 - 1.51 (m, 1H), 1.44 (s, 9H), 1.23 (d, *J* = 6.4 Hz, 12H) ¹³C NMR (126 MHz, CCDl₃) δ 154.56, 83.44, 78.82, 47.96, 47.77, 46.82, 46.46, 28.57, 28.23, 27.51, 24.72. ¹¹B NMR (160 MHz, cdcl₃) δ 33.62. δ HRMS (ESI) *m/z* calcd. for C₁₅H₂₈BNO₄Na [M+Na]⁺ 320.2009; Found 320.2000 11 carbon resonances appear as the rotomomers show differing carbon resonances at room temperature for the pyrrolidine ring only. The carbon peaks were found to be 3 carbon resonances for the boc group, 2 for the pinacol and 6 visible resonances for the pyrrolidine. The carbon connected to the boron is not visible in the spectra.



4,4,5,5-tetramethyl-2-(5-methylfuran-2-yl)-1,3,2-dioxaborolane(2h'):

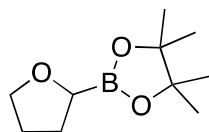
In a nitrogen filled glove box a round bottom flask (25 mL) was loaded with bis(1,5-cyclooctadiene)di-μ-methoxydiiridium(I) (9.9 mg, 0.015 mmol, 0.3 mol %), di-*tert*-butyl bipyridine(8.0 mg, 0.03 mmol, 0.6 mol %), bis(pinacolato)diboron(1.3 g, 5.1 mmol) and a stir bar. The RB was closed with a septa and removed from the glove box. 2-Methylfuran (5 mL) was added to the reaction mixture via syringe. The solution was stirred at room temperature for 3 hours. The reaction was opened up to air, and excess 2-methylfuran was removed in-vacuo. The residual oil was passed through a silica column (EtoAc:Hexanes 5:95) to yield a white solid (1.5g, 72% yield). Spectra matched reported

data from literature.¹²² ¹H NMR (500 MHz, CDCl₃) δ 6.98 (d, *J* = 3.2 Hz, 1H), 6.03 (dd, *J* = 3.2, 1.0 Hz, 1H), 2.86 (s, 3H), 1.33 (s, 12H).



4,4,5,5-tetramethyl-2-(5-methyltetrahydrofuran-2-yl)-1,3,2-dioxaborolane(2h):

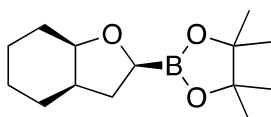
4,4,5,5-Tetramethyl-2-(5-methylfuran-2-yl)-1,3,2-dioxaborolane (208 mg, 1 mmol), 10% Pd/C (25 mg), and a stir bar were loaded into the liner of a 300 mL pressure reactor. Ethanol (5 mL) was added and the reactor was sealed and pressurized with hydrogen gas (700 psi). After 16 hours the reactor was opened and the reaction mixture was filtered through Celite and washed with methanol (3 X 5 mL). The solvent was removed under vacuum to yield a clear oil (165 mg, 78% yield). ¹H NMR (500 MHz, CDCl₃) δ 3.83 (m, 1H) 3.48 (m, 1H) 2.06-1.92 (br m, 1H) 1.83-1.75 (m, 1H) 1.44-1.34(m, 1H) ,1.30-1.25 (br s, 13H) 1.25-1.20 (m, 3H) ¹¹B NMR (160 MHz, CDCl₃) δ 32.63. The compound is not very stable in CDCl₃. Some boronate impurities are found in the boron NMR that was taken after the proton NMR.



4,4,5,5-tetramethyl-2-(tetrahydrofuran-2-yl)-1,3,2-dioxaborolane (2i):

2-(Furan-2-yl)-4,4,5,5-tetramethyl-1,3,2-dioxaborolane (194 mg, 1 mmol), 10% Pd/C (25 mg), and a stir bar were loaded into a glass liner in a 300 mL pressure reactor. Ethanol (5

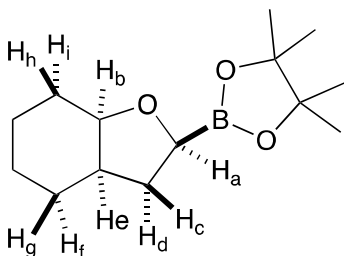
mL) was added and the reactor was sealed and pressurized with hydrogen gas (700 psi). After 16 hours the reaction mixture was filtered through Celite and washed with methanol (3 X 5 mL). The solvent was removed under vacuum to yield a clear oil (145 mg, 73% yield). ^1H NMR (500 MHz, CDCl_3) δ 3.81 (td, $J = 7.8, 5.9$ Hz, 1H), 3.60 – 3.41 (m, 2H), 1.91 – 1.72 (m, 2H), 1.63 – 1.52 (m, 1H), 1.46 (dq, $J = 11.9, 8.1, 5.9$ Hz, 1H), 1.00 (d, $J = 2.2$ Hz, 12H). δ ^{11}B NMR (160 MHz, C_6D_6) δ 32.6 All spectra matched previously reported literature data.¹²³



Cis-4,4,5,5-tetramethyl-2-(octahydrobenzofuran-2-yl)-1,3,2-dioxaborolane (2I):

2-(Benzofuran-2-yl)-4,4,5,5-tetramethyl-1,3,2-dioxaborolane (122 mg, 0.5 mmol), 5% Rh/C (50 mg), and a stir bar were loaded into a glass liner in a 300 mL pressure reactor. Ethanol (10 mL) was added and the reactor was sealed and pressurized with hydrogen gas (700 psi). After 24 hours the reaction mixture was filtered through Celite and washed with ethanol (3 X 5 mL). The solvent was removed under vacuum to yield a clear oil (103 mg, 81% yield) ^1H NMR (500 MHz, C_6D_6) δ 3.88 (dd, $J = 11.1, 6.9$ Hz, 1H) 3.67 (q, $J = 3.8$ Hz, 1H) 2.15-2.05 (m, 2H) 1.83-1.77 (m, 1H) 1.77-1.72 (m, 2H) 1.58-1.52 (m, 1H) 1.52-1.43 (m, 3H) 1.33-1.27 (m, 1H) 1.13-1.06 (m, 1H) 1.05 (s, 6H) 1.04 (s, 6H) ^{13}C NMR (126 MHz, CD_3OD) 83.7, 78.4, 38.0, 33.9, 27.8, 27.7 23.9, 23.6, 23.5 20.4 δ ^{11}B NMR (160 MHz, C_6D_6) δ 32.4. The methyl NMR signals from the pinacol became inequivalent and different signals were seen in both the proton and the carbon spectra. The carbon bound to boron signal was not seen by ^{13}C -NMR.

Assignment of stereochemistry



By gCOSY the multiplet at 2.15-2.05 was 2 distinct protons that did not show correlation to each other. The proton at 3.88 has a correlation with protons at 2.08 and 1.75. This indicates that 3.88 is H_a from Figure 20 as it only has a correlation to 2 other protons. As a result H_b is the other downfield proton at 3.67. H_b was found to correlate to protons at 2.12, 1.80 and 1.50. These are H_e, H_h and H_i. The proton at 2.12 did not have a correlation to 1.80. While 1.80 and 1.50 correlated to each other. These correlations indicate that 2.12 is the proton assigned as H_e and protons at 1.80 and 1.50 are H_h and H_i.

Based on the 1D-NOE data the excitation of H_a resulted in a NOE to protons at 3.67 (H_b), 2.12 ppm (H_e) and 1.75 ppm (H_d or c). Interestingly enough there was an inverse correlation to the proton at 2.05 (H_d or c). This indicated that the protons H_b and H_e were all on the same face of the ring fused molecule.

To further confirm this NOE data when H_b was excited showed NOE to 3.88 (H_a) as well as 2.12

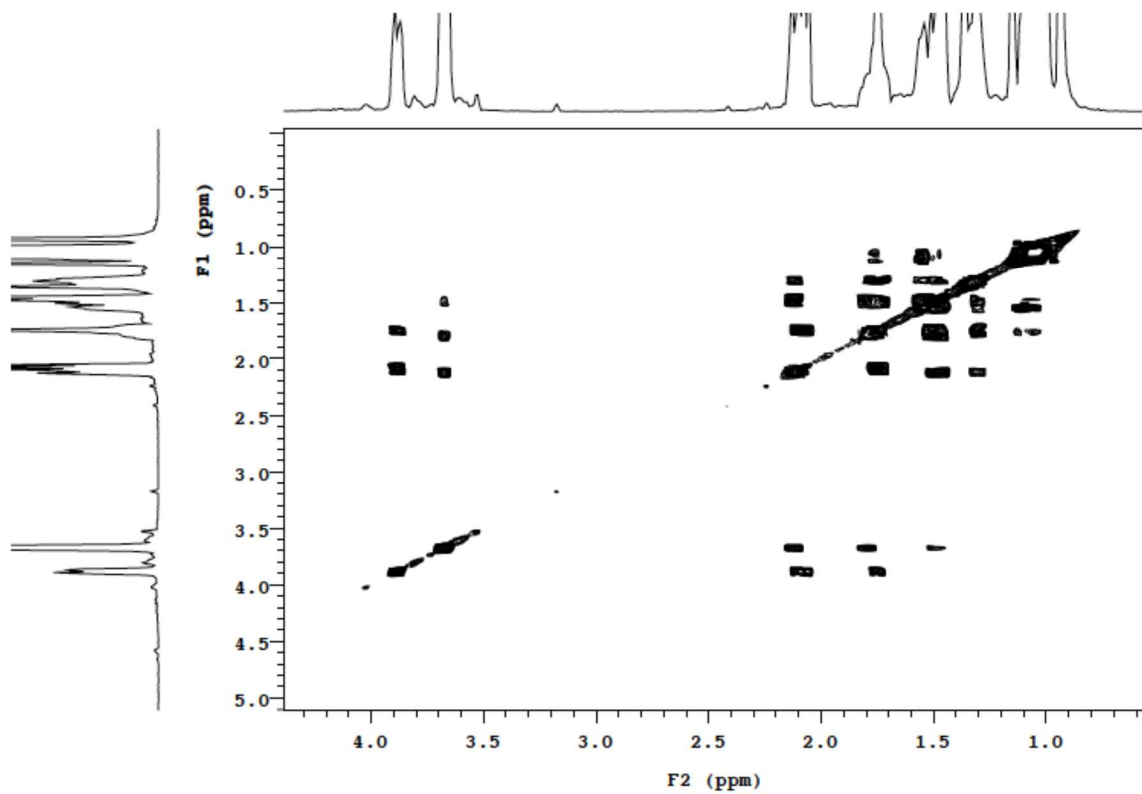


Figure 21. gCOSY of compound **21**

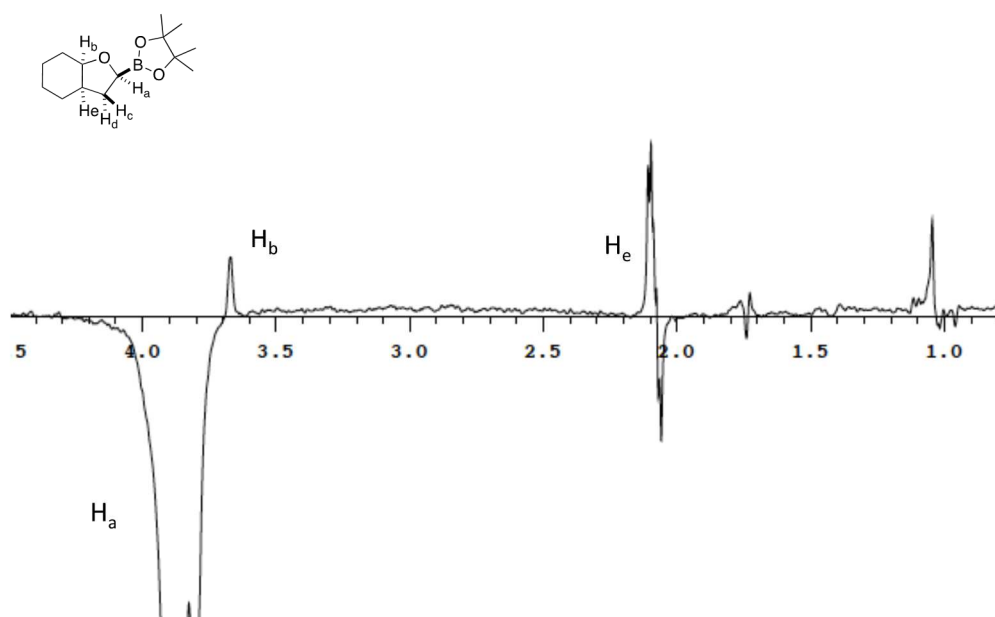


Figure 22. NOE between protons on **2I** showing cis stereochemistry 3.9ppm irradiated

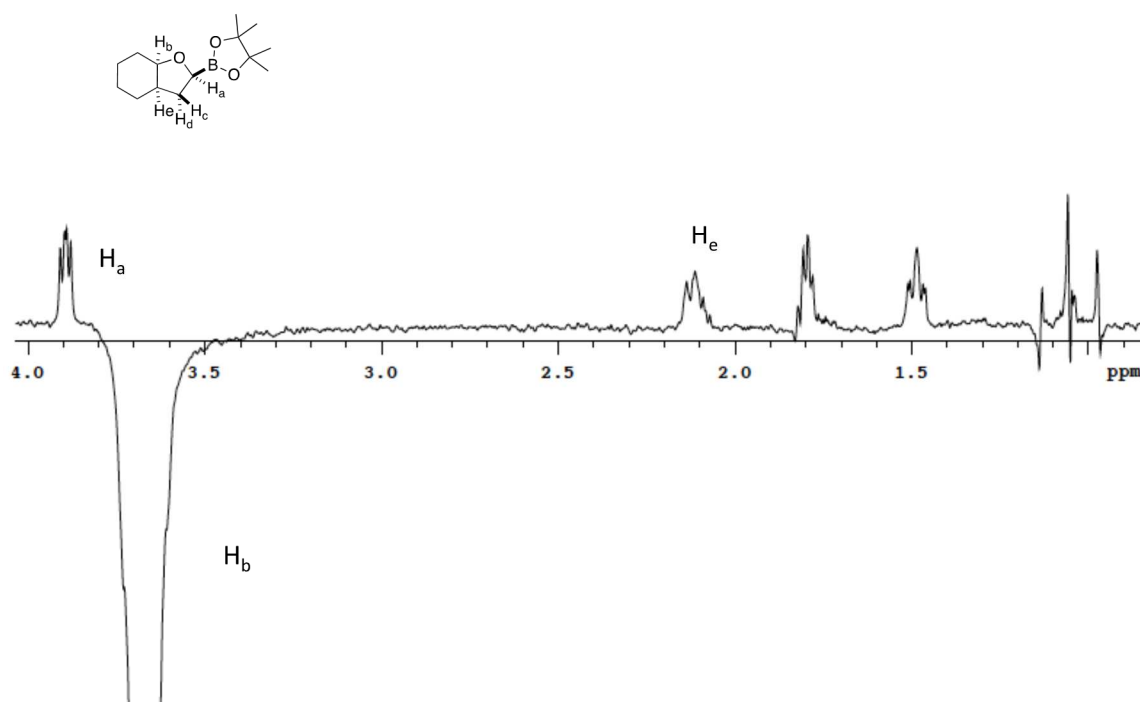
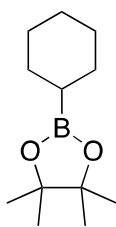


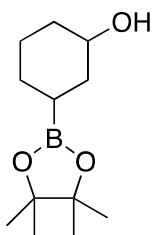
Figure 23. NOE between protons on **2l** showing cis stereochemistry 3.7ppm irradiated



2-cyclohexyl-4,4,5,5-tetramethyl-1,3,2-dioxaborolane (2o):

4,4,5,5-Tetramethyl-2-phenyl-1,3,2-dioxaborolane (2-4 mg, 1 mmol), 5% Rh/C (25 mg), and a stir bar were loaded into the pressure vessel. Ethanol (5 mL) was added and the reactor was sealed and pressurized with hydrogen gas (700 psi). After 16 hours the reactor was opened and the contents were filtered through Celite and washed with

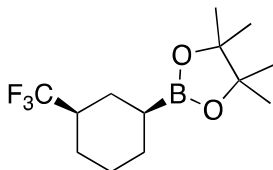
methanol (3 X 5 mL). The solvent was removed under vacuum to yield a clear oil (208 mg, 99% yield). All spectral data matched literature data.¹²⁴ ¹H NMR (500 MHz, CDCl₃) δ 1.71 – 1.52 (m, 5H), 1.40 – 1.25 (m, 5H), 1.23 (s, 12H), 0.98 (tt, *J* = 10.1, 2.8 Hz, 1H). ¹³C NMR (126 MHz, CDCl₃) δ 82.72, 27.95, 27.13, 26.75, 24.74.



3-(4,4,5,5-tetramethyl-1,3,2-dioxaborolan-2-yl)cyclohexan-1-ol (2p)

3-(4,4,5,5-Tetramethyl-1,3,2-dioxaborolan-2-yl)phenol (110 mg, 0.5 mmol), 5 % Rh/C (25 mg), and a stir bar were loaded into the pressure vessel. Ethanol (5 mL) was added and the reactor was sealed and pressurized with hydrogen gas (700 psi). After 16 hours the reactor was opened and the contents were filtered through Celite and washed with methanol (3 X 5 mL). The solvent was removed under vacuum to yield a clear oil (90.4 mg, 80% yield). ¹H NMR (500 MHz, CD₃OD) δ 3.82 – 3.37 (m, 1H), 1.95 – 1.83 (m, 1H), 1.83 – 1.69 (m, 1H), 1.66 – 1.57 (m, 1H), 1.57 – 1.54 (m, 1H), 1.48 – 1.27 (m, 3H), 1.23 (d, *J* = 4.9 Hz, 12H), 1.13 – 0.99 (m, 1H), 0.97 – 0.85 (m, 1H). ¹³C NMR (126 MHz, CD₃OD) δ 83.00 (d, *J* = 7.8 Hz) 82.72, 70.56, 67.70, 36.24, 35.30, 35.05, 34.19, 27.62, 26.87 – 26.22 (m), 25.58, 23.73 (dd, *J* = 5.0, 3.0 Hz), 22.66. ¹¹B NMR (160 MHz, CD₃OD) δ 33.86. HRMS (APCI) *m/z* calcd. for C₁₂H₂₂BO₃ [M-H]⁻ 225.1662; Found. 225.1655. Isomer ratios determined by comparison of 2 separate signals at 3.6 and 3.4

respectively. These proton signals combine to form 1H and they are in a 5:4 ratio. It is assumed that the major product is the cis stereochemical project based on the history of hydrogenation chemistry. However, specific evidence was not gathered for this compound.



4,4,5,5-tetramethyl-2-(3-(trifluoromethyl)cyclohexyl)-1,3,2-dioxaborolane (2q):

4,4,5,5-Tetramethyl-2-(3-(trifluoromethyl)phenyl)-1,3,2-dioxaborolane (136 mg, 0.5 mmol), 5% Rh/C (25 mg), and a stir bar were loaded into the pressure vessel. Ethanol (5 mL) was added and the reactor was sealed and pressurized with hydrogen gas (700 psi). After 16 hours the reactor was opened and the contents were filtered through Celite and washed with methanol (3 X 5 mL). The solvent was removed under vacuum to yield a clear oil (121 mg, 87 % yield). Both cis and trans diastereomers were seen via ¹⁹F-NMR in a 3:1 cis to trans ratio. ¹H NMR (500 MHz, CDCl₃) δ 2.06 – 1.70 (m, 6H), 1.47 – 1.32 (m, 1H), 1.32 – 1.07 (m, 22H), 0.91 (tt, *J* = 12.8, 3.1 Hz, 1H). ¹³C NMR (126 MHz, CDCl₃) δ 127.9 (q, *J* = 280 Hz, CF₃) 83.2, 83.1, 42.5 (q, *J* = 26.9 Hz), 40.1 (d, *J* = 26.1 Hz), 26.87, 26.77, 26.1 (q, *J* = 2.6 Hz), 25.8, 25.02(q, *J* = 2.2 Hz), 25.00 (q, *J* = 2.2 Hz), 24.77(d, *J* = 4.3 Hz), 24.7(d, *J* = 3.3 Hz), 23.86. ¹⁹F NMR (470 MHz, CDCl₃) δ -73.63 (d, *J* = 8.6 Hz), -74.05 (d, *J* = 8.3 Hz). ¹¹B NMR (160 MHz, CDCl₃) δ 34.08. HRMS (AP-) *m/z* calcd. for C₁₃H₂₁B₁O₂F₃ [M-H]⁻ 277.1587; Found. 277.1583. Isomer ratios were

determined from ^{19}F -NMR. ^{13}C NMR peak at 40.1 is likely part of a quartet from the minor isomer that correlates to the quarter at 42.5

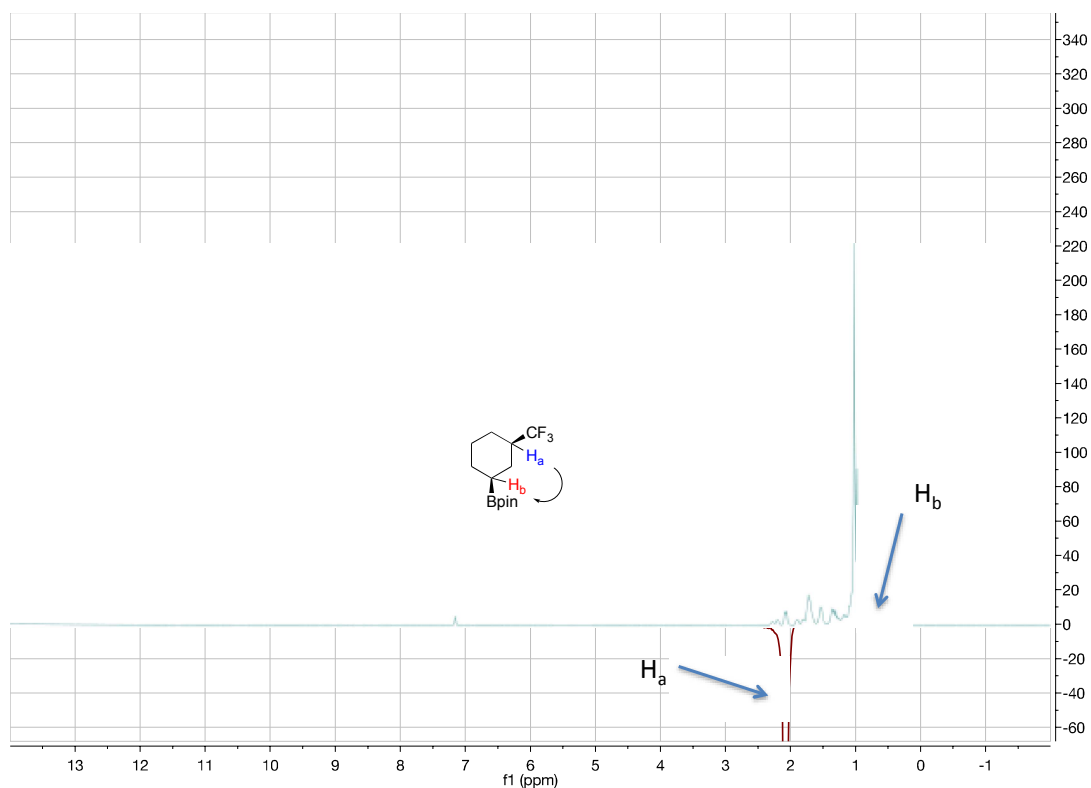
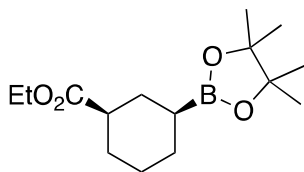


Figure 24. NOE between the major species of **2q** showing cis stereochemistry



ethyl-3-(4,4,5,5-tetramethyl-1,3,2-dioxaborolan-2-yl)cyclohexane-1-carboxylate (2r)

Ethyl 3-(4,4,5,5-tetramethyl-1,3,2-dioxaborolan-2-yl)benzoate (132 mg, 0.5 mmol), 5% Rh/C (25 mg), and a stir bar were loaded into the pressure vessel. Ethanol (5 mL) was added and the reactor was sealed and pressurized with hydrogen gas (700 psi). After 16 hours the reactor was opened and the contents were filtered through Celite and washed with methanol (3 X 5 mL). The solvent was removed under vacuum to yield a clear oil (129 mg, 96% yield). The reaction was isolated as a mixture of hydrogenated isomers in a 4.7:1 ratio as well as a small amount of starting material remaining. The determination of isomer ratio was found based on 2 quartets at 4.1 (minor) and 4.0 (major). ¹H NMR (500 MHz, C₆D₆) δ 4.04 – 3.94 (m, 2H), 2.36 – 2.19 (m, 2H), 1.98 (dtq, *J* = 10.7, 3.7, 1.8 Hz, 1H), 1.94 – 1.84 (m, 1H), 1.74 – 1.61 (m, 2H), 1.58 – 1.45 (m, 2H), 1.44 (s, 1H), 1.28 (qd, *J* = 13.0, 3.5 Hz, 1H), 1.12 (d, *J* = 14.7 Hz, 2H), 1.06 (d, *J* = 7.7 Hz, 12H), 0.99 (td, *J* = 7.2, 4.9 Hz, 3H) ¹³C NMR (126 MHz, C₆D₆) δ 175.27, 82.65, 82.45, 82.38, 59.36, 50.53, 50.51, 44.07, 43.04, 42.46, 30.58, 29.73, 28.33, 27.16, 26.95, 26.81, 26.45, 26.22, 24.48, 24.44, 13.92. ¹¹B NMR (160 MHz, C₆D₆) δ 34.15. HRMS (ES⁺) *m/z* calcd. for C₁₅H₂₇B₁O₄Na [M+Na] 305.1900; Found. 305.1893. All carbon peaks were reported for both isomers. Specific carbon resonances for each isomer were not determined. An unknown aromatic compound with peaks at 8.88 (s), 8.18 (d, *J* = 8.2Hz) and 8.07 (d, *J* = 7.3Hz) in a 1:1:1 ratio was found to be at 4% of the sample when compared to the peak at 4.04-3.94 ppm. While this impurity matched the splitting pattern and coupling constant of the starting material, the location of the resonances does not match. If this was the starting material the only peak that would potentially be visible in the carbon spectra would be the pinacol methyl protons which would make all 21 carbons show up from major isomer, minor and impurity compounds. An unknown impurity signal (potentially

water) was found at 0.2 that integrated to 1.9% when compared to the 1H at 4.04-3.94 ppm.

A second boron signal was observed at 31.1 ppm that was attributed to the minor isomer.

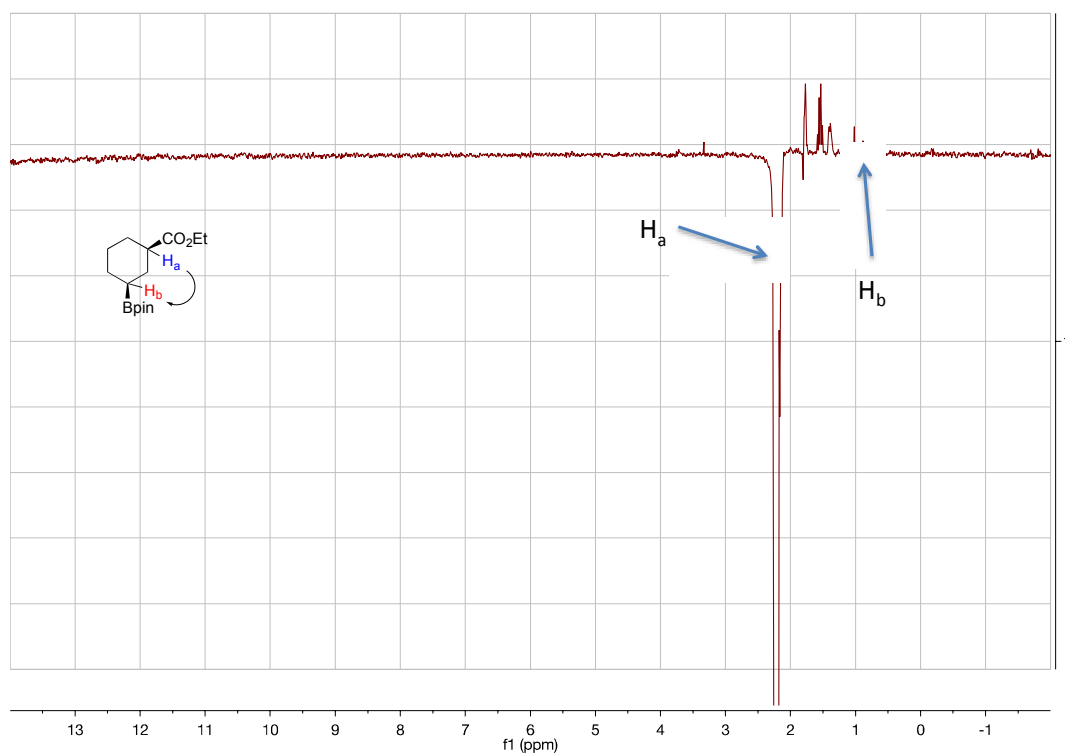
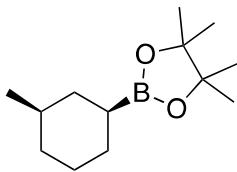


Figure 25. NOE between the major species of **2r** showing cis stereochemistry



4,4,5,5-tetramethyl-2-(3-methylcyclohexyl)-1,3,2-dioxaborolane (2s)

4,4,5,5-Tetramethyl-2-(*m*-tolyl)-1,3,2-dioxaborolane (116 mg, 0.5 mmol), 5% Rh/C (25 mg), and a stir bar were loaded into the pressure vessel. Ethanol (5 mL) was added and the reactor was sealed and pressurized with hydrogen gas (700 psi). After 16 hours the reactor was opened and the contents were filtered through Celite and washed with methanol (3 X 5 mL). The solvent was removed under vacuum to yield a clear oil (90 mg, 76% yield) NMR showed both *cis* and *trans* diastereomers were present in a 2:1 ratio based on the 2 different doublet signal at 0.91 ppm (minor isomer) compared to the signal at 0.84ppm (major isomer). Combined isomer peak shifts ¹H NMR (500 MHz, C₆D₆) δ 2.16 – 2.07 (tm, 1H *J* = 13.7 Hz), 1.92 (tm, *J* = 11.9 Hz, 1H), 1.74 – 1.35 (m, 2H), 1.34 – 1.10 (m, 2H), 1.02 (d, *J* = 3.5 Hz, 12H), 0.98 – 0.76 (m, 4H). ¹³C NMR (126 MHz, C₆D₆) δ 82.45, 82.22, 36.75, 36.20, 35.43, 35.31, 33.50, 31.28, 27.65, 27.56, 27.48, 25.42, 24.55, 24.53, 24.50, 23.03, 22.68. ¹¹B NMR (160 MHz, C₆D₆) δ 34.17.

Assignable peaks for major isomer: ¹H NMR (500 MHz, C₆D₆) δ 1.96 (tm, *J* = 11.5Hz), 0.88 (d, *J* = 6.5 Hz)

Assignable peaks for minor isomer: ¹H NMR (500 MHz, C₆D₆) δ 2.12 (tm, *J* = 13.7Hz), 0.96 (d, *J* = 6.5 Hz)

“tm” - triplet of multiplets.

HRMS (AP⁻) *m/z* calcd. for C₁₄H₂₈B₁O₃ [M+OMe]⁻ 255.2132; Found. 255.2133.

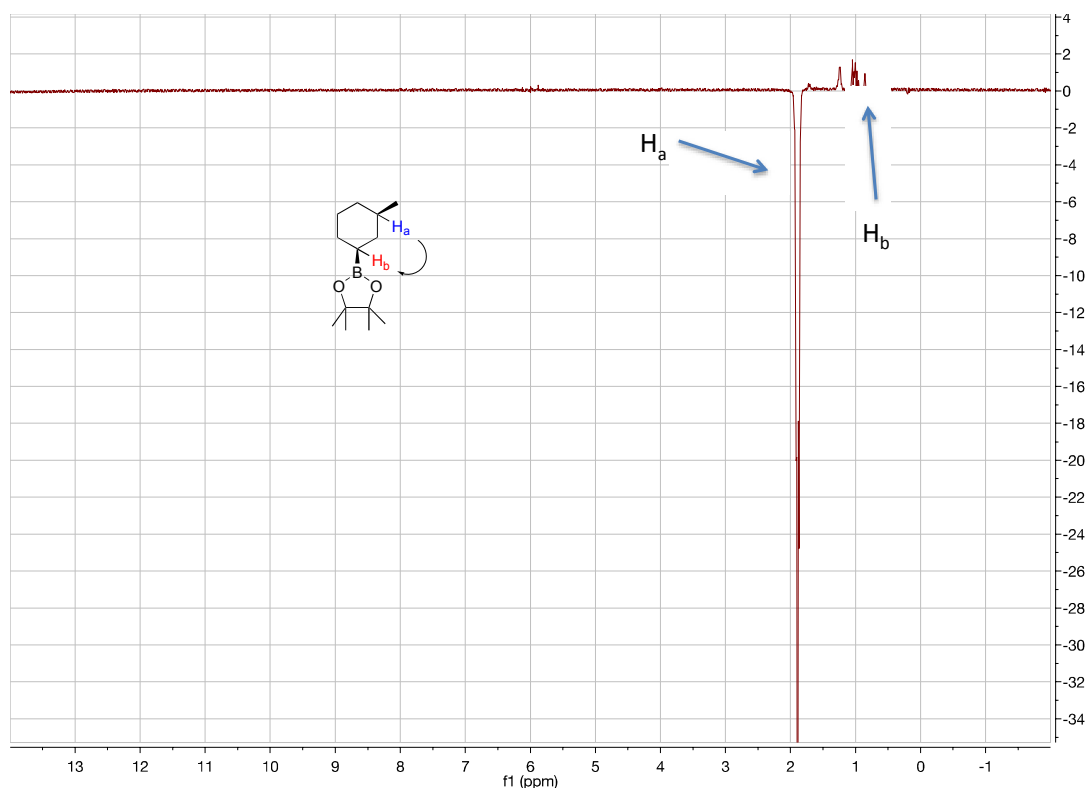
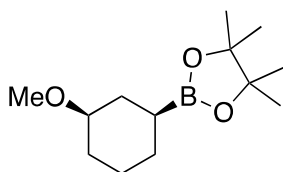


Figure 26. NOE between the major species of **2s** showing cis stereochemistry



2-(3-methoxycyclohexyl)-4,4,5,5-tetramethyl-1,3,2-dioxaborolane(2t)

2-(3-Methoxyphenyl)-4,4,5,5-tetramethyl-1,3,2-dioxaborolane (117 mg, 0.5 mmol), 5% Rh/C (25 mg), and a stir bar were loaded into the pressure vessel. Ethanol (5 mL) was added and the reactor was sealed and pressurized with hydrogen gas (700 psi). After 16 hours the reactor was opened and the contents were filtered through Celite and washed with methanol (3 X 5 mL). The solvent was removed under vacuum to yield a clear oil

(103 mg, 86% yield) $^1\text{H-NMR}$ showed 2 diastereomers in a 4.5:1 ratio based on the integrations of the methoxy groups at 3.14. $^1\text{H NMR}$ (500 MHz, C_6D_6) δ 3.14 (s, 3H), 2.96 (tt, $J = 9.7, 3.9$ Hz, 1H), 2.21 (d, $J = 12.5$ Hz, 1H), 1.92 – 1.85 (m, 1H), 1.85 – 1.67 (m, 2H), 1.62 (s, 2H), 1.54 – 1.41 (m, 1H), 1.41 – 1.23 (m, 2H), 1.15 (tddd, $J = 13.0, 10.1, 6.0, 2.4$ Hz, 1H), 1.02 (s, 12H). $^{13}\text{C NMR}$ (126 MHz, CDCl_3) δ 82.87, 82.66, 79.90, 55.49, 55.47, 32.75, 32.28, 27.90, 27.08, 27.04, 26.94, 26.70, 25.57, 24.74, 24.69, 24.64. $^{11}\text{B NMR}$ (160 MHz, C_6D_6) δ 33.86. HRMS (ESI+) m/z calcd. for $\text{C}_{13}\text{H}_{25}\text{B}_1\text{O}_3\text{Na}$ $[\text{M}+\text{Na}]^+$ 263.1794; Found. 263.1806. The exact peaks were not possible to be separated in the $^1\text{H-NMR}$ spectra due to overlapping signals. Signals in the carbon NMR were not determined to which isomer they corresponded. Major product found to be the cis isomer based on 1D-NOE spectra below. Definitive major isomer distinguishable peaks were found at 3.14 (s) 2.96 (tt, $J = 9.7, 3.9$ Hz). Minor isomer signals were found at 3.30-3.24 (m) and 3.16 (s).

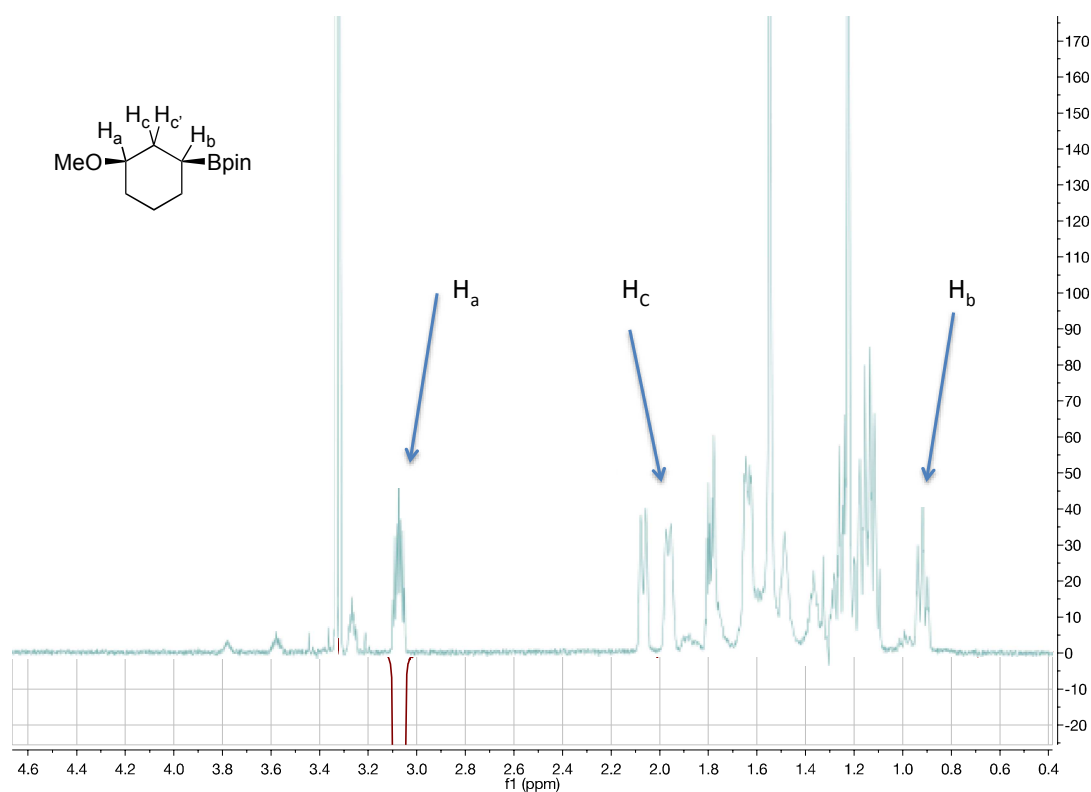
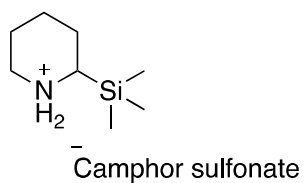


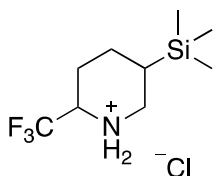
Figure 27. NOE between the major species of **2t** showing cis stereochemistry



2-(Trimethylsilyl)piperidin-1-ium (+)-camphorsulfonate (2u)

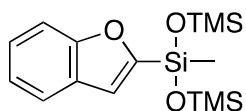
4,4,5,5-Tetramethyl-2-(*m*-tolyl)-1,3,2-dioxaborolane (1.51g, 10 mmol), 5% Rh/C (200 mg), (+) camphor sulfonic acid (2.32 g, 10 mmol), and a stir bar were loaded into the pressure vessel. Ethanol (20 mL) was added and the reactor was sealed and pressurized with hydrogen gas (700 psi). After 24 hours the reactor was opened and the contents were

filtered through Celite and washed with methanol (3 X 5 mL). The solvent was removed under vacuum to yield a clear oil (3.65 g, 95% yield) ^1H NMR (500 MHz, CDCl_3) δ 8.11 (m, 2H), 3.59 (t, $J = 11.5$ Hz, 1H), 3.28 (d, $J = 14.7$ Hz, 1H), 3.19 (q, $J = 5.2$ Hz, 1H), 3.10 – 2.92 (m, 1H), 2.78 (d, $J = 14.7$ Hz, 1H), 2.65 (ddd, $J = 14.9, 11.6, 4.0$ Hz, 1H), 2.58 – 2.45 (m, 1H), 2.32 (ddd, $J = 18.2, 4.8, 3.2$ Hz, 1H), 2.08 – 1.93 (m, 3H), 1.89 (s, 1H), 1.85 – 1.76 (m, 2H), 1.76 – 1.60 (m, 2H), 1.47 – 1.32 (m, 3H), 1.09 (s, 3H), 0.84 (s, 3H), 0.18 (d, $J = 5.2$ Hz, 9H). ^{13}C NMR (126 MHz, CDCl_3) δ 216.72, 58.45, 48.10, 48.08, 47.87, 47.32, 47.13, 47.10, 44.69, 42.92, 42.67, 27.00, 26.89, 24.75, 24.70, 24.61, 23.80, 23.77, 22.52, 22.48, 20.01, 19.85, -3.46. HRMS (ESI+) m/z calcd. for $\text{C}_8\text{H}_{20}\text{N}_1\text{Si}_1$ [M-Camphorsulfonate] $^+$ 158.1365; Found. 158.1366. Ion pairing with the (+)-camphorsulfonate resulted in seeing both R and S isomers of the 2-trimethylsilylpiperidine being distinct from each other in the proton NMR. This differentiation in the carbon NMR results in seeing up to 12 resonances from the piperidinium an 20 resonances from the camphorsulfonate. However, the TMS group is distinctly 1 signal by carbon NMR which indicates that some or many carbon signals fall on top of each other in the spectra. There is a signal at 8.6 that is in the region of a separate NH peak which integrates to 0.45 to the NH_2 of the piperidinium sulfonate of the product. At first it was thought that this signal was from de-silylated piperidinium camphorsulfonate, however the upfield resonances that should correspond to this signal were not seen. As such it is unknown what that peak is.



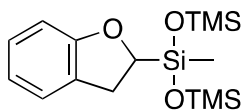
2-(Trifluoromethyl)-5-(trimethylsilyl)piperidin-1-ium chloride(2v)

2-(Trifluoromethyl)-5-(trimethylsilyl)pyridine (110 mg, 0.5 mmol), 5% Rh/C (25 mg), and a stir bar were loaded into the pressure vessel. Ethanol (5 mL) was added and the reactor was sealed and pressurized with hydrogen gas (700 psi). After 16 hours the reactor was opened and the contents were filtered through Celite and washed with methanol (3 X 5 mL). The solvent was removed under vacuum to yield a white solid (111 mg, 99% yield). ^1H NMR (500 MHz, D_2O) δ 4.13 (qdd, $J = 8.8, 6.1, 2.5$ Hz, 1H), 3.89 (dq, $J = 13.3, 6.7, 3.2$ Hz, 1H), 3.52 – 3.35 (m, 1H), 3.26 (dd, $J = 13.3, 4.2$ Hz, 1H), 2.98 (dtd, $J = 22.5, 13.3, 2.3$ Hz, 2H), 2.12 – 2.00 (m, 2H), 1.92 – 1.75 (m, 2H), 1.68 – 1.31 (m, 4H), 1.11 – 0.97 (m, 1H), -0.12 (s, 9H). ^{13}C NMR (126 MHz, D_2O) δ 127.7 (q, $J = 140$ Hz), 58.95, 58.70, 53.86 (q, $J = 30.4$ Hz), 47.64, 46.14, 23.99, 23.98, 23.81, 23.60, 23.17, 22.65, 20.23, -2.37, -2.56. ^{19}F NMR (470 MHz, D_2O) δ Major: -68.50 (d, $J = 8.8$ Hz), -75.53 (d, $J = 6.6$ Hz), Minor: -75.47 (d, $J = 6.7$ Hz), -75.75 (d, $J = 6.6$ Hz). HRMS (ESI+) m/z calcd. for $\text{C}_9\text{H}_{19}\text{N}_1\text{Si}_1\text{F}_3$ $[\text{M}-\text{Cl}]^+$ 226.1239; Found. 226.1237. A small amount of ethanol was present in the spectra clearly visible in the proton and carbon spectra. The ratio between the trimethylsilane signal and the piperdinium C-H signals is not correct which indicates that either the de-silylated product is present in significant quantity or silicate clusters have formed.



3-(Benzofuran-2-yl)-1,1,1,3,5,5,5-heptamethyltrisiloxane (2w')

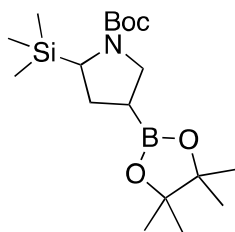
In a nitrogen filled glove box a Schlenk flask (100 mL) was filled with 2,3 benzofuran (1.18g, 10 mmol), bis(trimethylsiloxy)methylsilane (2.44g, 11 mmol) norborene (941mg, 10 mmol), [Ir(OMe)cod]₂ (74 mg, 1.1 mol %), dtbpy (62 mg, 2.4 mol %), THF (10 mL), and a stir bar. The flask was closed with a septa and removed from the glove box. The reaction mixture was heated at 80°C for 24 hours. The reaction was stopped, and the solvent removed by rotary evaporation. The residue was purified by column chromatography (hexanes:ethyl acetate 95:5) to yield a clear colorless oil (2.41g, 71% yield). ¹H NMR values matched literature precedent.¹²⁵ ¹H NMR (500 MHz, CDCl₃) δ 7.66 (dd, *J* = 8.0, 1.9 Hz, 1H), 7.62 – 7.55 (m, 1H), 7.36 (m, 1H), 7.27 (m, 1H), 7.09 (dt, *J* = 2.3, 1.0 Hz, 1H), 0.46 – 0.41 (m, 3H), 0.25 – 0.16 (m, 18H).



3-(2,3-Dihydrobenzofuran-2-yl)-1,1,1,3,5,5,5-heptamethyltrisiloxane(2w)

3-(Benzofuran-2-yl)-1,1,1,3,5,5,5-heptamethyltrisiloxane (169 mg, 0.5 mmol), 10% Pd/C (20 mg), and a stir bar were loaded into the pressure vessel. Ethanol (10 mL) was added and the reactor was sealed and pressurized with hydrogen gas (700 psi). After 16 hours the reactor was opened and the contents were filtered through Celite and washed with methanol (3 X 5 mL). The solvent was removed under vacuum to yield a clear oil (154 mg, 91% yield) ¹H NMR (500 MHz, C₆D₆) δ 7.00 (dd, *J* = 7.3, 1.3 Hz, 1H), 6.97 – 6.89

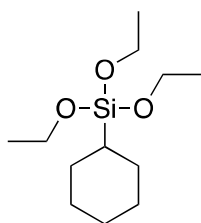
(m, 1H), 6.86 – 6.78 (m, 1H), 6.73 (td, $J = 7.3, 1.0$ Hz, 1H), 4.10 (t, $J = 11.1$ Hz, 1H), 3.11 (ddt, $J = 15.0, 11.4, 1.0$ Hz, 1H), 2.99 (dd, $J = 14.9, 10.8$ Hz, 1H), 0.17 (d, $J = 4.1$ Hz, 3H), 0.11 (s, 9H), 0.05 (s, 9H). ^{13}C NMR (126 MHz, C_6D_6) δ 161.23, 127.81, 127.55, 124.70, 119.98, 109.55, 74.95, 31.10, 1.49, 1.41, -2.91. HRMS (APCI+) m/z calcd. for $\text{C}_{15}\text{H}_{29}\text{O}_3\text{Si}_3$ $[\text{M}+\text{H}]^+$ 341.1424; Found. 341.1428. The silane region of the spectra contains an unknown impurity peaks in approximately a 10% level base on protons in the silicon region. It is undetermined what these impurities are but it is likely that in ethanol siloxane polymers were made. There are many other impurities that are not determined.



Cis-tert-butyl-4-(4,4,5,5-tetramethyl-1,3,2-dioxaborolan-2-yl)-2-(trimethylsilyl)pyrrolidine-1-carboxylate(2x):

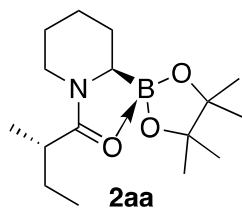
tert-Butyl 4-(4,4,5,5-tetramethyl-1,3,2-dioxaborolan-2-yl)-2-(trimethylsilyl)-1*H*-pyrrole-1-carboxylate (167 mg, 0.5 mmol), 5% Rh/C (25 mg), and a stir bar were loaded into the pressure vessel. Ethanol (5 mL) was added and the reactor was sealed and pressurized with hydrogen gas (700 psi). After 16 hours the reactor was opened and the contents were filtered through Celite and washed with methanol (3 X 5 mL). The solvent was removed under vacuum to yield a white solid (116 mg, 70% yield) with a m.p. of 73.5-75 °C. ^1H NMR (500 MHz, CDCl_3) δ 3.75 (t, $J = 9.5$ Hz, 1H), 3.55-3.30 (m, 1H) 3.28-3.10 (m, 1H) 3.10 (q, $J = 11.7, 9.7$ Hz, 1H), 2.11 (m, 1H), 1.68 – 1.54 (m, 1H), 1.46 (m, 9H), 1.25 (s,

12H), 0.07 (s, 9H). ^{13}C NMR (126 MHz, CDCl_3) δ 154.4, 83.3, 50.05, 48.58, 31.68, 28.60, 26.89, 24.76, 24.72, -2.04. ^{11}B NMR (160 MHz, C_6D_6) δ 33.61. Small impurities around 10% are due to *tert*-Butyl 3-(4,4,5,5-tetramethyl-1,3,2-dioxaborolan-2-yl)-1*H*-pyrrole-1-carboxylate which comes from the desilylated compound. There is a peak in the carbon nmr at 78.3 that is impurity.

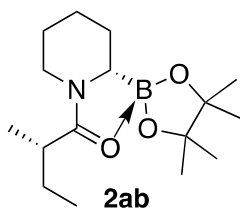


Cyclohexyltriethoxysilane(2y)

Triethoxy phenylsilane (123 mg, 0.5 mmol), 5% Rh/C (25 mg), and a stir bar were loaded into the pressure vessel. Hexanes (10 mL) were added and the reactor was sealed and pressurized with hydrogen gas (700 psi). After 16 hours the reactor was opened and the contents were filtered through Celite and washed with Hexanes (3 X 10 mL). The solvent was removed under vacuum to yield a clear oil (103 mg, 84% yield) ^1H NMR (500 MHz, CDCl_3) δ 3.81 (q, $J = 7.0$ Hz, 6H), 1.89 – 1.55 (m, 6H), 1.21 (t, $J = 7.1$ Hz, 16H), 0.79 (tt, $J = 12.4, 3.0$ Hz, 2H). ^{13}C NMR (126 MHz, CDCl_3) δ 58.40, 27.69, 27.66, 26.80, 26.77, 26.68, 22.84, 18.31. ^{29}Si NMR (99 MHz, CDCl_3) δ -48.51.

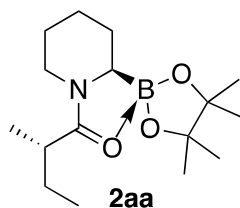


(S)-2-Methyl-1-((R)-2-(4,4,5,5-tetramethyl-1,3,2-dioxaborolan-2-yl)piperidin-1-yl)butan-1-one (2za):



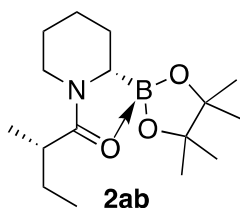
(S)-2-Methyl-1-((S)-2-(4,4,5,5-tetramethyl-1,3,2-dioxaborolan-2-yl)piperidin-1-yl)butan-1-one (2zb)

In a 2-dram vial 2-(4,4,5,5-tetramethyl-1,3,2-dioxaborolan-2-yl)piperidin-1-ium bromide (435 mg, 1.5 mmol) was loaded along with a stir bar and ethyl acetate (10 mL). To this stirred suspension was added (S)-2-methylbutyric anhydride (0.3 mL, 1.5 mmol) followed by 1,8-diazabicyclo[5.4.0]undec-7-ene (0.45 mL, 3 mmol). The reaction mixture was stirred for 30 minutes. The solvent was removed by rotary evaporation. Silica column chromatography (MeOH:EtOAc:hexanes 1:10:89 to 2:20:78) was performed to yield 3 differing solutions across multiple fractions. Upon removal of solvent via rotary evaporation solution A (a clear solid 47.8 mg, 11% yield) contained compound **2za**. Fraction B a clear crystalline solid contained a mixture of 2 different components. Fraction C (a white solid, 65.4 mg, 15% yield) contained **2zb**. Suitable crystals for x-ray crystallography were obtained by slow evaporation of hexanes of 2za.



(S)-2-methyl-1-((R)-2-(4,4,5,5-tetramethyl-1,3,2-dioxaborolan-2-yl)piperidin-1-yl)butan-1-one (2za):

^1H NMR (500 MHz, C_6D_6) δ 2.87 (dd, $J = 13.1, 4.5$ Hz, 1H), 2.34 – 2.24 (m, 1H), 2.16 (td, $J = 12.9, 3.2$ Hz, 1H), 1.85 – 1.72 (m, 2H), 1.64 – 1.53 (m, 1H), 1.53 – 1.47 (m, 1H), 1.42 (d, $J = 8.2$ Hz, 12H), 1.11 – 0.93 (m, 3H), 0.90 – 0.77 (m, 1H), 0.76 (d, $J = 6.8$ Hz, 3H), 0.59 (t, $J = 7.4$ Hz, 3H). ^{13}C NMR (126 MHz, C_6D_6) δ 176.32, 79.45, 44.25, 33.16, 27.53, 26.54, 25.98, 25.65, 25.56, 24.51, 16.03, 11.24. ^{11}B NMR (160 MHz, C_6D_6) δ 13.65. HRMS (ESI+) m/z calcd. for $\text{C}_{16}\text{H}_{31}\text{B}_1\text{N}_1\text{O}_3$ $[\text{M}+\text{H}]^+$ 296.2397; Found. 296.2404.



(S)-2-methyl-1-((S)-2-(4,4,5,5-tetramethyl-1,3,2-dioxaborolan-2-yl)piperidin-1-yl)butan-1-one (2zb)

^1H NMR (500 MHz, C_6D_6) δ 2.87 (dt, $J = 13.0, 2.9$ Hz, 1H), 2.30 (dd, $J = 12.8, 3.7$ Hz, 1H), 2.19 (td, $J = 12.9, 3.2$ Hz, 1H), 1.85 – 1.74 (m, 2H), 1.58 (dtd, $J = 14.1, 12.8, 3.4$ Hz, 1H), 1.53 – 1.43 (m, 2H), 1.41 (d, $J = 7.1$ Hz, 12H), 1.10 – 0.92 (m, 3H), 0.89 – 0.80 (m, 1H), 0.76 (d, $J = 6.9$ Hz, 3H), 0.60 (t, $J = 7.5$ Hz, 3H). ^{13}C NMR (126 MHz, C_6D_6) δ 176.55, 79.51, 74.13, 44.36, 33.33, 27.35, 26.32, 26.08, 25.62, 25.40, 24.82, 24.50, 16.26, 11.23. ^{11}B NMR (160 MHz, C_6D_6) δ 13.57. HRMS (ESI+) m/z calcd. for $\text{C}_{16}\text{H}_{31}\text{B}_1\text{N}_1\text{O}_3$ $[\text{M}+\text{H}]^+$ 296.2397; Found. 296.2406

Two singlets appear in the spectra of compound **2zb** at 2.47 and 1.11 respectively. They are in a 1:6 ratio to each other and are free pinacol in the sample. Relative to the bound pinacol the free pinacol makes up a 28.4% mol to mol ratio of the sample.

4.3 Experimental information for Chapter 3

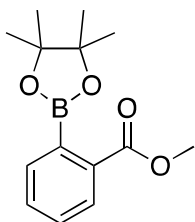
General procedure for Table 9

In a nitrogen-filled glove box, a 3 mL Wheaton® conical vial was charged with [Ir(OMe)COD]₂ (6.6 mg, 0.01 mmol), a monodentate pyridine (0.02 mmol), and bis(pinacolato)diboron (254 mg, 1 mmol). Tetrahydrofuran (2 mL) was added via syringe. A triangular stir bar was added followed by methyl benzoate (126 µL, 1.0 mmol). The conical vial was capped, removed from the glove box and heated to 70 °C for 14 hours. A GC/FID sample was made containing reaction solution (10 µL), 0.5 M naphthalene in ethyl acetate (100 µL) and ethyl acetate (890 µL). The results of the GC/FID were compared to a calibration curve of methyl 2-(4,4,5,5-tetramethyl-1,3,2-dioxaborolan-2-yl)benzoate. Each ligand tested was run in duplicate. The *ortho*:(*meta*+*para*) ratio was estimated based on the GC/FID integrations.

General procedure for Table 10

In a nitrogen filled glove box, a 3 mL Wheaton® conical vial was charged with [Ir(OMe)COD]₂ (6.6 mg, 0.01 mmol), a monodentate pyridine (0.02 mmol), and bis(pinacolato)diboron (127 mg, 1 mmol). Tetrahydrofuran (1.5 mL) was added via syringe. A triangular stir bar was added followed by methyl benzoate (126 µL, 1.0 mmol). The conical vial was capped, removed from the glove box and heated to 70 °C for 14 hours. A GC/FID sample was made containing reaction solution (10 µL), 0.5 M naphthalene in ethyl acetate (100 µL) and ethyl acetate (890 µL). The results of the GC/FID were compared to a calibration curve of methyl 2-(4,4,5,5-tetramethyl-1,3,2-

dioxaborolan-2-yl)benzoate. Each ligand tested was run in duplicate. The *ortho*:(*meta*+*para*) ratio was estimated based on the GC/FID integrations.



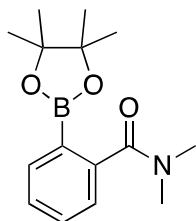
Methyl 2-(4,4,5,5-tetramethyl-1,3,2-dioxaborolan-2-yl)benzoate (3z)⁸

“Closed system” - In a nitrogen filled glove box a 3 mL Wheaton® conical vial was charged with [Ir(OMe)COD]₂ (6.6 mg, 0.01 mmol), 2-methoxyisonicotinonitrile (2.6 mg, 0.02 mmol) and bis(pinacolato)diboron (305 mg, 1.2 mmol). Tetrahydrofuran (1.5 mL) was added via syringe. A triangular stir bar was added followed by addition of methyl benzoate (126 µL, 1.0 mmol). The conical vial was capped, removed from the glove box and heated to 70 °C for 16 hours. The solution was opened to air and concentrated using a rotary evaporator. Column chromatography (10:90 EtOAc : hexanes) on the residue yielded a clear colorless oil (135 mg, 55% yield). ¹H NMR (500 MHz, CDCl₃, ppm) δ 7.94 (d, 1H, *J* = 7.8 Hz) 7.55-7.48 (m, 2H) 7.45-7.40 (m, 1H) 3.92 (s, 3H) 1.43 (s, 12H). Data matched literature reference.¹²⁶

“Open system” – In a nitrogen filled glove box a 10 mL Schlenk flask was charged with [Ir(OMe)COD]₂ (6.6 mg, 0.01 mmol), 2-methoxyisonicotinonitrile (2.6 mg, 0.02 mmol), and bis(pinacolato)diboron (192 mg, 0.77 mmol). Tetrahydrofuran (1.5 mL) was added via syringe. A small stir bar was added to the Schlenk flask followed by addition of methyl benzoate (126 µL, 1.0 mmol) via a microliter syringe. A condenser fitted with

septa was attached to the Schlenk flask. The whole apparatus was removed from the glove box and connected to a nitrogen line through a needle inserted into the septa under positive nitrogen flow. An oil bath was used to heat the reaction to 70 °C for 4 hours. Column chromatography (5:95 EtOAc:hexanes) yielded a clear colorless oil (130 mg, 64% yield based on B₂pin₂, 50% yield based on arene). ¹H NMR (500 MHz, CDCl₃, ppm) δ 7.94 (d, 1H, *J* = 7.8 Hz) 7.55-7.48 (m, 2H) 7.45-7.40 (m, 1H) 3.92 (s, 3H) 1.43 (s, 12H). Data matched literature reference.¹²⁶

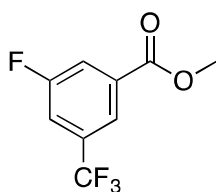
Diborylated methyl benzoate (28% by GC/FID ratio) was observed in the crude reaction material for both open and closed systems by GC/FID but never recovered. Other mono borylated isomers were observed in trace amounts by GC/FID in the crude reaction but upon workup only *ortho* borylated product was observed in the ¹H-NMR.



***N,N*-Dimethyl-2-(4,4,5,5-tetramethyl-1,3,2-dioxaborolan-2-yl)benzamide (3aa)⁹**

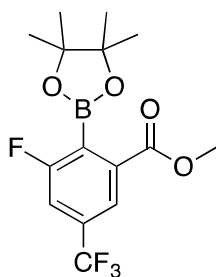
In a nitrogen filled glove box a 3 mL Wheaton® conical vial was charged with [Ir(OMe)COD]₂ (6.6 mg, 0.01 mmol), 2-methoxyisonicotinonitrile (2.6 mg, 0.02 mmol), *N,N*-dimethylbenzamide (149 mg, 1.0 mmol), and bis(pinacolato)diboron (305 mg, 1.2 mmol). Tetrahydrofuran (1.5 mL) was added via syringe. A triangular stir bar was added and the conical vial was capped. The reaction vial was removed from the glove box and heated to 70 °C for 16 hours. The solution was opened to air and concentrated using a rotary evaporator. Column chromatography (50:50 EtOAc:hexanes) on the residue

yielded a white solid (211 mg, 77% yield). ^1H NMR (500 MHz, CDCl_3 , ppm) δ 7.82 (dd, 1H, $J=7.8, 0.9$ Hz) 7.45 (td, 1H $J=7.8, 1.4$ Hz) 7.37 (td, 1H, $J=7.3, 1.0$ Hz) 7.30 (d, 1H, $J=7.1$ Hz) 2.97 (br s, 6H) 1.32 (s, 12H). Data matched literature reference.¹²⁷ There were 2 impurity peaks at 1.26 and 1.23 that integrated to 3% relative to the pinacol ester on compound **3aa**. There was also an impurity at 2.02 that is likely acetone that integrated to less than 0.2% based on adjustment for number of protons.



Methyl 3-fluoro-5-(trifluoromethyl)benzoate (3ab):

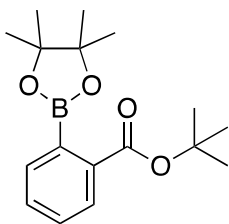
A 50 mL round bottom flask was charged with 3-fluoro-5-(trifluoromethyl) benzoic acid (865 mg, 4.15 mmol), methanol (20 mL), and concentrated sulfuric acid (0.5 mL). The flask was fitted with a condenser, a stir bar was added and the reaction solution was refluxed for 3 hours. To the reaction mixture 20 mL of diethyl ether was added and the solution was washed with saturated potassium carbonate (3 x 50 mL), the organic layer was dried over magnesium sulfate and concentrated under vacuum to yield a clear colorless oil (712 mg, 77 %) ^1H NMR (500 MHz, CDCl_3 , ppm) δ 8.11 (s, 1H) 7.92 (d, 1H, $J=9.0$ Hz) 7.52 (d, 1H, $J=8.3$ Hz) 3.97 (s, 3H). ^{13}C NMR (125 MHz, CDCl_3 , ppm) 164.6 (d, $J_{\text{CF}}=2.7$ Hz), 163.3, 161.3, 133.4 (d, $J_{\text{CF}}=8.0$ Hz), 122.9 (q, $J_{\text{CF}}=274.9$ Hz), 122.3 (t, $J_{\text{CF}}=4.0$ Hz), 120.0 (d, $J_{\text{CF}}=22.9$ Hz), 117.1 (dq, $J_{\text{CF}}=24.6, 3.6$ Hz), 52.8. ^{19}F NMR (470 MHz, CDCl_3 , ppm) δ -63.02, -109.59 ($J=8.0$ Hz). Anal. calcd. for $\text{C}_9\text{H}_6\text{F}_4\text{O}_2$ C 48.66 H 2.72; found C 48.83 H 3.33.



Methyl 3-fluoro-2-(4,4,5,5-tetramethyl-1,3,2-dioxaborolan-2-yl)-5-(trifluoromethyl)benzoate (3ab)

In a nitrogen filled glove box a 3 mL Wheaton® conical vial was charged with [Ir(OMe)COD]₂ (6.6 mg, 0.01 mmol), 2-methoxyisonicotinonitrile (2.6 mg, 0.02 mmol), and bis(pinacolato)diboron (305 mg, 1.2 mmol). Tetrahydrofuran (1.5 mL) was added via syringe followed by methyl 3-fluoro-5-(trifluoromethyl)benzoate (222 mg, 1.0 mmol). A triangular stir bar was added and the conical vial was capped. The reaction vial was removed from the glove box and heated to 70 °C for 16 hours. The vial was opened to air and concentrated using a rotary evaporator. Column chromatography (5:95 EtOAc:hexanes) on the residue yielded a light brown solid (237 mg, 84% yield) with a m.p. 73-74 °C. ¹H NMR (500 MHz, CDCl₃, ppm) δ 8.04 (d, 1H, *J* = 1.0 Hz) 7.46 (d, 1H, *J* = 7.8 Hz) 3.97 (s, 3H) 1.45 (s, 12H). ¹³C NMR (125 MHz, CDCl₃, ppm) δ 166.1 (d, *J* = 2.6 Hz), 165.9, 164.0, 136.2 (d, *J*_{CF} = 9.8 Hz), 133.7 (dq, *J* = 34.3, 8.8 Hz), 122.8 (dq, *J*_{CF} = 274.8, 2.9 Hz), 121.5 (t, *J*_{CF} = 3.9 Hz), 116.3 (dq, *J*_{CF} = 27.8, 4.1 Hz), 85.0, 53.1, 24.8. ¹⁹F NMR (470 MHz, CDCl₃, ppm) δ -63.02, -103.04 (*J* = 9.0 Hz). ¹¹B NMR (160 MHz, CDCl₃, ppm) 30.53. HRMS (ESI-) *m/z* calcd. for C₁₄H₁₄BO₄F₄ [M-CH₃]⁻ 333.0924; found 333.0935. Regiochemistry was assigned based on size of the aromatic coupling constants. Having 1 aromatic proton with a coupling constant as low as 1 Hz indicates

that the proton is only influenced by long-range coupling. This means that only 1 proton in the aromatic region is on a carbon adjacent to a carbon-fluorine bond.

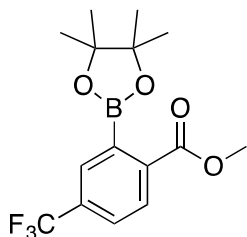


***tert*-Butyl (2-(4,4,5,5-tetramethyl-1,3,2-dioxaborolan-2-yl))benzoate (3ac)**

“Closed system” - In a nitrogen filled glove box a 3 mL Wheaton® conical vial was charged with [Ir(OMe)COD]₂ (6.6 mg, 0.01 mmol), 2-methoxyisonicotinonitrile (2.6 mg, 0.02 mmol), and bis(pinacolato)diboron (305 mg, 1.2 mmol). Tetrahydrofuran (1.5 mL) was added via syringe. A triangular stir bar was added followed by addition of *tert*-butyl benzoate (126 μL, 1.0 mmol). The conical vial was capped, removed from the glove box and heated to 70 °C for 16 hours. The solution was opened to air and concentrated using a rotary evaporator. Column chromatography (10:90 EtOAc:hexanes) yielded a white solid (252 mg, 83% yield). ¹H NMR (500 MHz, CDCl₃, ppm) δ 7.82 (d, 1H, *J* = 7.8 Hz) 7.48-7.44 (m, 2H) 7.37 (m, 1H) 1.59 (s, 9H) 1.42 (s, 12H). Data matched previously reported literature data.¹²⁷ There existed small amounts of impurities between 1.4 and 1.2 it is believed that those come from boronates. They could also possibly come from a solvent mixture but this is unknown. The integrations of these impurities add up to 12% relative to that of the pinacol ester of the target compound.

“Open system” - In a nitrogen filled glove box a 10 ml Schlenk flask was charged with [Ir(OMe)COD]₂ (6.6 mg, 0.01 mmol), 2-methoxyisonicotinonitrile (2.6 mg, 0.02 mmol),

and bis(pinacolato)diboron (305 mg, 1.2 mmol) followed by addition of 1.5 mL of THF. *tert*-butyl benzoate (178 μ L, 1.0 mmol) was added to the solution via microliter syringe. The flask was fitted with a condenser with septa on top of it and the whole apparatus was removed from the glove box. The apparatus was connected to a Schlenk line via a needle under positive nitrogen pressure. The solution was heated to 70 $^{\circ}$ C for 9 hours. After heating was done, the solvent was removed using a rotary evaporator and the oily residue was purified by column chromatography (5:95 EtOAc:hexanes) which yielded a white solid (226 mg, 74% yield). 1 H NMR (500 MHz, CDCl_3 , ppm) δ 7.82 (d, 1H, $J = 7.8$ Hz) 7.48-7.44 (m, 2H) 7.38-7.34 (m, 1H) 1.59 (s, 9H) 1.42 (s, 12H). Data matched previously reported literature.¹²⁷

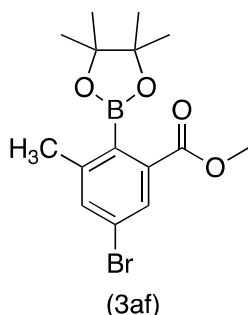
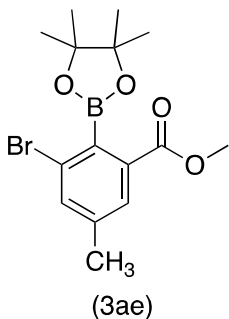


Methyl 2-(4,4,5,5-tetramethyl-1,3,2-dioxaborolan-2-yl)-4-(trifluoromethyl)benzoate (3ad)

“Closed system” - In a nitrogen filled glove box a 3 mL Wheaton® conical vial was charged with $[\text{Ir}(\text{OMe})\text{COD}]_2$ (6.6 mg, 0.01 mmol), 2-methoxyisonicotinonitrile (2.6 mg, 0.02 mmol), and bis(pinacolato)diboron (305 mg, 1.2 mmol). Tetrahydrofuran (1.5 mL) was added via syringe. A triangular stir bar was added followed by addition of methyl 4-(trifluoromethyl)benzoate (160 μ L, 1.0 mmol). The conical vial was capped, removed from the glove box and heated to 70 $^{\circ}$ C for 16 hours. The solution was opened to air and concentrated using a rotary evaporator. Column chromatography (5:95 EtOAc:hexanes)

on the residue yielded a clear colorless oil (215 mg, 65% yield). $^1\text{H-NMR}$ (500 MHz, CDCl_3 , ppm) δ 8.04 (d, 1H, $J= 7.6$ Hz) 7.75 (s, 1H) 7.69 (d, 1H, $J= 7.6$ Hz) 3.95 (s, 3H) 1.44 (s, 12H). Data matched literature reference.¹²⁷ A small amount of boronate impurities were on the spectra at 1.26 ppm with an integration of 5% relative to the pinacol ester peak from the target compound

“Open system” – In a nitrogen filled glove box a 10 mL Schlenk flask was charged with $[\text{Ir}(\text{OMe})\text{COD}]_2$ (6.6 mg, 0.01 mmol), 2-methoxyisonicotinonitrile (2.6 mg, 0.02 mmol), and bis(pinacolato)diboron (192 mg, 0.77 mmol). Tetrahydrofuran (1.5 mL) was added via syringe. A small stir bar was added to the Schlenk flask followed by addition of methyl 4-(trifluoromethyl)benzoate (160 μL , 1.0 mmol) via a microliter syringe. A condenser fitted with a septa was attached to the Schlenk flask. The whole apparatus was removed from the glove box and connected to a nitrogen line through a needle inserted into the septa under positive nitrogen flow. An oil bath was used to heat the reaction at 70 $^\circ\text{C}$ for 4.5 hours. Column chromatography (5:95 EtOAc:hexanes) yielded a clear colorless oil (192 mg, 76% based on B_2pin_2 , 58% based on arene) $^1\text{H NMR}$ (500 MHz, CDCl_3 , ppm) δ 8.04 (d, 1H, $J= 7.6$ Hz) 7.75 (s, 1H) 7.69 (d, 1H, $J= 7.6$ Hz) 3.95 (s, 3H) 1.44 (s, 12H). Data matched literature reference.¹²⁷



Methyl 3-bromo-5-methyl-2-(4,4,5,5-tetramethyl-1,3,2-dioxaborolan-2-yl)benzoate (3ae)

Methyl 3-bromo-5-methyl-6-(4,4,5,5-tetramethyl-1,3,2-dioxaborolan-2-yl)benzoate (3af)

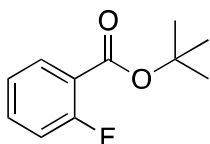
In a nitrogen filled glove box a 10 mL Schlenk flask was charged with $[\text{Ir}(\text{OMe})\text{COD}]_2$ (6.6 mg, 0.01 mmol), 2-methoxyisonicotinonitrile (2.6 mg, 0.02 mmol), and bis(pinacolato)diboron (192 mg, 0.77 mmol). Tetrahydrofuran (1.5 mL) was added via syringe. A small stir bar was added to the Schlenk flask followed by addition of methyl 3-bromo-5-methyl benzoate (162 μL , 1 mmol) via a microliter syringe. A condenser fitted with a septa was attached to the Schlenk flask. The whole apparatus was removed from the glove box and connected to a nitrogen line through a needle inserted into the septa under positive nitrogen flow. An oil bath was used to heat the reaction flask to 70 $^{\circ}\text{C}$ for 48 hours. Column chromatography (4:96 EtOAc:hexanes) yielded compound 3ae as white solid (129.5 mg, 37% yield); m.p. 58-60 $^{\circ}\text{C}$, and compound 3af as a white solid (73.3 mg, 21% yield); m.p. 97-98 $^{\circ}\text{C}$. Starting material (66 mg, 29%) was also recovered. Structure assignments are based on likely positions relative to the size of the adjacent group. A methyl group is slightly larger than that of a bromine and as such the borylation occurs adjacent to the bromine more readily. However, 2D experiments to confirm these assignments were not performed.

Methyl 3-bromo-5-methyl-2-(4,4,5,5-tetramethyl-1,3,2-dioxaborolan-2-yl)benzoate (3ae)

^1H NMR (500 MHz, CDCl_3 , ppm) δ 7.93 (d, 1H, J = 1.7 Hz) 7.48 (d, 1H, J = 2.0 Hz) 3.91 (s, 3H) 2.43 (s, 3H) 1.45 (s, 12H). ^{13}C NMR (125 MHz, CDCl_3 , ppm) δ 167.5, 143.5, 136.1, 135.0, 128.9, 122.7, 84.1, 52.6, 25.3, 21.3. ^{11}B NMR (160 MHz, CDCl_3 , ppm) δ 30.8. HRMS (ESI) m/z calcd. for $\text{C}_{15}\text{H}_{20}\text{BBrNaO}_4$ $[\text{M}+\text{Na}]^+$ 377.0539, found 377.0547.

Methyl 3-bromo-5-methyl-6-(4,4,5,5-tetramethyl-1,3,2-dioxaborolan-2-yl)benzoate (3af)

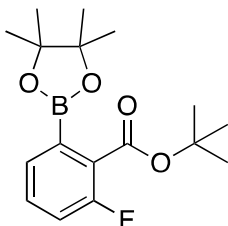
^1H NMR (500 MHz, CDCl_3 , ppm) δ 7.74 (s, 1H) 7.52 (s, 1H) 3.91 (s, 3H) 2.35 (s, 3H) 1.48 (s, 12H). ^{13}C NMR (125 MHz, CDCl_3 , ppm) δ 167.3, 140.6, 136.6, 135.0, 128.4, 126.7, 84.4, 52.5, 25.3, 20.9. ^{11}B NMR (160 MHz, CDCl_3 , ppm) δ 30.2. Anal calcd. for $\text{C}_{15}\text{H}_{20}\text{BBrO}_4$: C 50.75 H 5.68. Found C 50.99 H 5.58.



***tert*-Butyl 2-fluorobenzoate (3ah')**

A round bottom flask (250 mL) was charged with toluene (40 mL), magnesium sulfate (5.2 g, 43.2 mmol), and a stir bar. Concentrated sulfuric acid (0.55 mL) was added to the vigorously stirred suspension. After 15 minutes 2-fluorobenzoic acid (1.48 g, 10.5 mmol) was added and the suspension was stirred for 15 minutes. The round bottom flask was fitted with a septa and *tert*-butanol (4.6 mL, 48.4 mmol) was added via syringe. The suspension was stirred at room temperature for 18 hours. Saturated potassium carbonate (3 x 75 mL) was used to wash the solution. The organic layer was separated and dried over magnesium sulfate. Upon concentration under vacuum, a clear colorless oil (1.51 g,

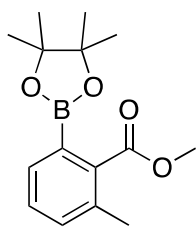
73% yield) was obtained. ^1H NMR (500 MHz, CDCl_3 , ppm) δ 7.87 (td, 1H, $J= 7.9, 1.9$ Hz) 7.51-7.45 (m, 1H) 7.18 (t, 1H, $J= 7.5$ Hz) 7.11 (dd, 1H, $J= 10.5, 8.6$ Hz) 1.61 (s, 9H). ^{19}F NMR (470 MHz, CDCl_3 , ppm) δ -110.3. Data matched literature reference.¹²⁸



***tert*-Butyl 2-fluoro-6-(4,4,5,5-tetramethyl-1,3,2-dioxaborolan-2-yl)benzoate (3ah)**

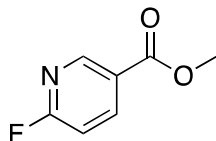
In a nitrogen filled glove box a 3 mL Wheaton® conical vial was charged with $[\text{Ir}(\text{OMe})\text{COD}]_2$ (6.6 mg, 0.01 mmol), 2-methoxyisonicotinonitrile (2.6 mg, 0.02 mmol), and bis(pinacolato)diboron (305 mg, 1.2 mmol). Tetrahydrofuran (1.5 mL) was added via syringe followed by *tert*-butyl 2-fluorobenzoate (196 mg, 1.0 mmol). A triangular stir bar was added and the conical vial was capped. The reaction vial was removed from the glove box and heated to 70 °C for 16 hours. The solution was opened to air and concentrated using a rotary evaporator. ^{19}F -NMR of the crude reaction mixture showed 6 different products plus starting material (22%) with a majority of the mixture being *ortho*-borylation to the ester (57%). Column chromatography (10:90 Et_2O :hexanes) on the residue afforded a white solid (148 mg, 46% yield) m.p.: 36-37 °C. ^1H NMR (500 MHz, CDCl_3 , ppm) δ 7.43-7.35 (m, 2H) 7.12 (ddd, 1H, $J= 10.2, 7.7, 1.6$ Hz) 1.61 (s, 9H) 1.37 (s, 12H). ^{13}C NMR (125 MHz, CDCl_3 , ppm) δ 165.8, 160.7, 158.7, 131.5 (d, $J_{\text{CF}}= 8.0$ Hz), 129.2 (d, $J_{\text{CF}}= 3.7$ Hz), 126.8 (d, $J_{\text{CF}}= 14.4$ Hz), 84.2, 82.4, 28.2, 24.8. ^{19}F NMR (470 MHz, CDCl_3 , ppm) δ -114.4 (dd, $J= 10.1, 5.1$ Hz). ^{11}B NMR (160 MHz, CDCl_3 , ppm) δ 30.7. HRMS (ESI) m/z calcd. for $\text{C}_{17}\text{H}_{24}\text{BFNaO}_4$ $[\text{M}+\text{Na}]^+$ 345.1653; found

345.1663. Determination of regiochemistry was performed by comparing the spectra from literature of CHB of methyl 2-fluoro benzoate where ortho-borylation to both the ester¹²⁹ and the fluorine¹³⁰ are known. With borylation ortho to the fluorine there is a clear and defined triplet at 7.20 while with borylation ortho to the ester there is a clear and defined ddd at 7.16 on the methyl ester. The aromatic splitting pattern matched that of borylation ortho to the ester.



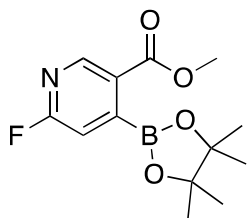
Methyl 2-methyl-6-(4,4,5,5-tetramethyl-1,3,2-dioxaborolan-2-yl)benzoate (3aj)

In a nitrogen filled glove box a 3 mL Wheaton® conical vial was charged with [Ir(OMe)COD]₂ (6.6 mg, 0.01 mmol), 2-methoxyisonicotinonitrile (2.6 mg, 0.02 mmol), and bis(pinacolato)diboron (305 mg, 1.2 mmol). Tetrahydrofuran (1.5 mL) was added via syringe. A triangular stir bar was added followed by addition of methyl *o*-toluate (140 μL, 1.0 mmol). The conical vial was capped, removed from the glove box and heated to 70 °C for 16 hours. The solution was opened to air and concentrated using a rotary evaporator. Column chromatography (5:95 EtOAc:hexanes) on the residue yielded a clear colorless oil (196 mg, 71% yield). ¹H NMR (500 MHz, CDCl₃, ppm) δ 7.55 (d, 1H, *J* = 7.6 Hz) 7.32 (t, 1H, *J* = 7.5 Hz) 7.27 (d, 1H, *J* = 7.5 Hz) 3.89 (s, 3H) 2.39 (s, 3H) 1.34 (s, 12H). Spectral data matched literature reference.^{129,131} Unknown methyl groups appear in the spectra around 2.5 there are 3 other methyl groups that would be from species off of an aromatic. This integrates to a 4:1 product to impurity ratio.



Methyl 6-fluoronicotinate (3ao')

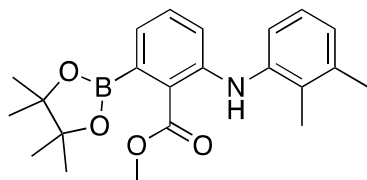
In a 100 mL round bottomed flask 6-fluoro-nicotinic acid (570 mg, 4.04 mmol) was dissolved in methanol (4 mL) and toluene (6 mL). The solution was slowly treated with trimethylsilyl diazomethane (2.2 mL, 2M in dichloromethane). After 2 hours of stirring the solution had a slightly yellow color. The solution was dried under vacuum to yield a white solid (509 mg, 81% yield) m.p. 52-53 °C. ¹H NMR (500 MHz, CDCl₃, ppm) δ 8.88 (d, 1H, *J*=2.0 Hz) 8.40 (td, 1H, *J*= 8.1, 2.4 Hz) 7.00 (dd, 1H, *J*= 8.6, 2.9 Hz) 3.95 (s, 3H). ¹³C NMR (125 MHz, CDCl₃, ppm) δ 166.8, 164.8 (d, *J*_{CF}= 17.3 Hz), 150.4 (d, *J*_{CF}= 17.1 Hz), 142.6 (d, *J*_{CF}= 8.6 Hz), 124.4 (d, *J*_{CF}= 4.6 Hz), 109.5 (d, *J*_{CF}= 37.3 Hz), 52.5. ¹⁹F NMR (470 MHz, CDCl₃, ppm) δ -61.28 (d, 1F, *J*= 6.0 Hz). Data matched literature reference.¹³²



Methyl 6-fluoro-4-(4,4,5,5-tetramethyl-1,3,2-dioxaborolan-2-yl)nicotinate (3ao)

In a nitrogen filled glove box a 3 mL Wheaton® conical vial was charged with [Ir(OMe)COD]₂ (6.6 mg, 0.01 mmol), 2-methoxyisonicotinonitrile (2.6 mg, 0.02 mmol), methyl 6-fluoronicotinate (155 mg, 1.0 mmol), and bis(pinacolato)diboron (305 mg, 1.2

mmol). Tetrahydrofuran (1.5 mL) was added via syringe. A triangular stir bar was added and the conical vial was capped. The reaction vial was removed from the glove box and heated to 70 °C for 16 hours. The solution was opened to air and concentrated using a rotary evaporator. Column chromatography (5:95 EtOAc:hexanes) on the residue yielded a white solid (237 mg, 84% yield); m.p. 83-85 °C. ¹⁹F-NMR revealed about 3% of methyl 6-fluoro-5-(4,4,5,5-tetramethyl-1,3,2-dioxaborolan-2-yl)nicotinate¹³¹ that was unable to be separated. ¹H NMR (500 MHz, CDCl₃, ppm) δ 8.80 (s, 1H) 7.02 (d, 1H, *J* = 2.4 Hz) 3.96 (s, 3H) 1.42 (s, 12H). ¹³C NMR (125 MHz, CDCl₃, ppm) δ 166.1 (d, *J*_{CF} = 14.6 Hz), 164.1, 149.3 (d, *J*_{CF} = 16.0), 127.0 (d, *J*_{CF} = 3.6 Hz), 112.7 (d, *J*_{CF} = 36.3 Hz), 85.1, 52.7, 24.8. ¹⁹F NMR (470 MHz, CDCl₃, ppm) δ -63.38. ¹¹B NMR (160 MHz, CDCl₃, ppm) δ 30.5. HRMS (ESI) *m/z* calc. for (C₁₃H₁₈NBO₄F) [M+H]⁺ 282.1315; found 282.1312.



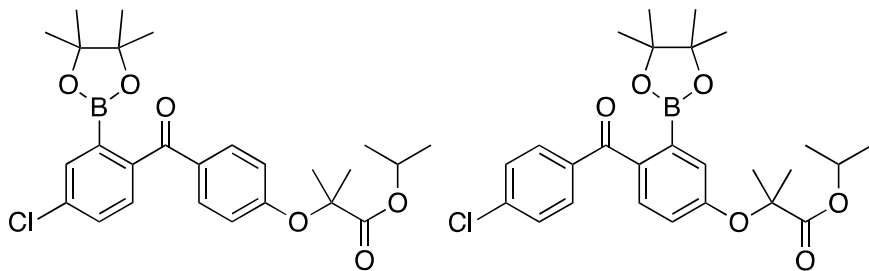
Methyl 2-((2,3-dimethylphenyl)amino)-6-(4,4,5,5-tetramethyl-1,3,2-dioxaborolan-2-yl)benzoate (3az)

In a glove box, a 15 mL pressure tube was charged with [Ir(OMe)COD]₂ (3.3 mg, 0.005 mmol), 2-methoxyisonicotinonitrile (1.3 mg, 0.01 mmol), methyl 2-((2,3-dimethylphenyl)amino)benzoate (128 mg, 0.5 mmol), and bis(pinacolato)diboron (152 mg, 0.6 mmol). Tetrahydrofuran (2 mL) was added via syringe and a stir bar was added. The pressure tube was closed up, removed from the glove box and heated in an oil bath to

85 °C for 16 hours. The reaction was stopped and the volatiles were removed under vacuum. Column chromatography (5:95 EtOAc:Hexane) yielded an off white solid m.p. 96-98 °C (69.0 mg, 38% yield). ¹H NMR (500 MHz, CDCl₃, ppm) δ 8.80 (s, 1H), 7.21 (dd, 1H, *J*= 8.8, 6.6 Hz) 7.12-7.06 (m, 2H) 7.02-6.99 (m, 1H) 6.77(dd, 1H, *J*= 14.5, 0.8 Hz) 6.75 (dd, 1H, *J*= 16.2, 1.4 Hz) 3.92 (s, 3H) 2.32 (s, 3H) 2.14 (s, 3H) 1.40 (s, 12H). ¹³C NMR (125 MHz, CDCl₃, ppm) δ 169.4, 148.5, 138.9, 138.2, 133.1, 132.3, 126.6, 125.9, 122.9, 121.0, 115.2, 113.8, 83.7, 51.8, 25.0, 20.6, 13.9. ¹¹B NMR (160 MHz, CDCl₃, ppm) δ 30.8 (s, br). HRMS (ESI) *m/z* calcd. for C₂₂H₂₉BNO₄ [M+H]⁺ 382.2190, found 382.2201.

(2-((2,3-Dimethylphenyl)amino)phenyl)methanol (3az'):

Also isolated from this reaction by column chromatography was starting material (43.8 mg, 35%) and a yellow oil (2-((2,3-dimethylphenyl)amino)phenyl)methanol (20.4 mg, 18% yield). ¹H NMR (500 MHz, CDCl₃, ppm) δ 7.21-7.17 (m, 2H) 7.09 (t, 1H, *J*= 8.3 Hz) 7.05 (t, 1H, *J*= 7.6 Hz) 7.00 (d, 1H, *J*= 8.7 Hz) 7.89 (d, 1H, *J*= 7.7 Hz) 6.82 (t, 1H, *J*= 7.6 Hz) 4.76 (s, 2H) 2.33 (s, 3H) 2.15 (s, 3H). ¹³C NMR (125 MHz, CDCl₃, ppm) δ 144.6, 140.7, 137.9, 129.4, 129.2, 128.0, 127.0, 125.9, 124.2, 119.2, 118.2, 115.8, 64.9, 20.7, 13.6. Spectral data matched literature.¹³³



(3ba)

(3bb)

Isopropyl 2-(4-(4-chloro-2-(4,4,5,5-tetramethyl-1,3,2-dioxaborolan-2-yl)benzoyl)phenoxy)-2-methylpropanoate (3ba)

Isopropyl 2-(4-(4-chlorobenzoyl)-3-(4,4,5,5-tetramethyl-1,3,2-dioxaborolan-2-yl)phenoxy)-2-methylpropanoate (3bb):

In a nitrogen filled glove box a 10 mL Schlenk flask was charged with [Ir(OMe)COD]₂ (6.6 mg, 0.01 mmol), 2-methoxyisonicotinonitrile (2.6 mg, 0.02 mmol), isopropyl 2-(4-(4-chlorobenzoyl)phenoxy)-2-methylpropanoate (360 mg, 1.0 mmol), and bis(pinacolato)diboron (229 mg, 0.9 mmol). Tetrahydrofuran (2 mL) was added via syringe. A condenser fitted with a septa was attached to the Schlenk flask. The whole apparatus was removed from the glove box and connected to a nitrogen line through a needle inserted into the septa under positive nitrogen flow. An oil bath was used to heat the reaction mixture to 70 °C for 16 hours. Column chromatography (0:100-20:80 Et₂O:hexanes) yielded a clear colorless oil (240 mg, 55% based on B₂pin₂) as a mixture of products in a 5:1 ratio determined by NMR spectroscopy.

Chemical assignments were determined after a series of 2D NMR. The ipso carbon of the aromatic ether is expected to be around the 160 ppm range while the ipso carbon of the aromatic chloride is expected to be around 133 ppm.¹⁰ Using these known expected values the ipso carbon of the ether was correlated to the protons of the two compounds. The minor isomer had proton chemical shifts that were more distinctly visible. The minor component had a proton peak at 7.11 that is a doublet with a j coupling of 2.6 Hz. That is much too small of a coupling constant to be an ortho C-H coupling. As a result that was

labeled the proton adjacent to the boron. This proton, labeled A in the 2D spectra, had a 2D correlation to a carbon peak at 123 for the gHSQC and for gHMBCAD had signals to carbons at 134.8 and 117.7 ppm. The proton for the minor isomer should have shown a correlation to a more downfield carbon near 160 had it been adjacent to the ether. However that was not the case.

Undetermined signals from the inseparable mixture: δ 7.70-7.65 (m, 3.6 H) 7.47-7.39 (m, 3.0 H) 7.10(d, 0.34H, J = 2.5 Hz) 6.82-6.79 (m, 2H) 6.77 (dd, 0.35H, J = 8.5, 2.8 Hz) 5.08 (sept, 1.3H, J = 6.0 Hz) 1.65-1.62 (m, 8.3H) 1.27 (s, 4.3H), 1.22 (s, 4.2H) 1.20 (s, 4.3H) 1.19 (s, 12.2H). ^{13}C NMR (125 MHz, CDCl_3 , ppm) δ 195.9, 195.5, 173.2, 173.1, 159.7, 158.5, 142.2, 138.3, 136.7, 136.5, 134.8, 133.8, 131.8, 131.7, 131.2, 130.0, 129.7, 128.5, 123.2, 117.3, 84.3, 84.0, 79.3, 79.2, 69.3, 25.3, 24.7, 24.5, 21.5. ^{11}B NMR (160 MHz, CDCl_3 , ppm) δ 30.2. HRMS (ESI) m/z calcd. for $\text{C}_{26}\text{H}_{33}\text{BClO}_6$ $[\text{M}+\text{H}]^+$ 487.2063; found 487.2066.

Known peaks for **Isopropyl 2-(4-(4-chloro-2-(4,4,5,5-tetramethyl-1,3,2-dioxaborolan-2-yl)benzoyl)phenoxy)-2-methylpropanoate (3ba):**

^1H NMR (500 MHz, CDCl_3 , ppm) δ 5.08 (sept, 1H, J = 6.0 Hz) 1.19 (s, 12H). ^{13}C NMR (125 MHz, CDCl_3 , ppm) δ 195.9, 173.1, 159.7, 84.3, 79.3, 69.3, 25.3, 24.5, 21.5.

Known peaks for **Isopropyl 2-(4-(4-chlorobenzoyl)-3-(4,4,5,5-tetramethyl-1,3,2-dioxaborolan-2-yl)phenoxy)-2-methylpropanoate (3bb):**

^1H NMR (500 MHz, CDCl_3 , ppm) δ 7.47 (d, 1H, $J= 8.4$ Hz) 7.11 (d, 1H, $J= 2.6$ Hz) 6.78 (dd, 1H, $J= 8.4, 2.6$ Hz) 5.08 (sept, 1H, $J= 6.0$ Hz). ^{13}C NMR (125 MHz, CDCl_3 , ppm) δ 195.5, 173.3, 158.5, 123.3, 84.8, 79.2, 69.3, 25.3, 24.7, 21.5.

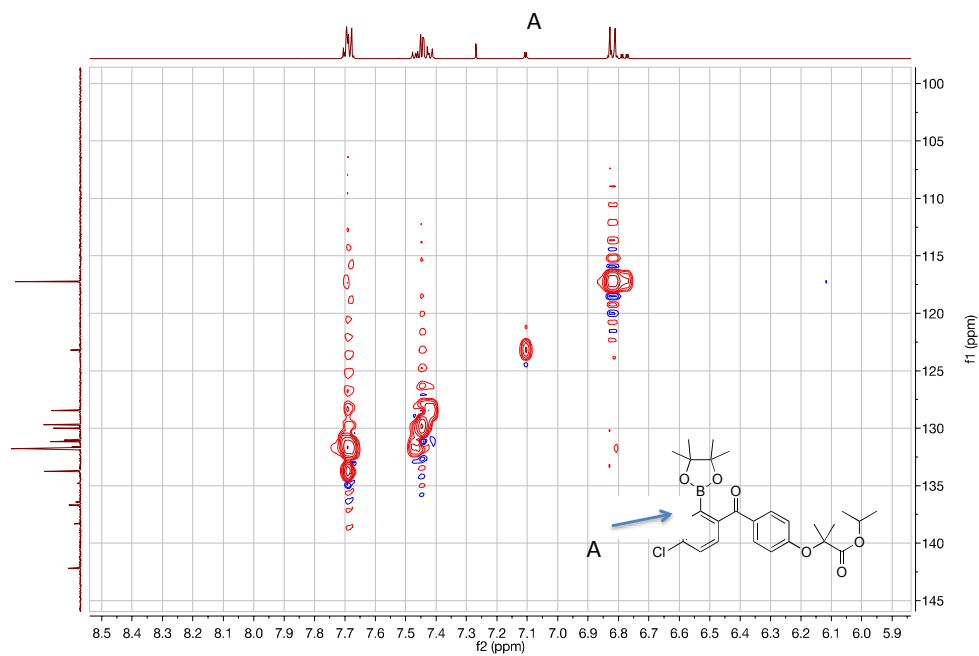


Figure 28. gHMBC for assignments of 3ba and 3bb.

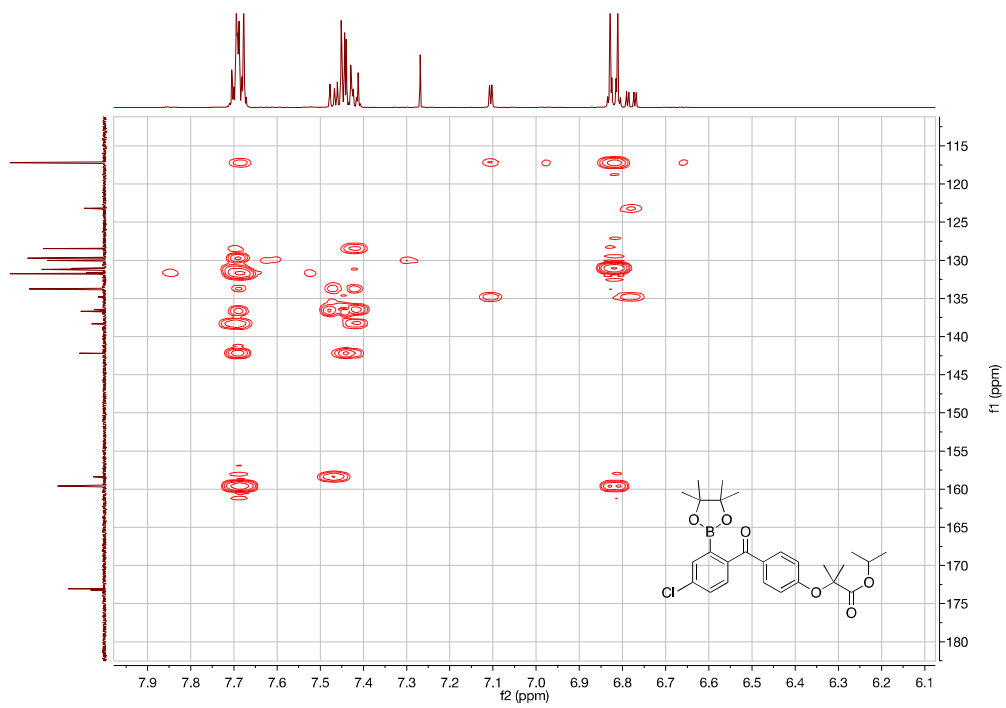


Figure 29. gHMBCAD for assignments of 3ba an 3bb.

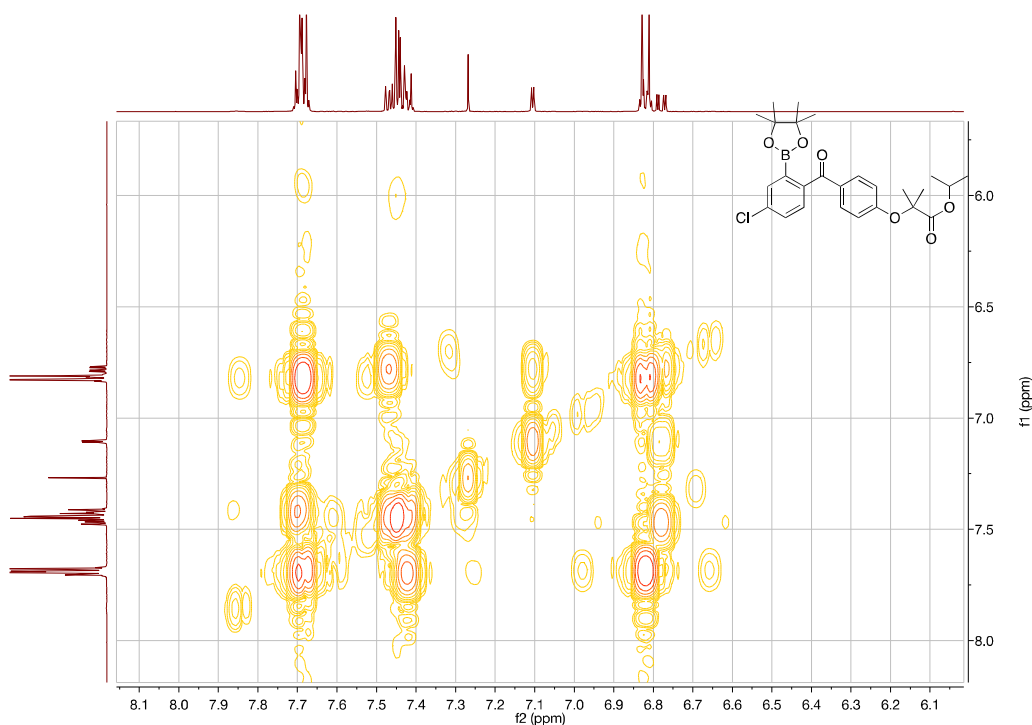


Figure 30. gCOSY for assignments of 3ba and 3bb.

Procedure for Table 16

In a nitrogen filled glove box a stock solution of 2-methoxyisonicotinonitrile (26.1 mg, 0.2 mmol) in tetrahydrofuran (1 mL) was made. Various amounts of this stock solution (0 μ L, 50 μ L, 100 μ L, 200 μ L, and 400 μ L) were added to 10 mL Schlenk flasks containing a stir bar, $[\text{Ir}(\text{OMe})\text{COD}]_2$ (6.6 mg, 0.01 mmol), bis(pinacolato)diboron (305 mg, 1.2 mmol), and *tert*-butyl benzoate (178 μ L, 1.0 mmol). Tetrahydrofuran was added to the Schlenk flask to bring the total amount of tetrahydrofuran up to 1.5 mL (Stock solution plus solvent). The flask was fitted with a condenser with septa on top of it and the whole apparatus was removed from the glove box. The apparatus was connected to a Schlenk

line under positive nitrogen pressure and heated to 70 °C. GC/FID was used to monitor the reactions over time.

Procedure for Scheme 40:

In a nitrogen filled glove box, a 3 mL Wheaton® conical vial was charged with [Ir(OMe)COD]₂ (6.6 mg, 0.01 mmol), 2-methoxyisonicotinonitrile (2.6 mg, 0.02 mmol), and bis(pinacolato)diboron (127 mg, 0.5 mmol). Tetrahydrofuran (1.5 mL) was added via syringe. A triangular stir bar was added followed by methyl benzoate (63 µL, 0.5 mmol) and cyclopropyl phenyl ketone (69.1 µL, 0.5 mmol). The conical vial was capped, removed from the glove box and heated to 70 °C for 3 hours. After 3 hours the solution was cooled and sample for GC/FID was taken. The following results were obtained: cyclopropyl phenyl ketone conversion was 62% and conversion of methyl benzoate was 10%.

General procedure for catalyst concentration reactions Figure 16:

In a nitrogen filled glove box, a well plate was set up with concurrent reactions. To each reaction was added from a stock solution bis(pinacolato)diboron (100 µL, 2M in THF), methyl benzoate (25 µL, 0.2 mmol) dodecane (10 µL) as an internal standard, and changing amounts of iridium and ligand solution such that the iridium to ligand ratio remained at 1:1. The reaction volume was brought up to 0.4 mL with extra THF. The well plate was capped, removed from the glove box and heated on a temperature controlled hot plate at 80 °C for 18h. The crude reaction conversions and selectivity ratios were determined by GC/FID and shown below.

Table 17. Underlying data for Figure 16

Entry	[Ir] ₂ molarity	o:m+p*
1	0.002461408	26.85
2	0.004922816	19.83
3	0.009845633	14.7
4	0.019691265	10.01
5	0.029536898	7.05
6	0.03938253	4.97

General procedure for catalyst concentration reactions Figure 17:

In a nitrogen filled glove box, a well plate was set up with concurrent reactions. To each reaction was added from a stock solution bis(pinacolato)diboron (100 μ L, 2M in THF), methyl benzoate (25 μ L, 0.2 mmol) dodecane (10 μ L) as an internal standard, and a changing amount of iridium from a 0.04M[Ir(OMe)cod]₂ solution. The reaction volume was brought up to 0.4 mL with extra THF. The well plate was capped, removed from the glove box and heated on a temperature controlled hot plate at 80 °C for 18h. The crude reaction conversions and selectivity ratios were determined by GC/FID and shown below.

Table 18. Underlying data for Figure 17

Entry	[Ir] ₂ (mols/L)	Conversion (%)	o:m+p
1	0.002461408	20.7	40
2	0.004922816	16.6	11
3	0.009845633	16.1	1.8
4	0.019691265	20.5	0.823
5	0.029536898	26.5	0.85
6	0.03938253	27.2	0.52

APPENDICES

APPENDIX A

NMR Spectra

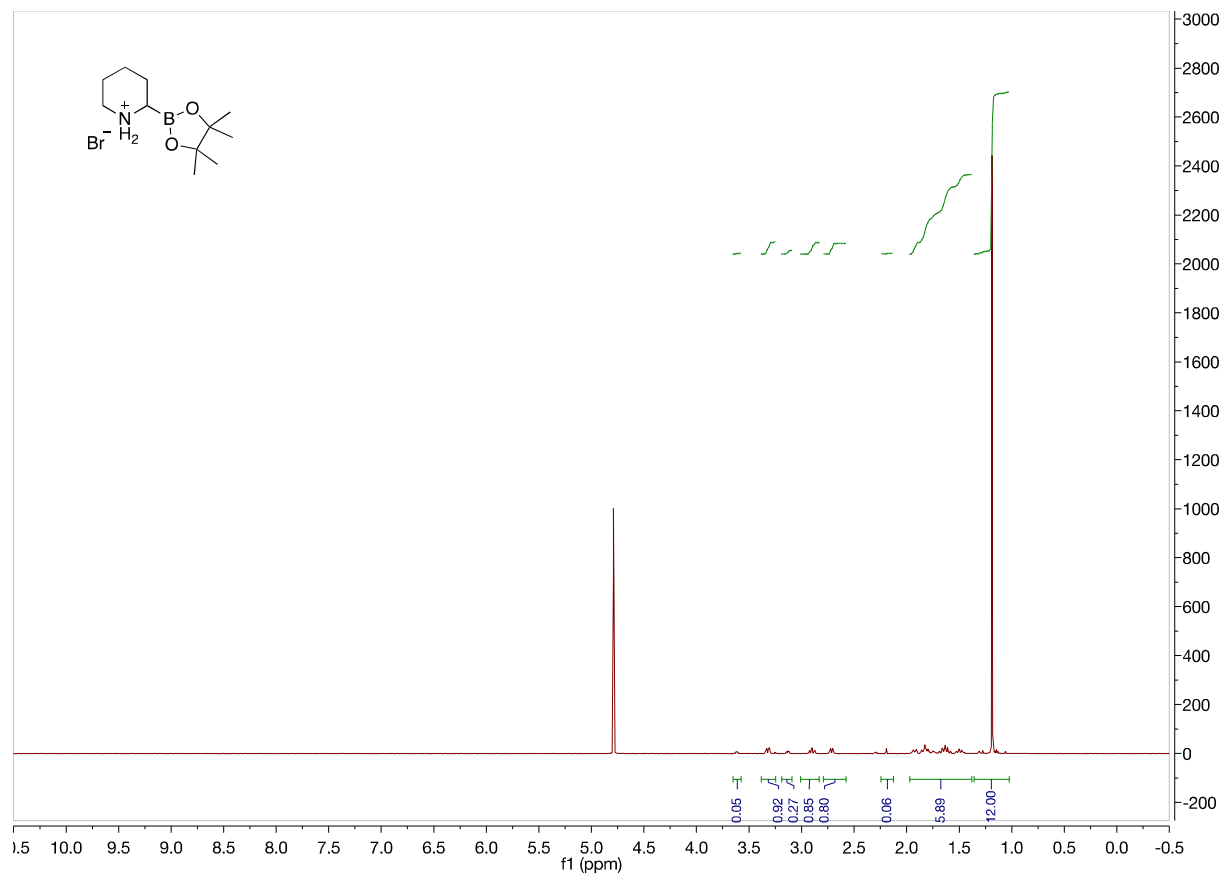


Figure A1. 500 MHz ^1H NMR of **2b** in D_2O

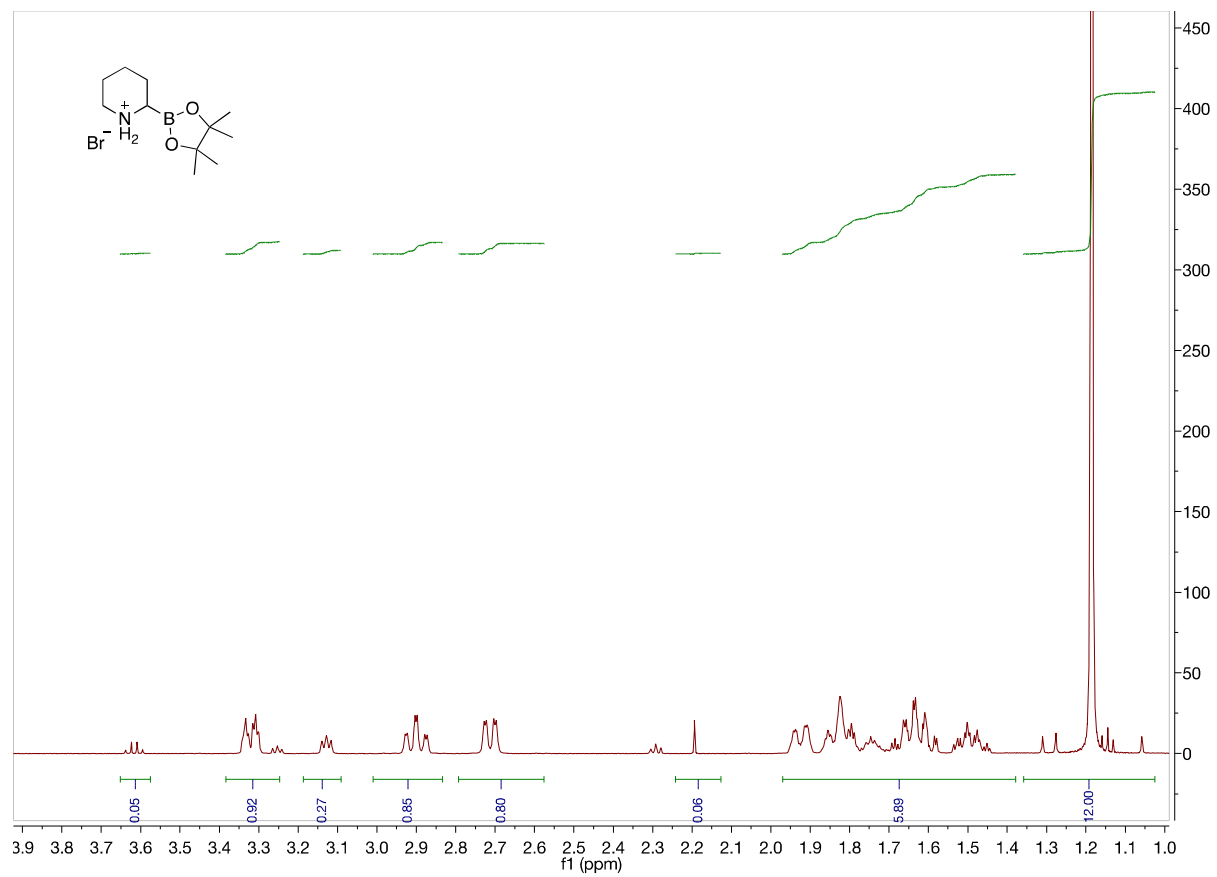


Figure A2. 500 MHz ^1H NMR of **2b** in D_2O from 3.9 to 1.0 ppm

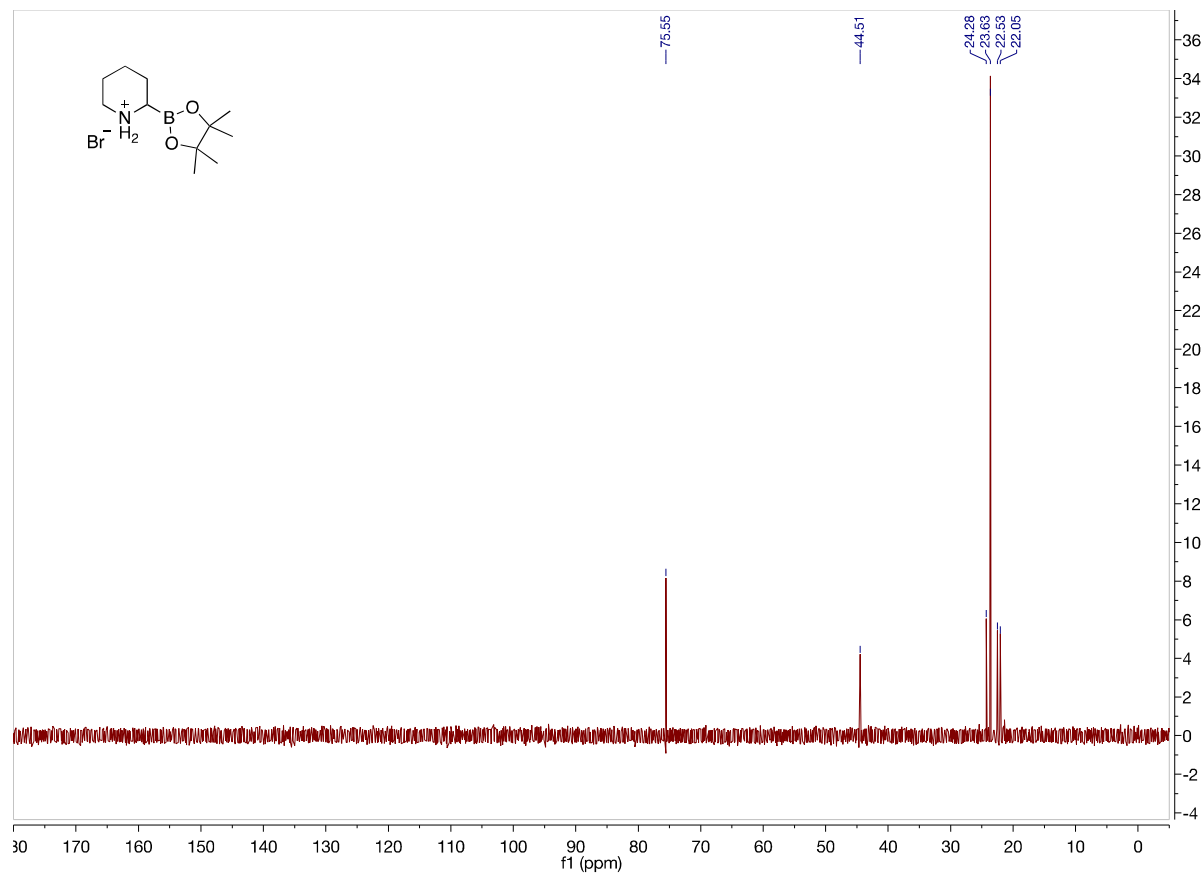


Figure A3. 125 MHz ^{13}C NMR of **2b** in D_2O

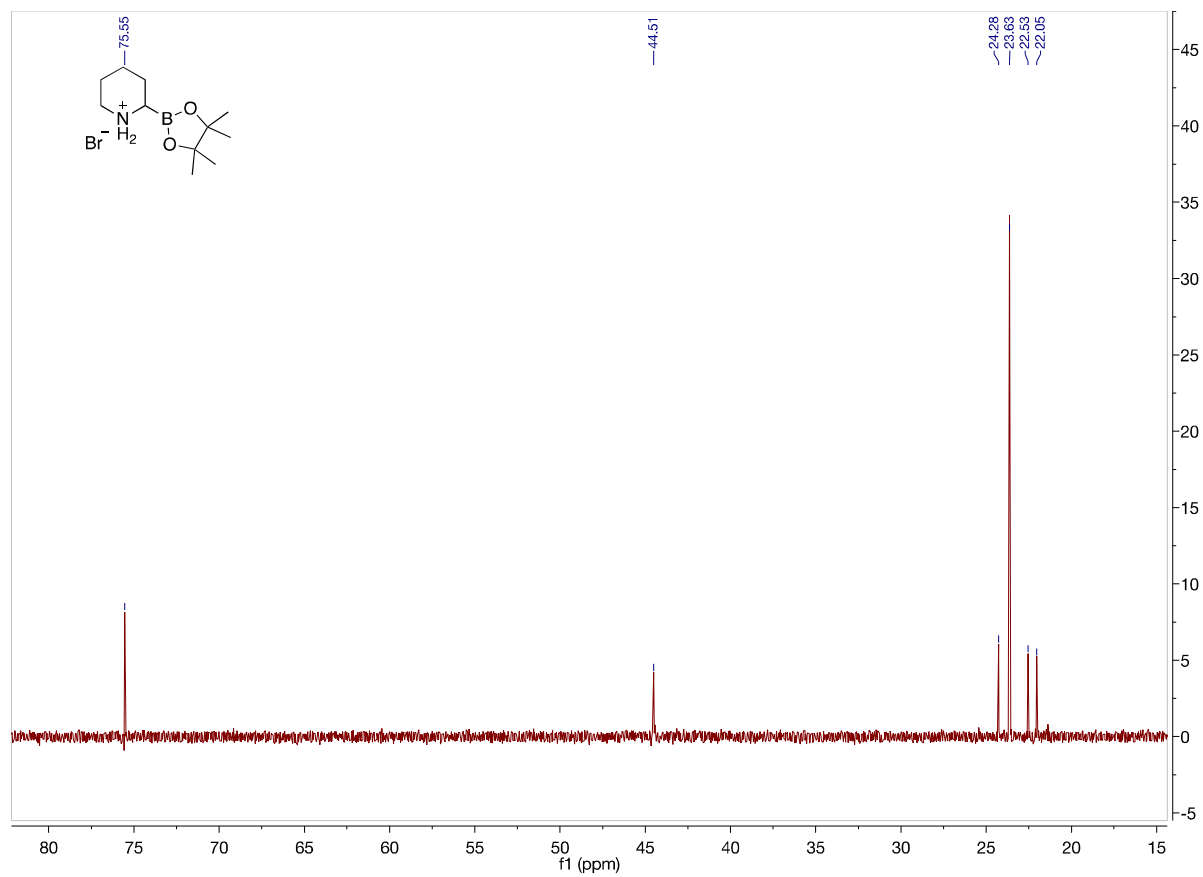


Figure A4. 125 MHz ¹³C NMR of **2b** in D₂O from 85 to 15 ppm

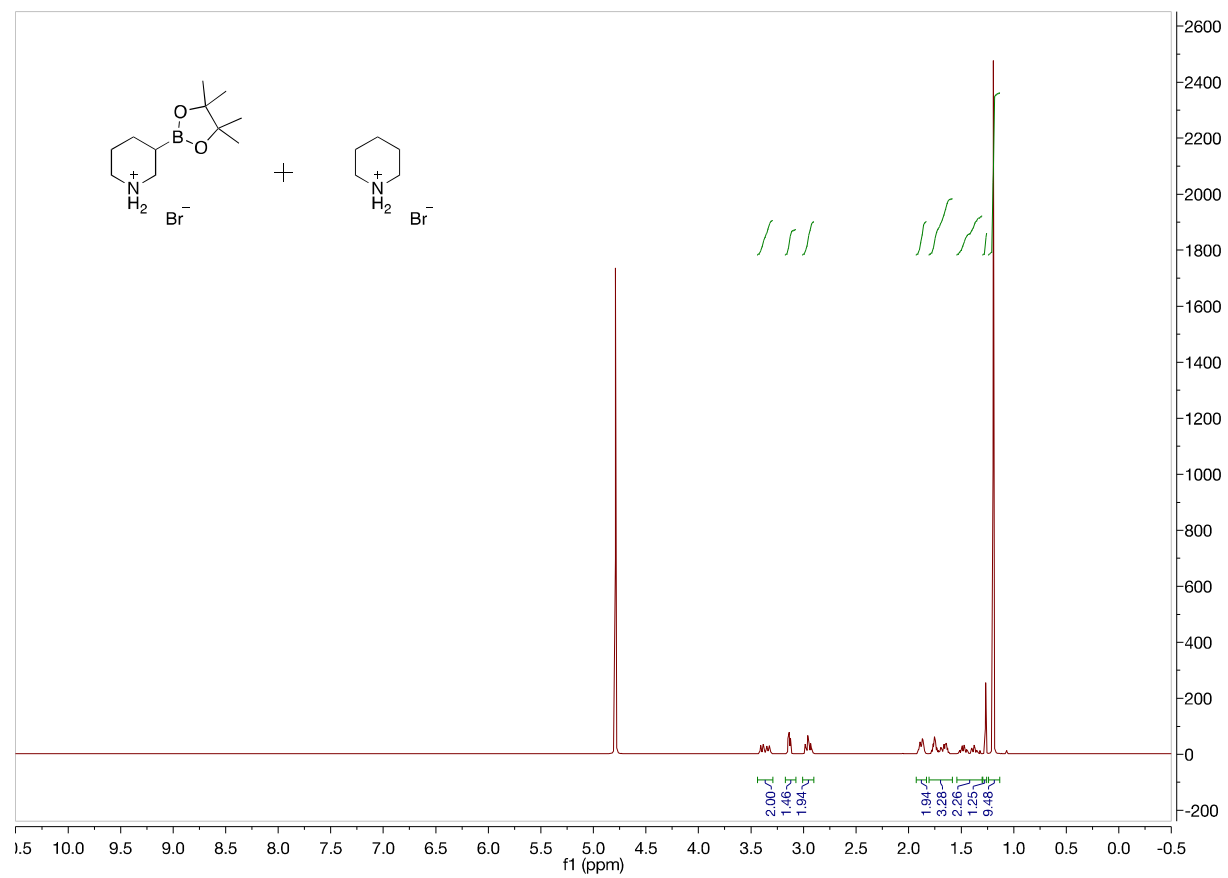


Figure A5. 500 MHz ^1H NMR of **2c** in D_2O

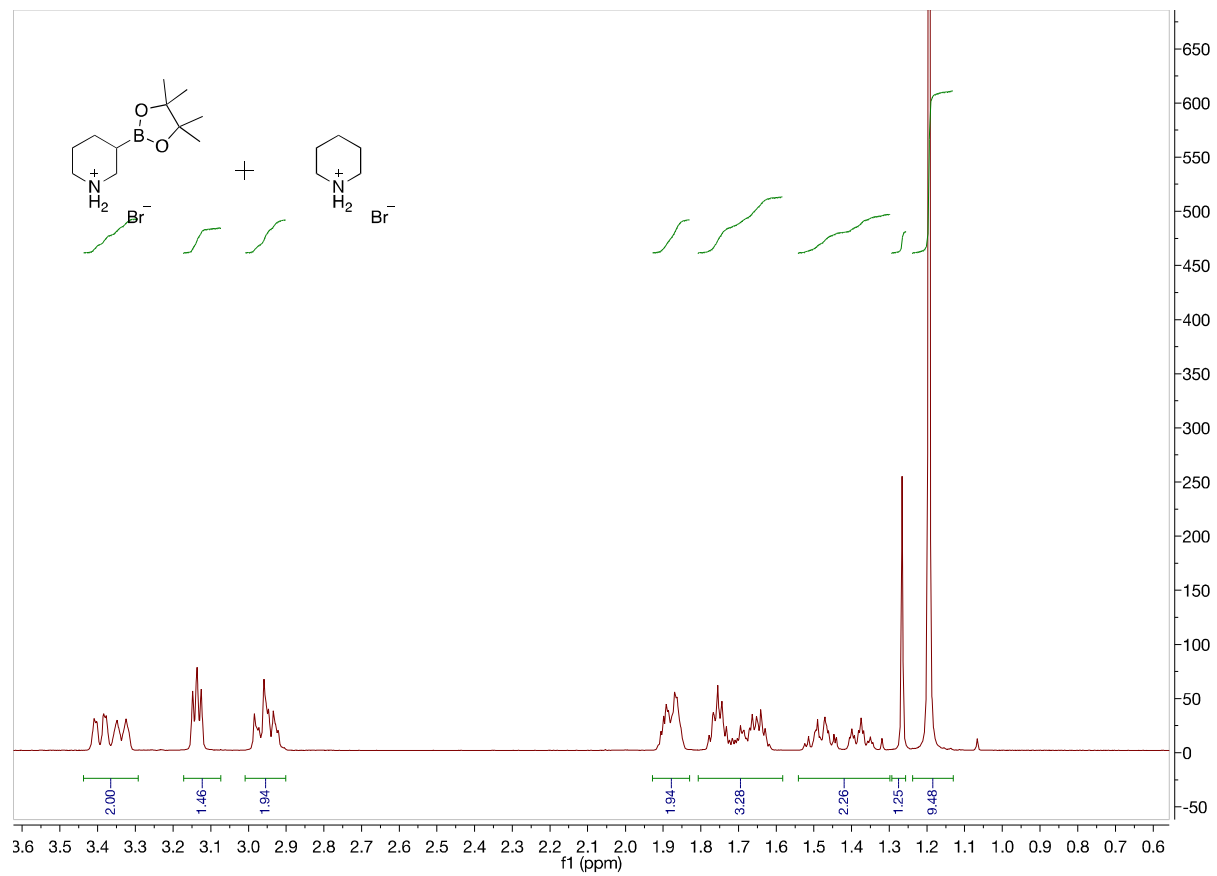


Figure A6. 500 MHz ^1H NMR of **2c** in D_2O from 3.6 to 0.6 ppm

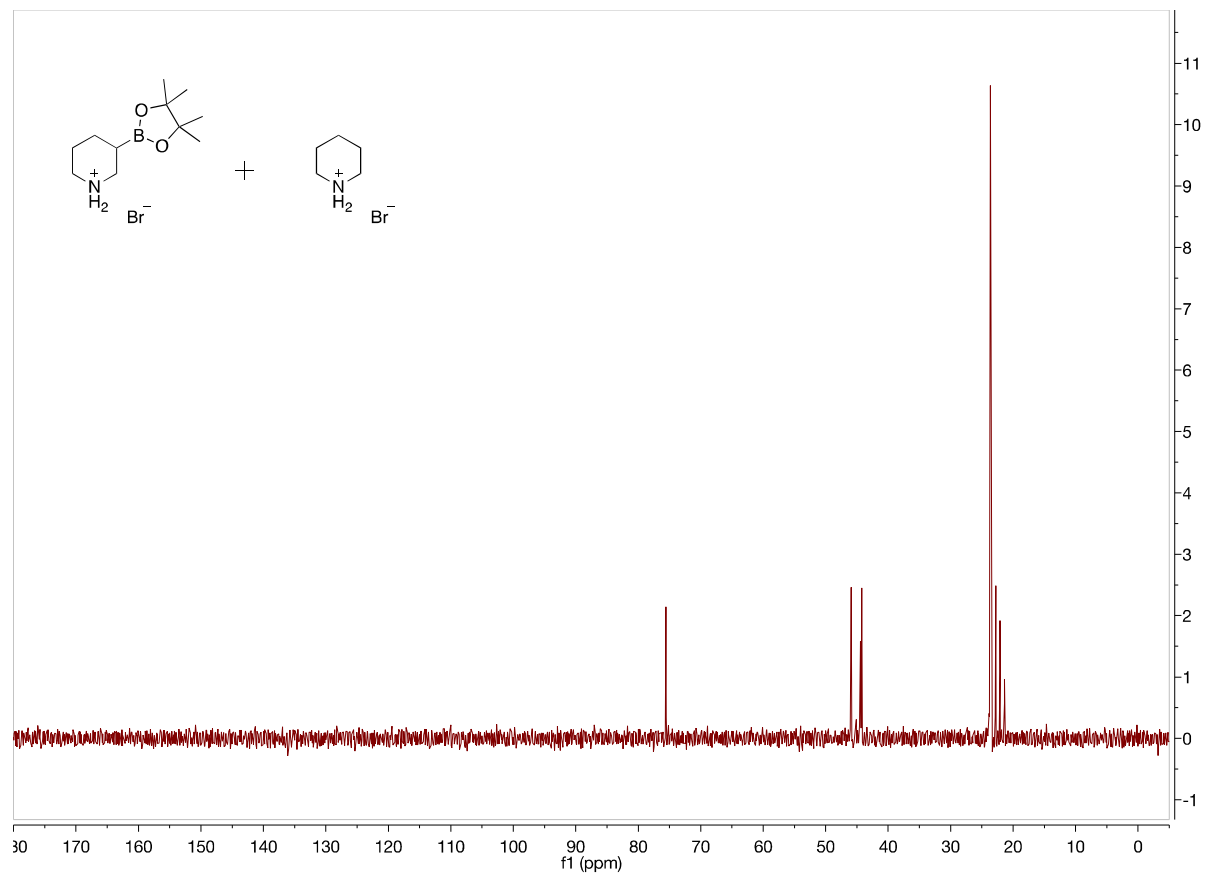


Figure A7. 125 MHz ^{13}C NMR of **2c** in D_2O

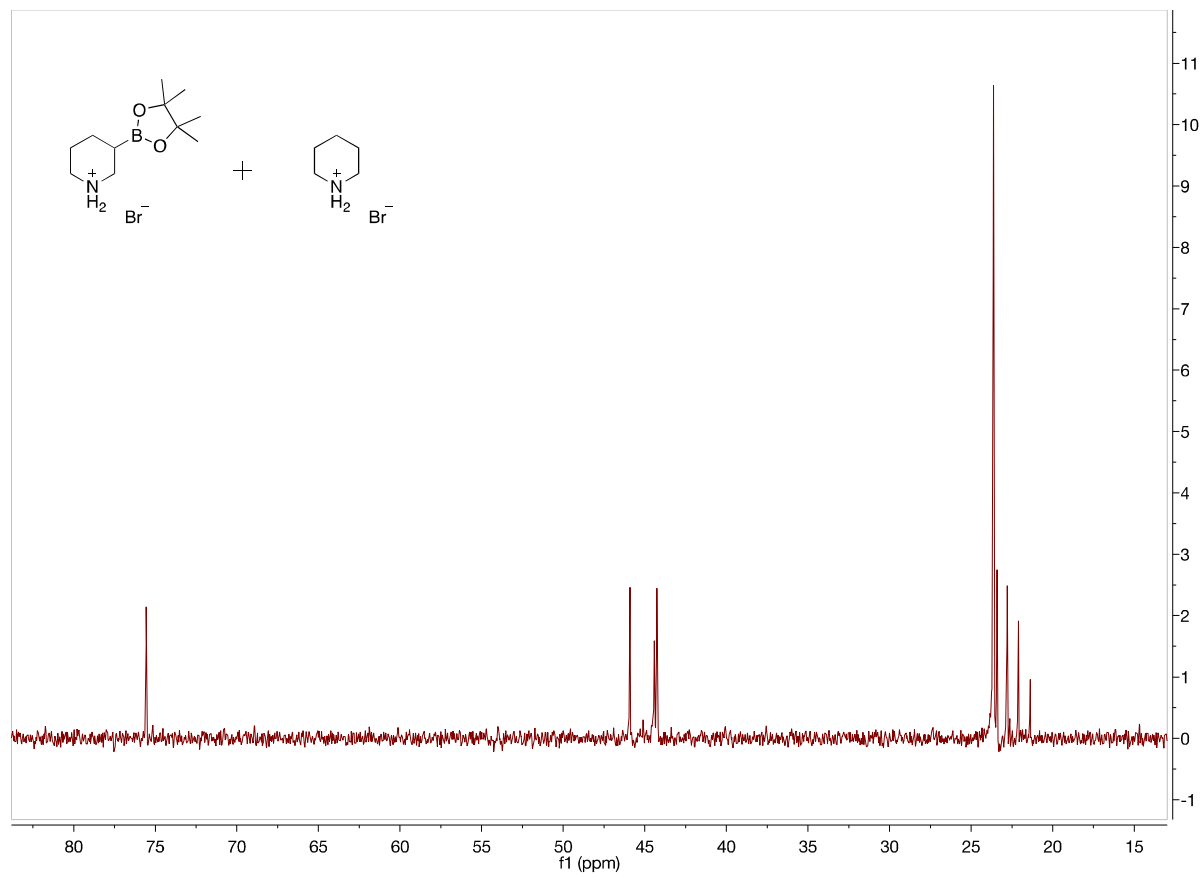


Figure A8. 125 MHz ^{13}C NMR of **2c** in D_2O from 85 to 15 ppm

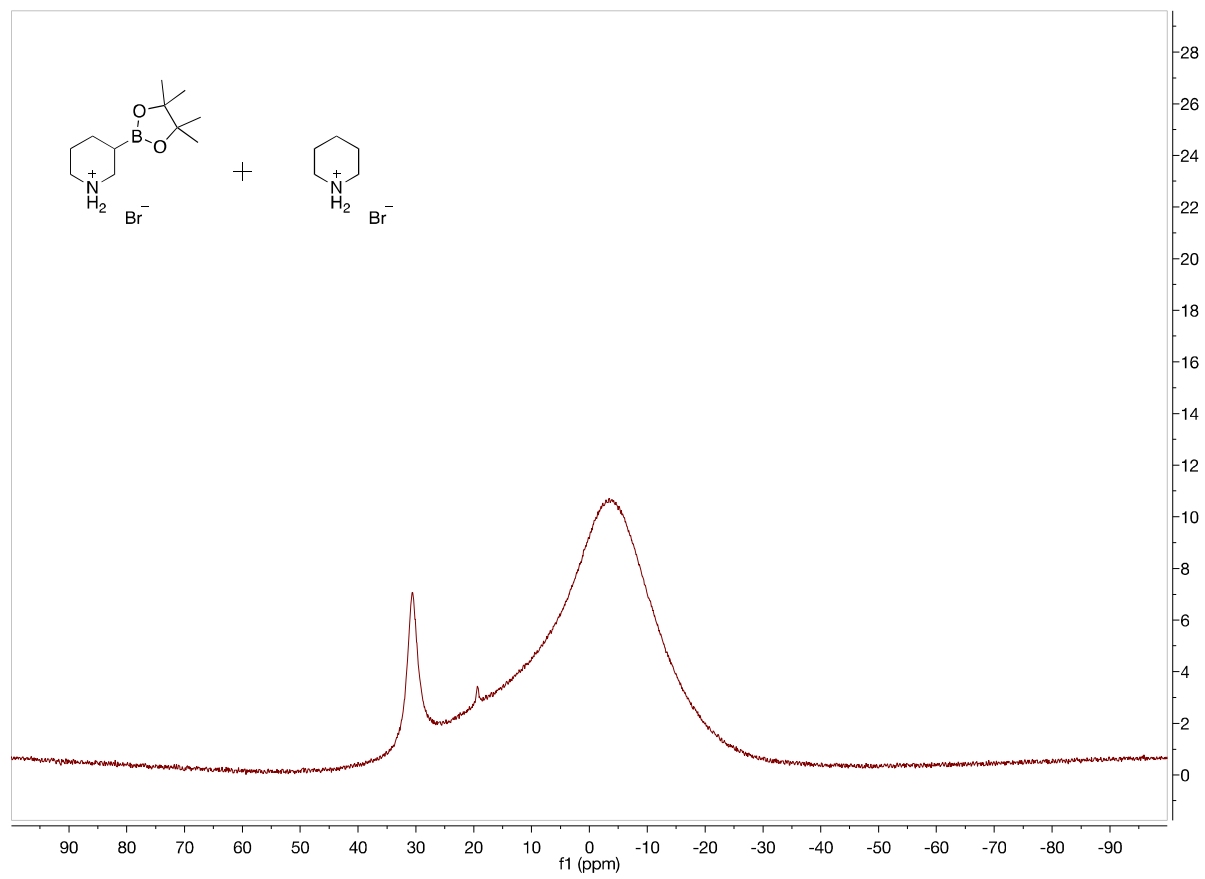


Figure A9. 160 MHz ^{11}B NMR of **2c** in D_2O

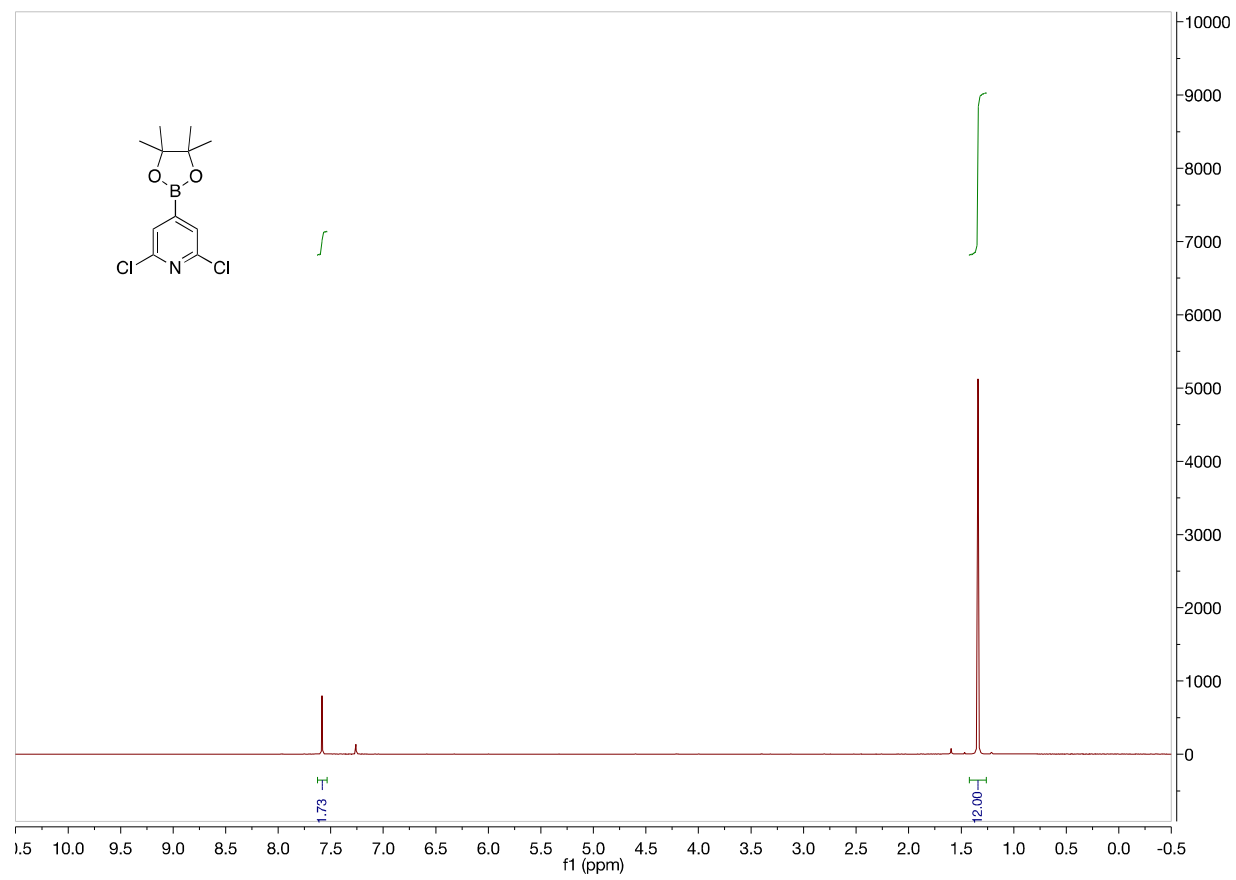


Figure A10. 500 MHz ^1H NMR of **2d'** in CDCl_3

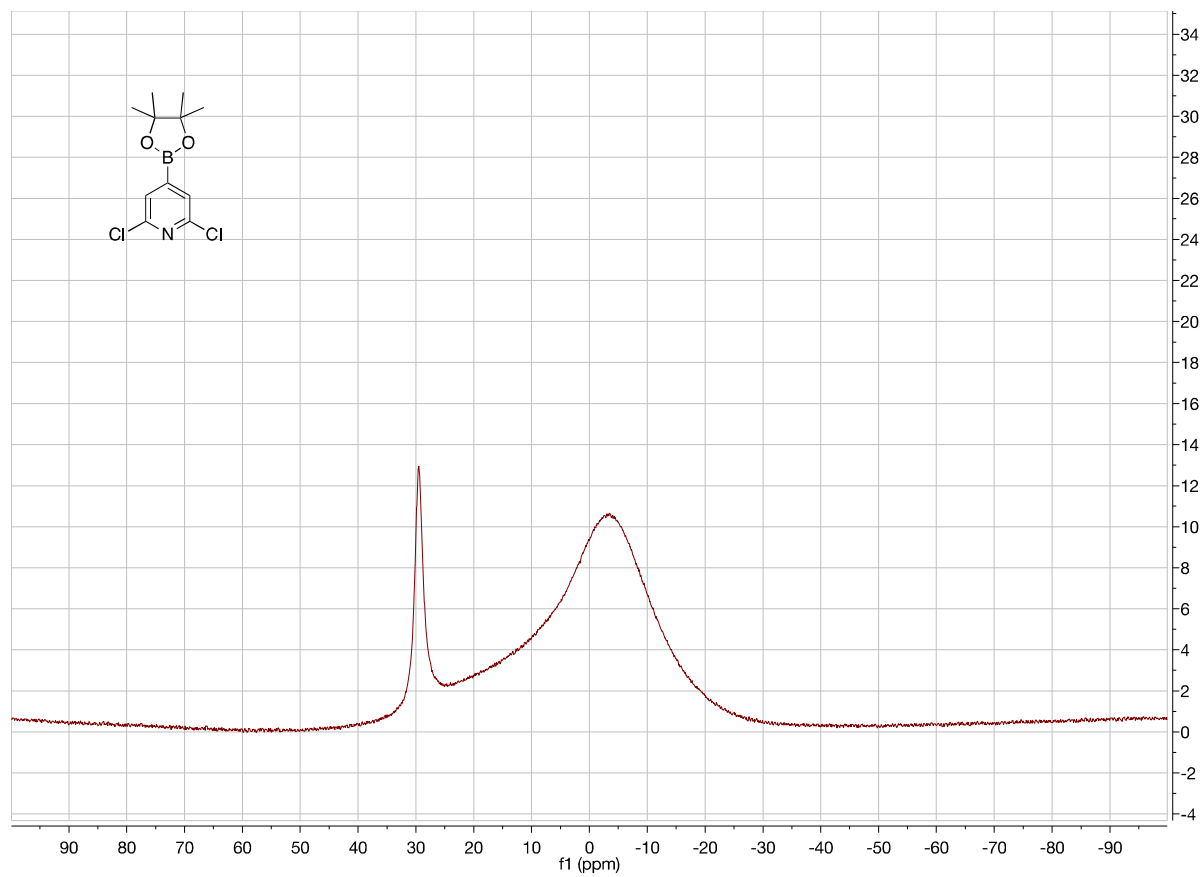


Figure A11. 160 MHz ^{11}B NMR of **2d'** in D_2O

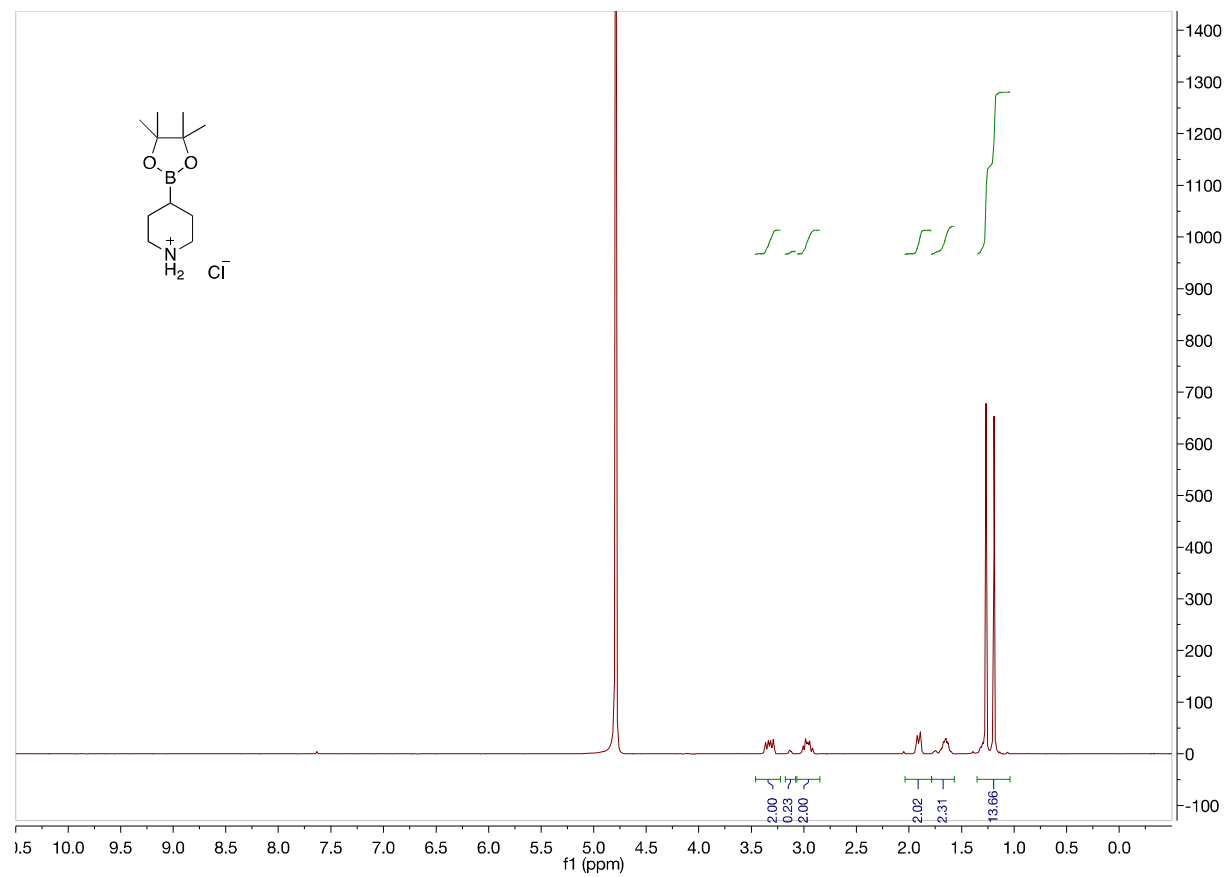


Figure A12. 500 MHz ^1H NMR of **2d** in D_2O

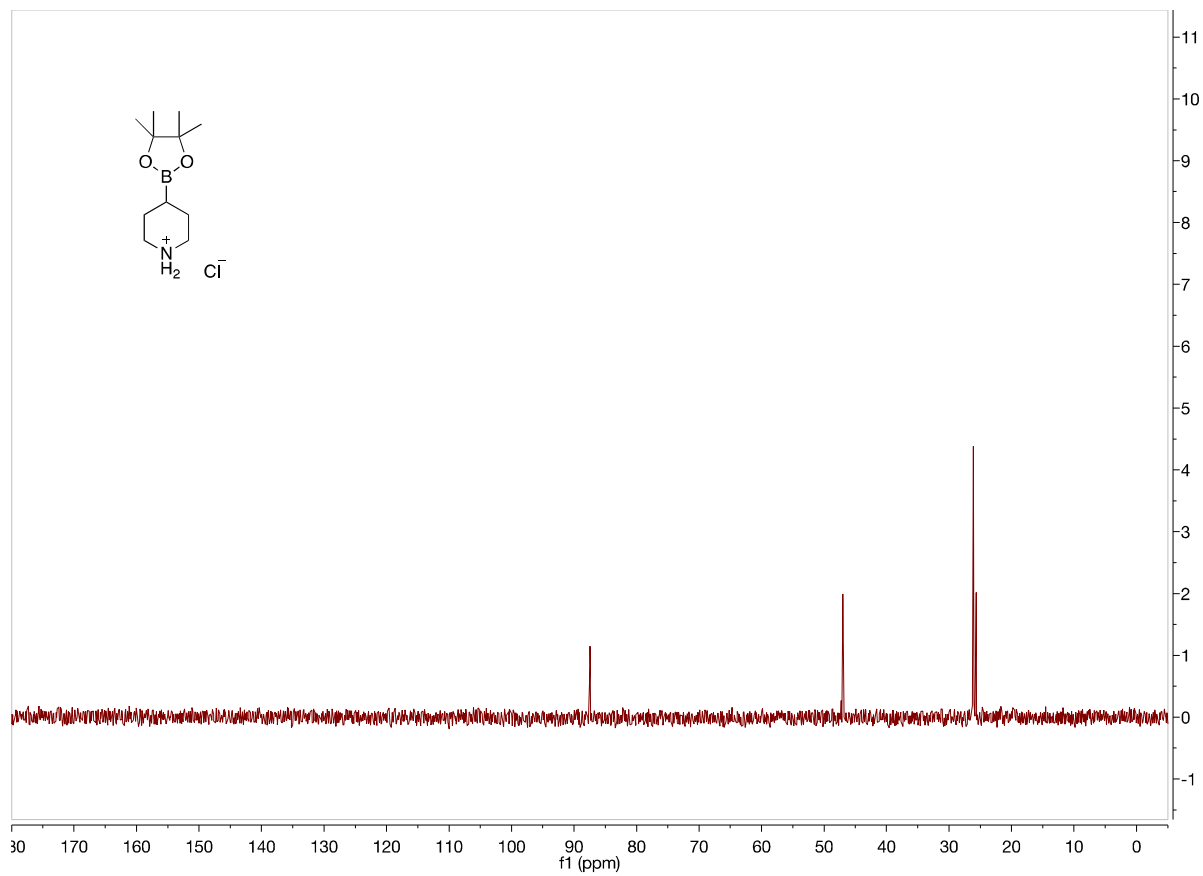


Figure A13. 125 MHz ^{13}C NMR of **2d** in D_2O

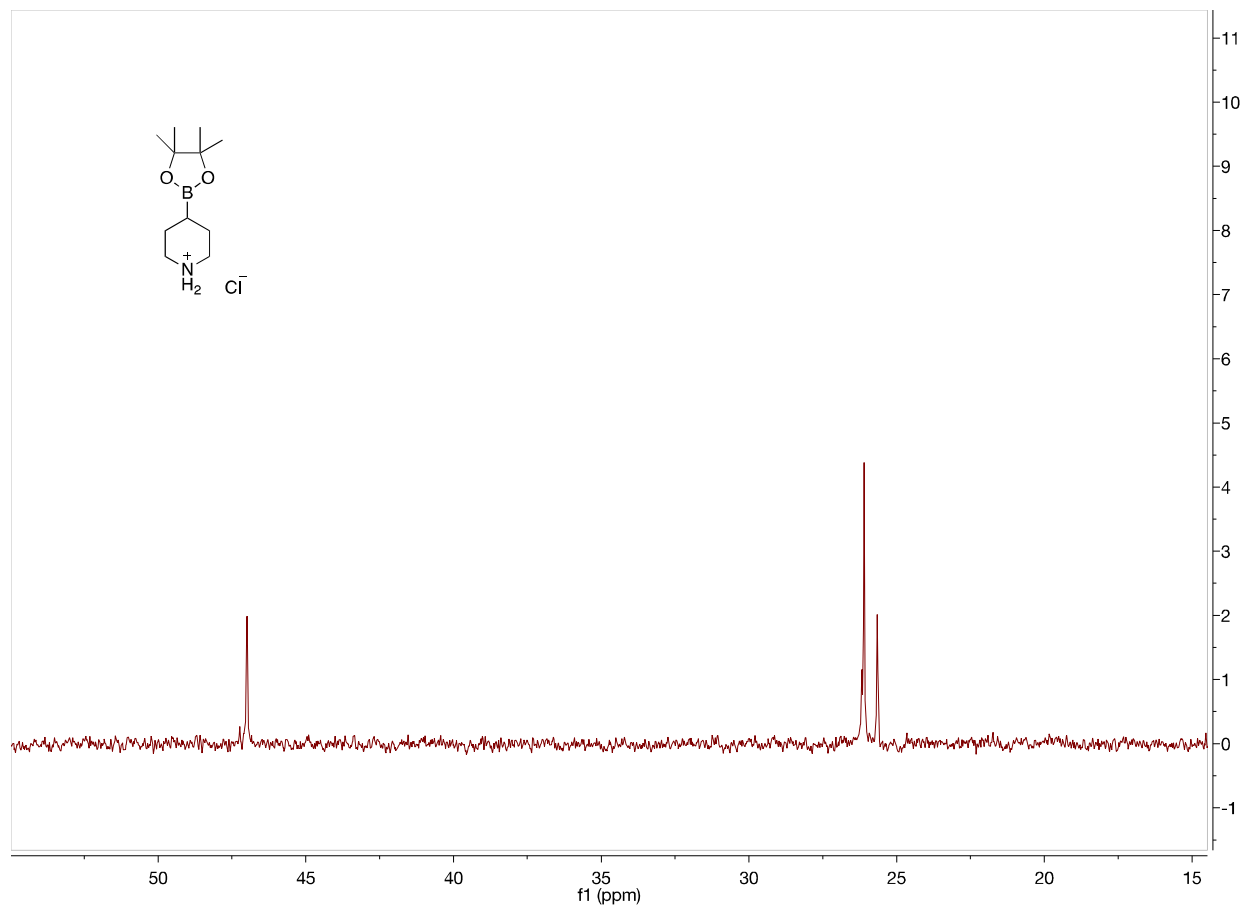


Figure A14. 125 MHz ^{13}C NMR of **2d** in D_2O from 60 to 15 ppm

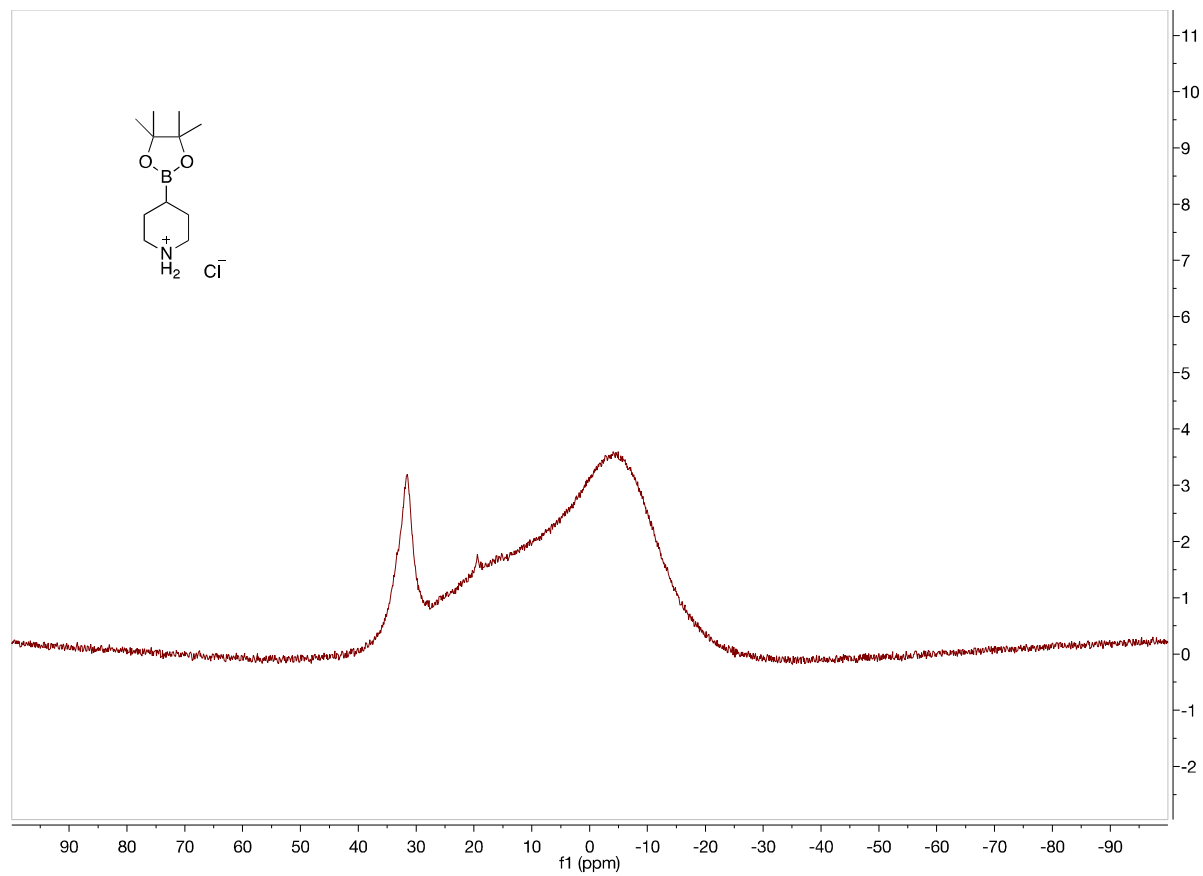


Figure A15. 160 MHz ^{11}B NMR of **2d** in D_2O

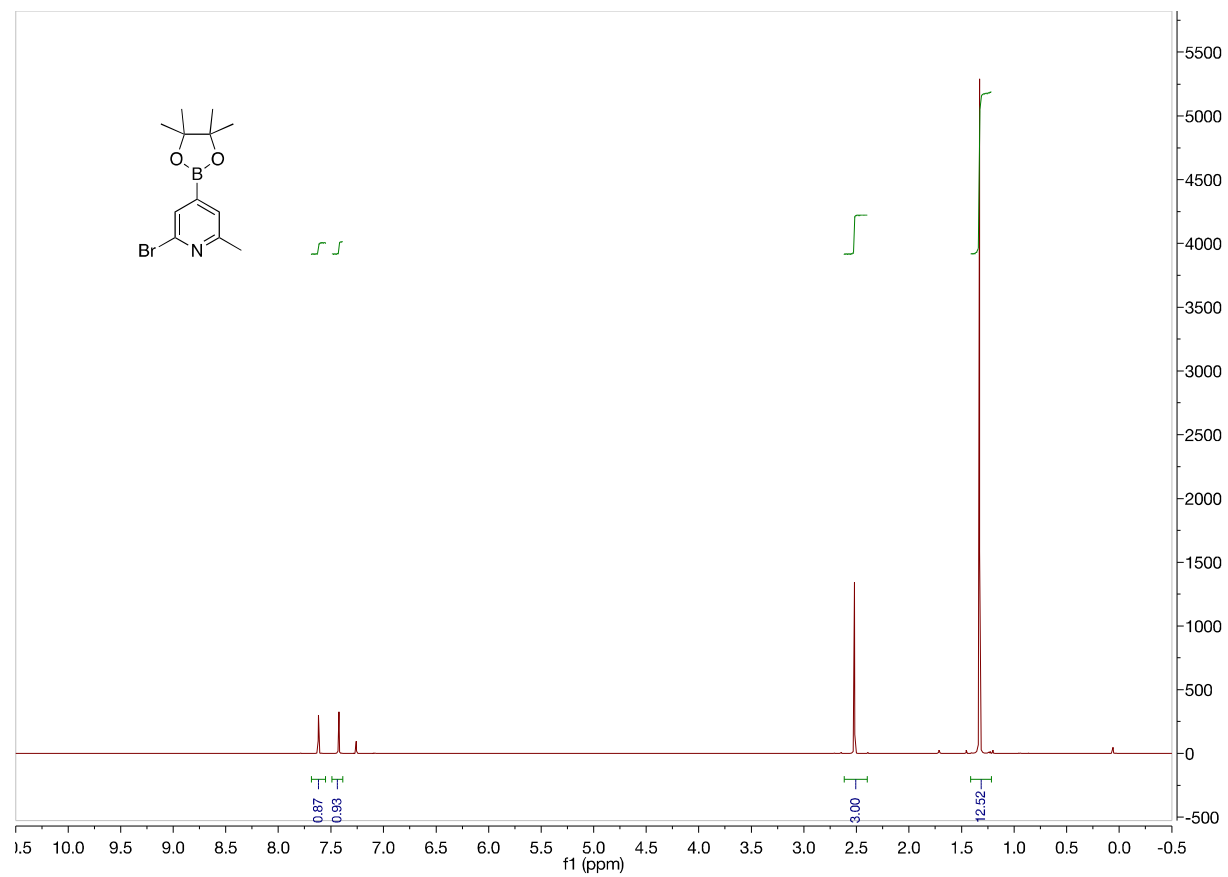


Figure A16. 500 MHz ^1H NMR of **2e'** in CDCl_3

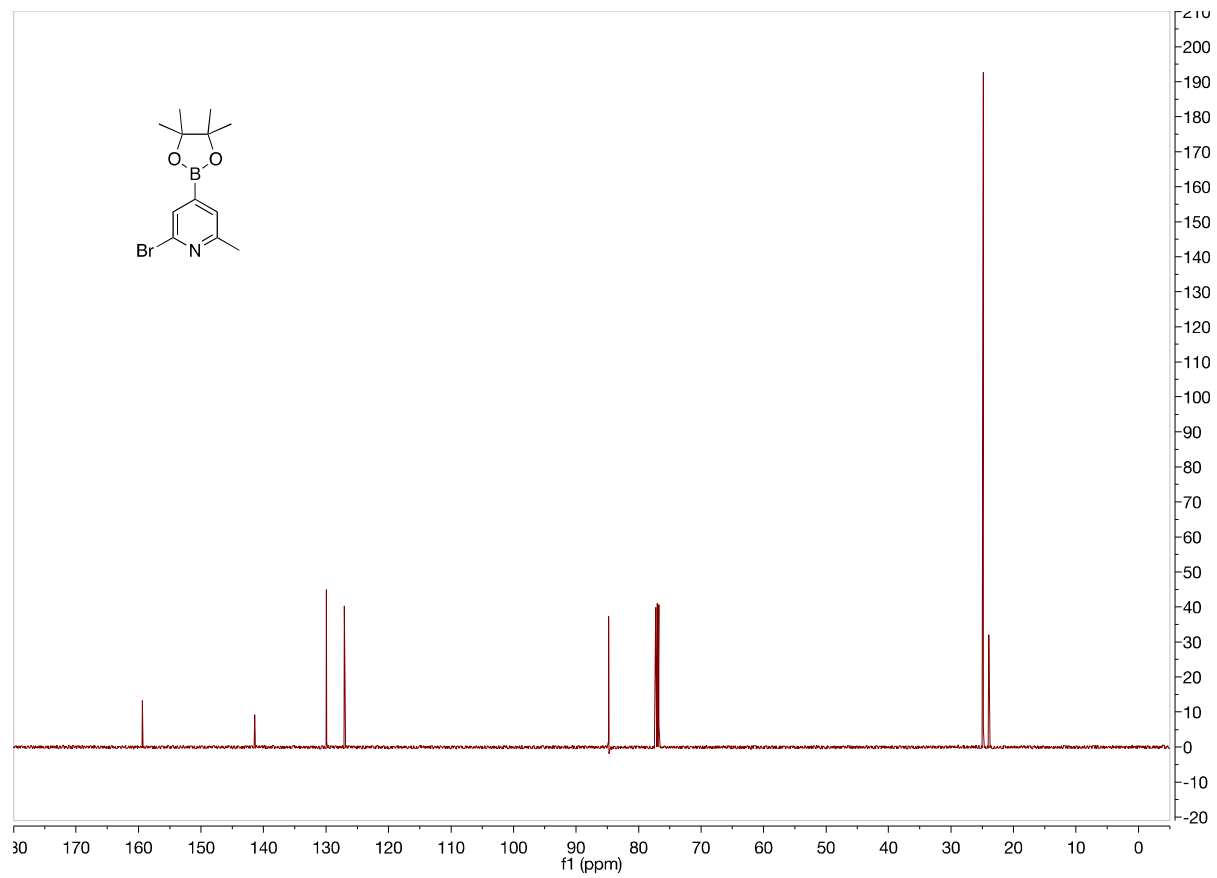


Figure A17. 125 MHz ^{13}C NMR of **2e'** in CDCl_3

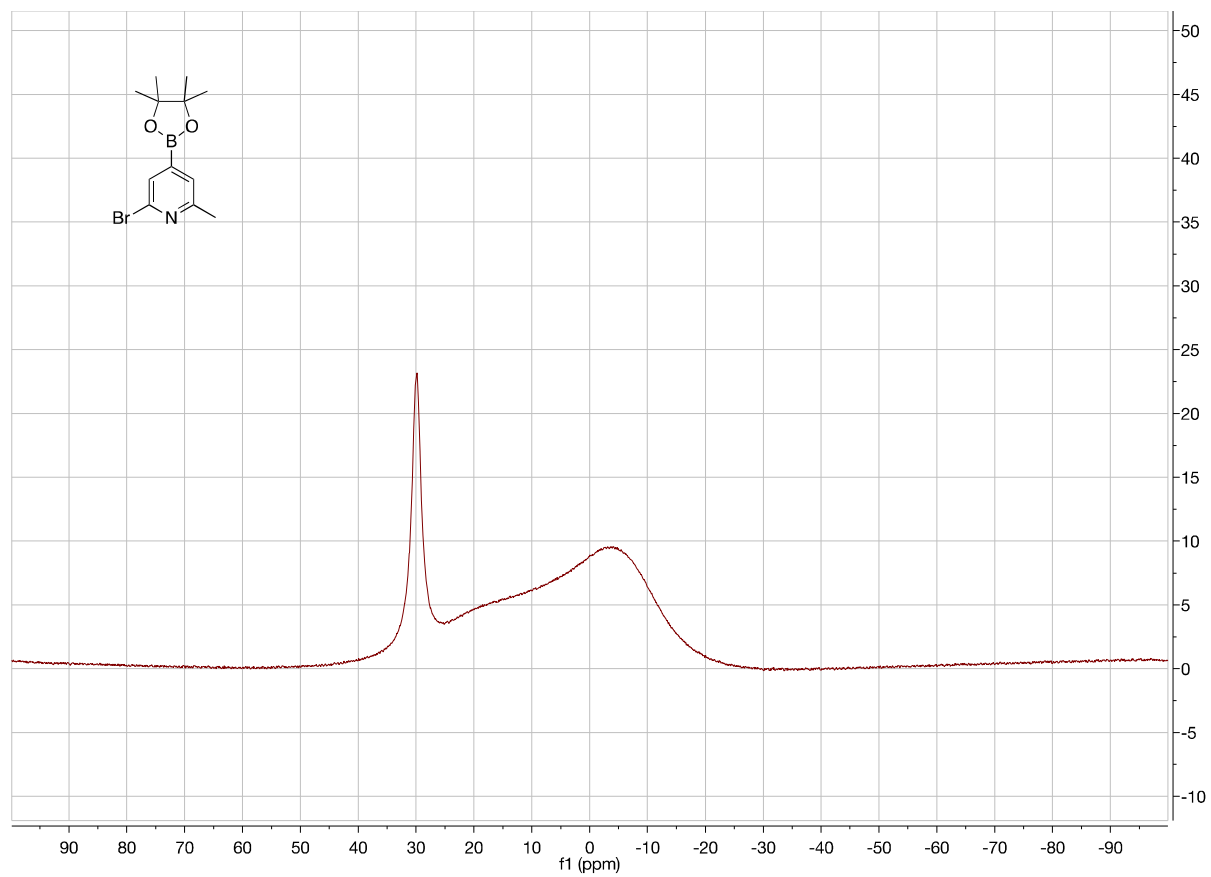


Figure A18. 160 MHz ^{11}B NMR of **2e'** in CDCl_3

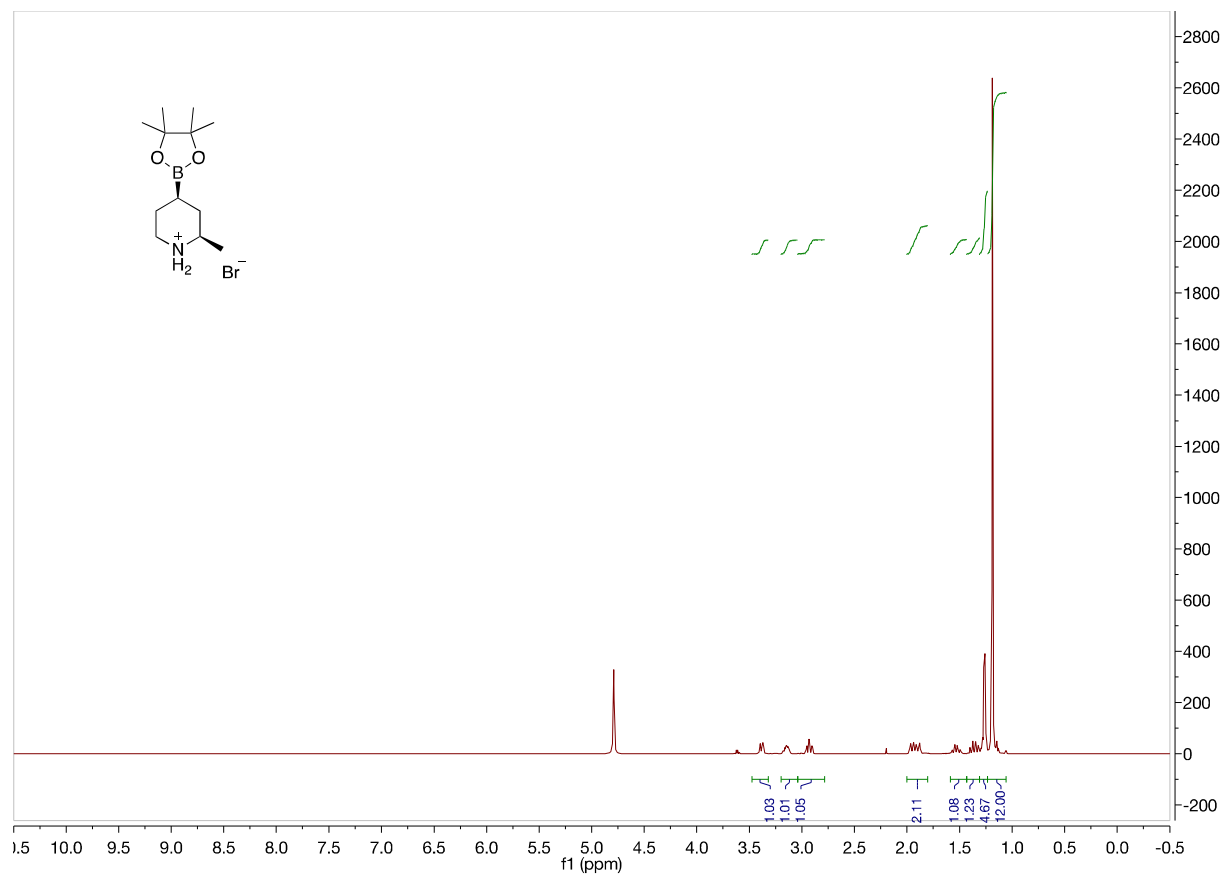


Figure A19. 500 MHz ^1H NMR of **2e** in D_2O

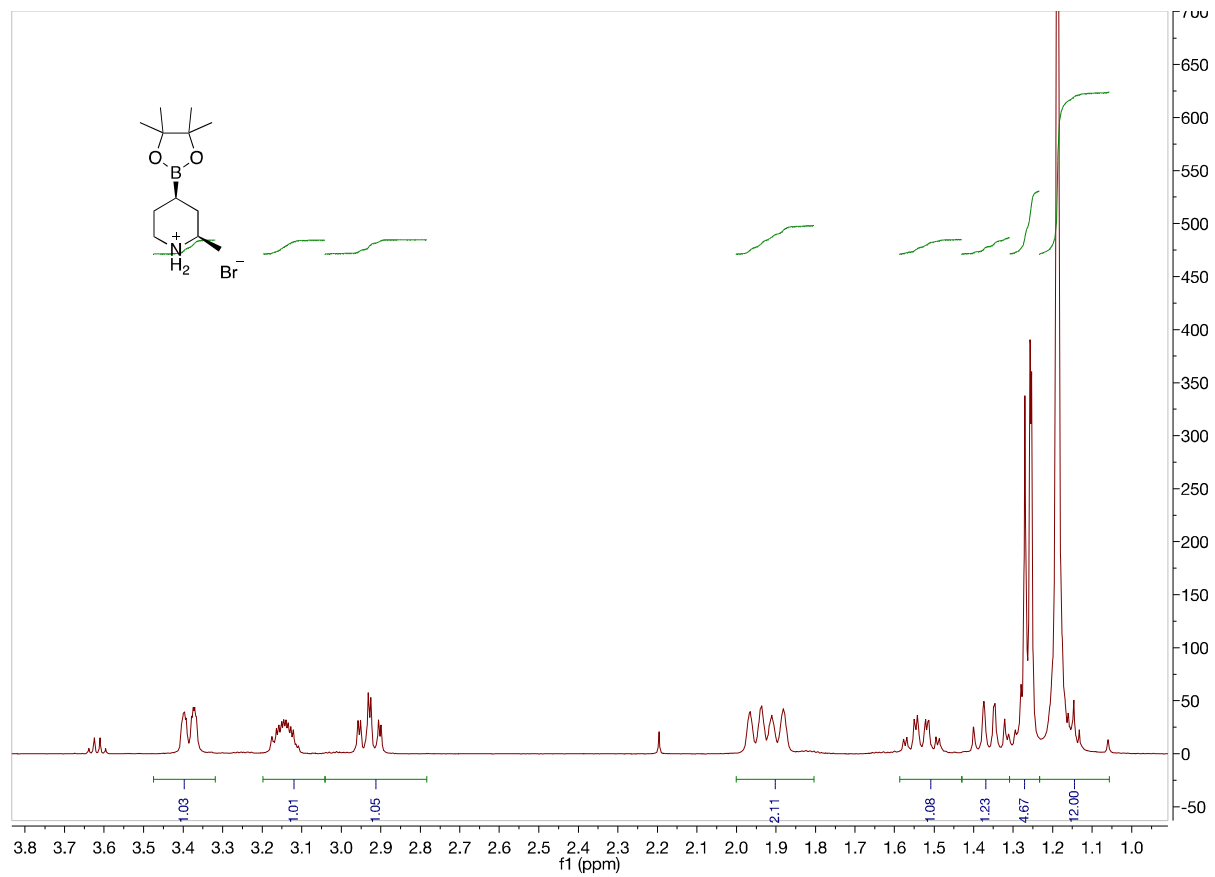


Figure A20. 500 MHz ^1H NMR of **2e** in D_2O from 3.8 to 1.0 ppm

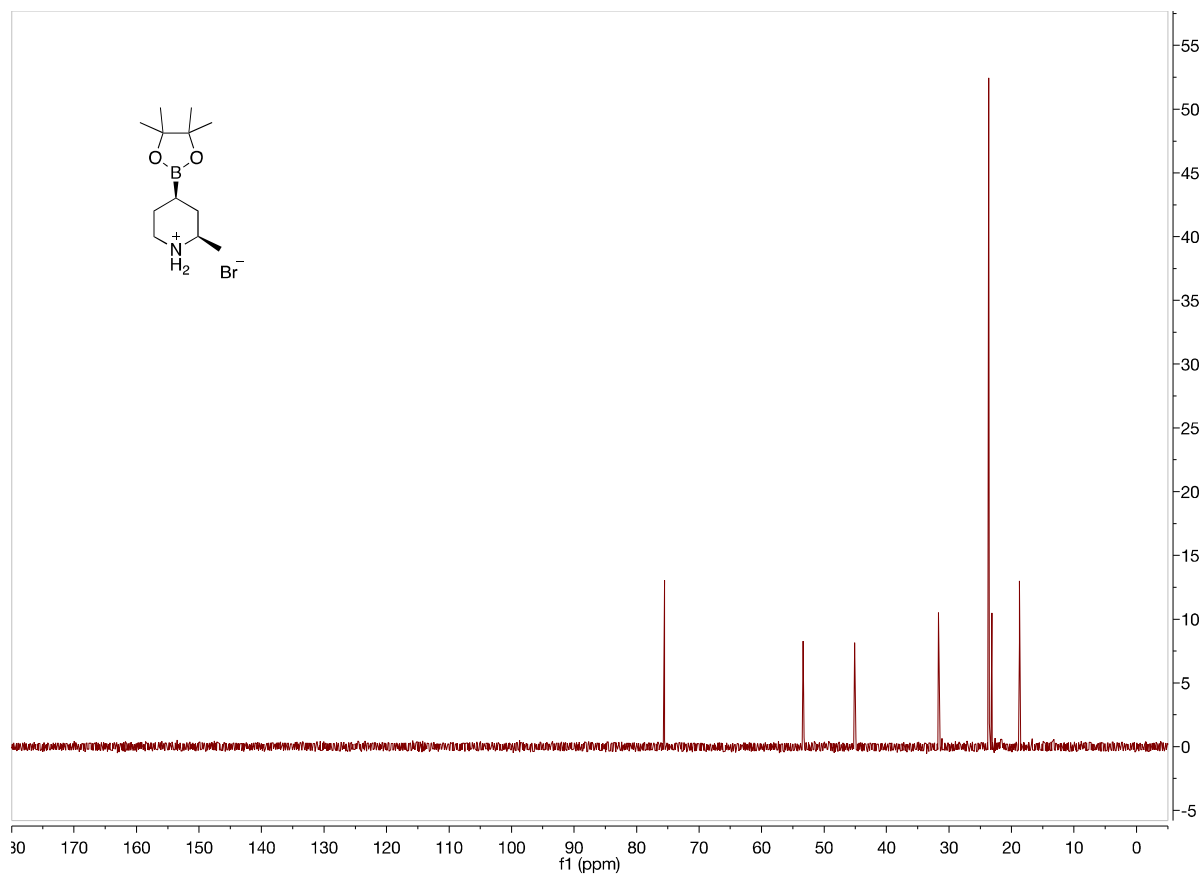


Figure A21. 125 MHz ^{13}C NMR of **2e** in D_2O

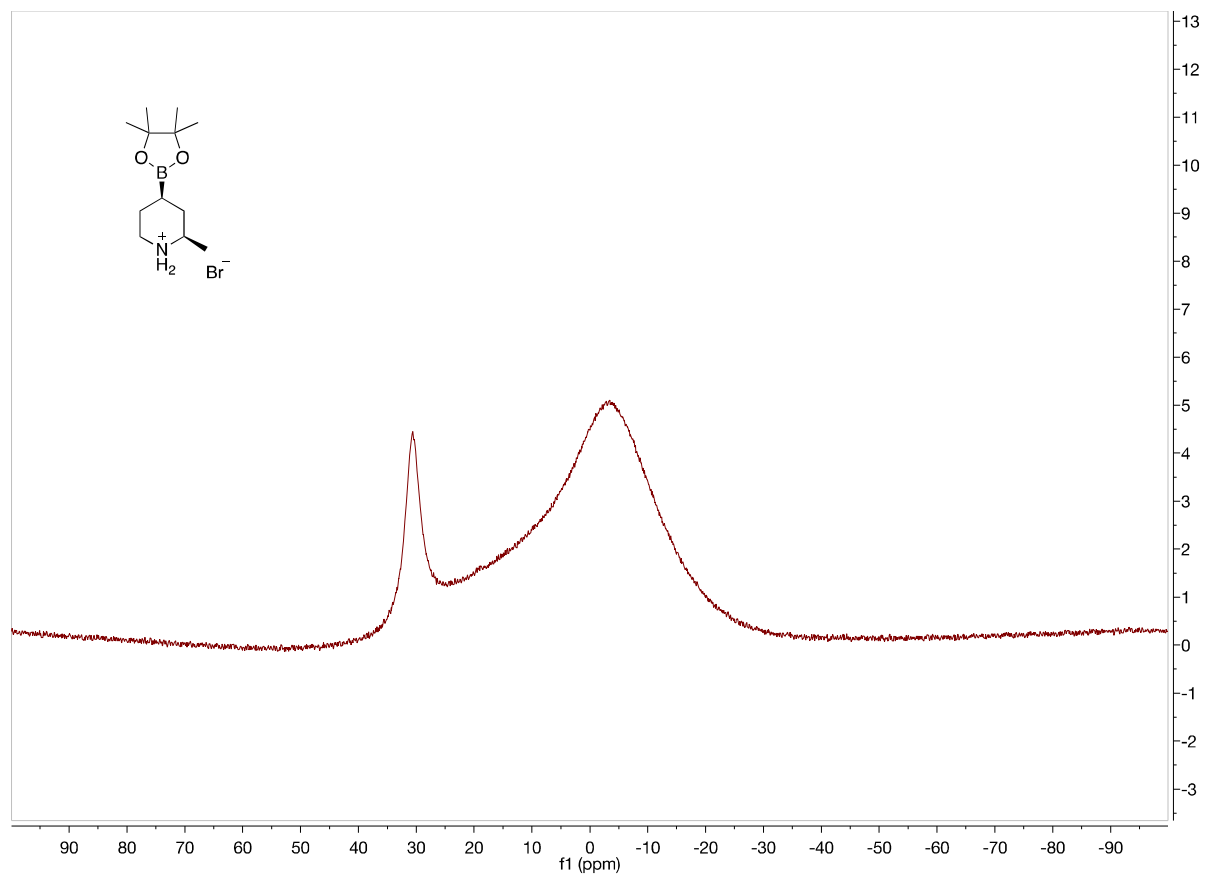


Figure A22. 160 MHz ^{11}B NMR of **2e** in D_2O

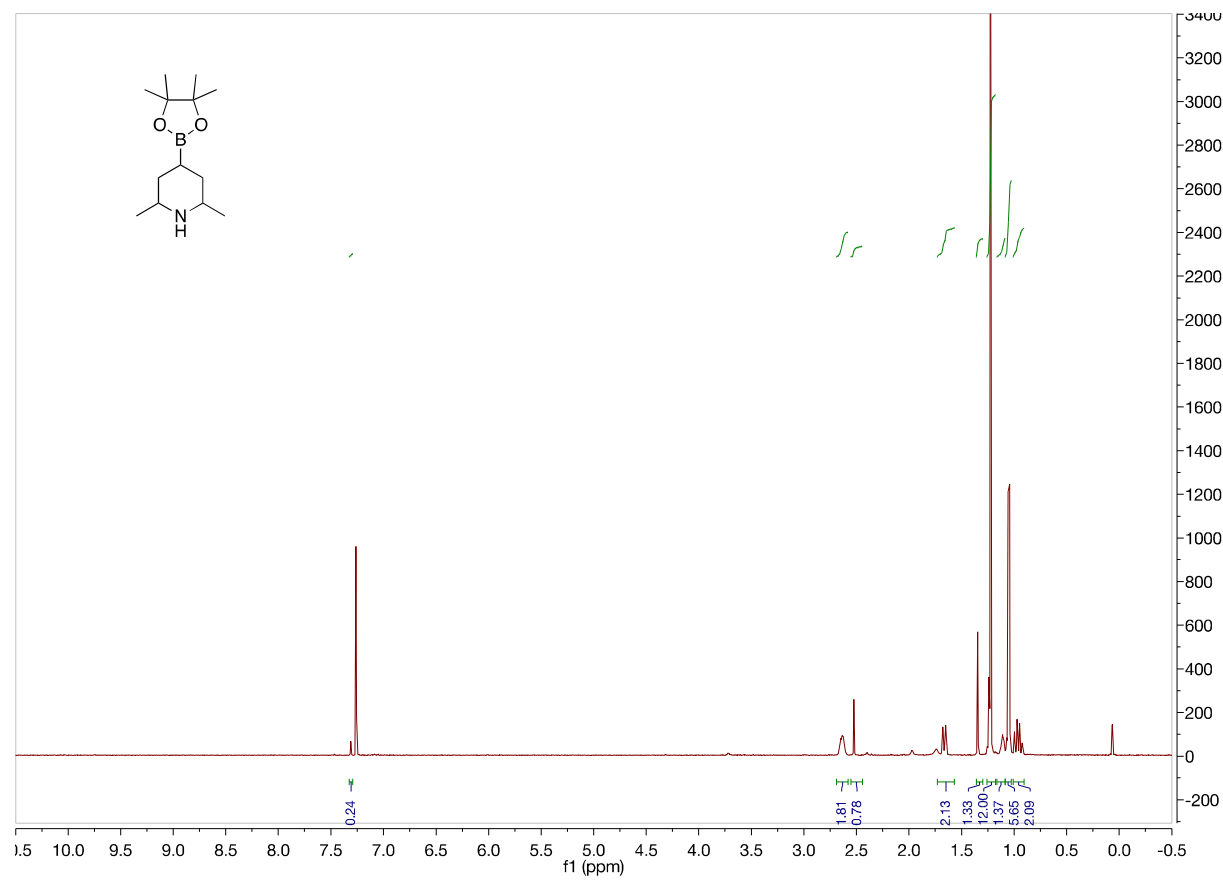


Figure A23. 500 MHz ¹H NMR of **2f** in CDCl₃

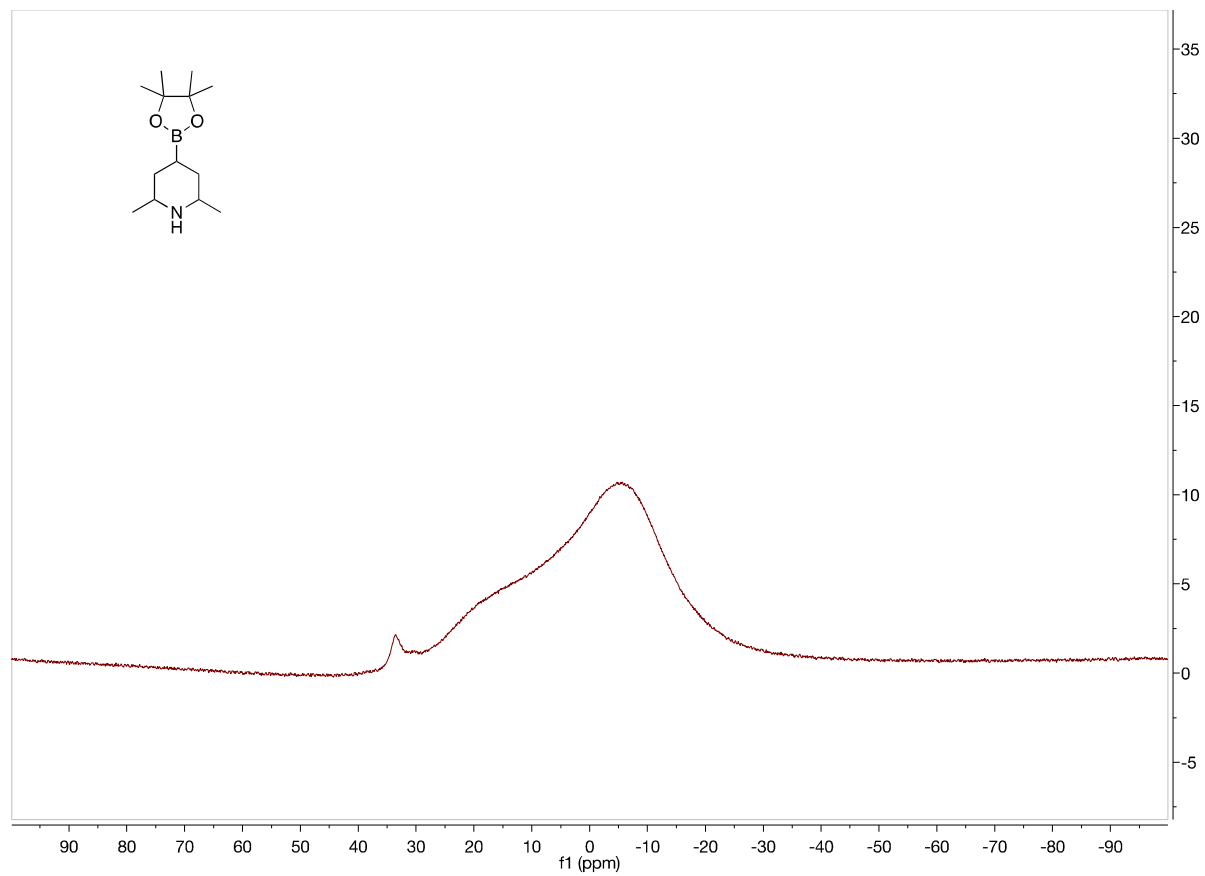


Figure A24. 160 MHz ^{11}B NMR of **2f** in CDCl_3

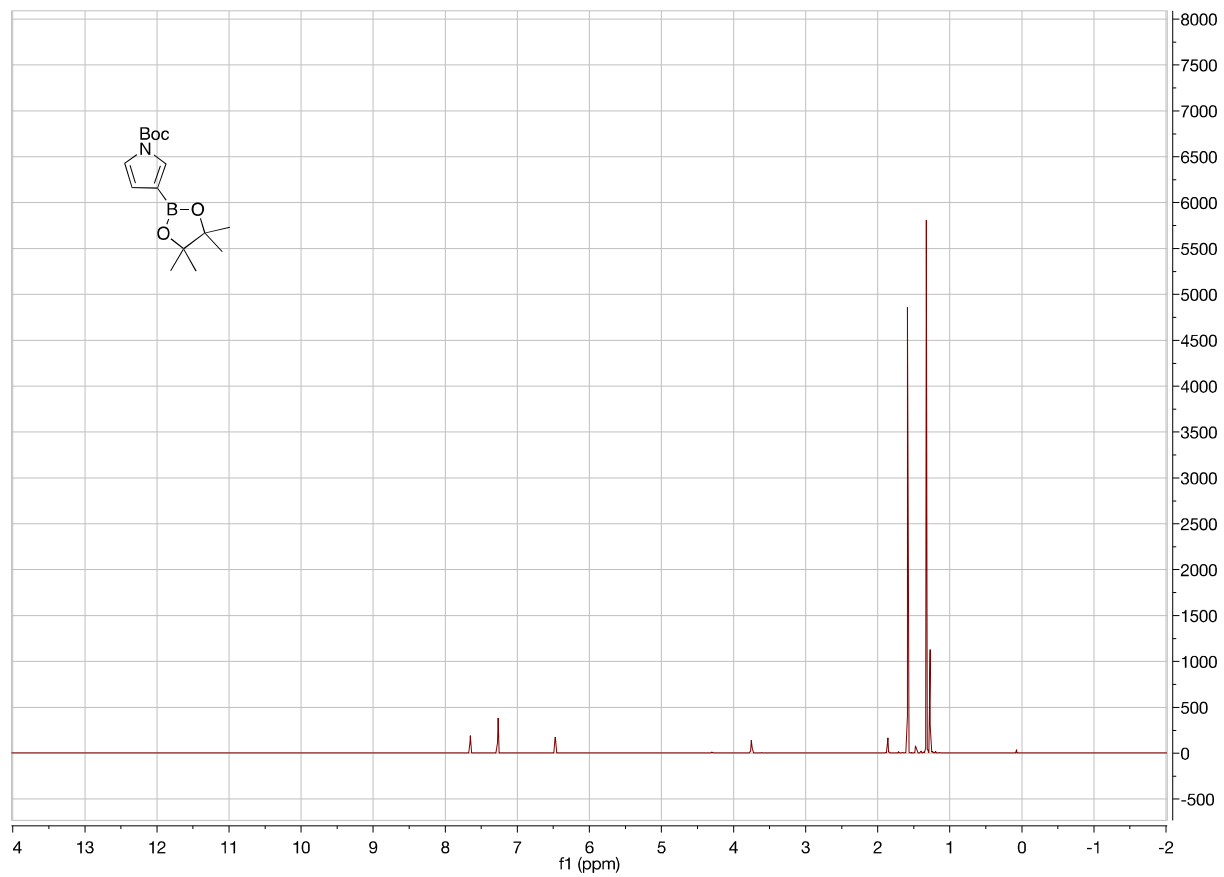


Figure A25. 500 MHz ¹H NMR of **2g'** in CDCl₃

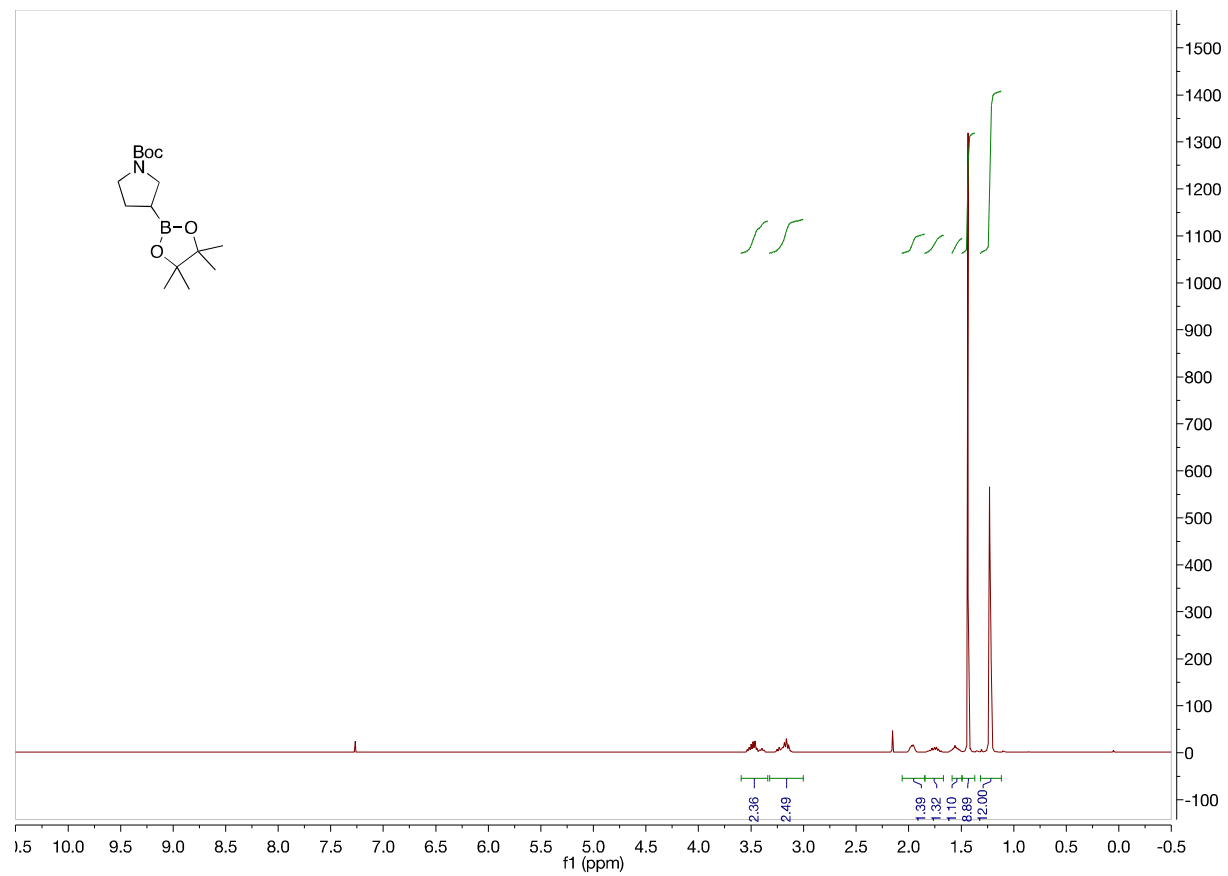


Figure A26. 500 MHz ^1H NMR of **2g** in CDCl_3

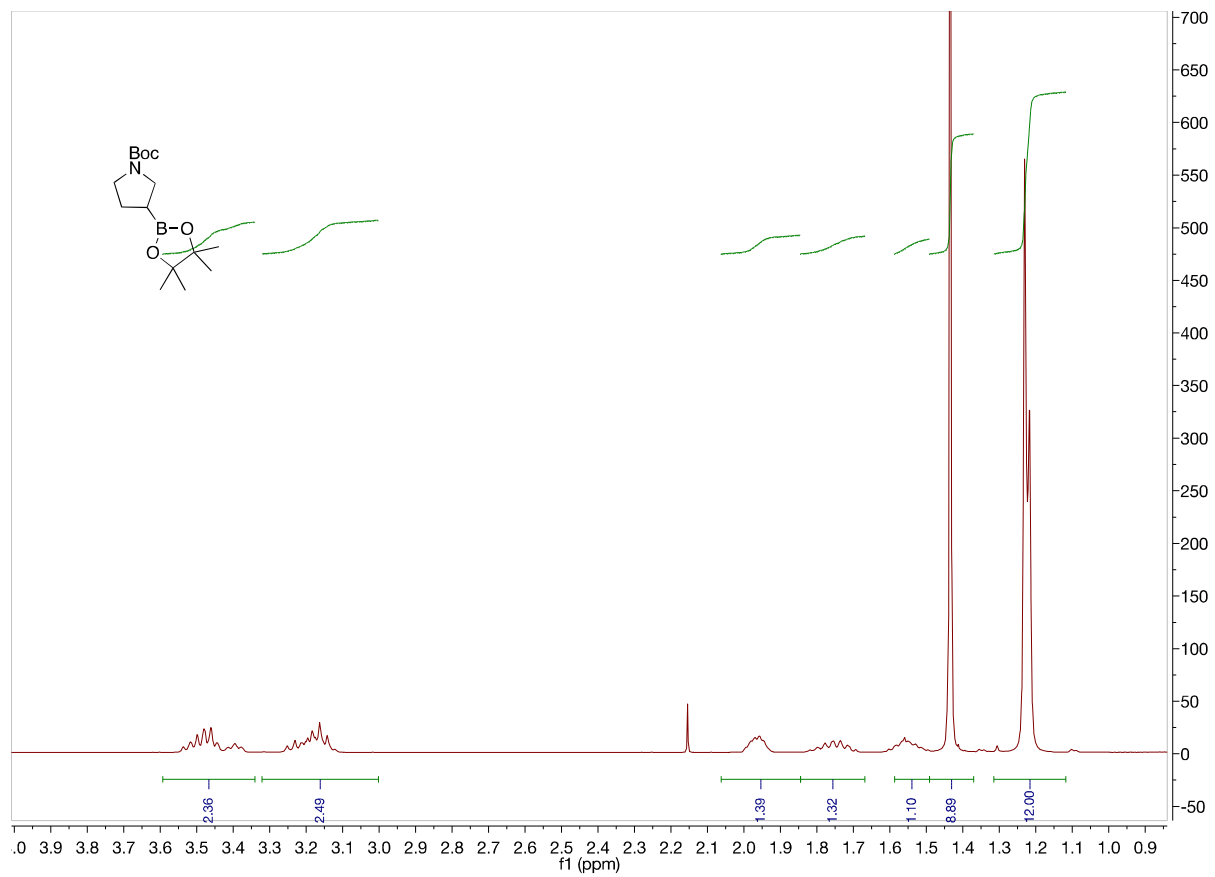


Figure A27. 500 MHz ^1H NMR of **2g** in CDCl_3 from 4.0 to 0.9 ppm

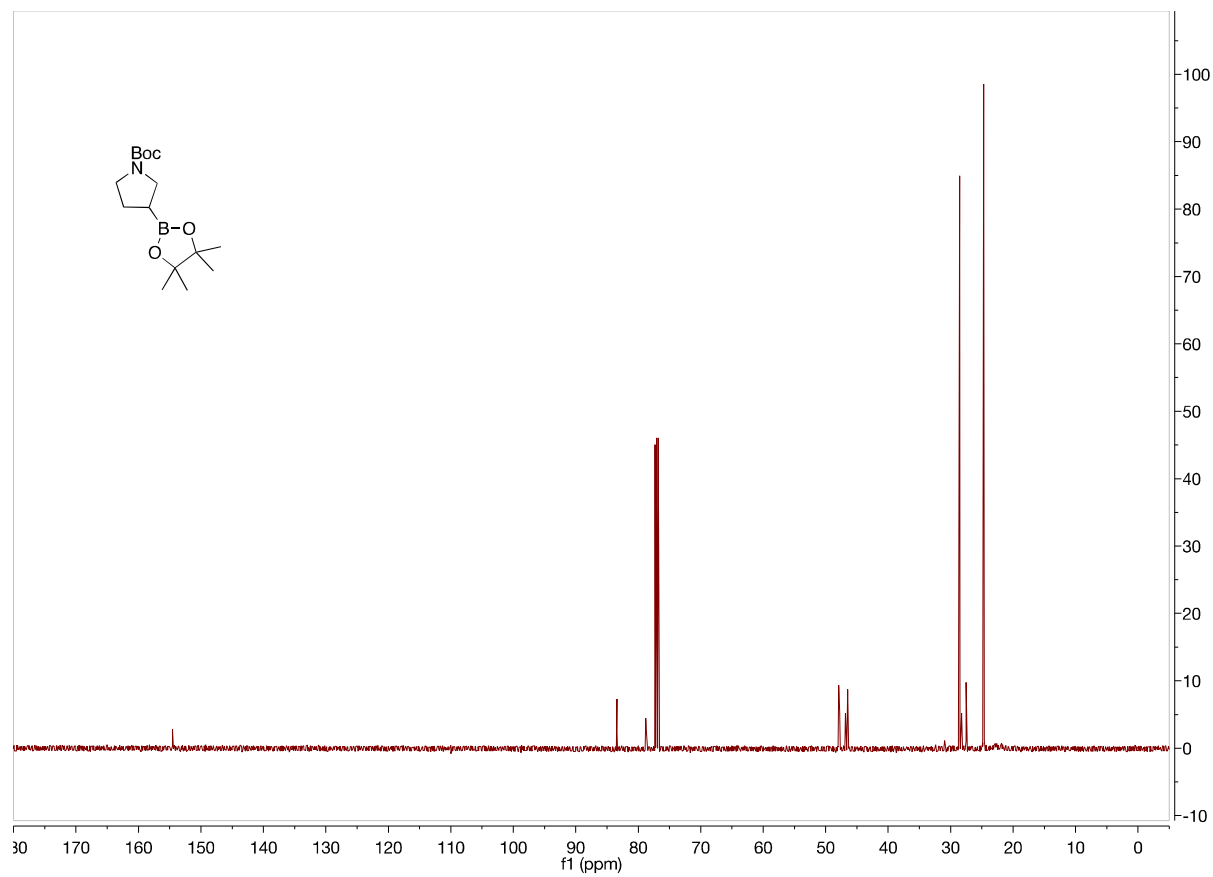


Figure A28. 125 MHz ^{13}C NMR of **2g** in CDCl_3

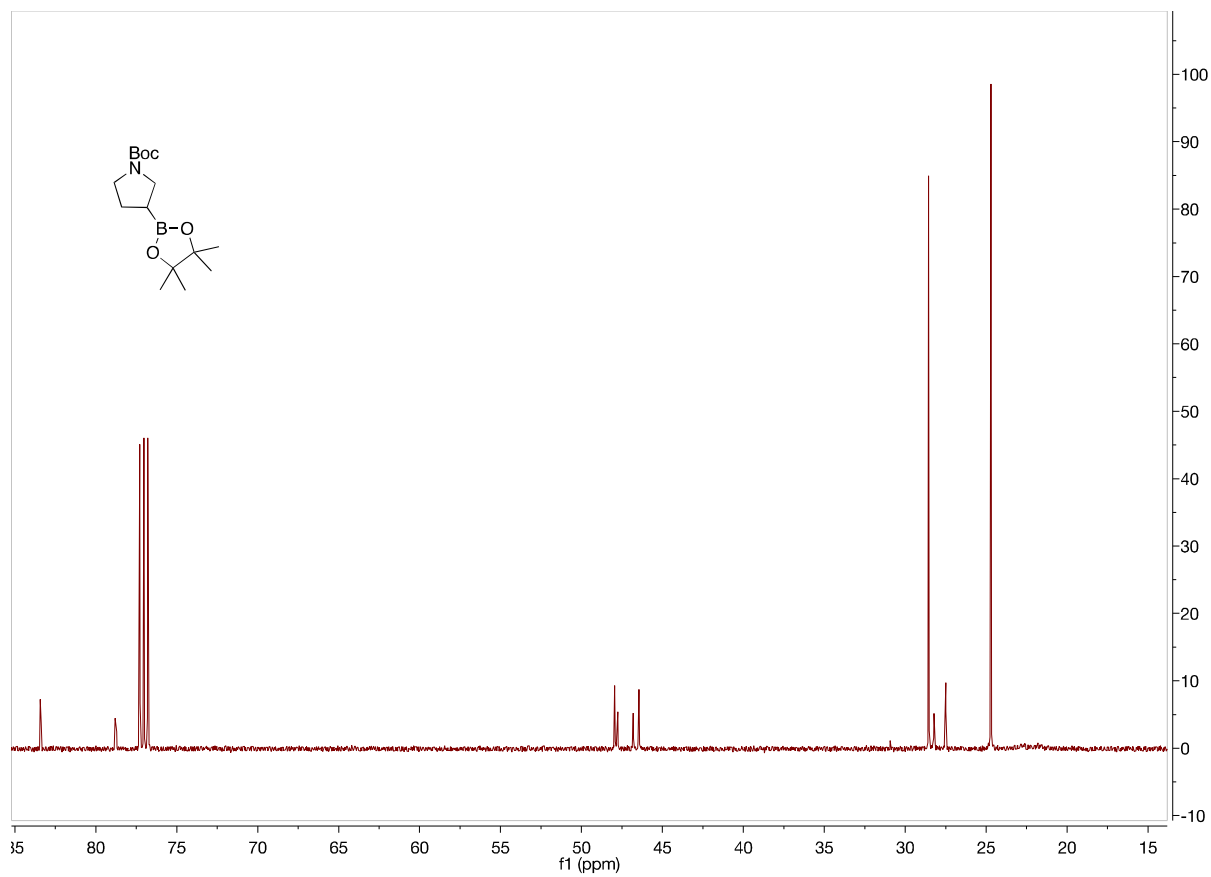


Figure A29. 125 MHz ^{13}C NMR of **2g** in CDCl_3 from 85 to 15 ppm

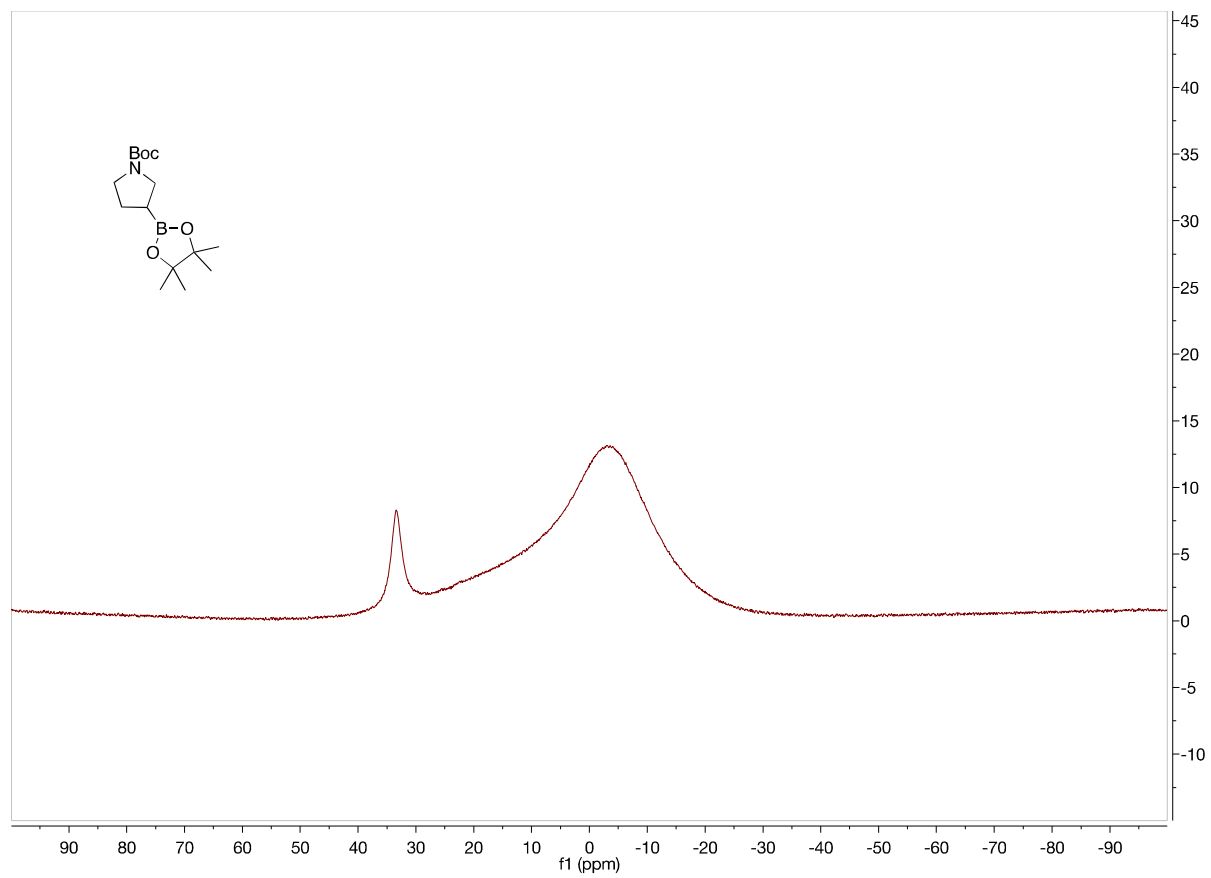


Figure A30. 160 MHz ^{11}B NMR of **2g** in CDCl_3

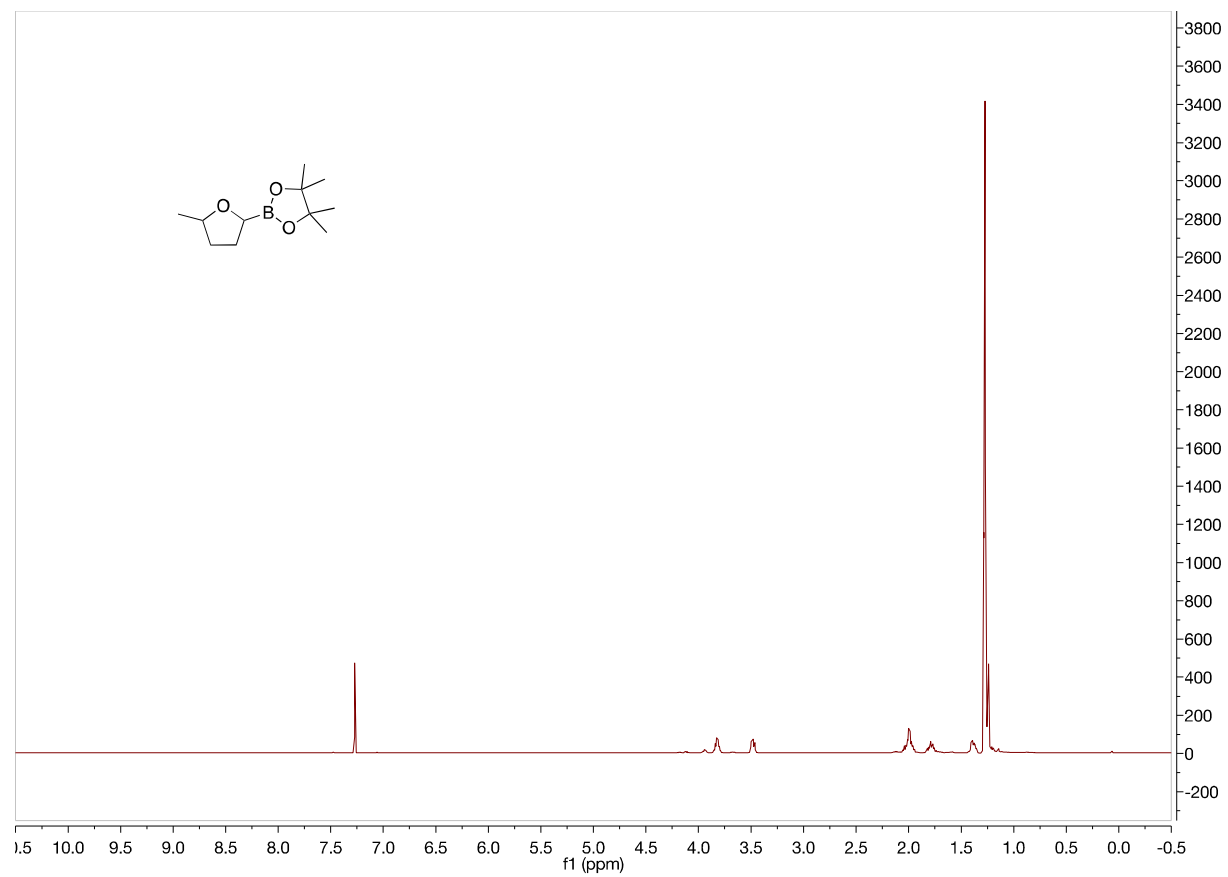


Figure A31. 500 MHz ¹H NMR of **2h** in CDCl₃

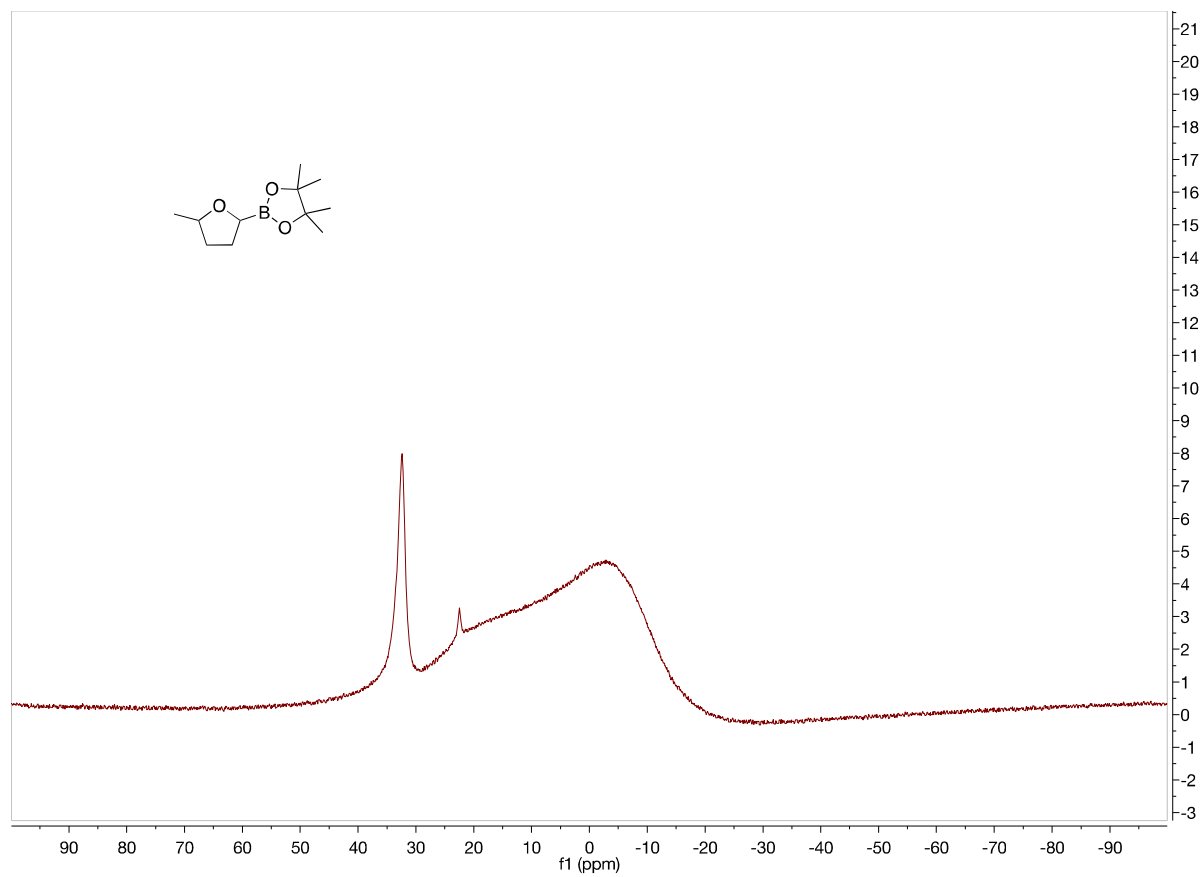


Figure A32. 160 MHz ^{11}B NMR of **2h** in CDCl_3

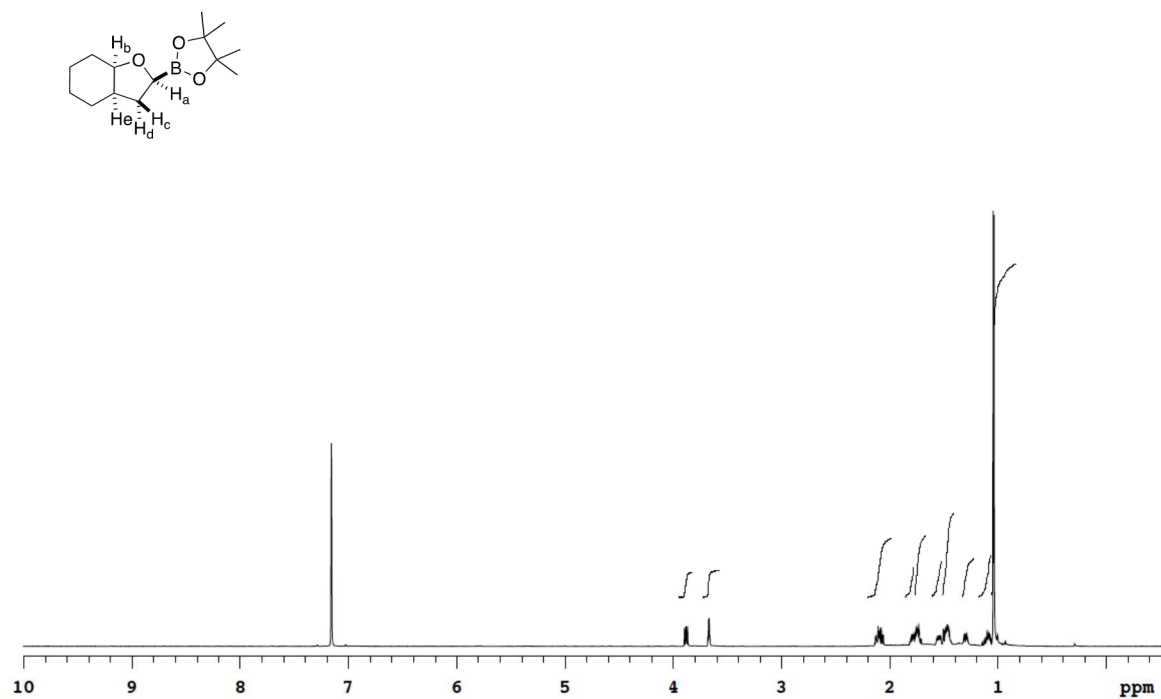


Figure A33. 500 MHz ^1H NMR of **21** in C_6D_6

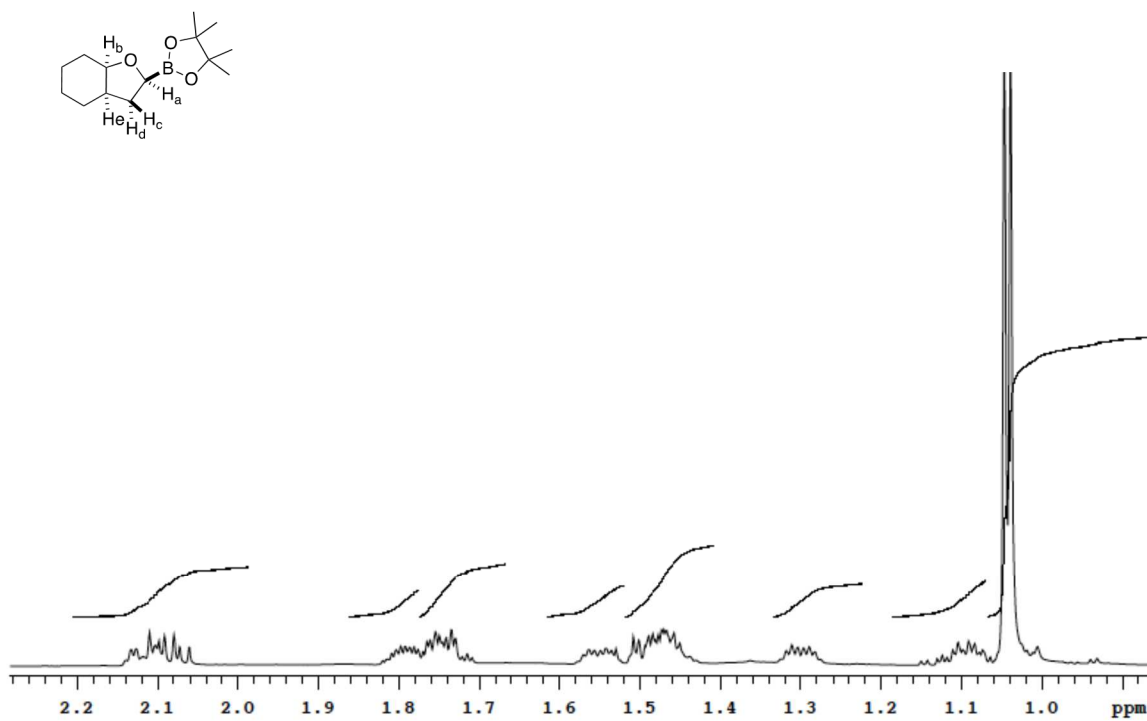


Figure A34. 500 MHz ^1H NMR of **2l** in C_6D_6 from 2.3ppm to 0.9ppm

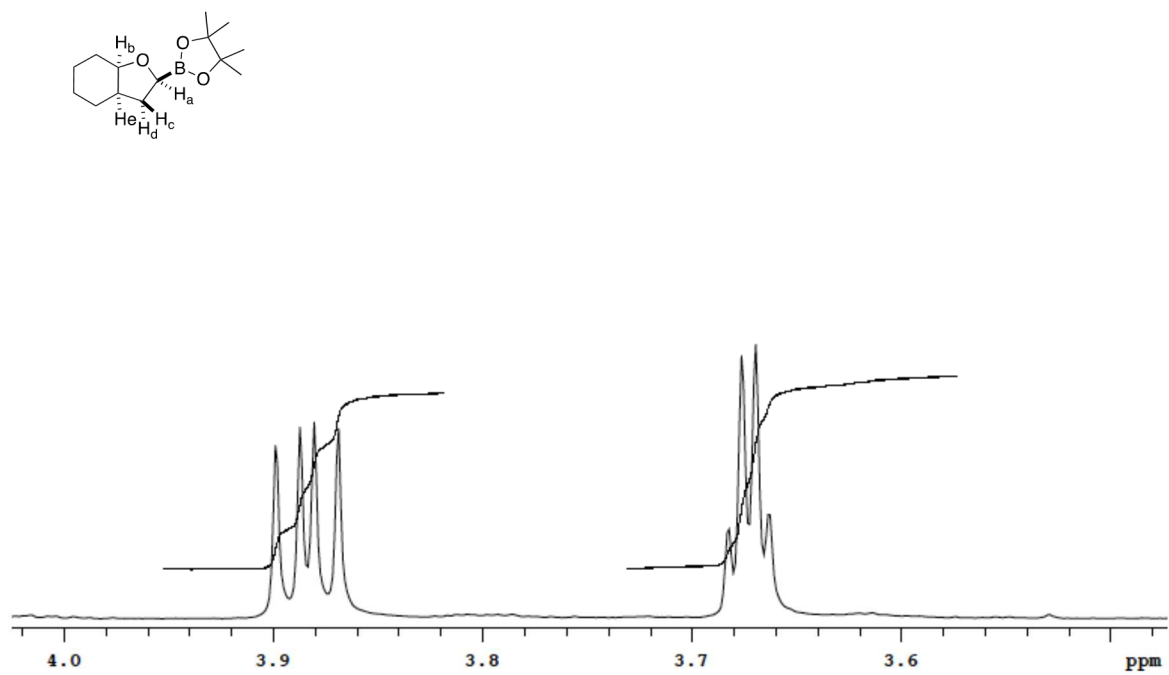


Figure A35. 500 MHz ^1H NMR of **21** in C_6D_6 from 4.1ppm to 3.5ppm

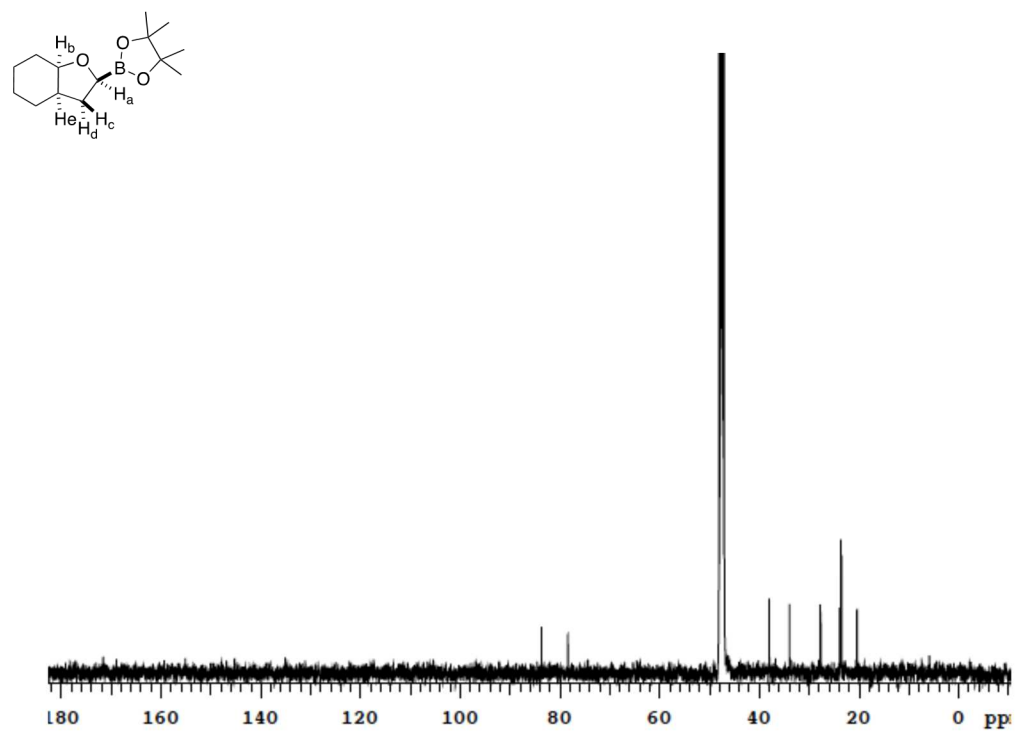


Figure A36. 125 MHz ¹³C NMR of **21** in C₆D₆

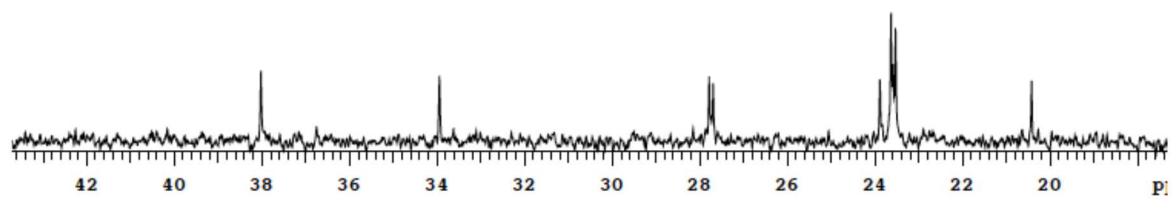
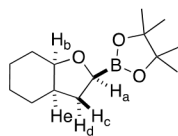


Figure A37. 125 MHz ^{13}C NMR of **21** in C_6D_6 from 43ppm to 18 ppm

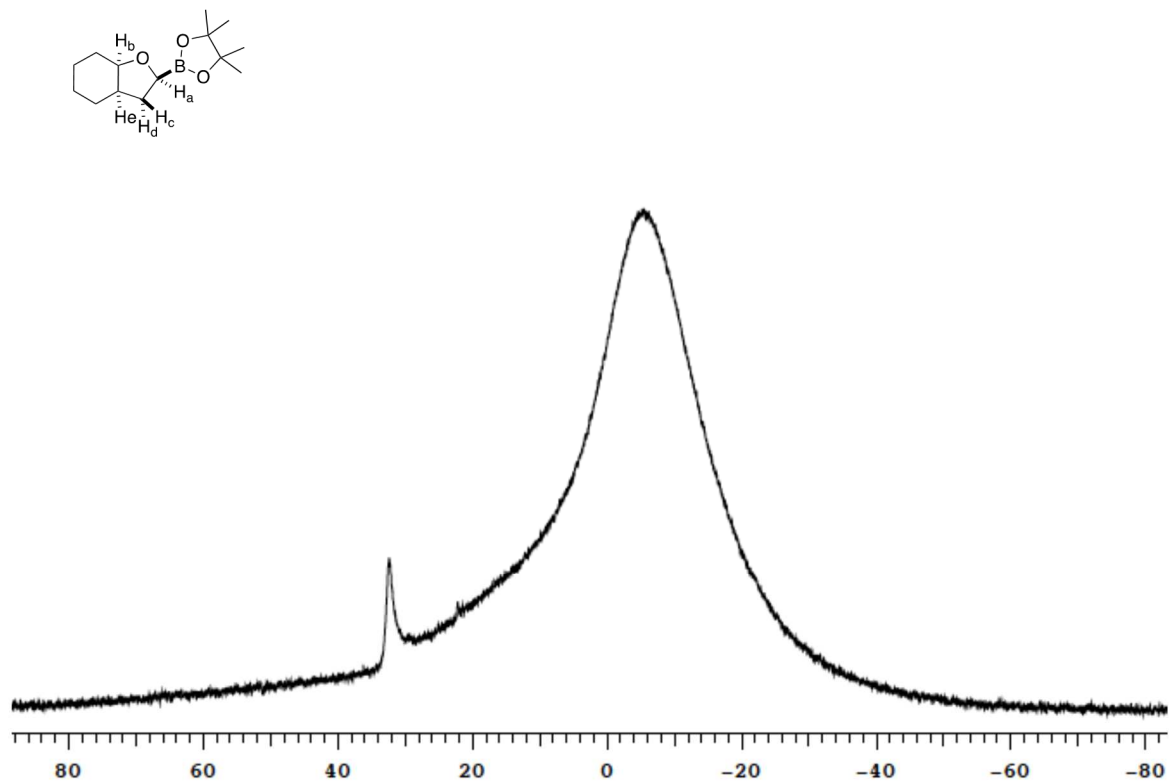


Figure A38. 160 MHz ^{11}B NMR of **2l** in C_6D_6

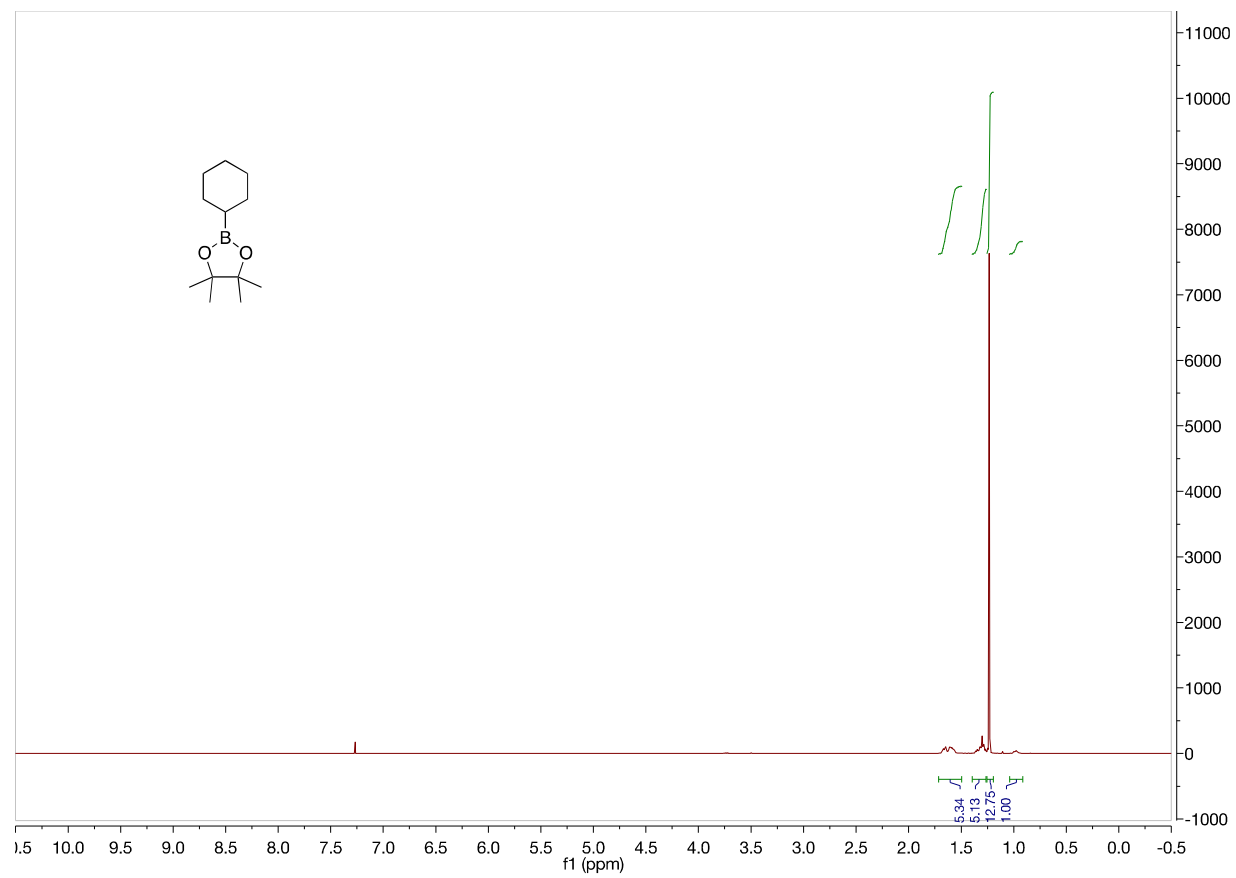


Figure A39. 500 MHz ^1H NMR of **2o** in CDCl_3

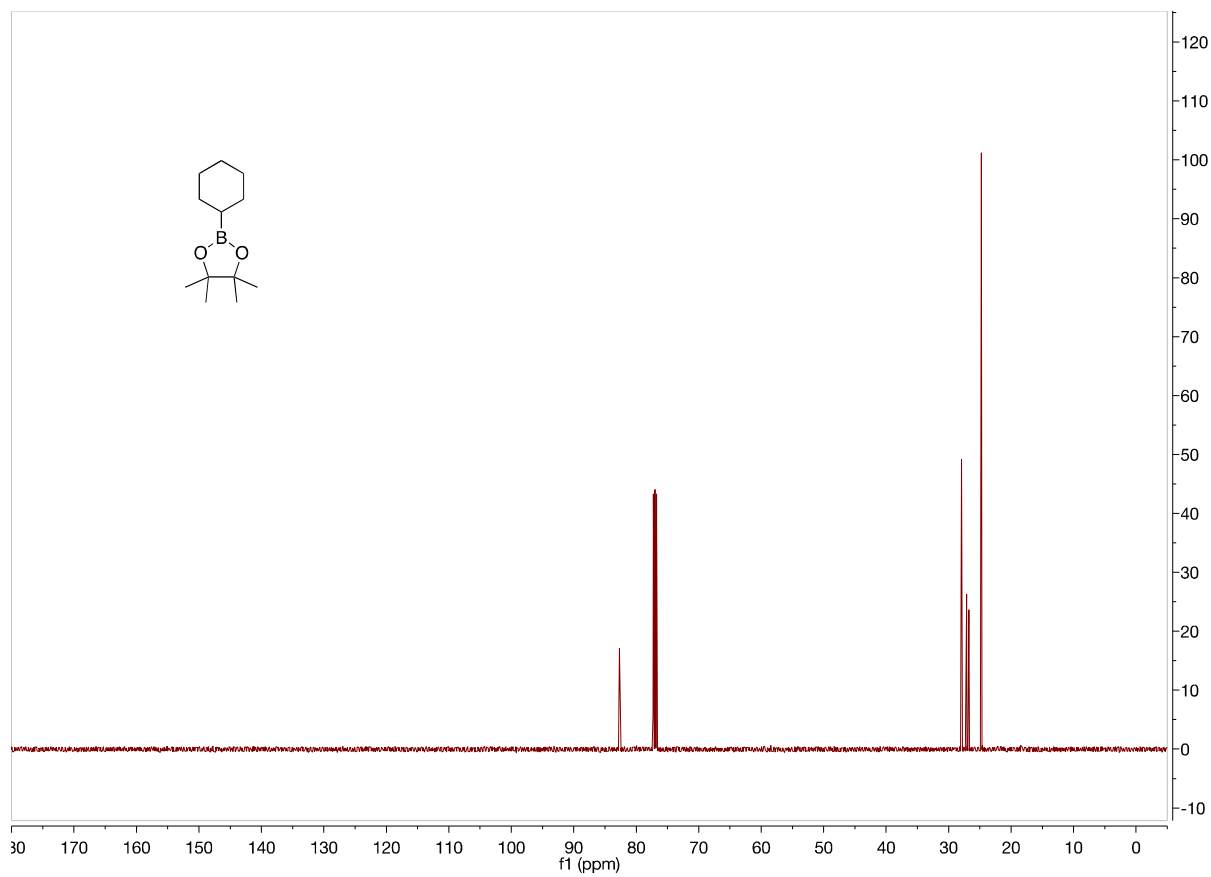


Figure A40. 125 MHz ^{13}C NMR of **2o** in CDCl_3

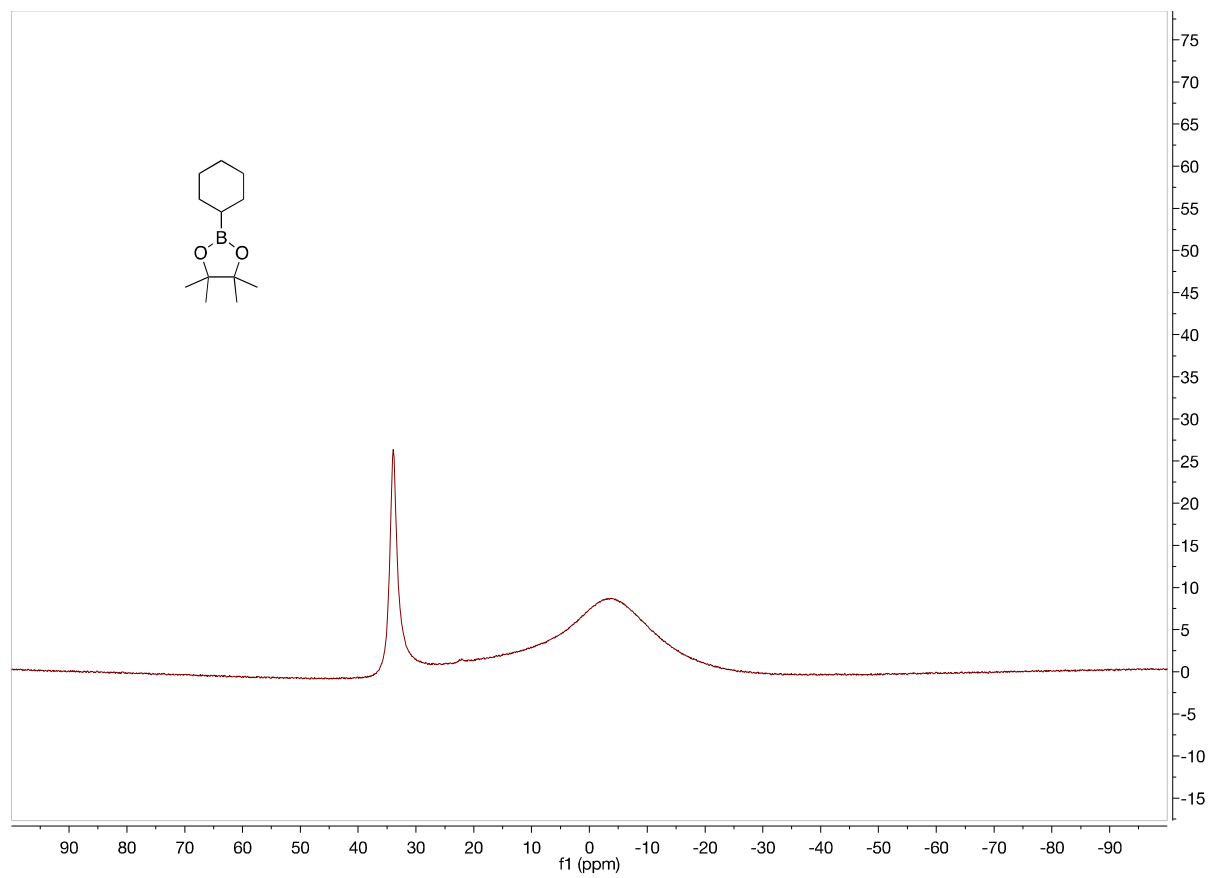


Figure A41. 160 MHz ^{11}B NMR of **2o** in CDCl_3

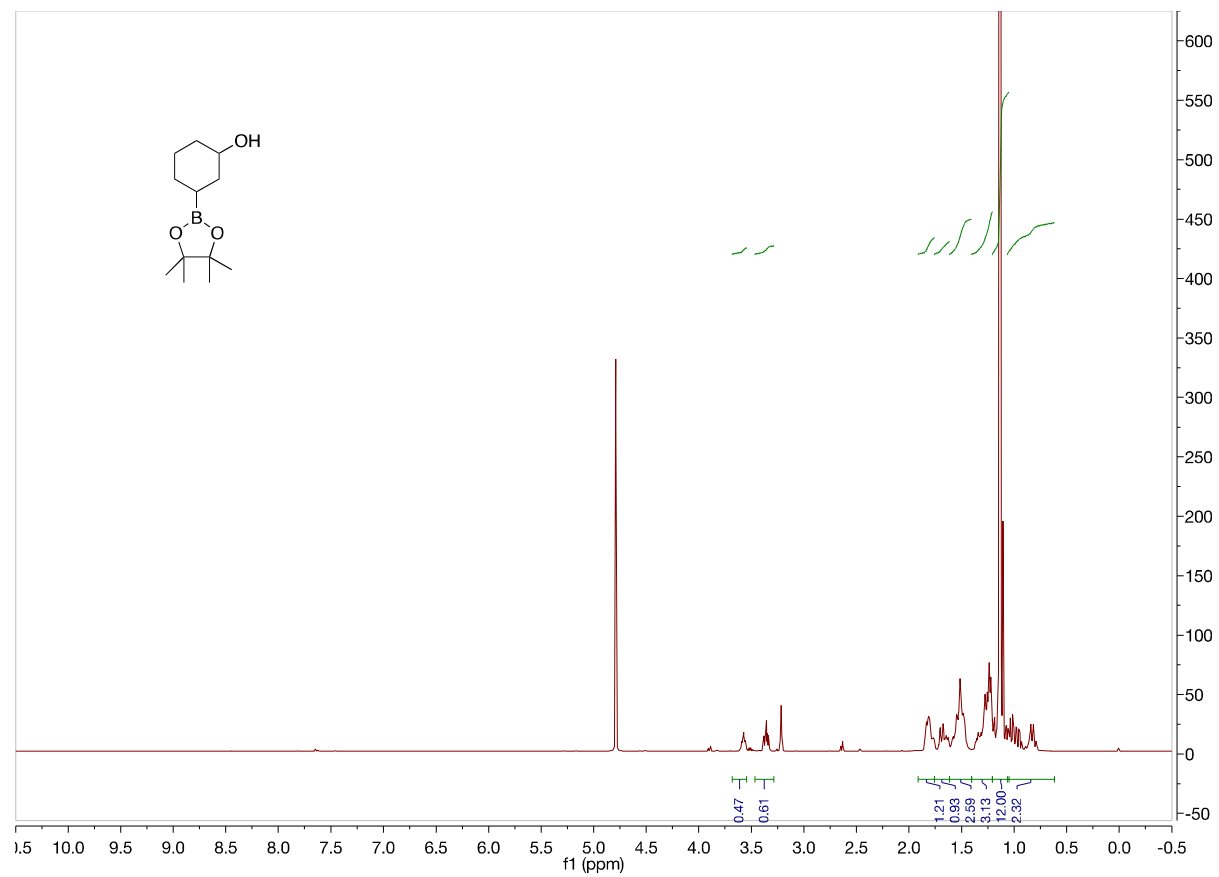


Figure A42. 500 MHz ^1H NMR of **2p** in D_2O

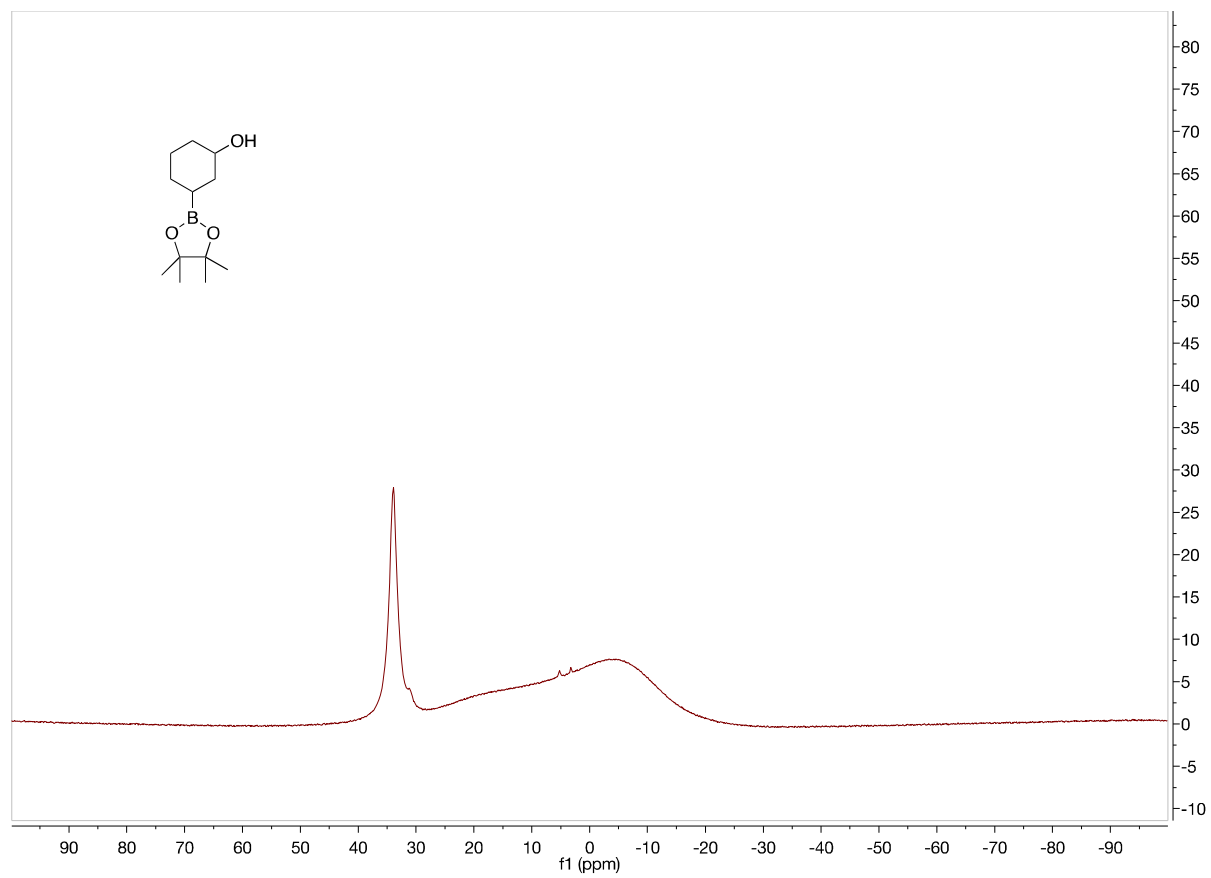


Figure A43. 160 MHz ^{11}B NMR of **2p** in D_2O

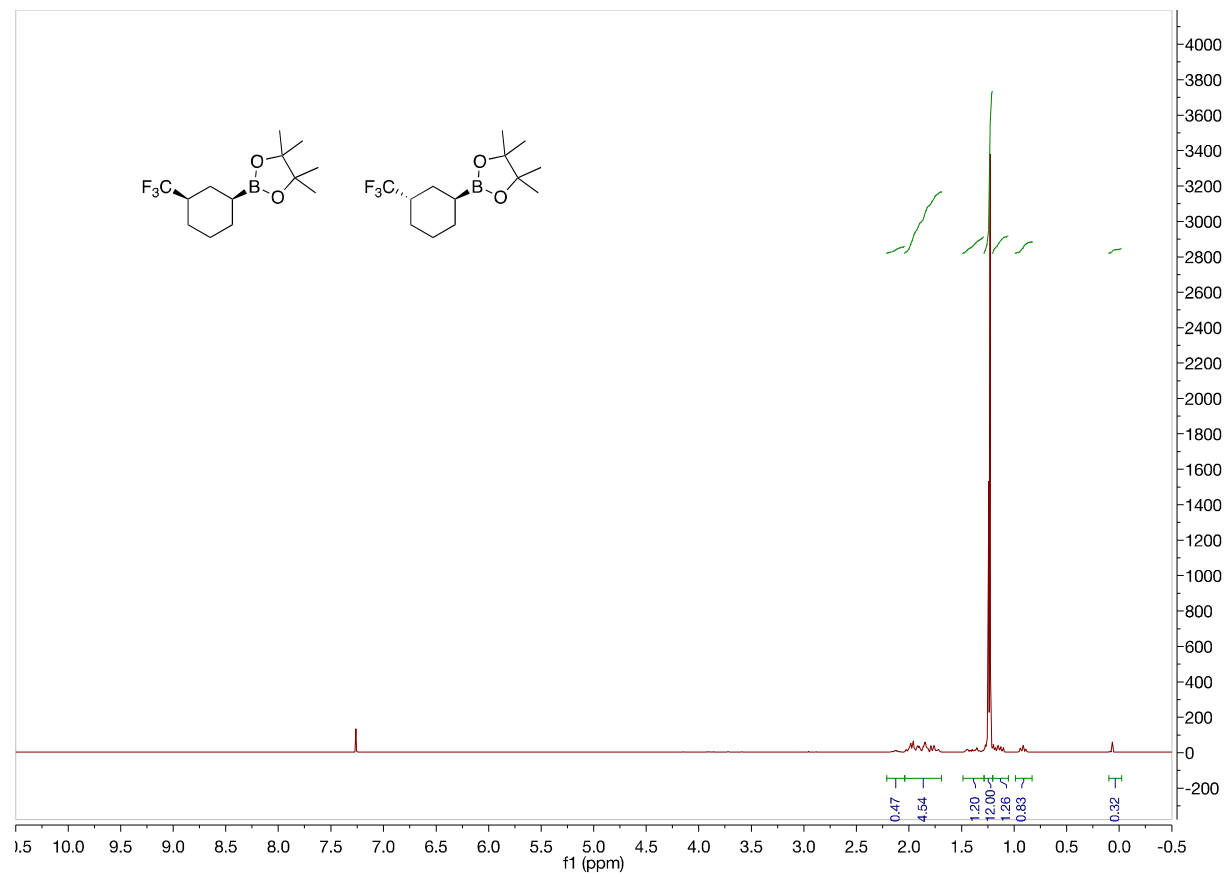


Figure A44. 500 MHz ^1H NMR of **2q** in CDCl_3

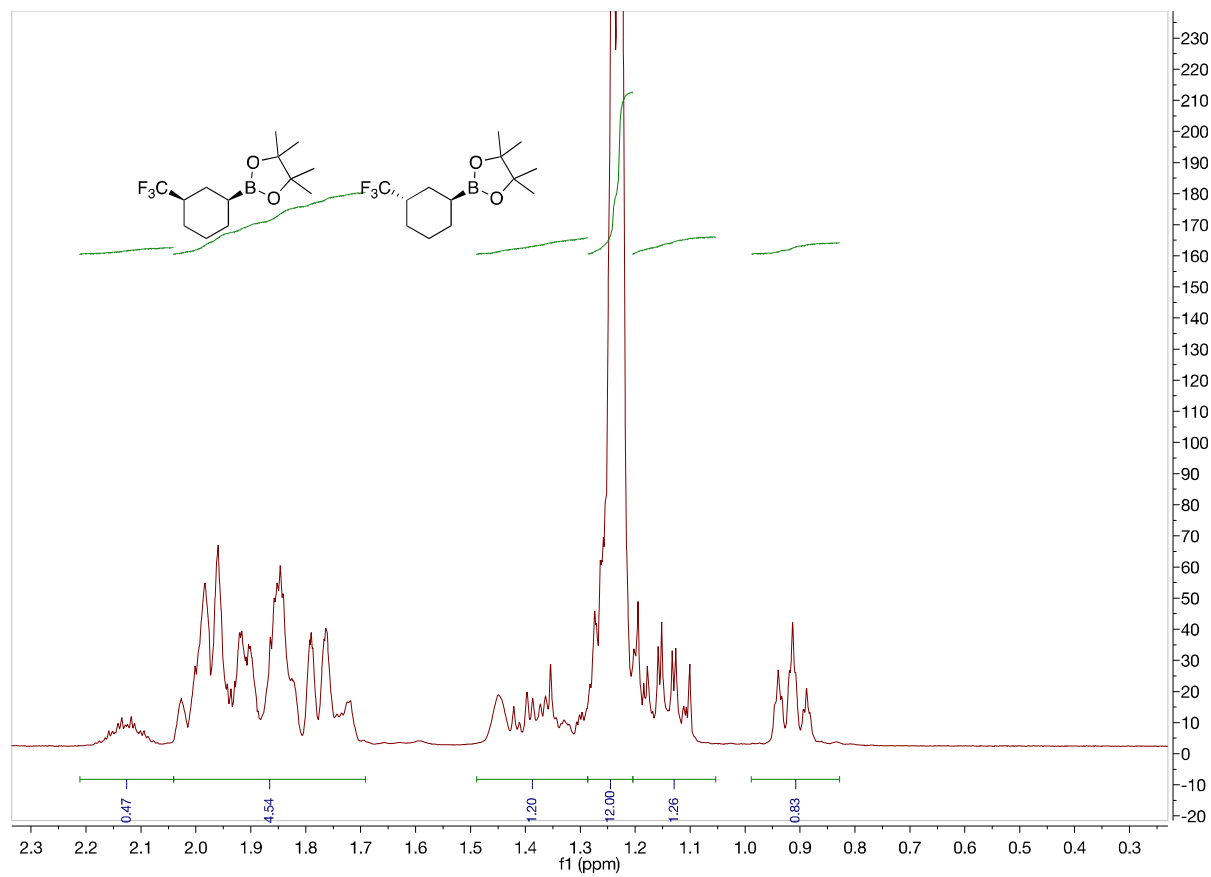


Figure A45. 500 MHz ^1H NMR of **2q** in CDCl_3

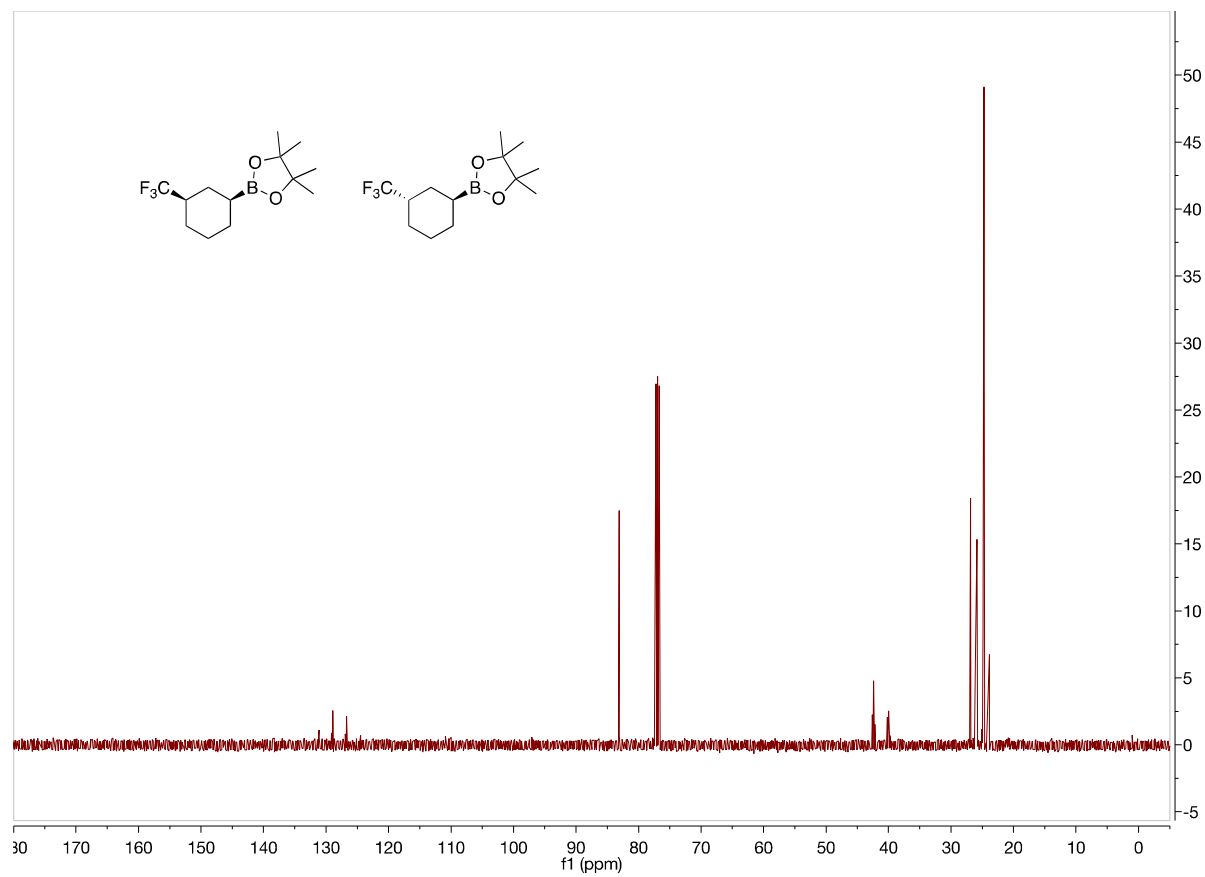


Figure A46. 125 MHz ^{13}C NMR of **2q** in CDCl_3

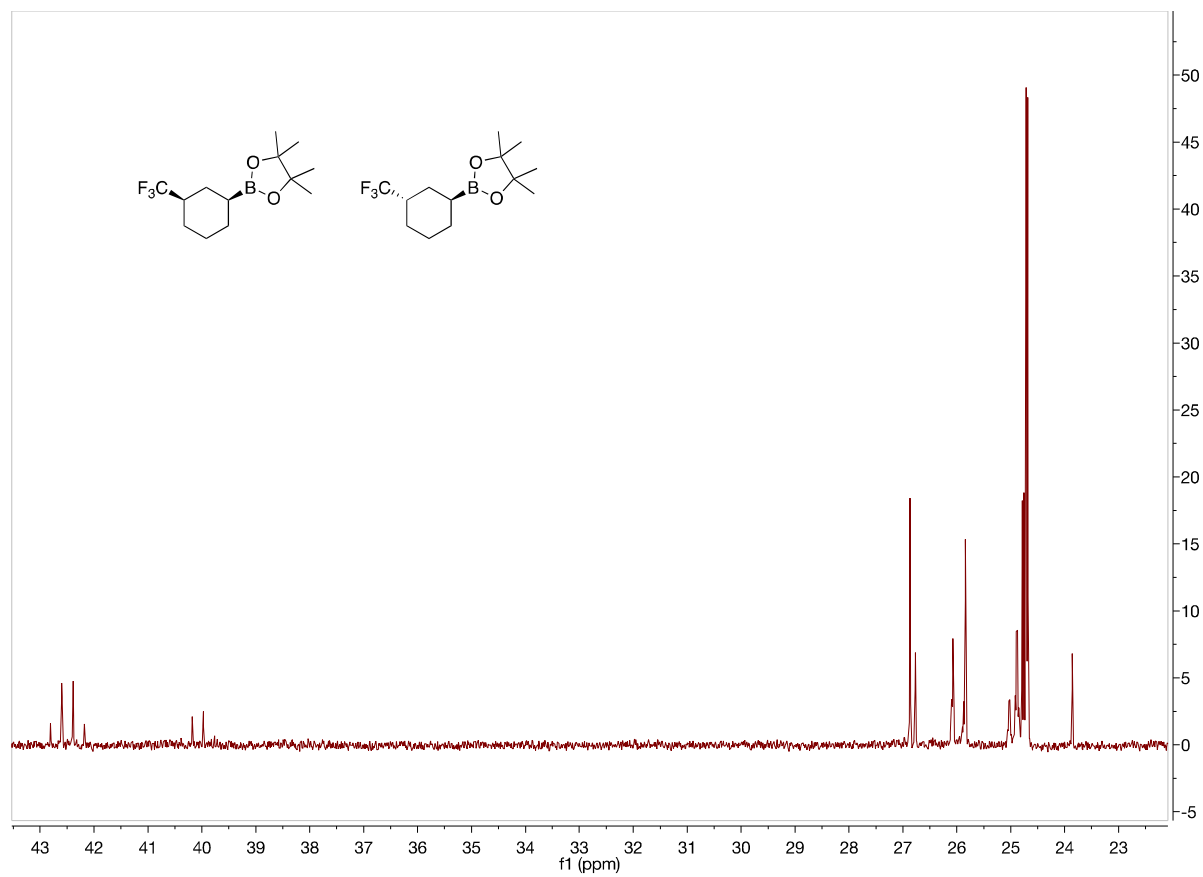


Figure A47. 125 MHz ^{13}C NMR of **2q** in CDCl_3 from 44 to 22 ppm

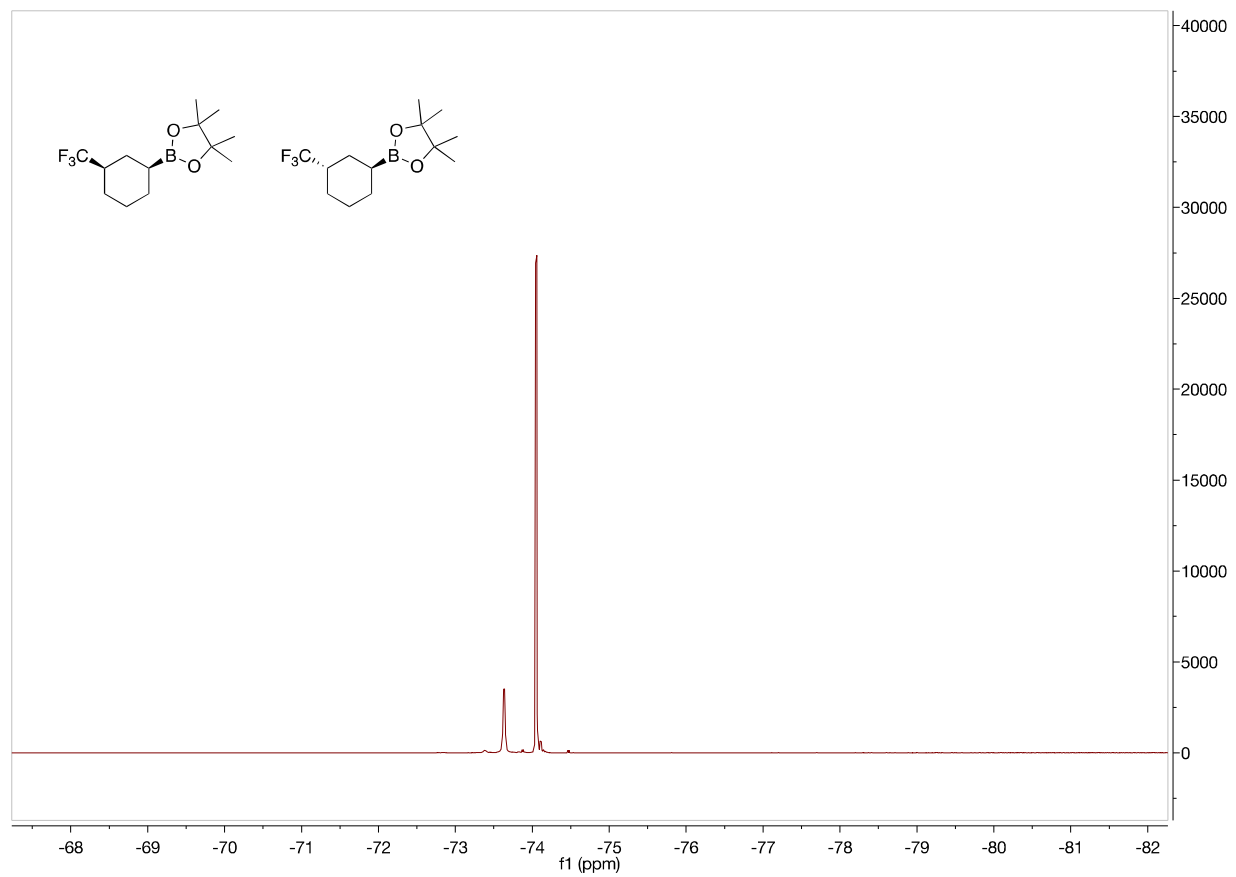


Figure A48. 470 MHz ^{19}F NMR of **2q** in CDCl_3

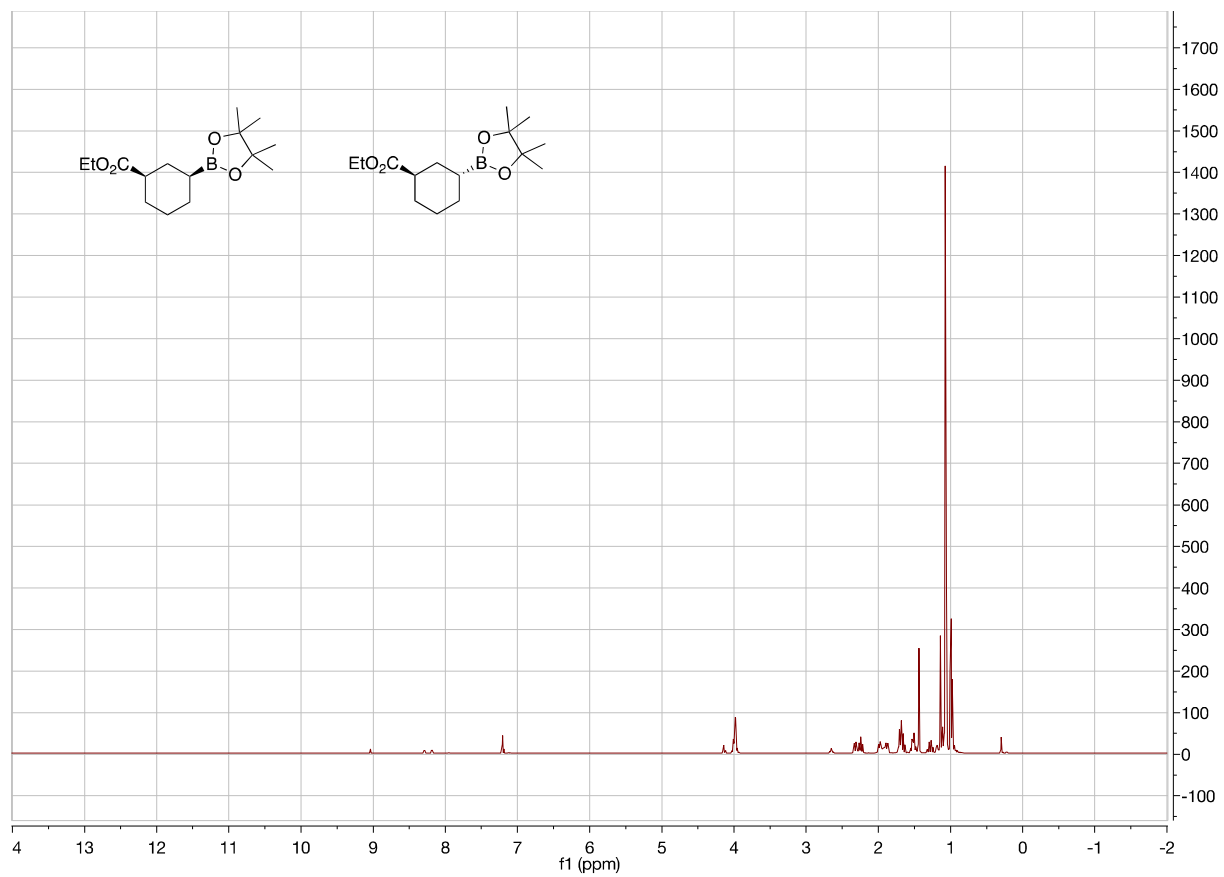


Figure A49. 500 MHz ^1H NMR of **2r** in C_6D_6

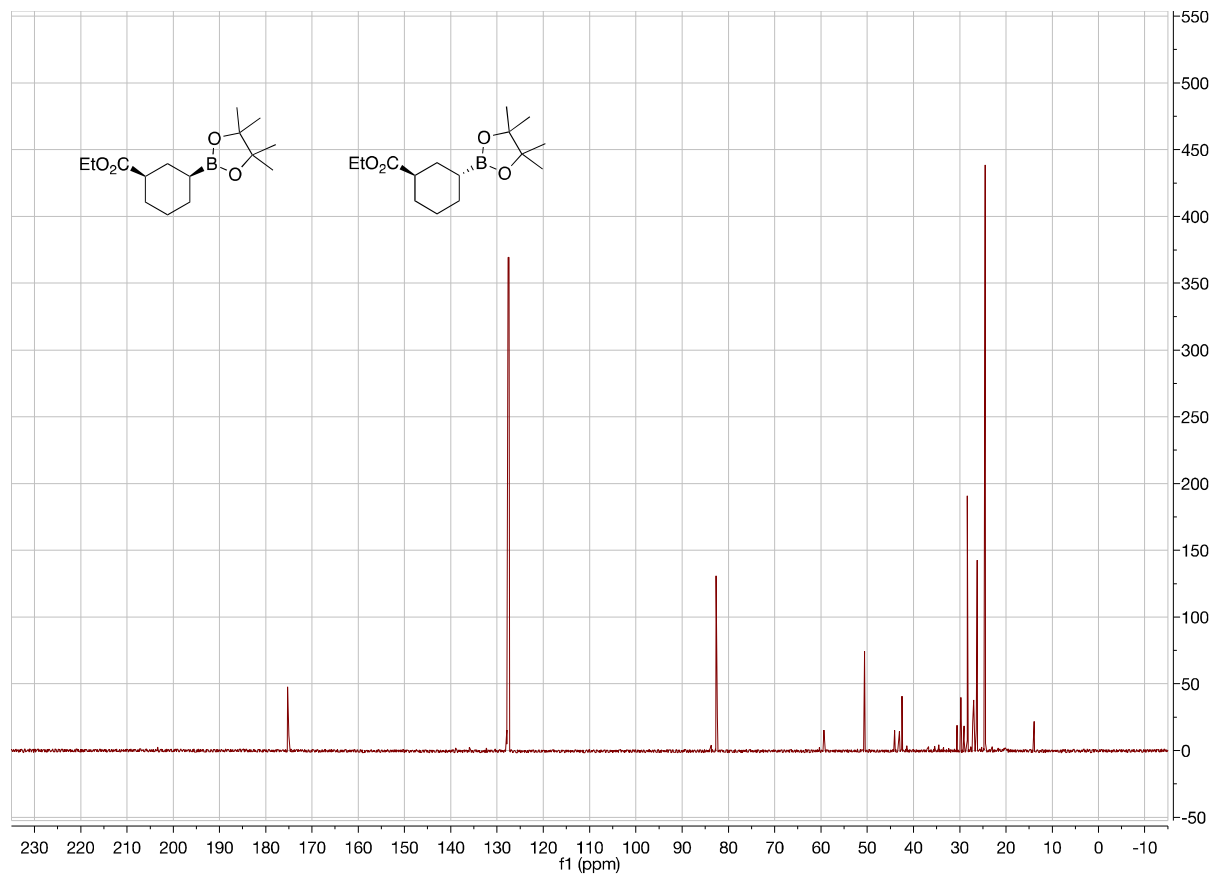


Figure A50. 125 MHz ^{13}C NMR of **2r** in C_6D_6

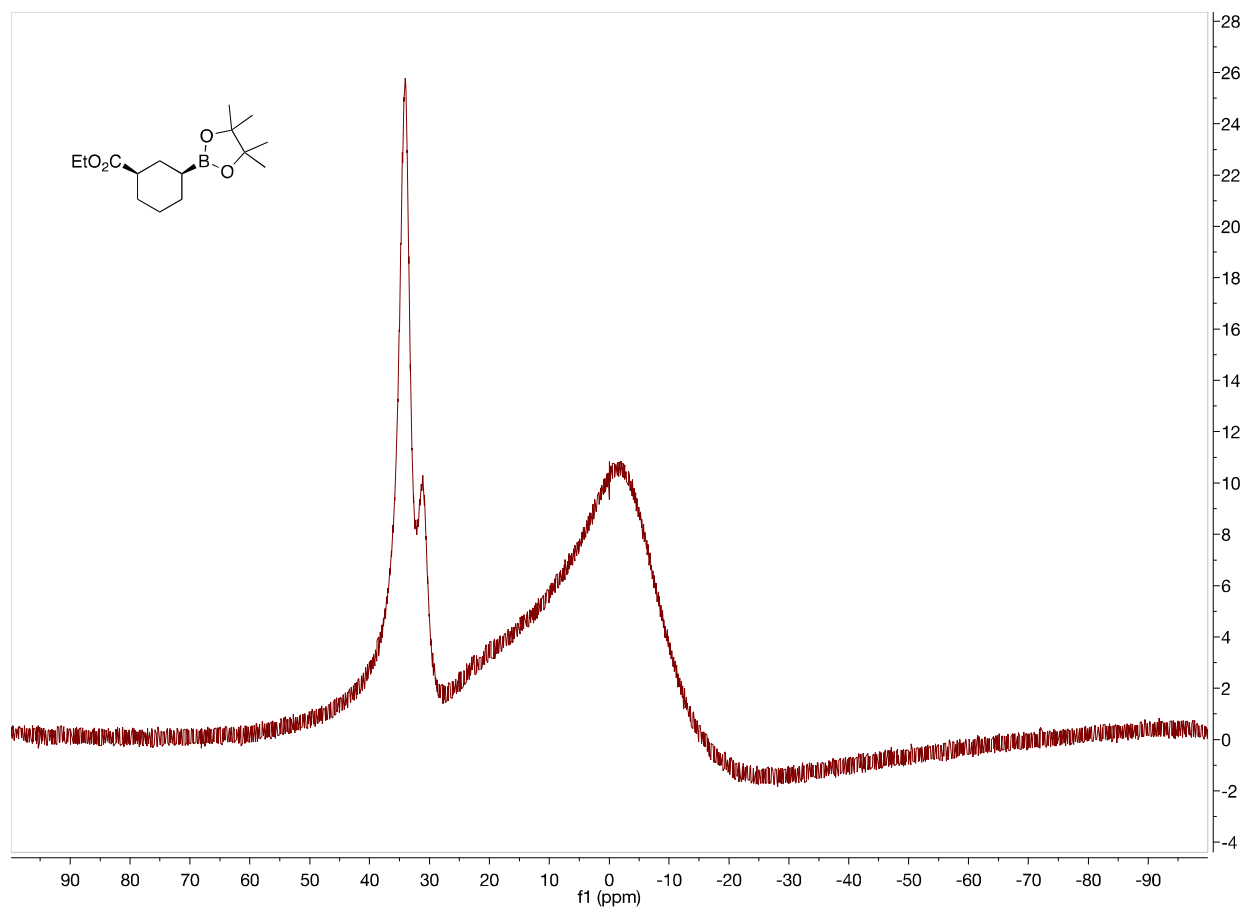


Figure A51. 160 MHz ^{11}B NMR of **2r** in C_6D_6

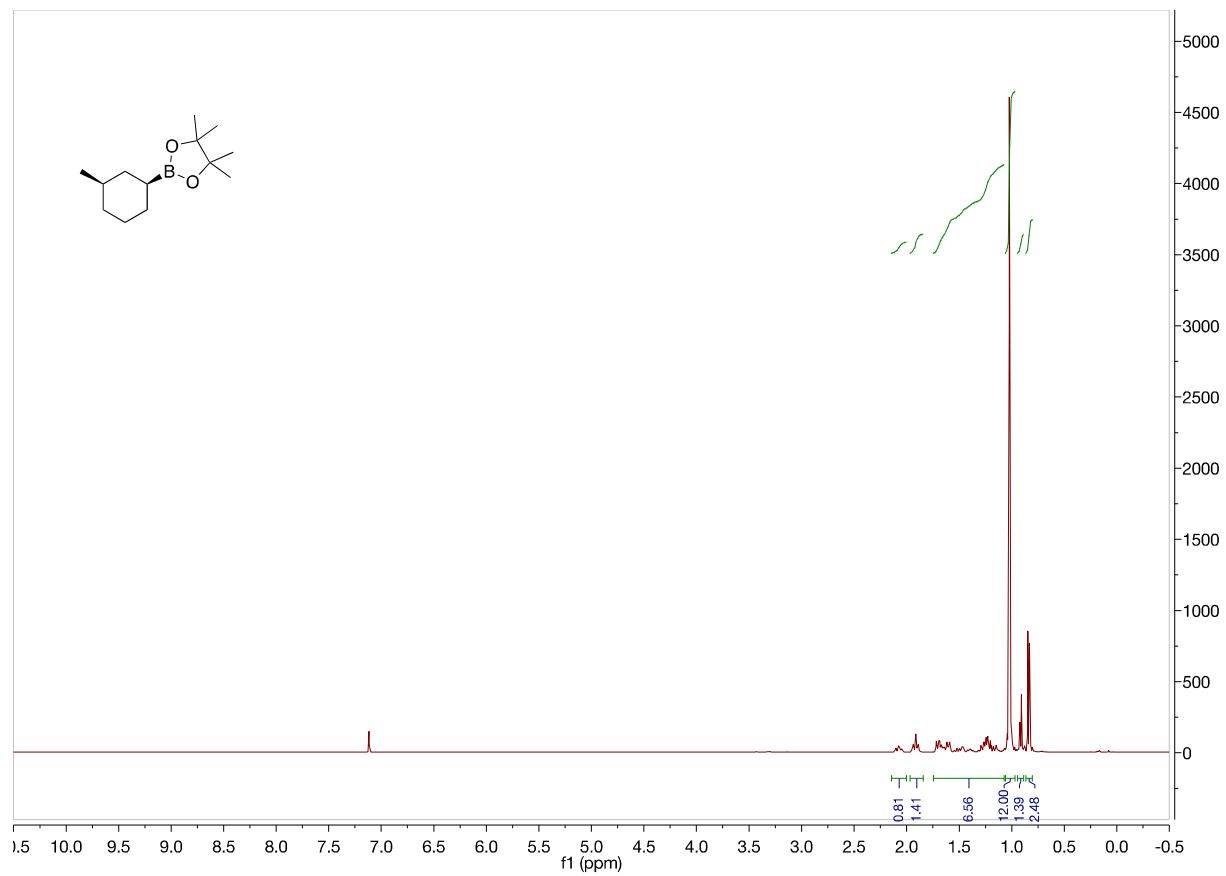


Figure A52. 500 MHz ^1H NMR of **2s** in C_6D_6

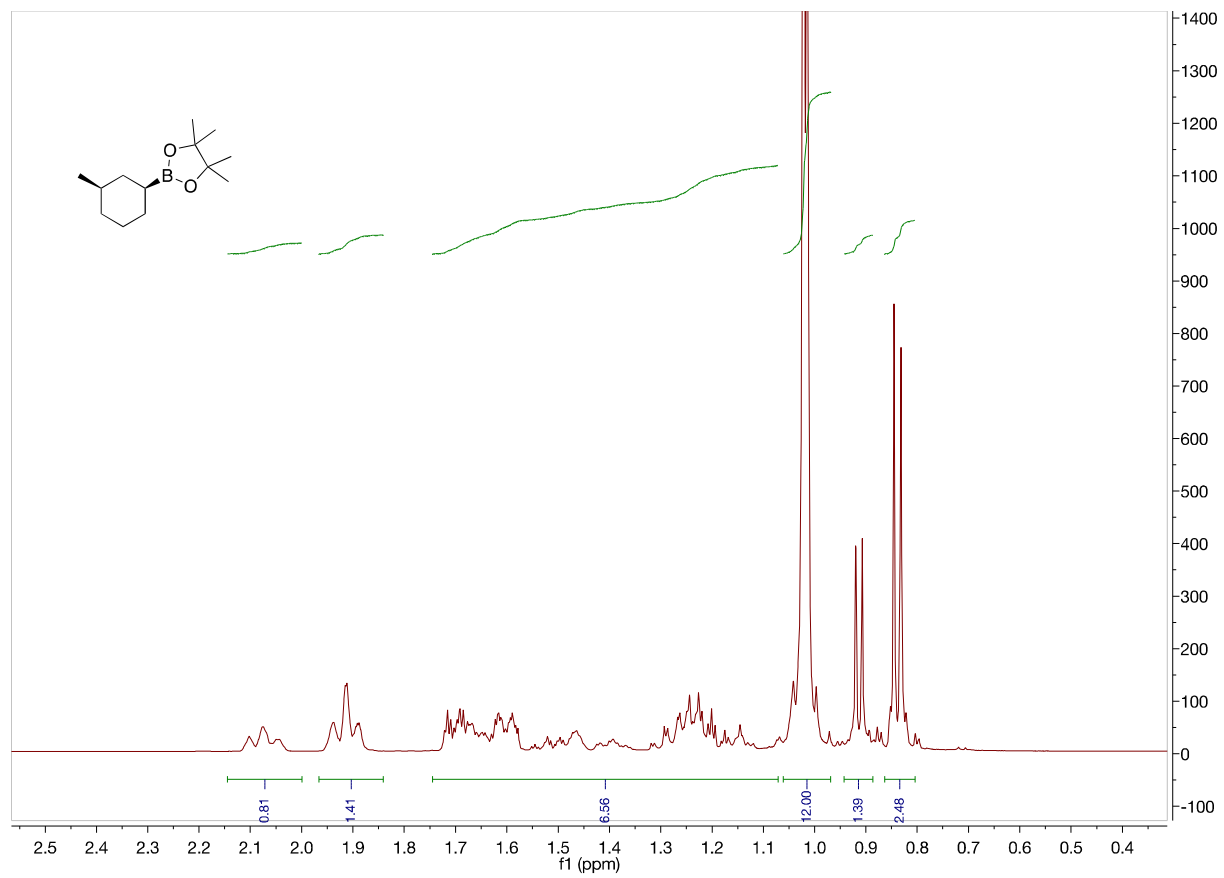


Figure A53. 500 MHz ¹H NMR of **2s** in C₆D₆ from 2.5 to 0.4 ppm

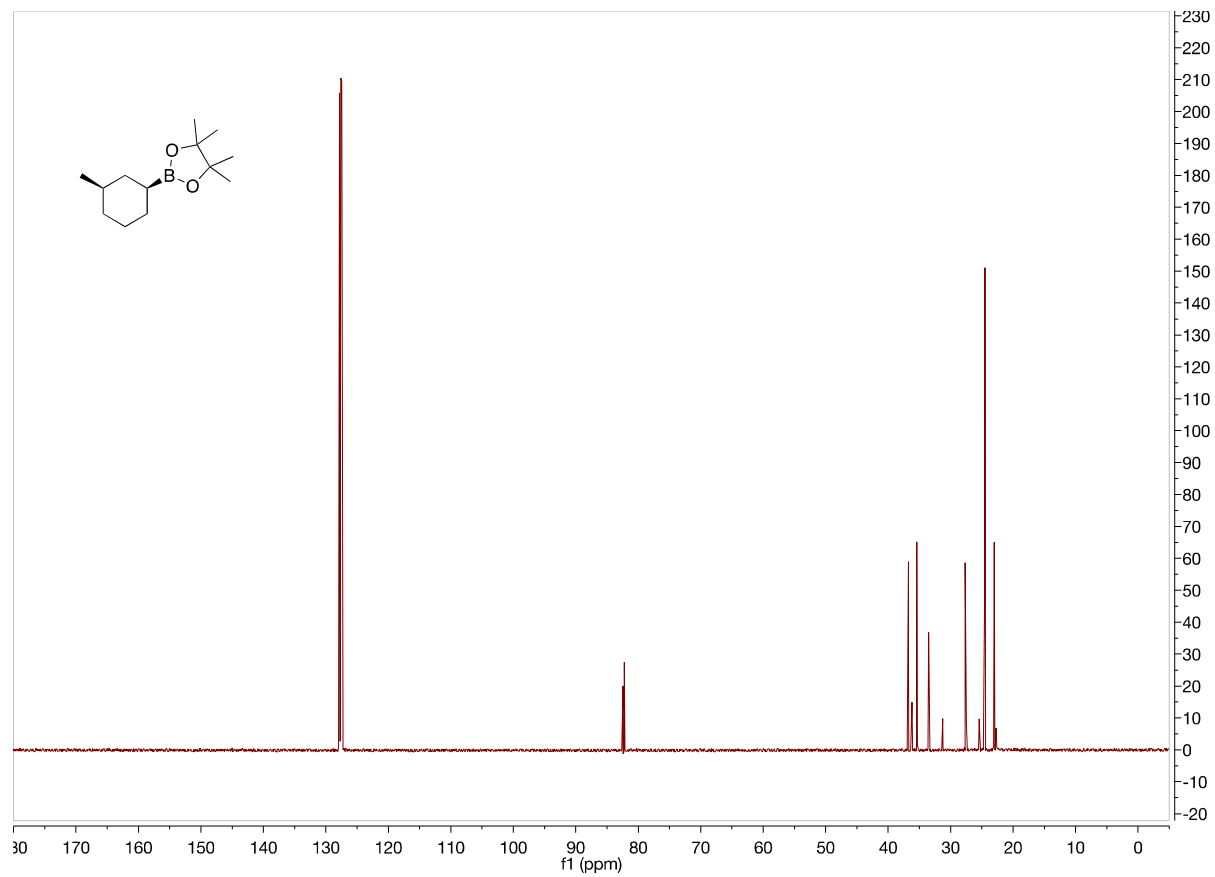


Figure A54. 125 MHz ¹³C NMR of **2s** in C₆D₆

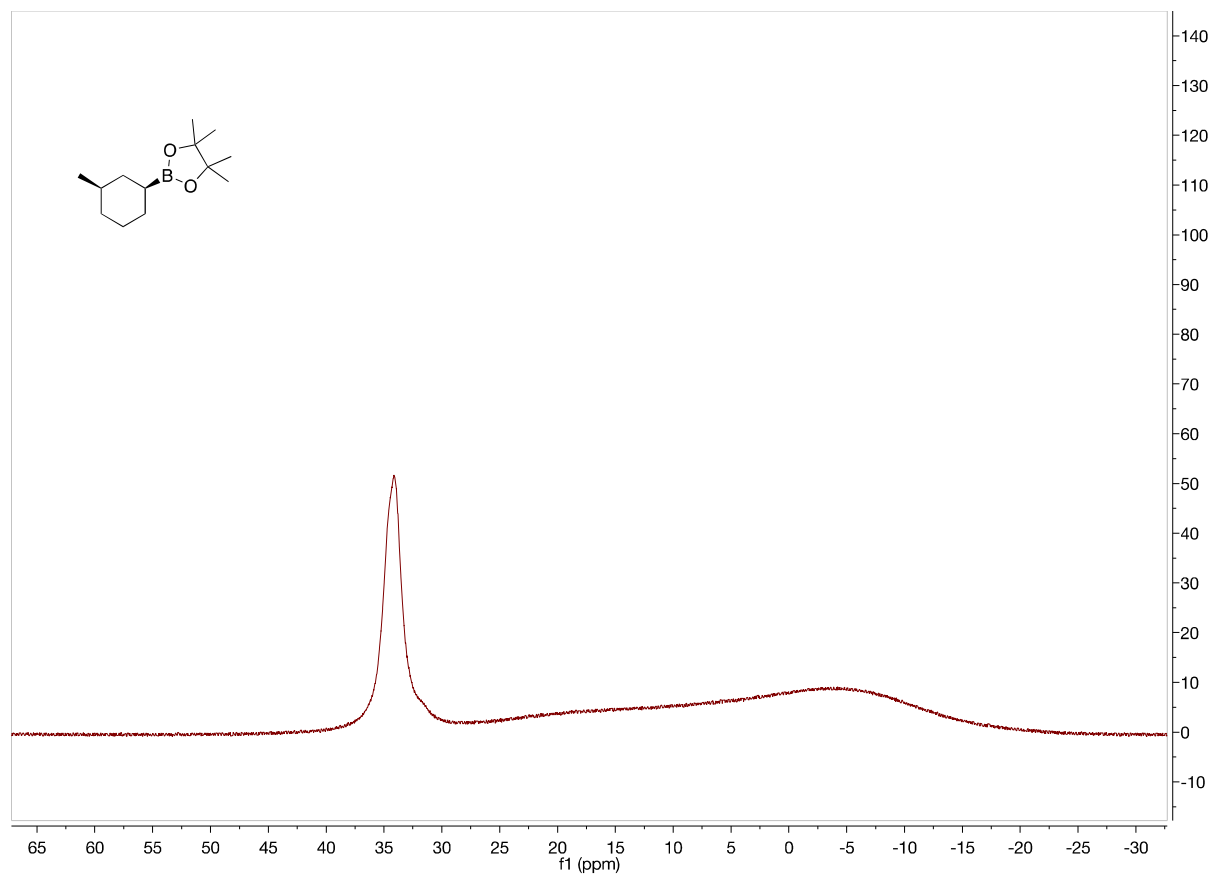


Figure A55. 160 MHz ^{11}B NMR of **2s** in C_6D_6

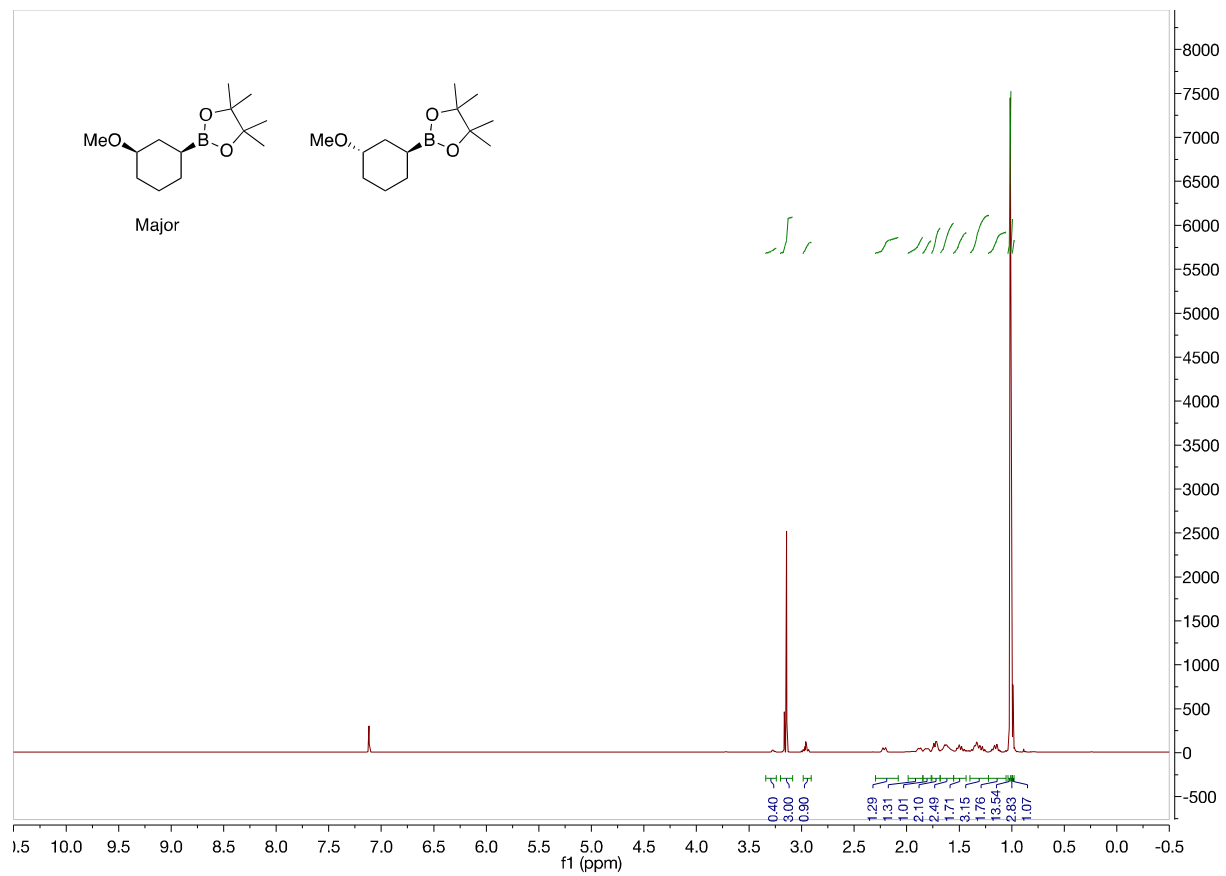


Figure A56. 500 MHz ^1H NMR of **2t** in C_6D_6

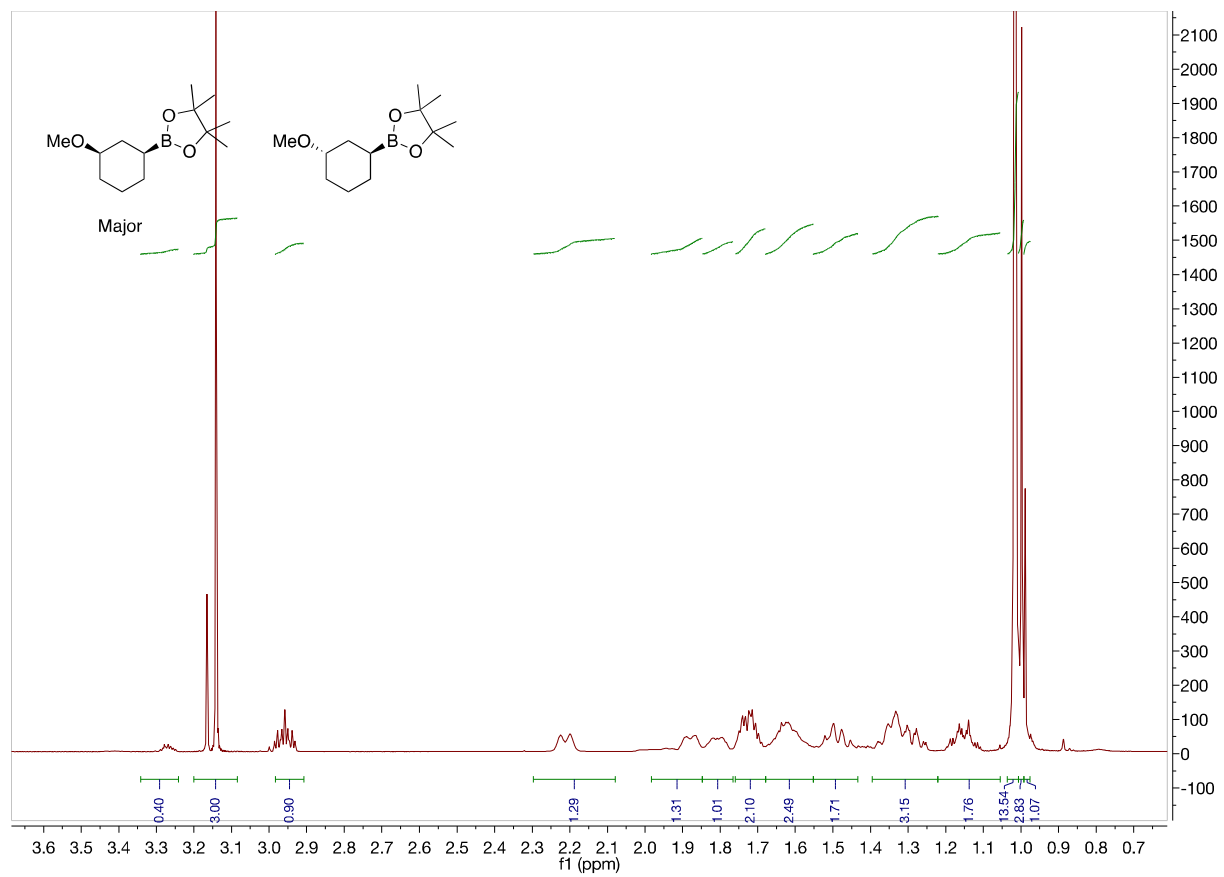


Figure A57. 500 MHz ^1H NMR of **2t** in C_6D_6 from 3.6 to 0.7 ppm

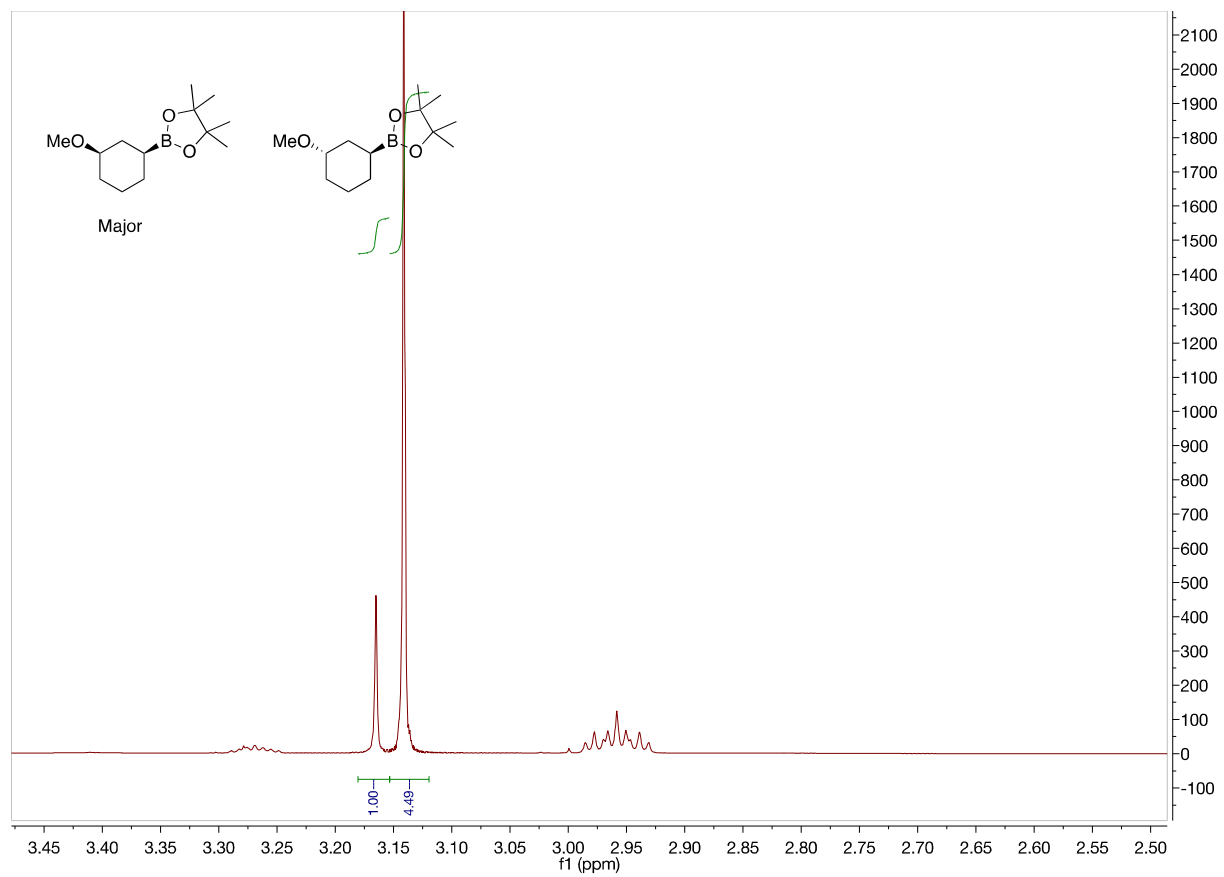


Figure A58. 500 MHz ^1H NMR of **2t** in C_6D_6 from 3.45 to 2.5 ppm

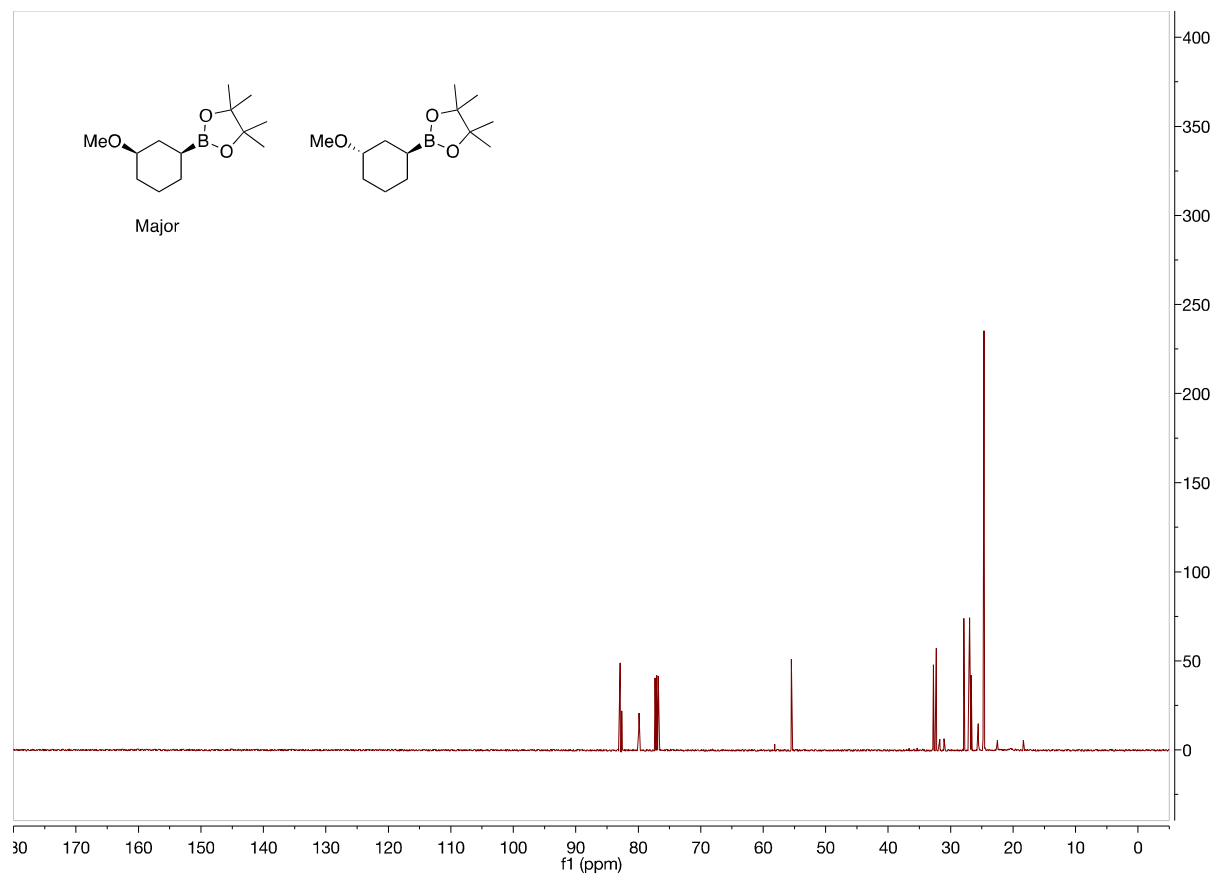


Figure A59. 125 MHz ^{13}C NMR of **2t** in CDCl_3

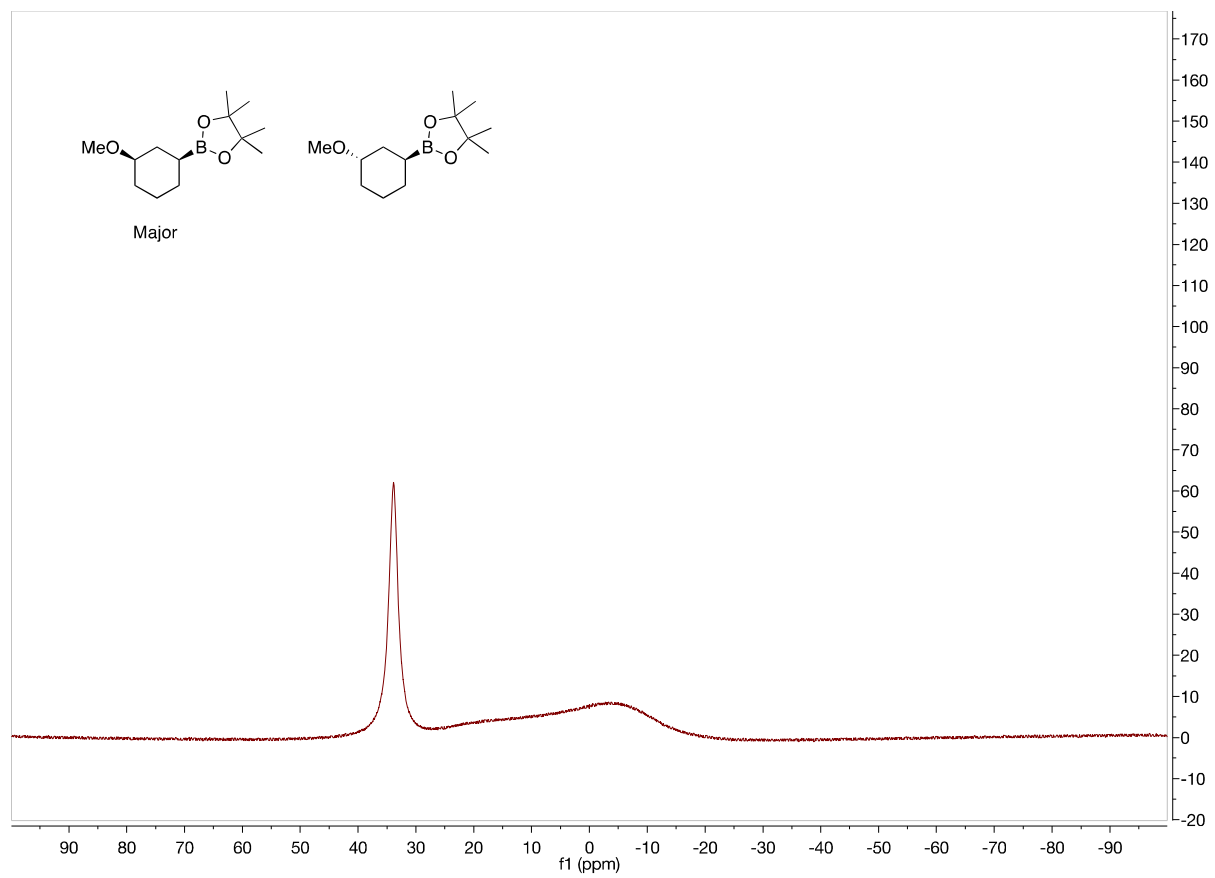


Figure A60. 160 MHz ^{11}B NMR of **2t** in CDCl_3

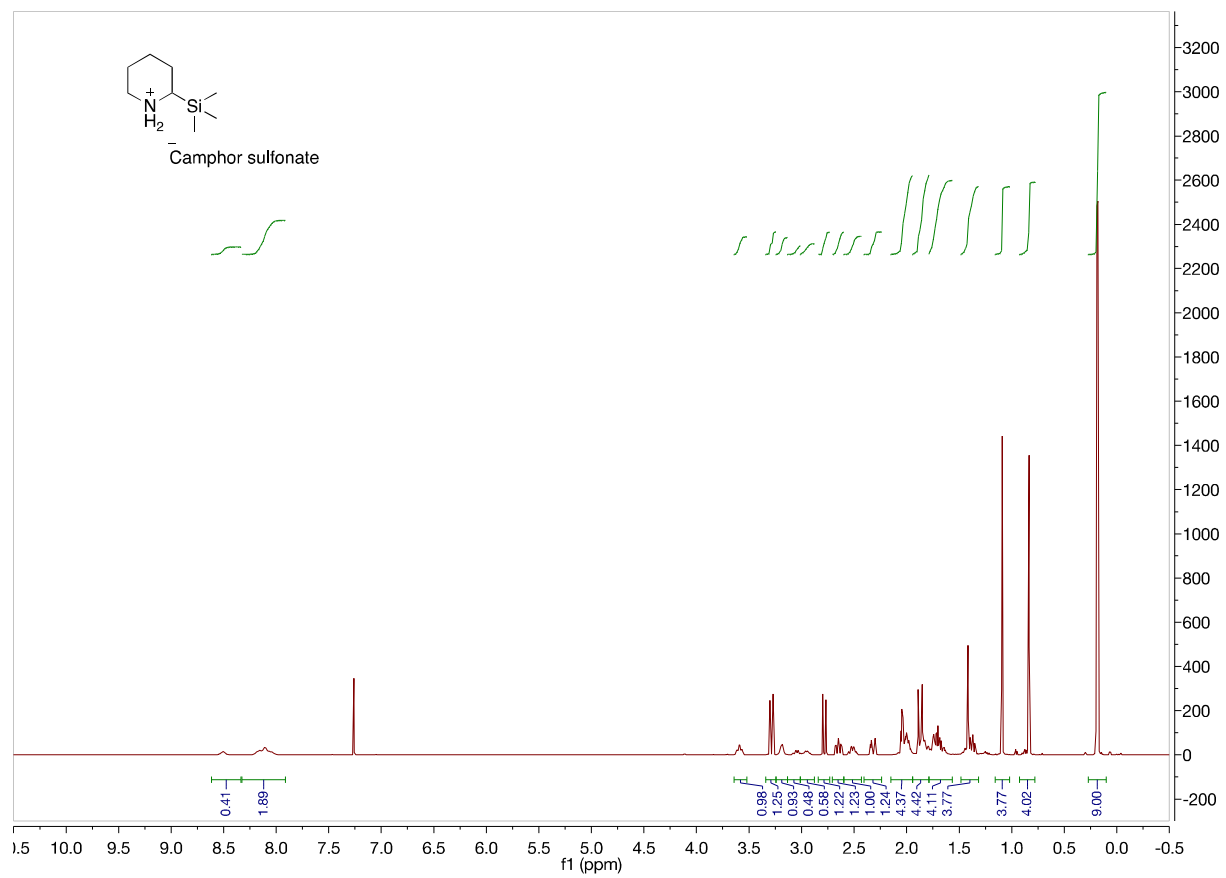


Figure A61. 500 MHz ^1H NMR of **2u** in CDCl_3

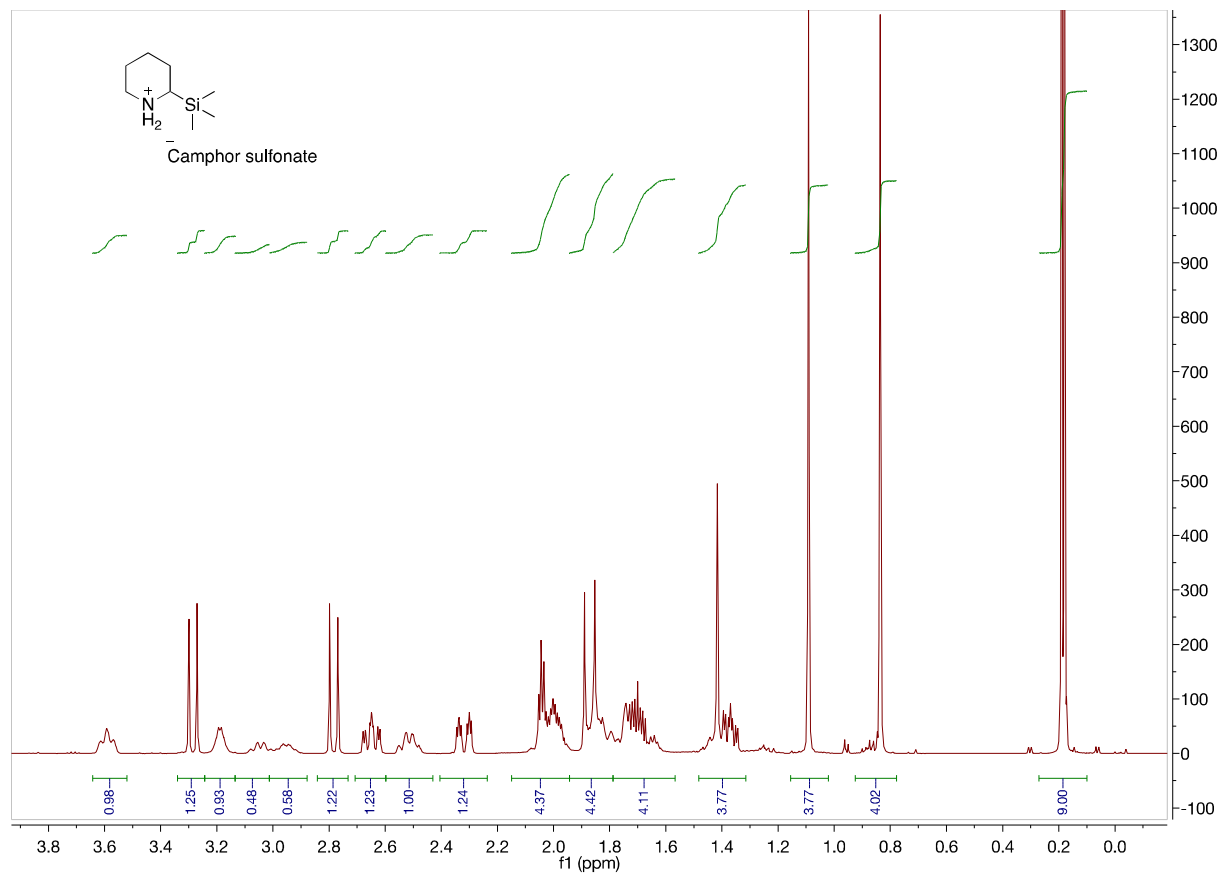


Figure A62. 500 MHz ^1H NMR of **2u** in CDCl_3 from 3.8 to 0.0 ppm

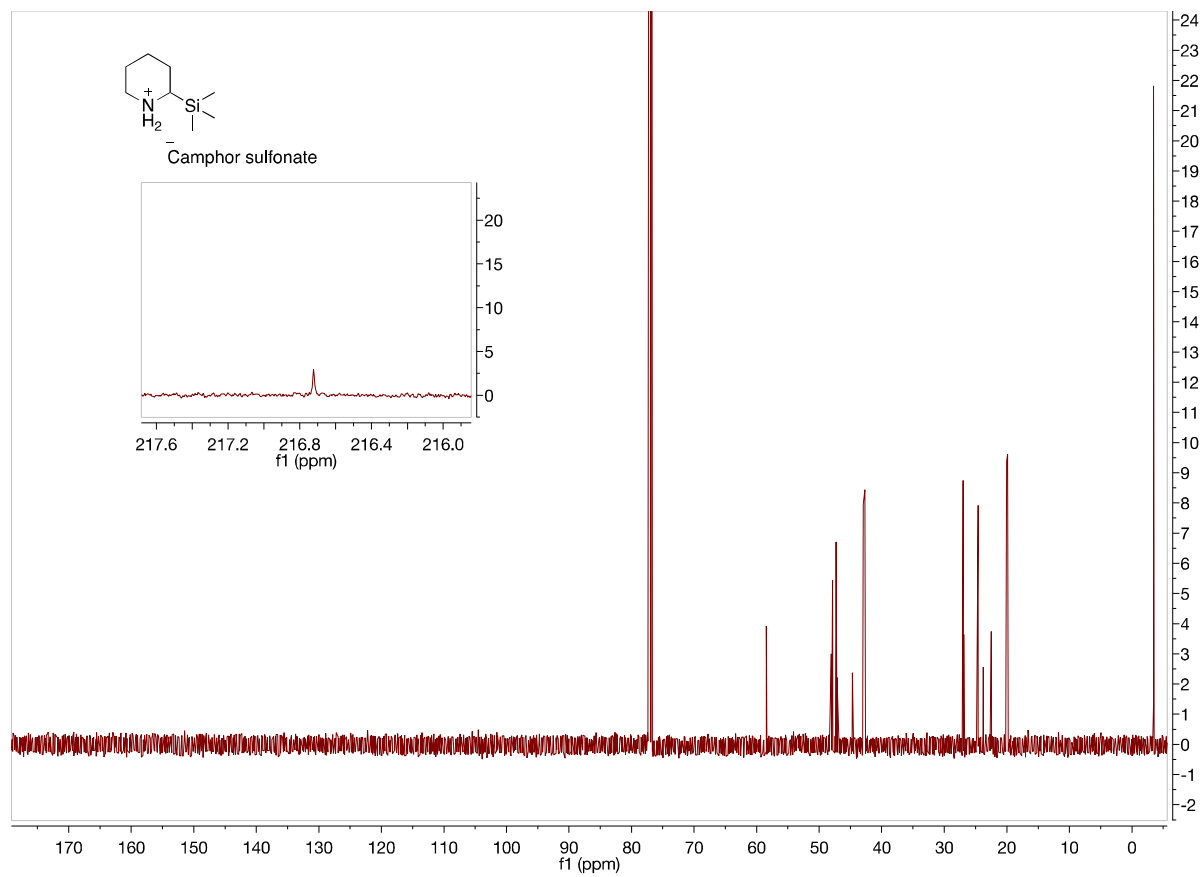
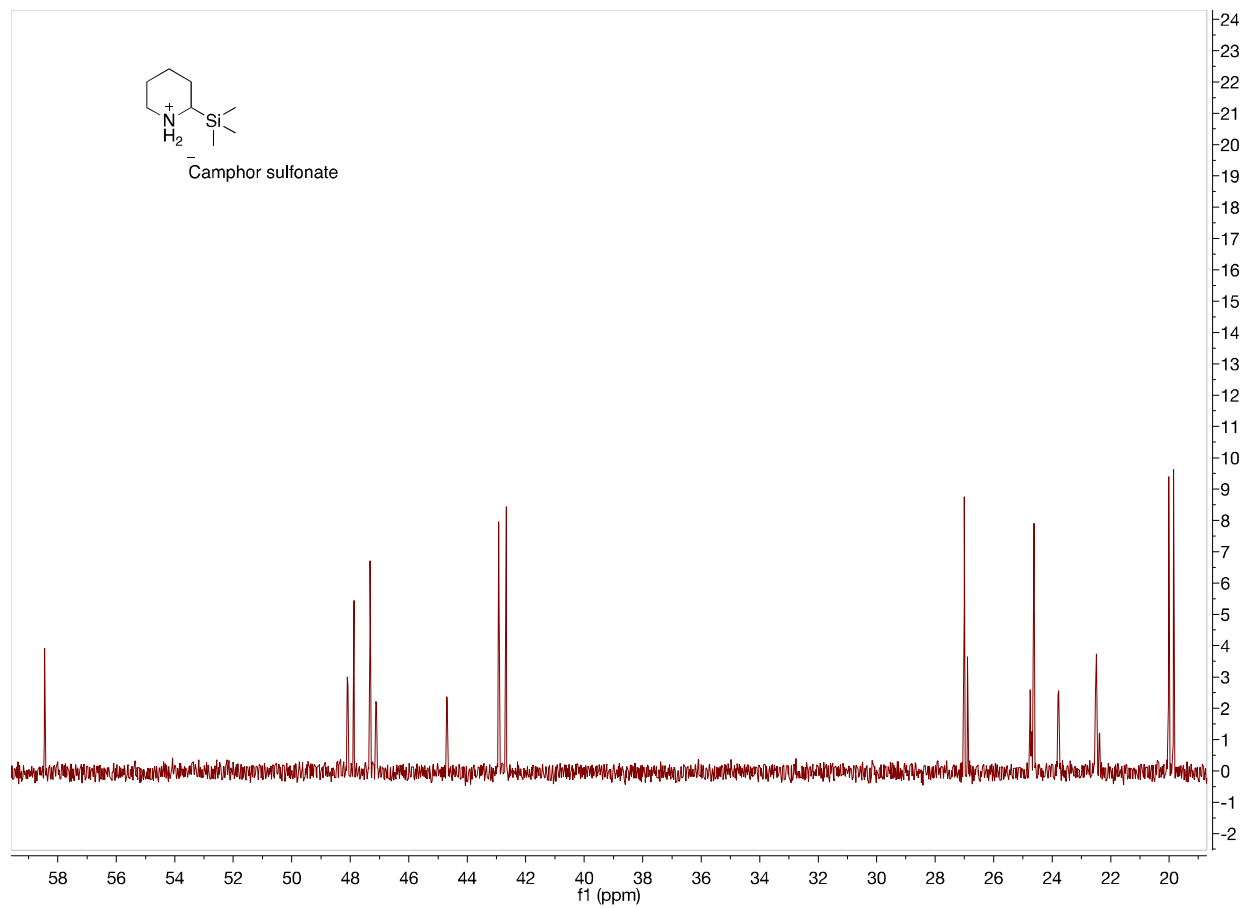


Figure A63. 125 MHz ^{13}C NMR of **2u** in CDCl_3



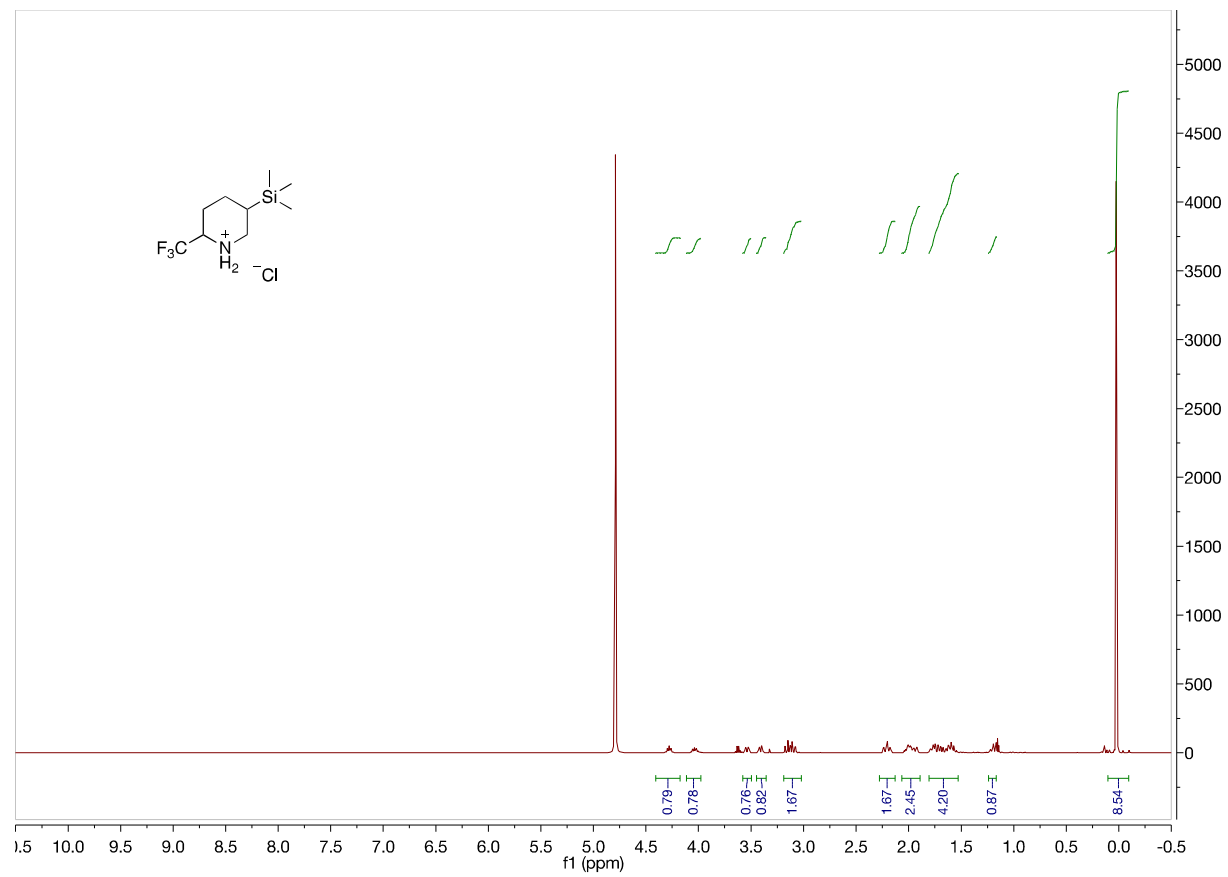


Figure A65. 500 MHz ^1H NMR of **2v** in D_2O

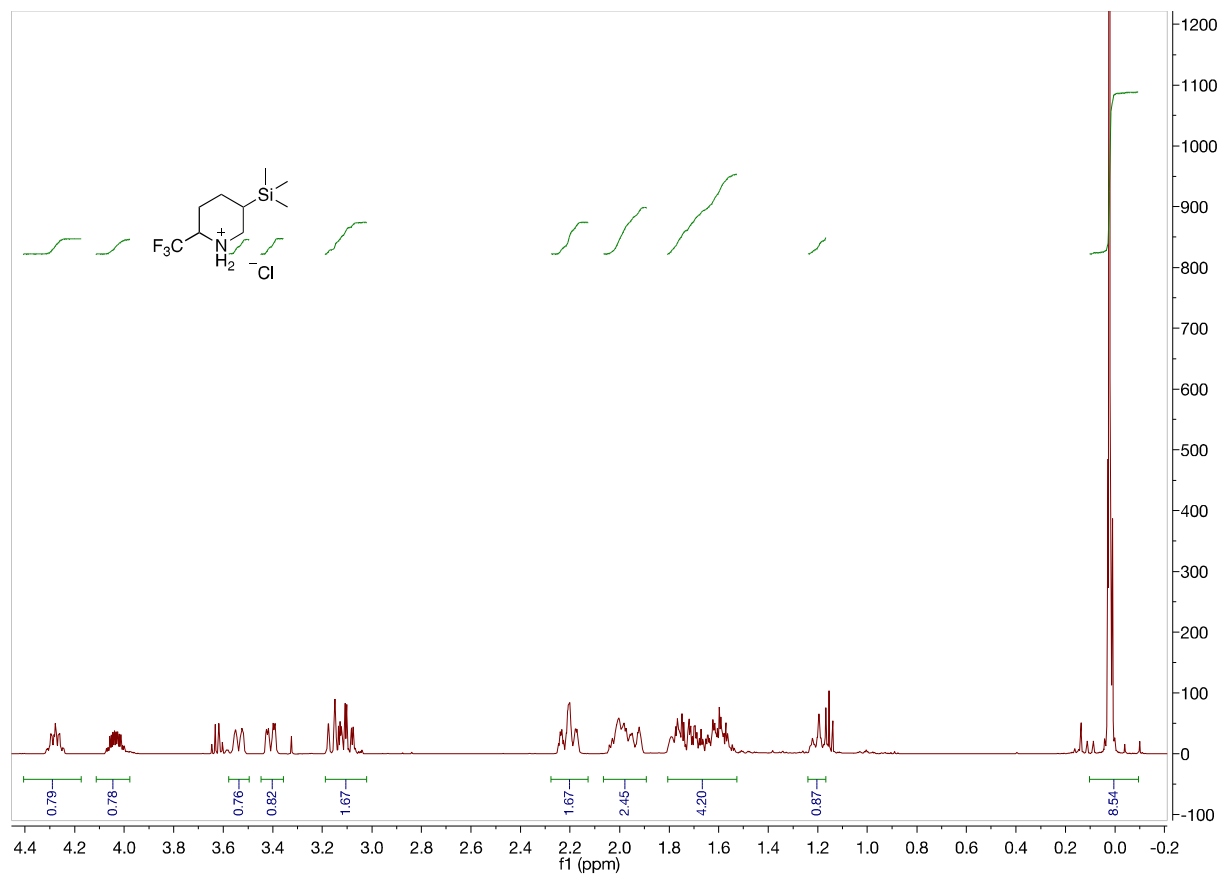


Figure A66. 500 MHz ^1H NMR of **2v** in D_2O from 4.4 to -0.2ppm

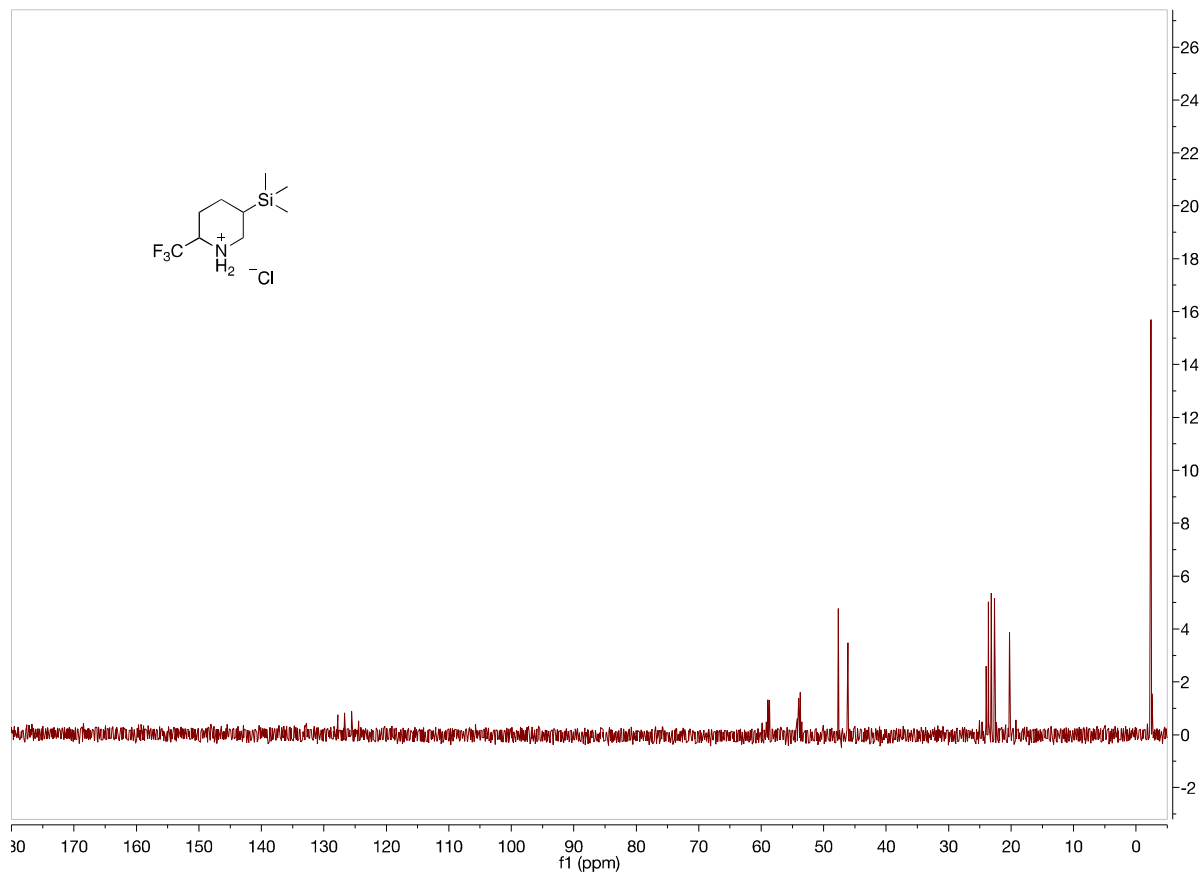


Figure A67. 125 MHz ^{13}C NMR of **2v** in D_2O

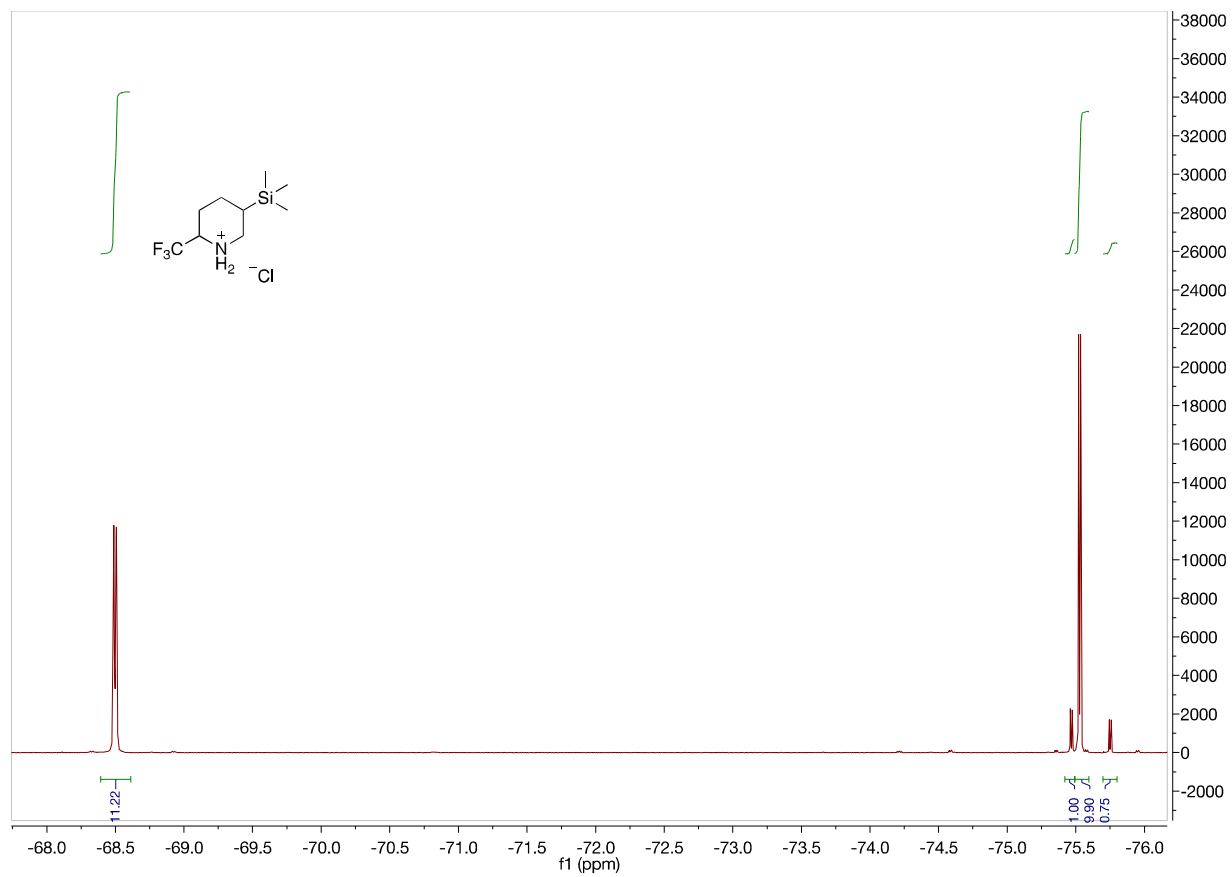


Figure A68. 470 MHz ^{19}F NMR of **2v** in D_2O

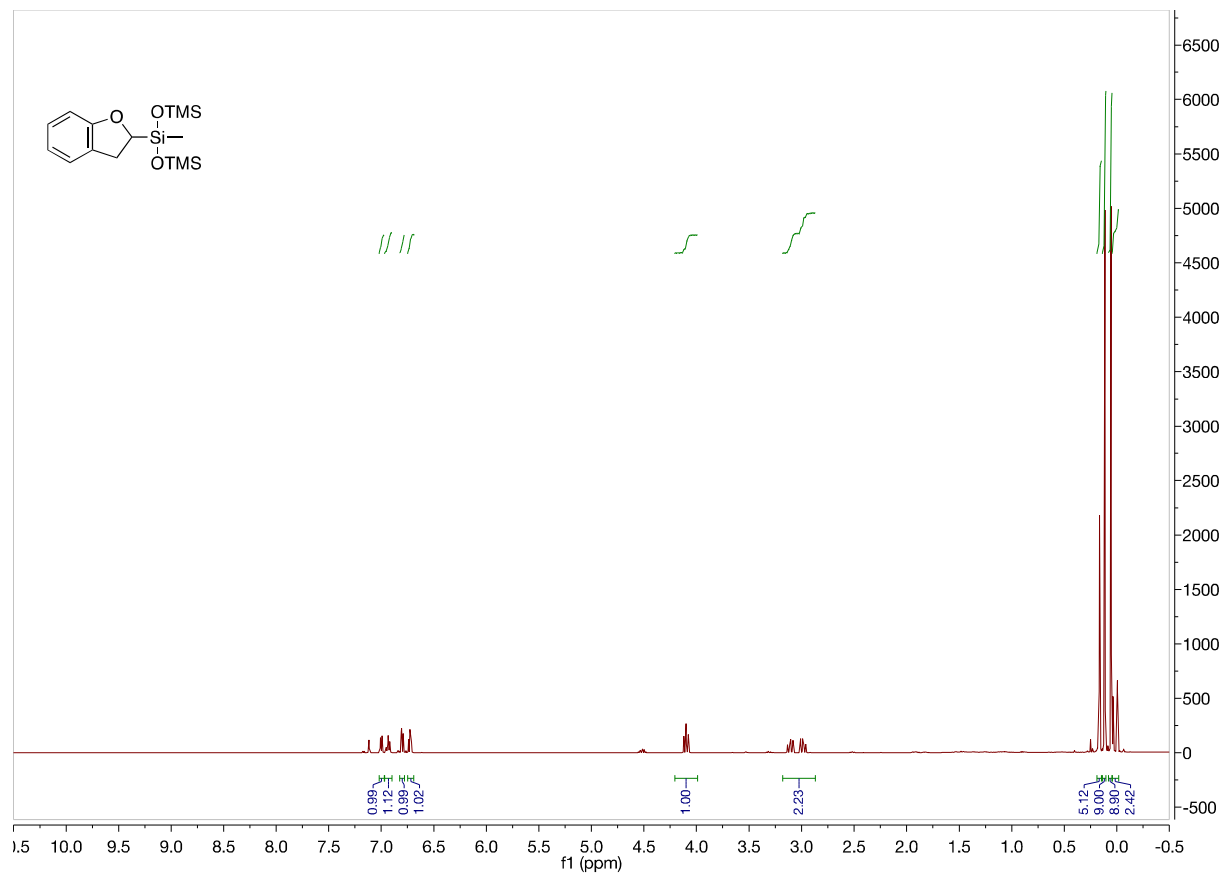


Figure A69. 500 MHz ¹H NMR of **2w** in C₆D₆

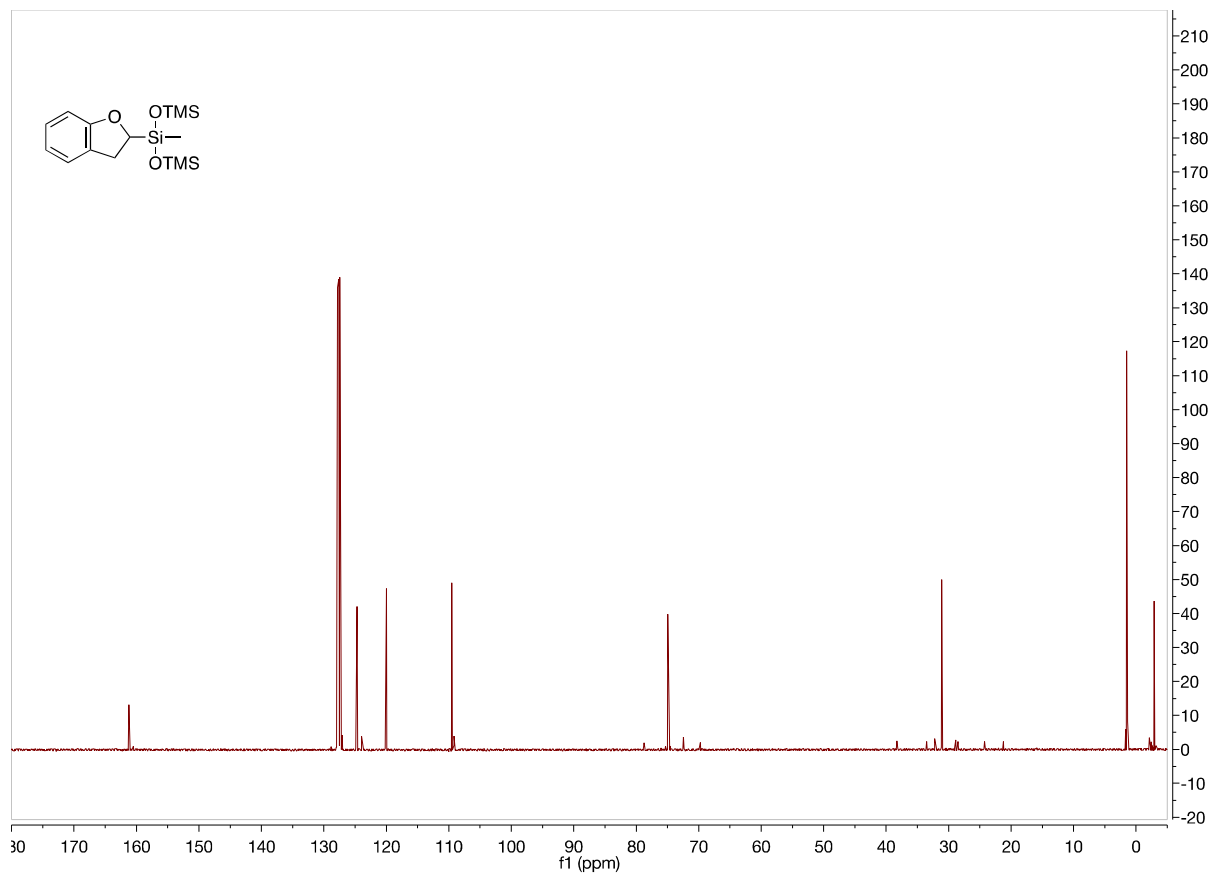


Figure A70. 125 MHz ¹³C NMR of **2w** in C₆D₆

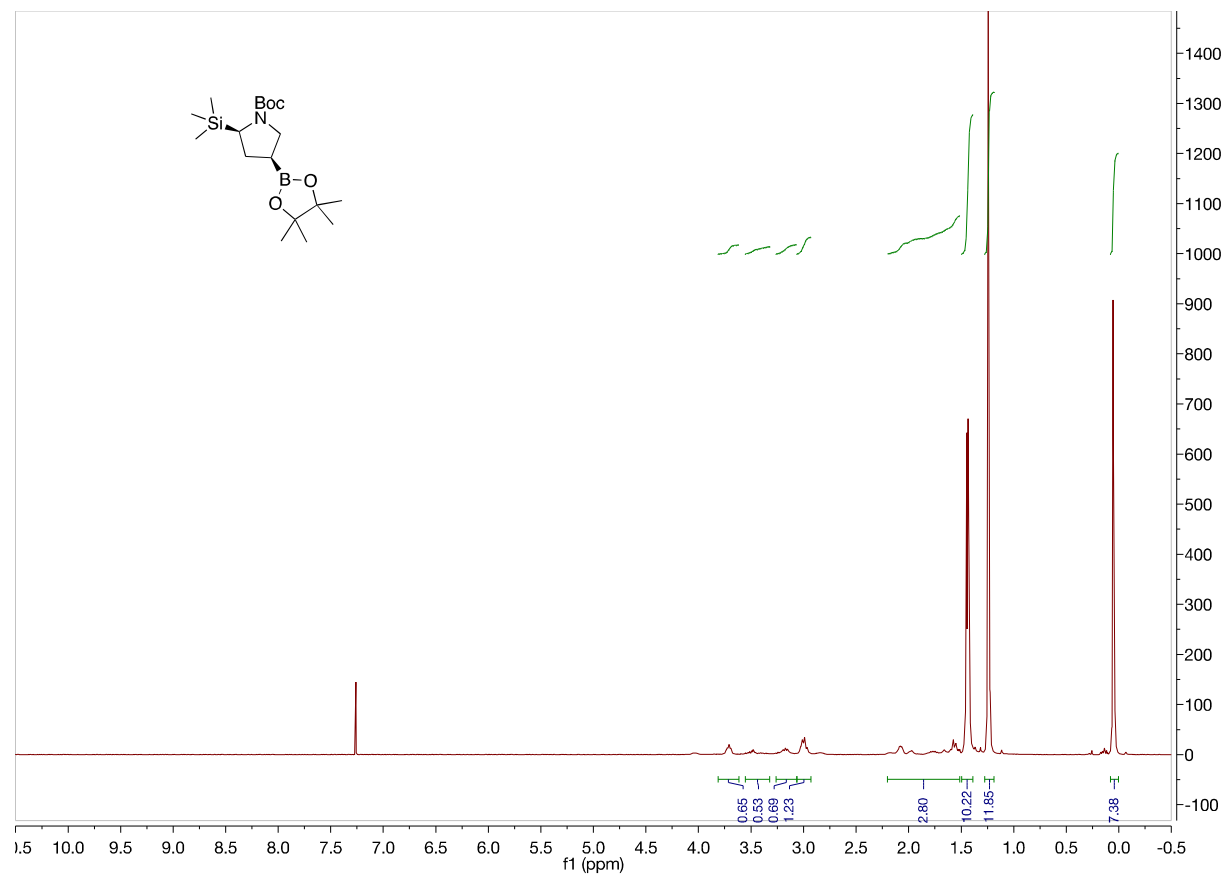


Figure A71. 500 MHz ^1H NMR of **2x** in CDCl_3

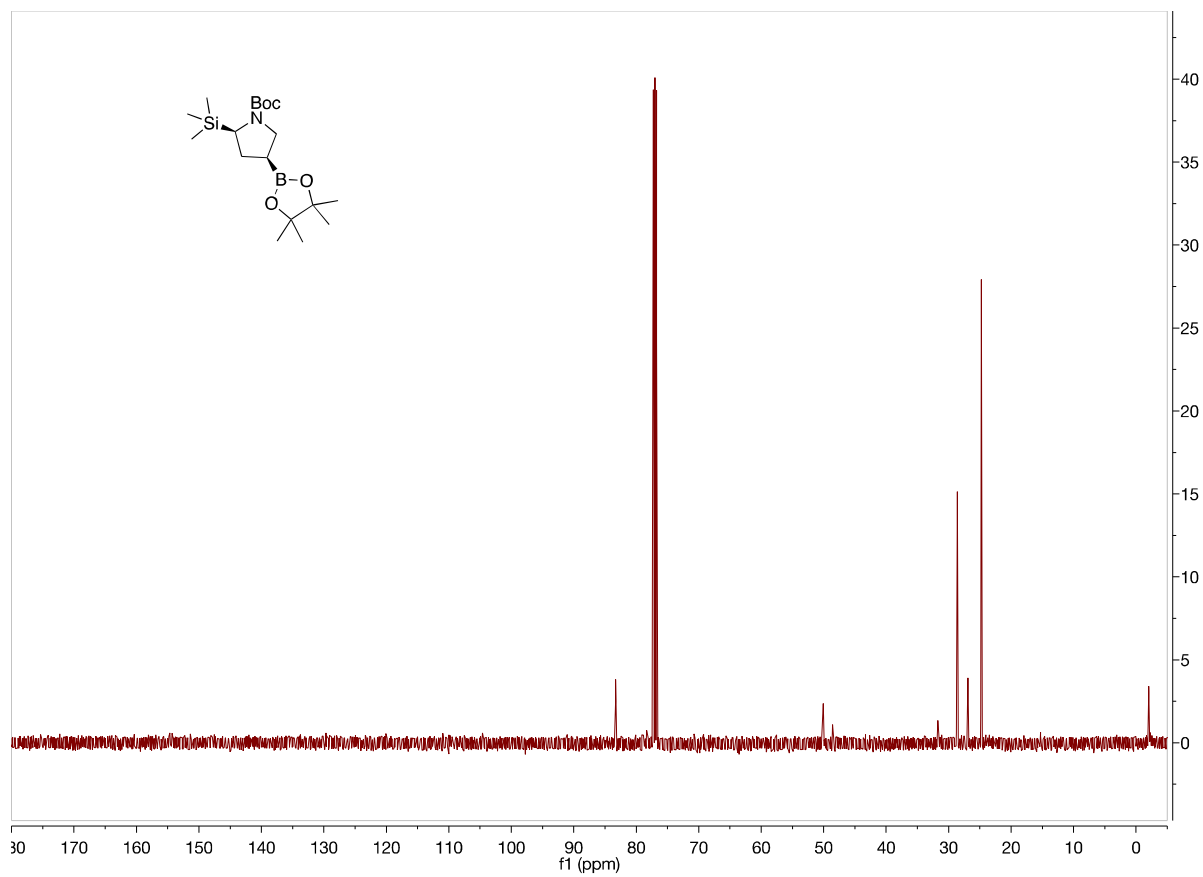


Figure A72. 125 MHz ¹³C NMR of **2x** in CDCl₃

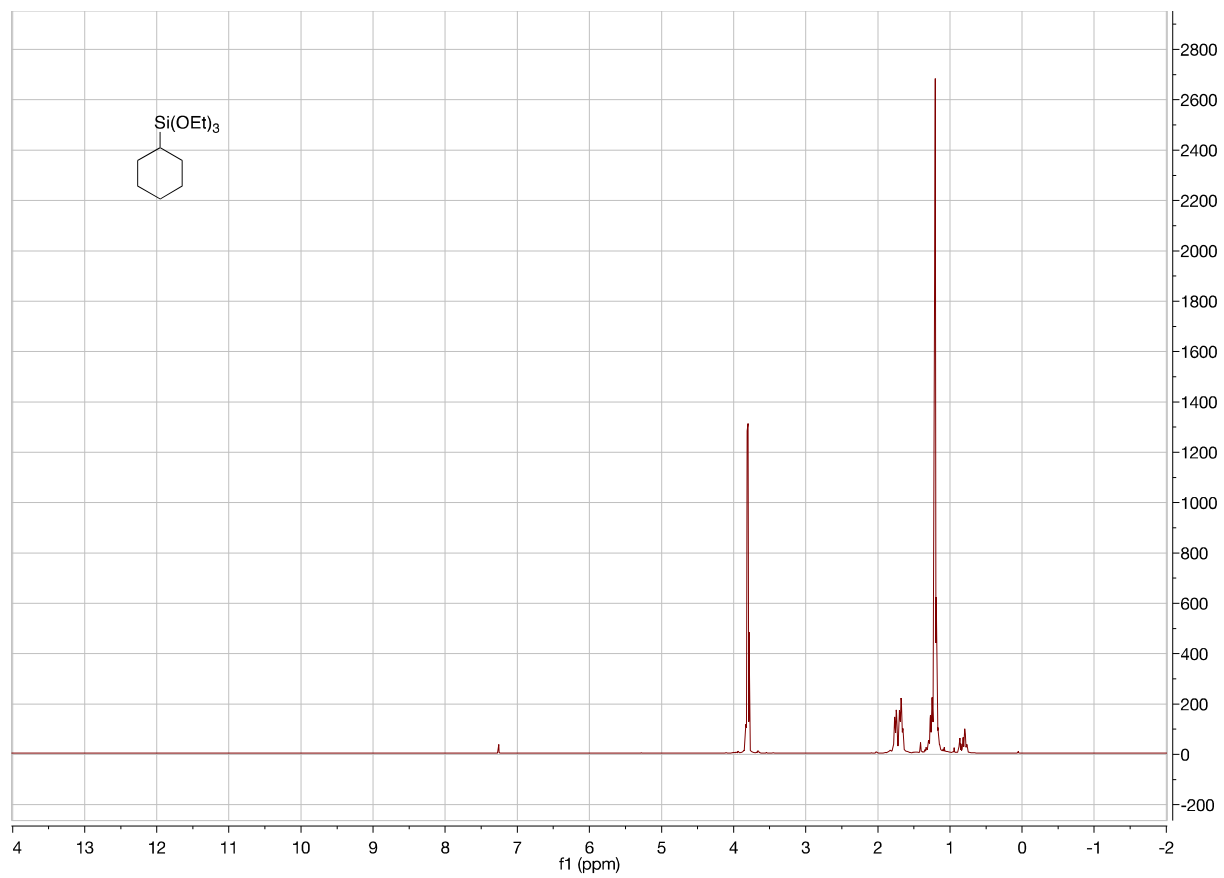


Figure A73. 500 MHz ^1H NMR of **2y** in C_6D_6

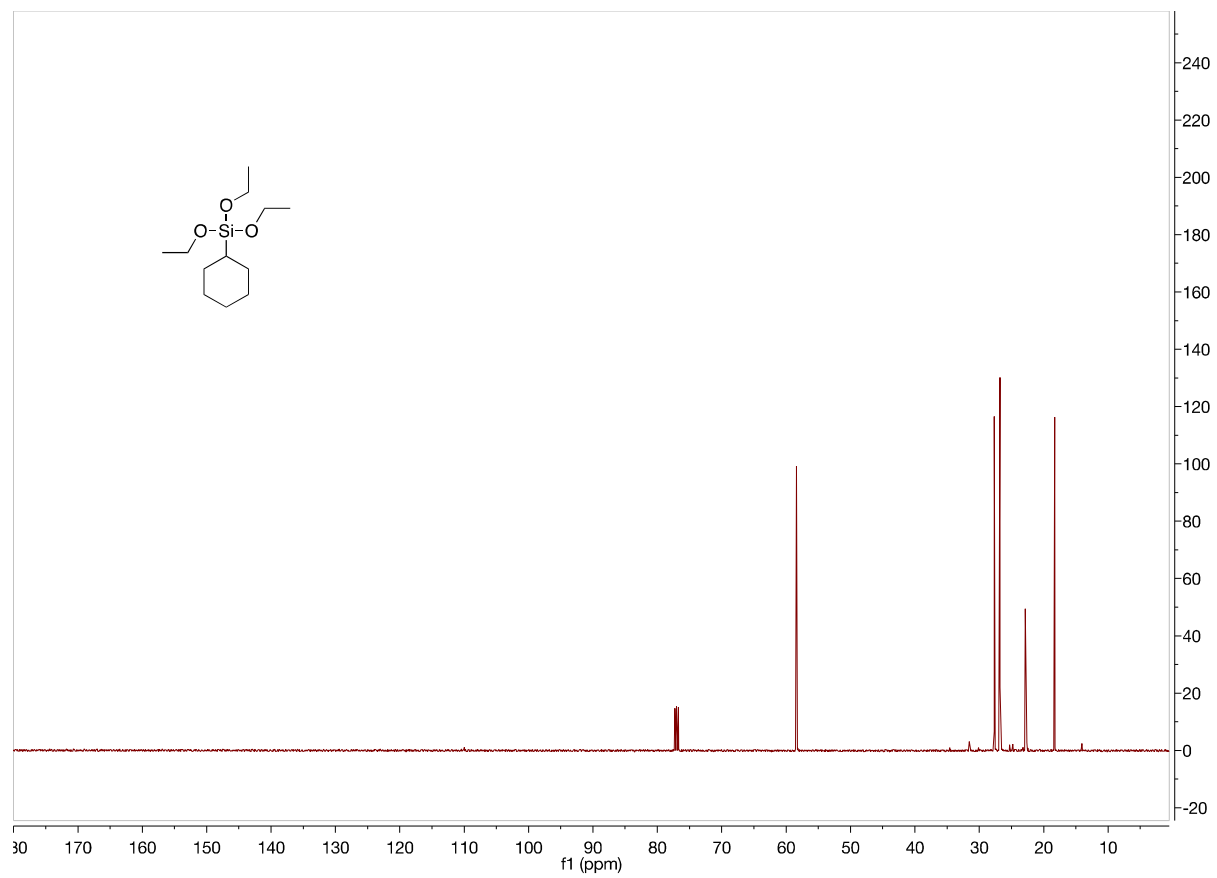


Figure A74. 125 MHz ^{13}C NMR of **2y** in CDCl_3

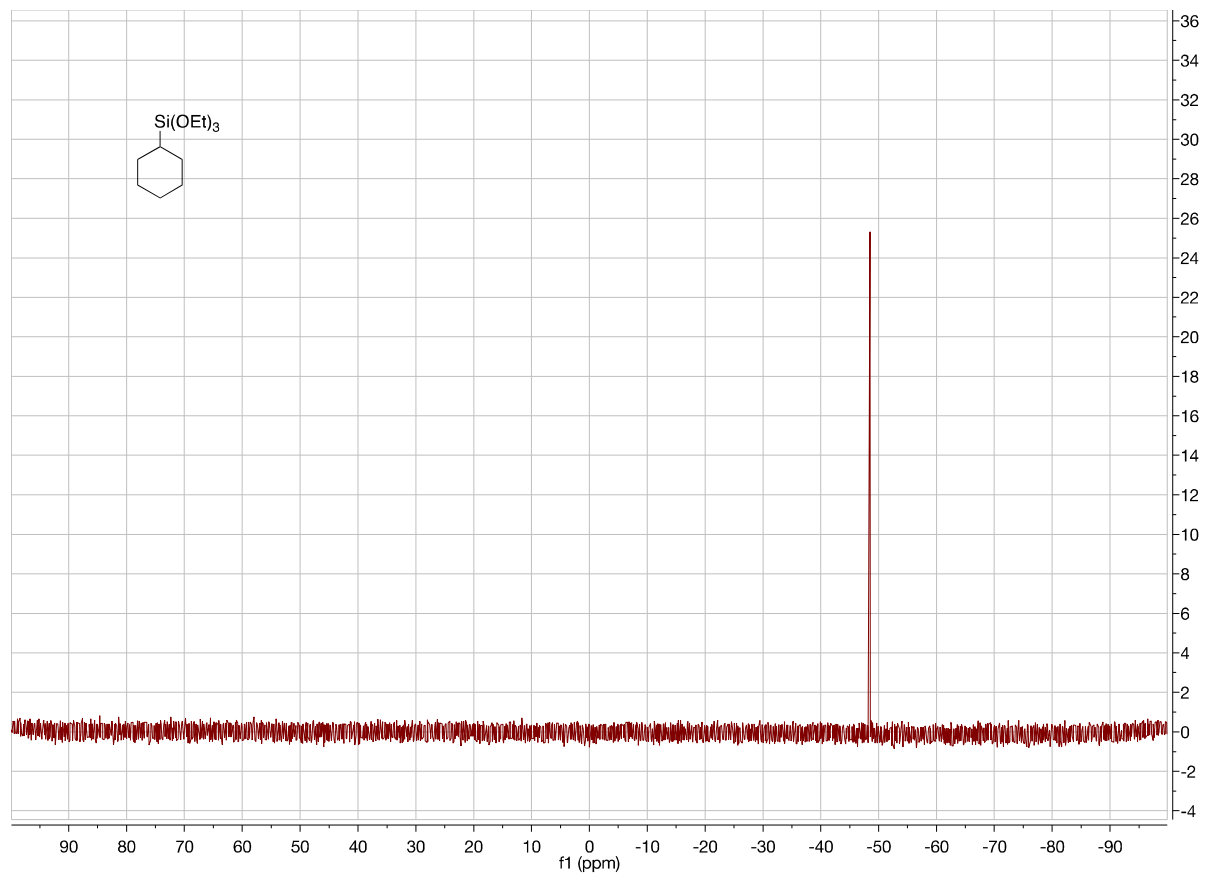


Figure A75. 99 MHz ^{29}Si NMR of **2y** in CDCl_3

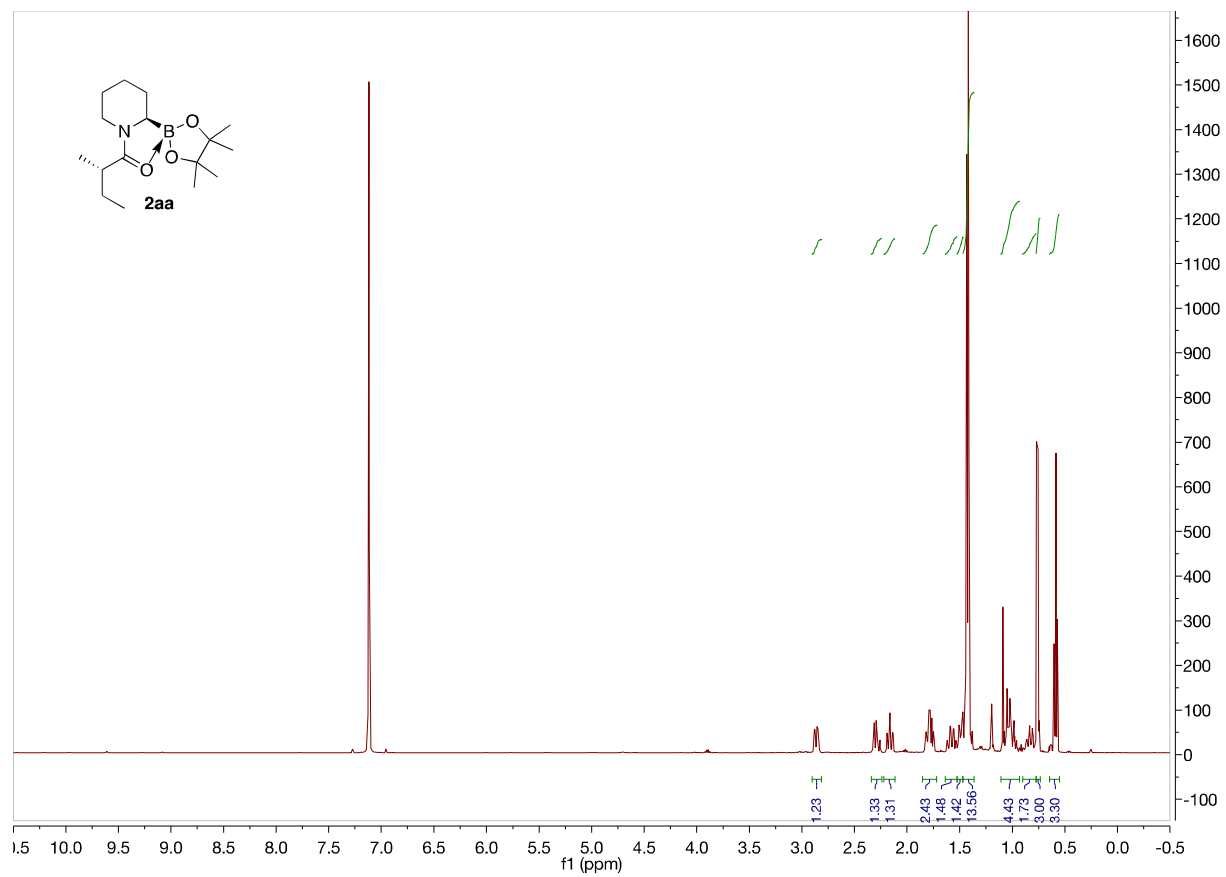


Figure A76. 500 MHz ¹H NMR of **2za** in C₆D₆

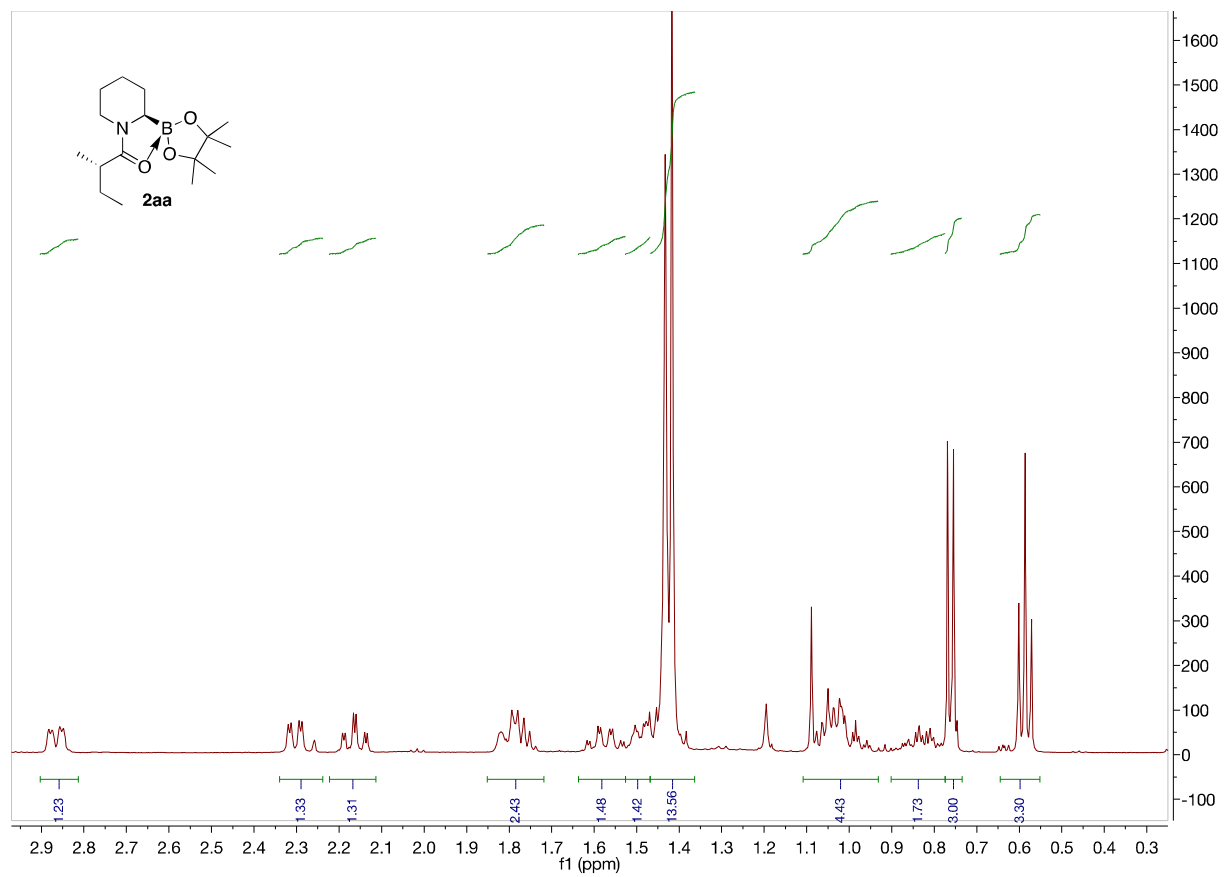


Figure A77. 500 MHz ¹H NMR of **2za** in C₆D₆ from 3.0 to 0.3 ppm

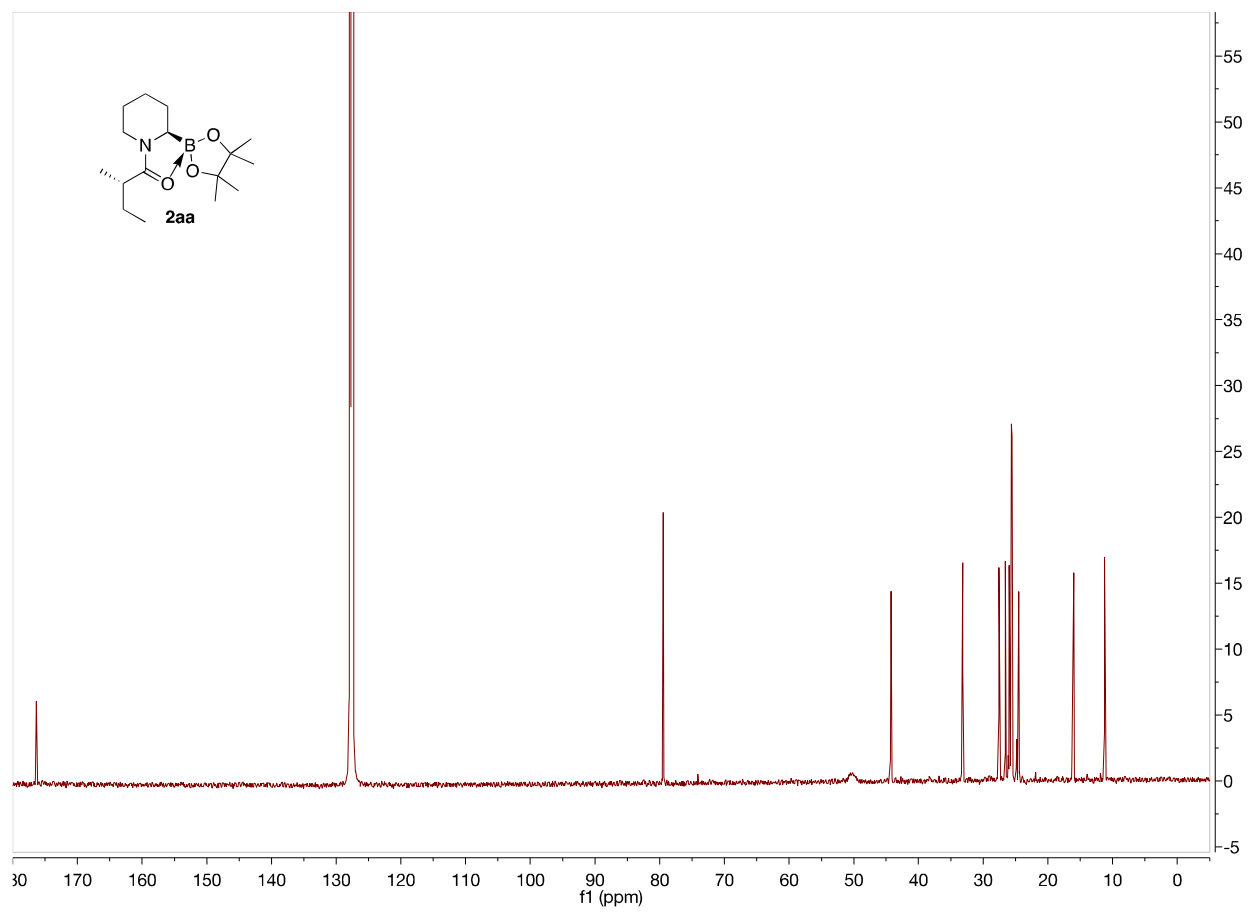


Figure A78. 125 MHz ^{13}C NMR of **2za** in C_6D_6

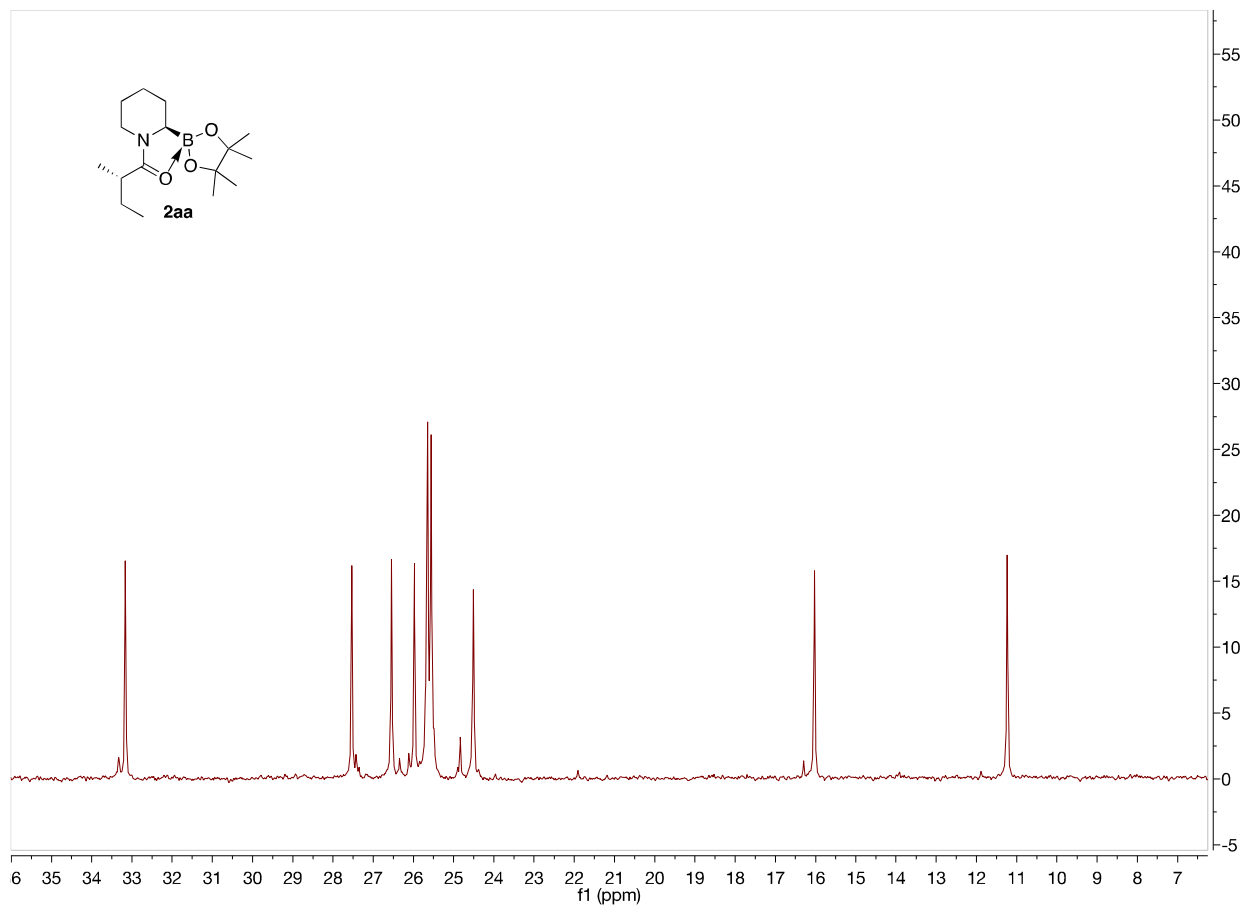


Figure A79. 125 MHz ^{13}C NMR of **2za** in C_6D_6 from 36 to 6 ppm

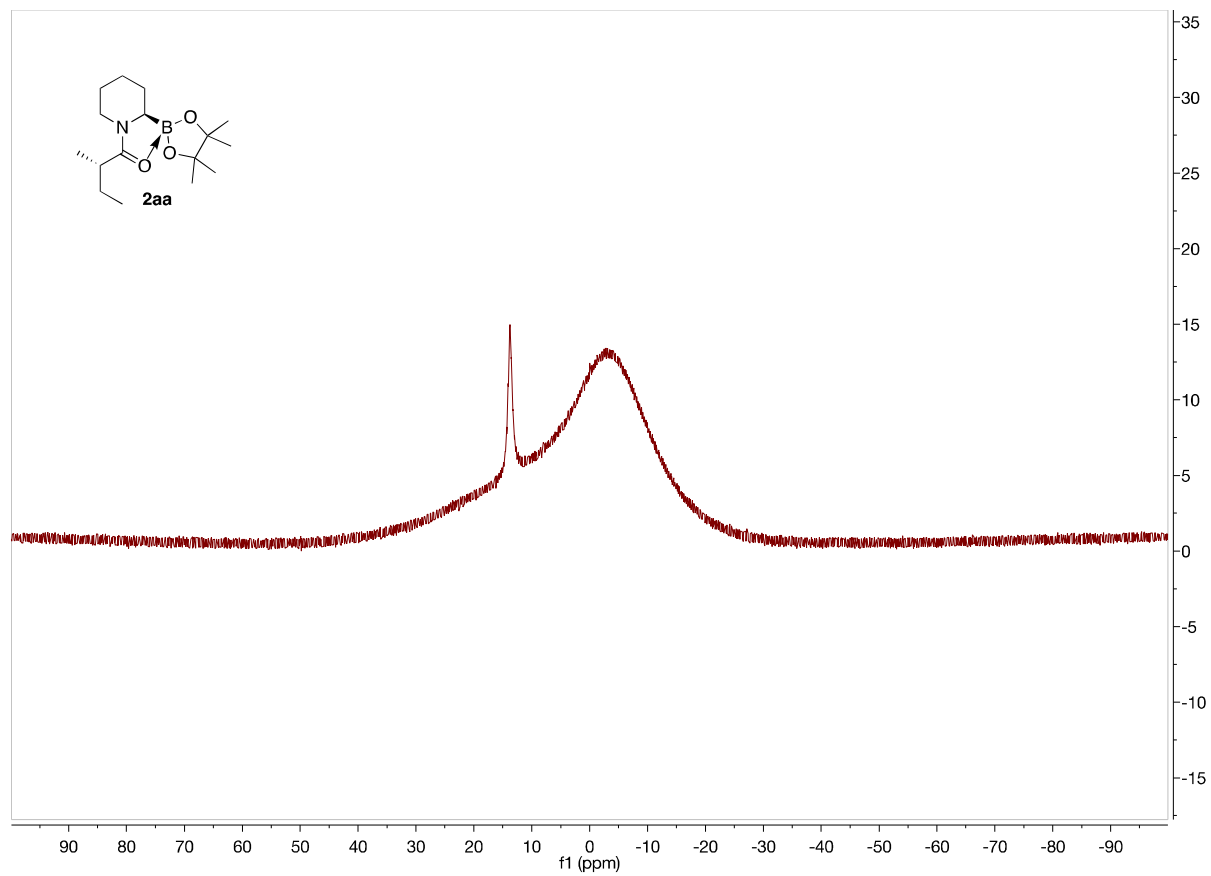


Figure A80. 160 MHz ^{11}B NMR of **2a** in C_6D_6

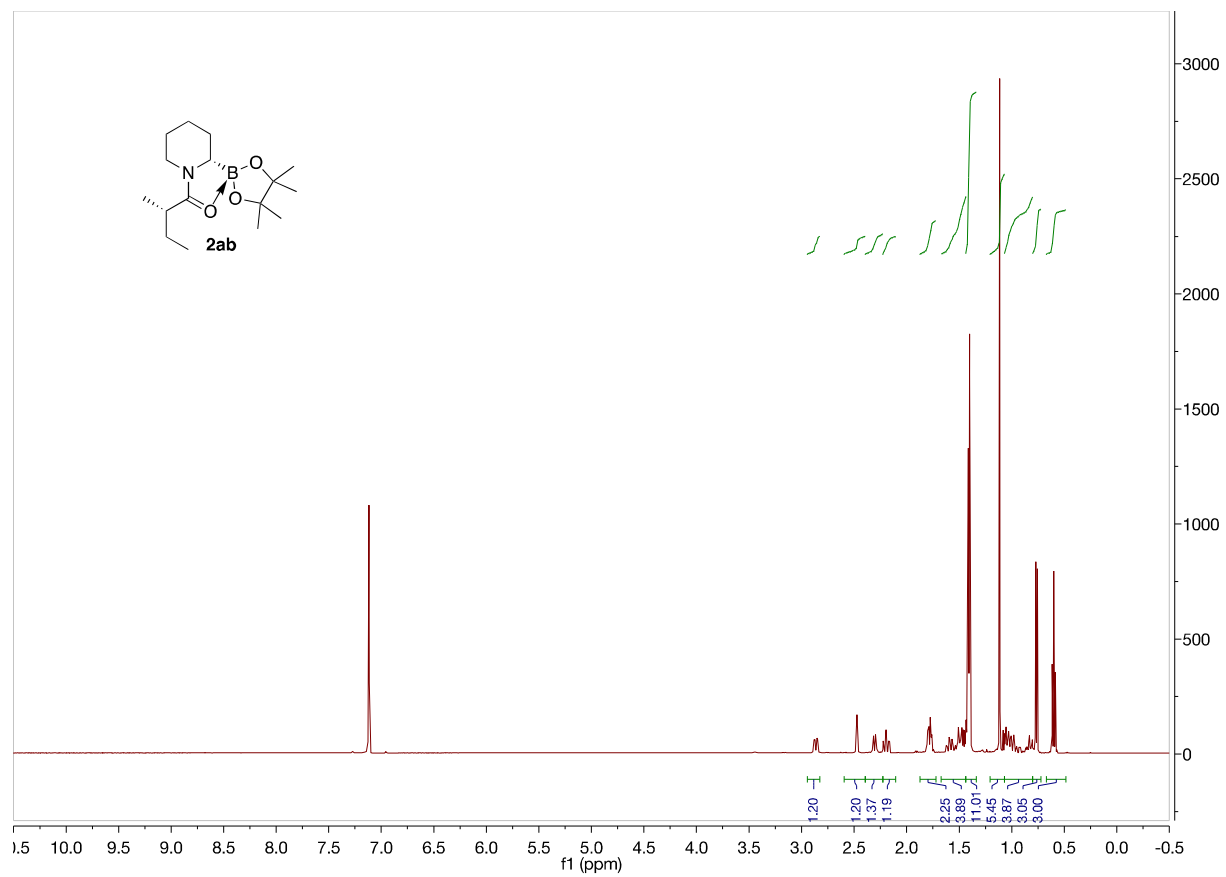


Figure A81. 500 MHz ¹H NMR of **2zb** in C₆D₆

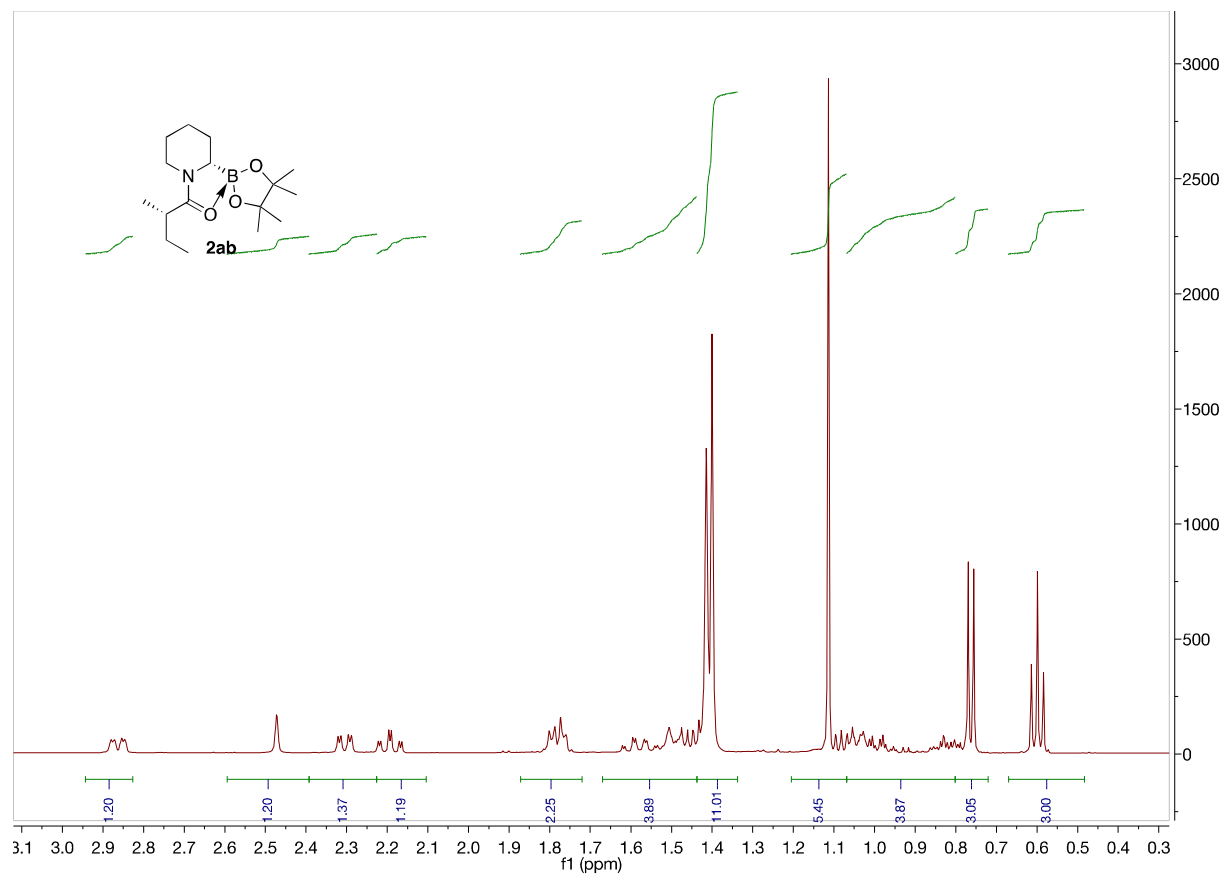


Figure A82. 500 MHz ^1H NMR of **2zb** in C_6D_6

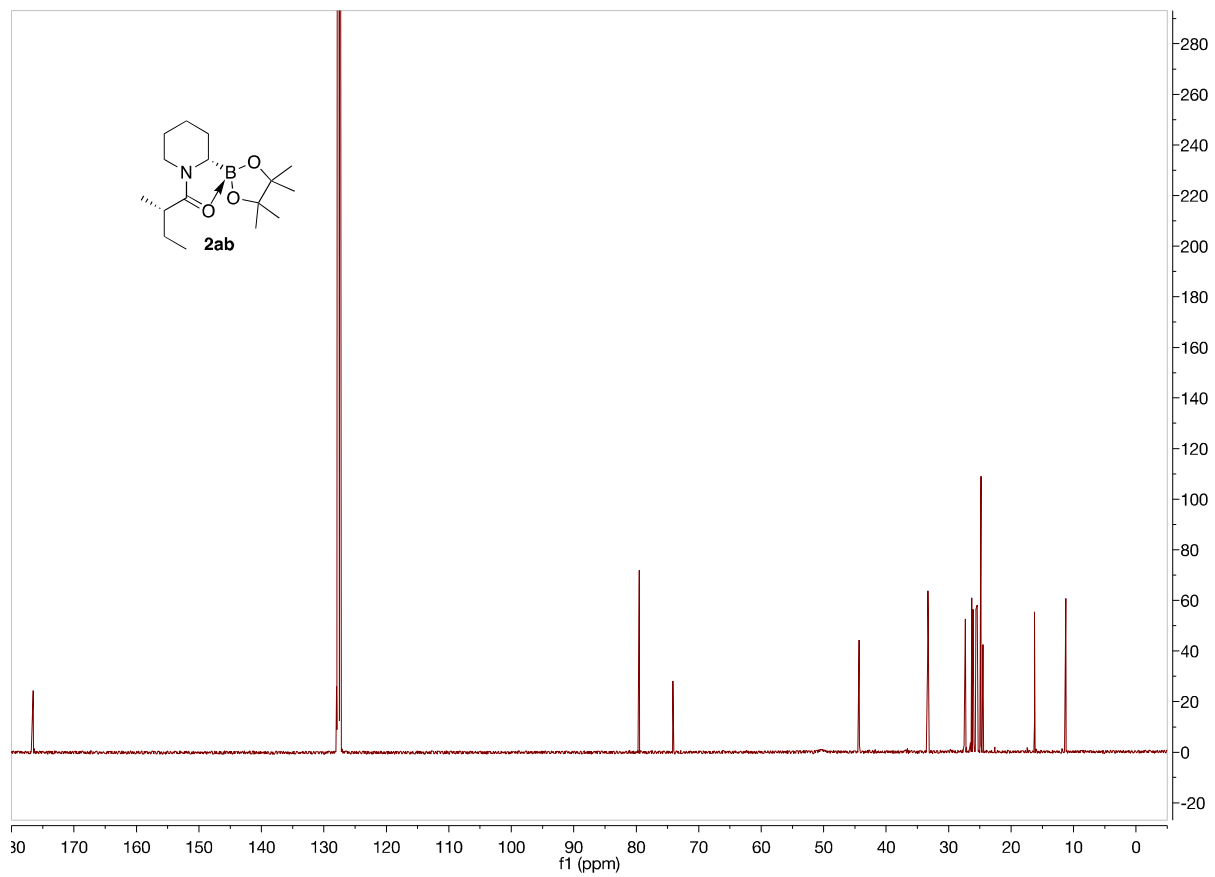


Figure A83. 125 MHz ^{13}C NMR of **2zb** in C_6D_6

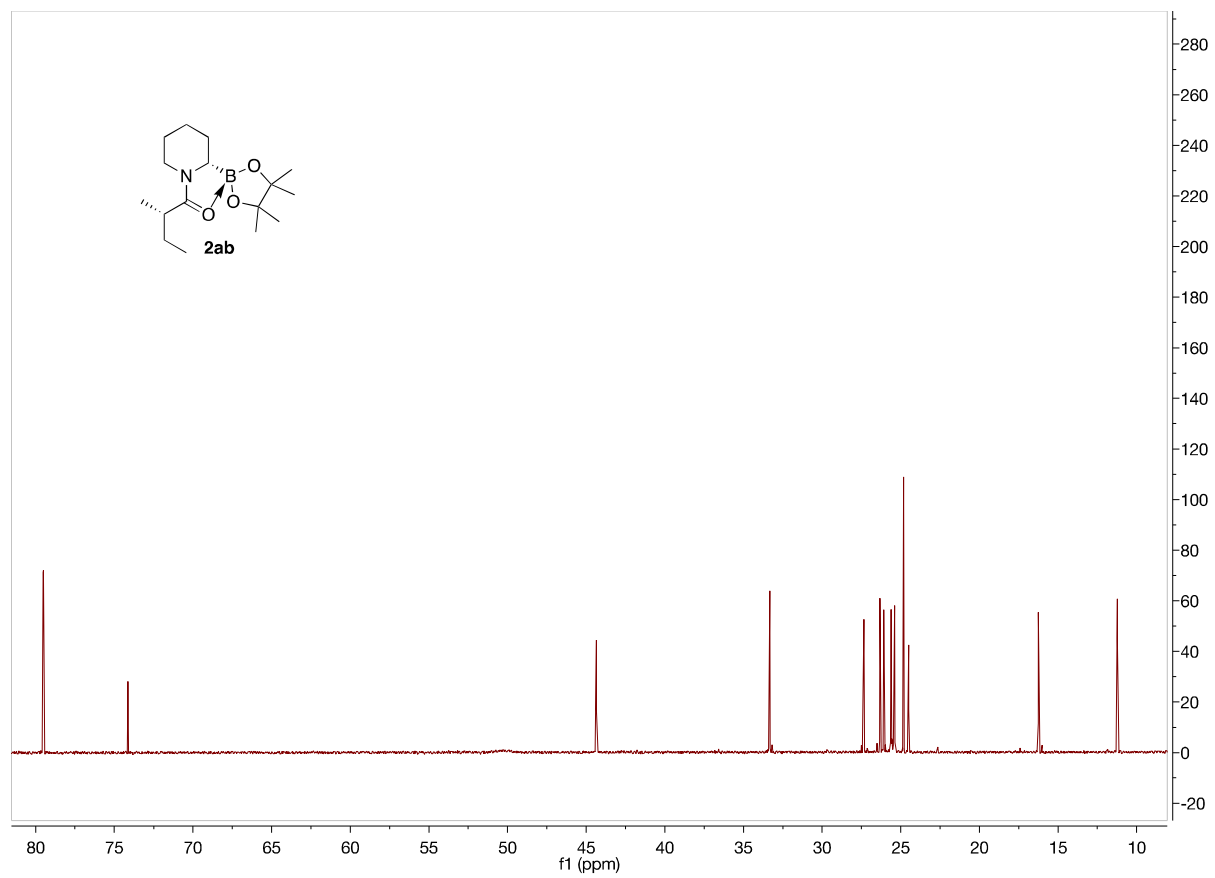


Figure A84. 125 MHz ^{13}C NMR of **2zb** in C_6D_6 from 85 to 5 ppm

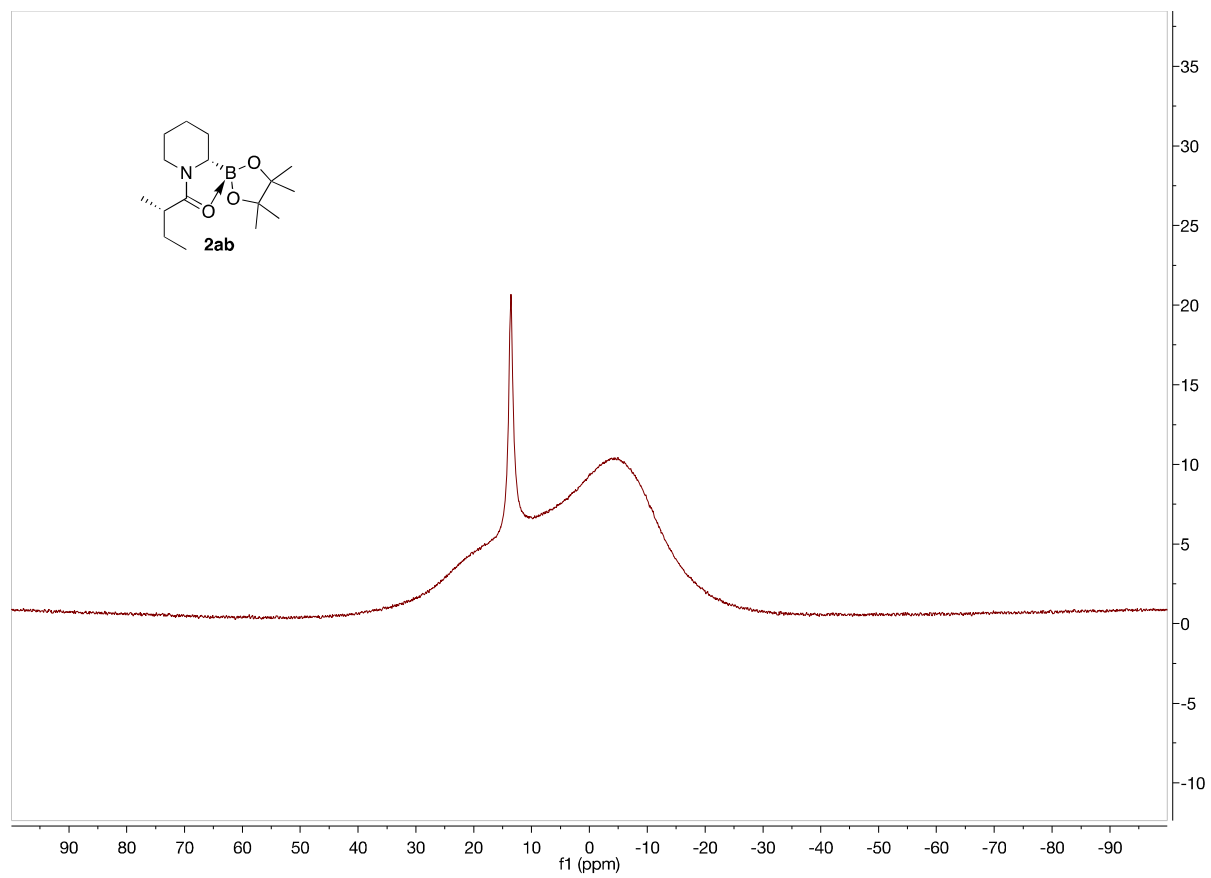


Figure A85. 160 MHz ^{11}B NMR of **2ab** in C_6D_6

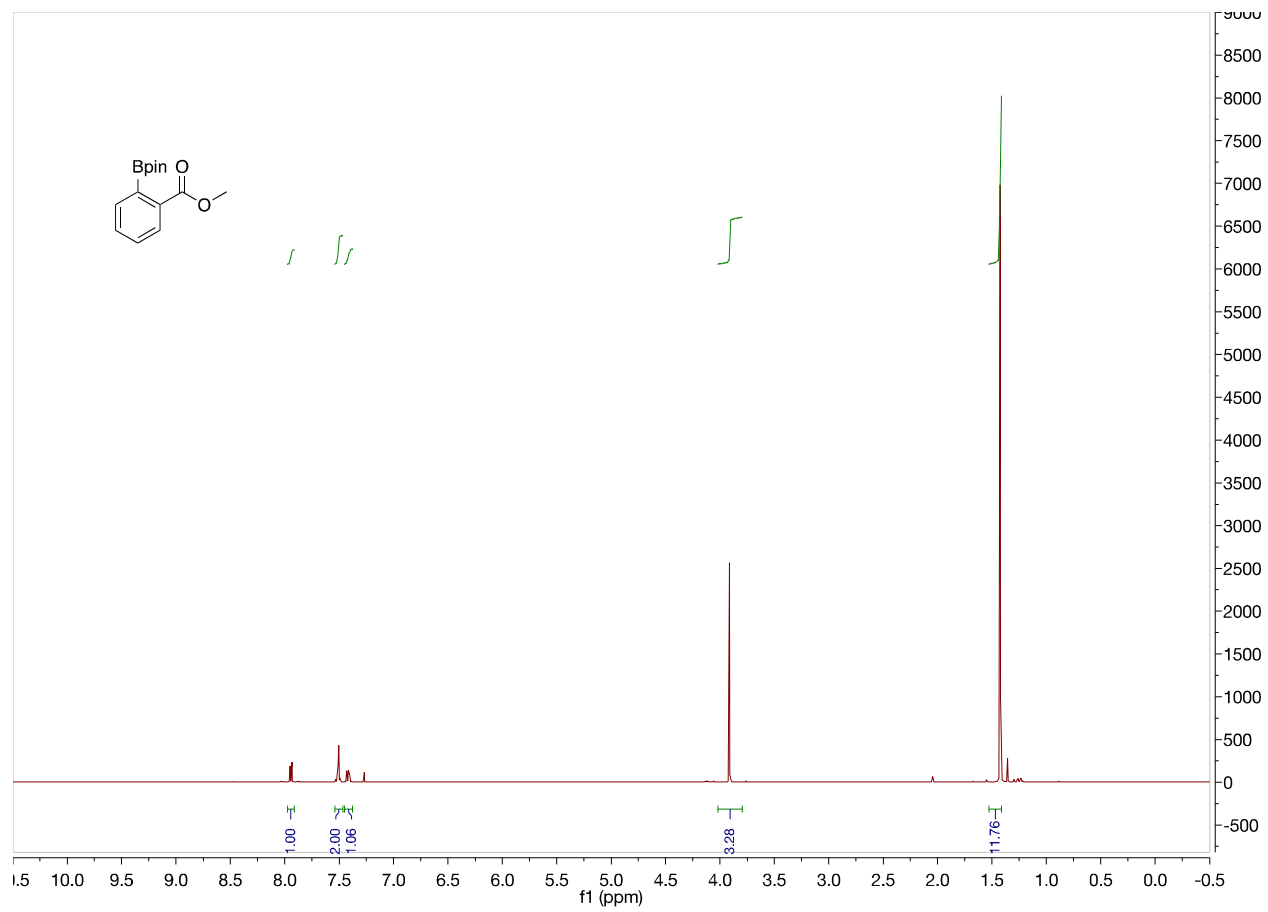


Figure A86. 500 MHz ¹H NMR of **3z** in CDCl₃

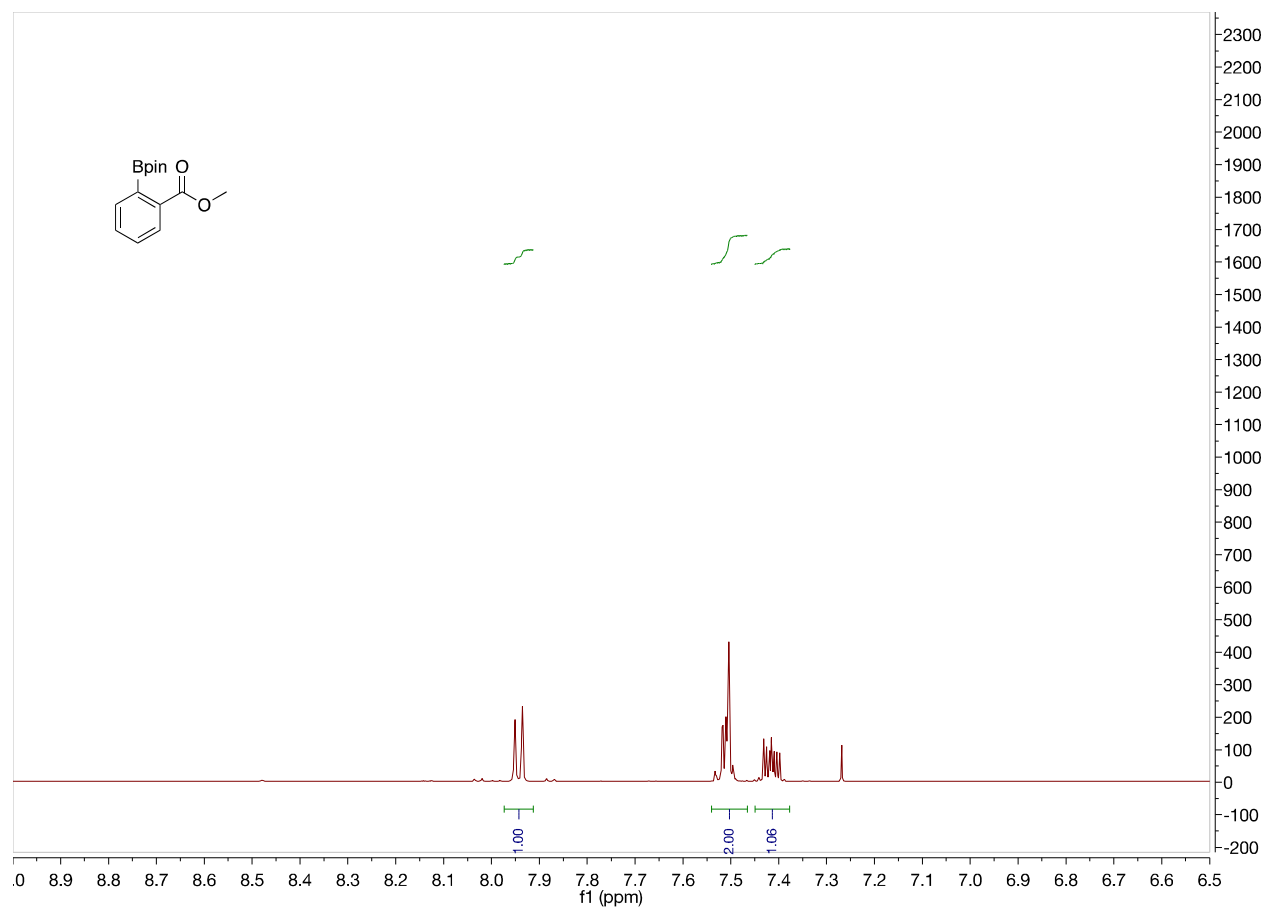


Figure A87. 500 MHz ^1H NMR of **3z** in CDCl_3 from 9.0 to 6.5 ppm

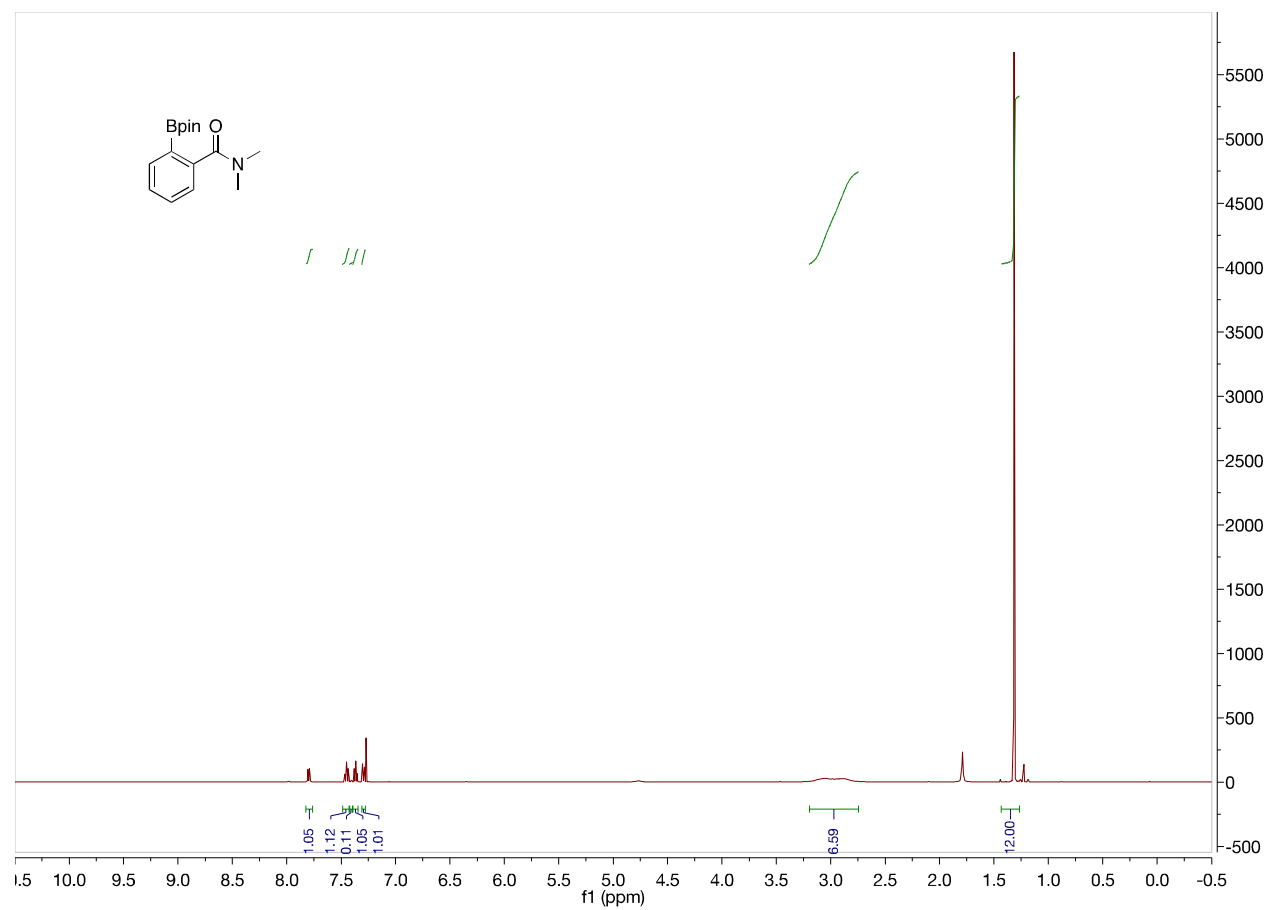


Figure A88. 500 MHz ^1H NMR of **3aa** in CDCl_3

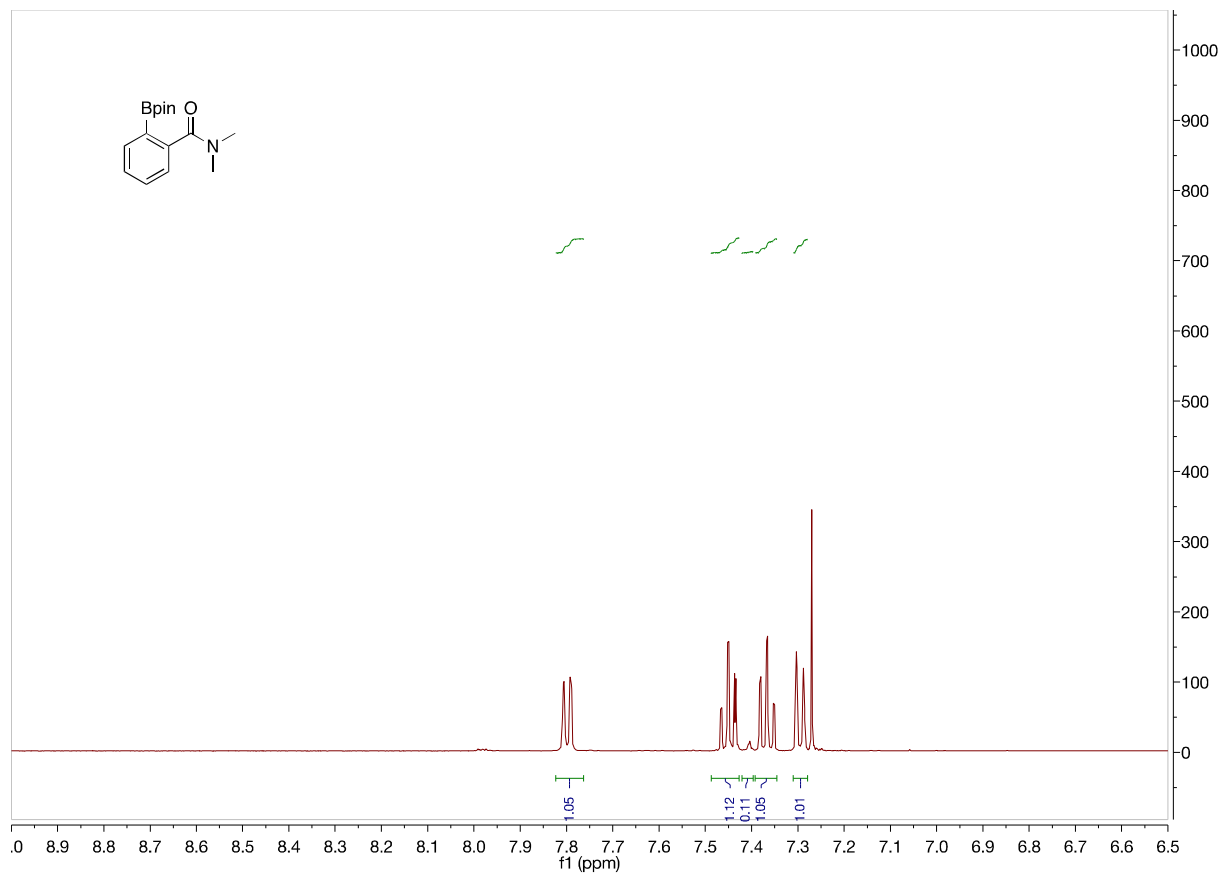


Figure A89. 500 MHz ^1H NMR of **3aa** in CDCl_3 from 9.0 to 6.5 ppm

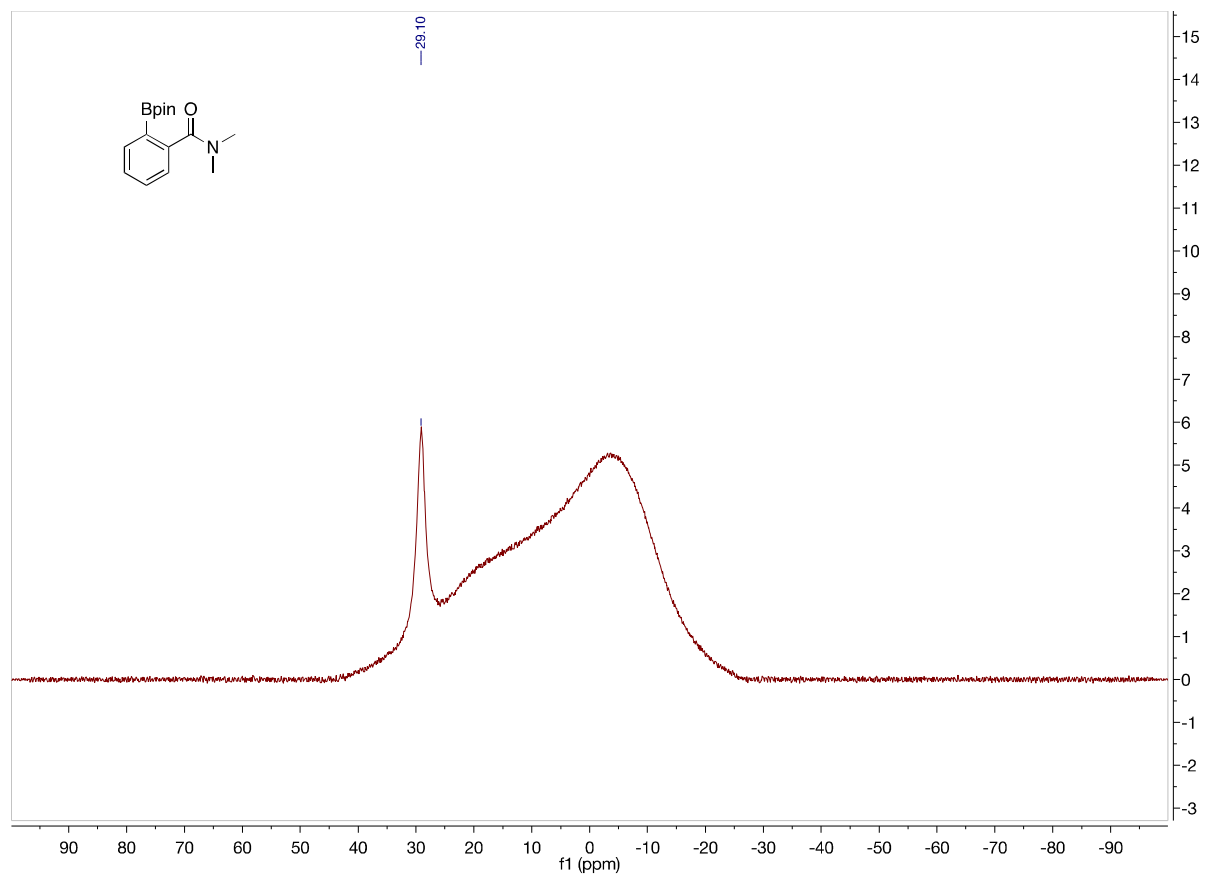


Figure A90. 160 MHz ^{11}B NMR of **3aa** in CDCl_3

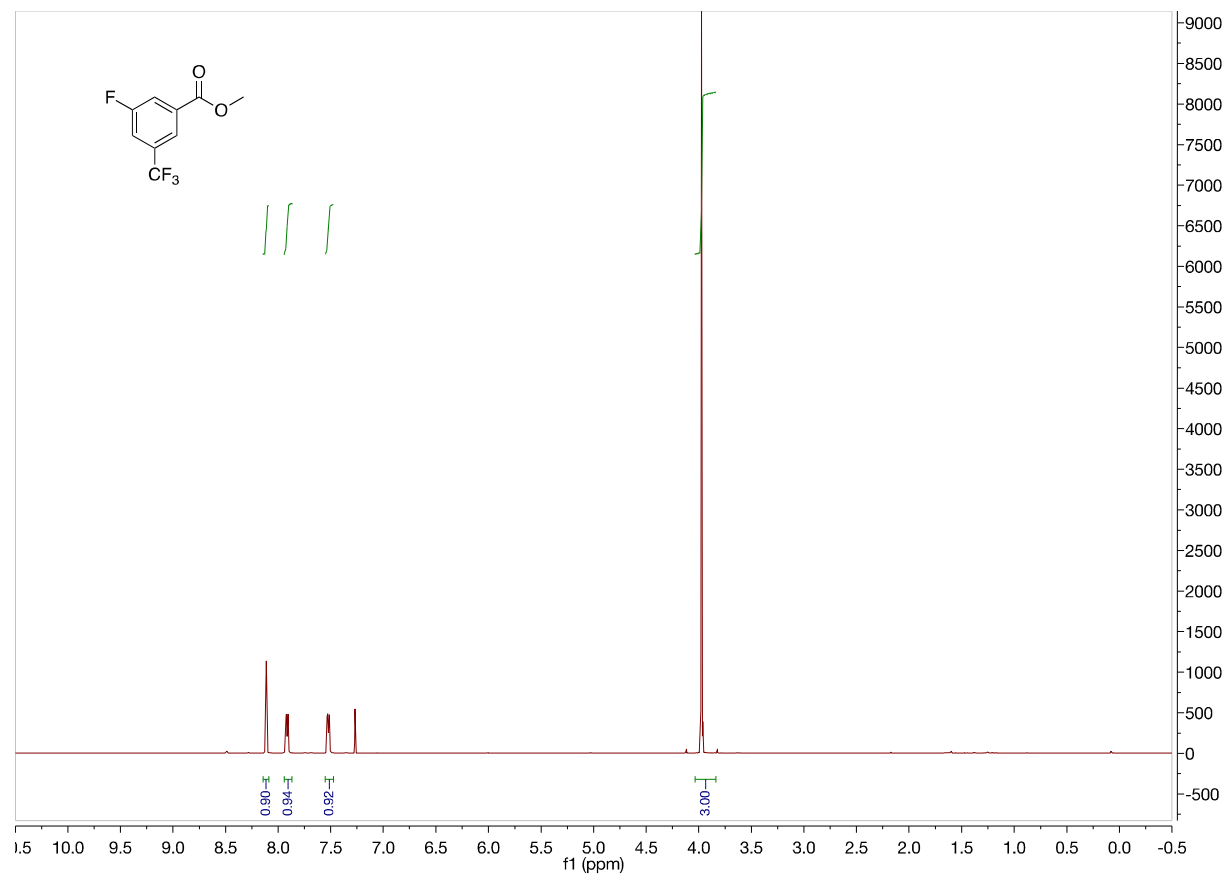


Figure A91. 500 MHz ¹H NMR of **3ab'** in CDCl₃

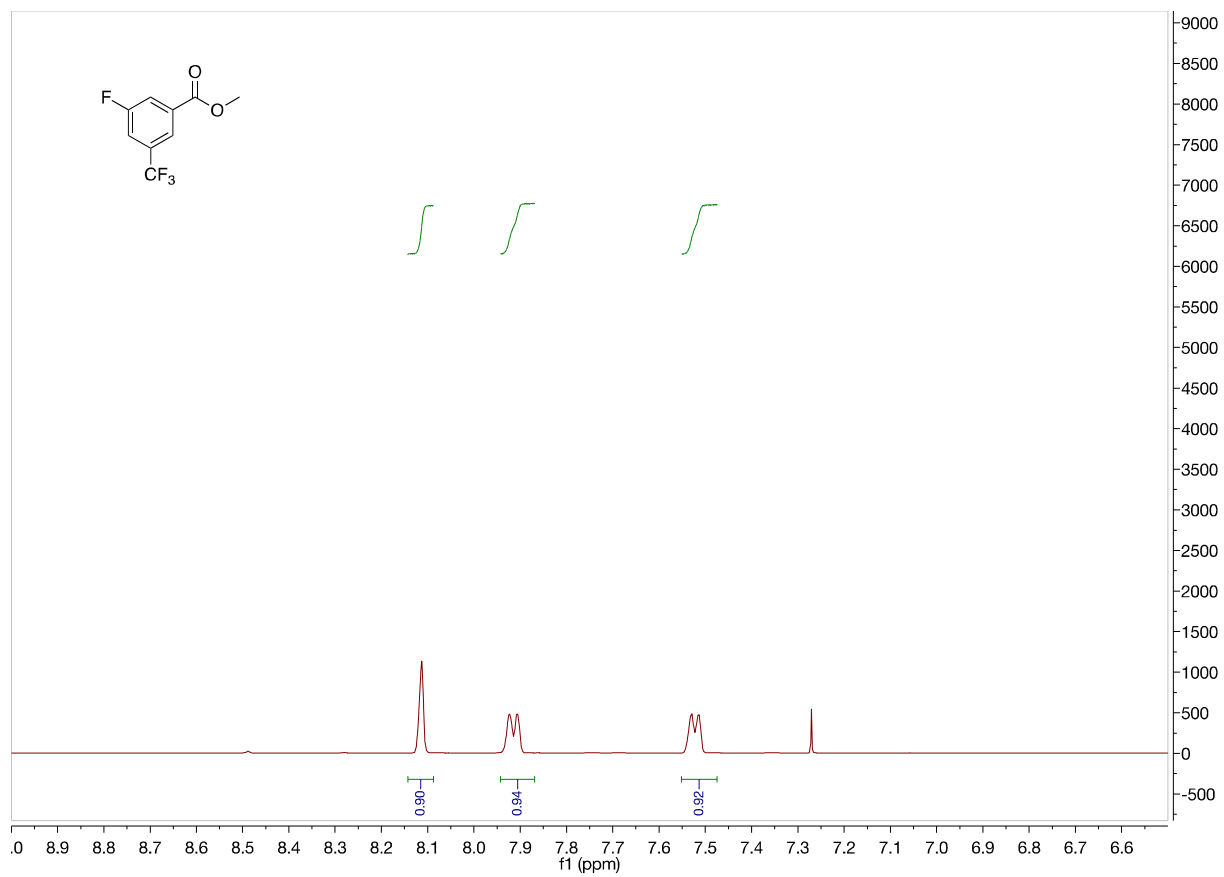


Figure A92. 500 MHz ¹H NMR of **3ab'** in CDCl₃ from 9.0 to 6.5 ppm

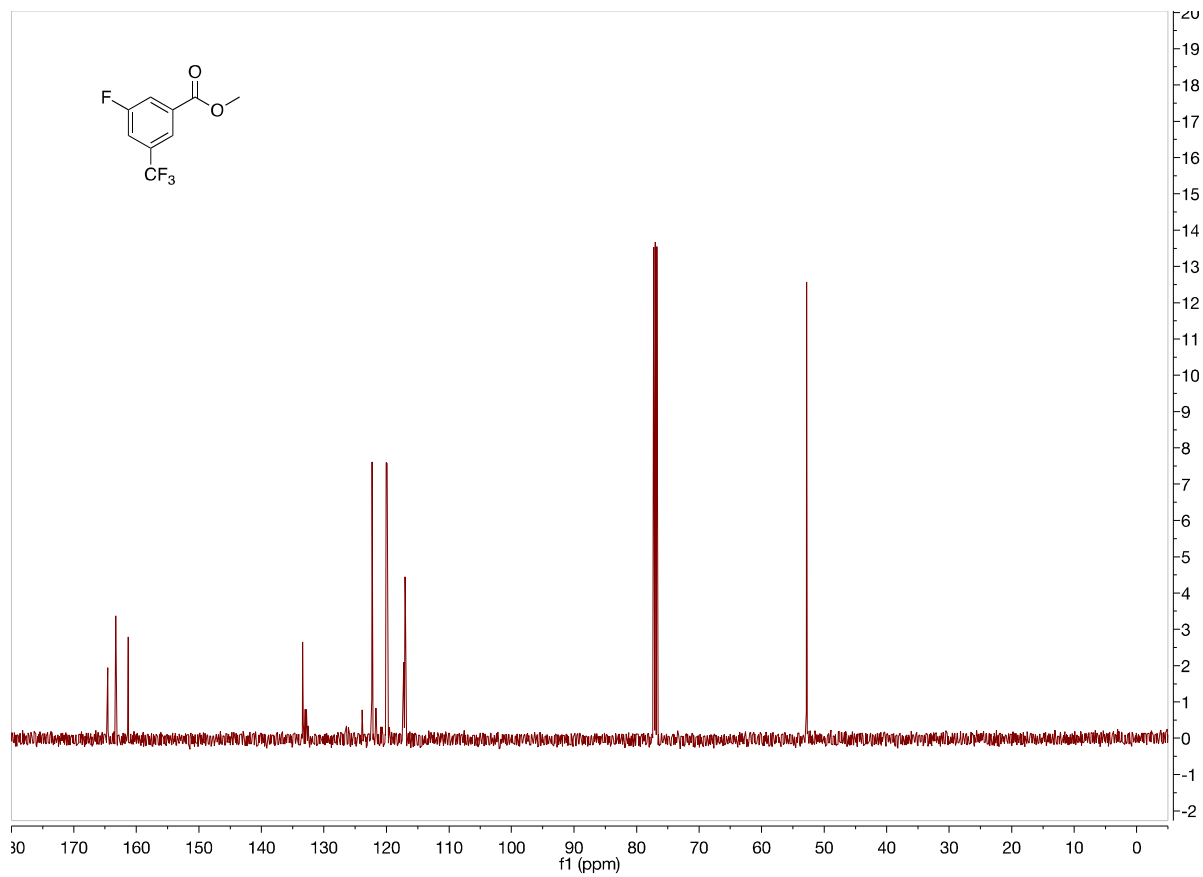


Figure A93. 125 MHz ^{13}C NMR of **3ab'** in CDCl_3

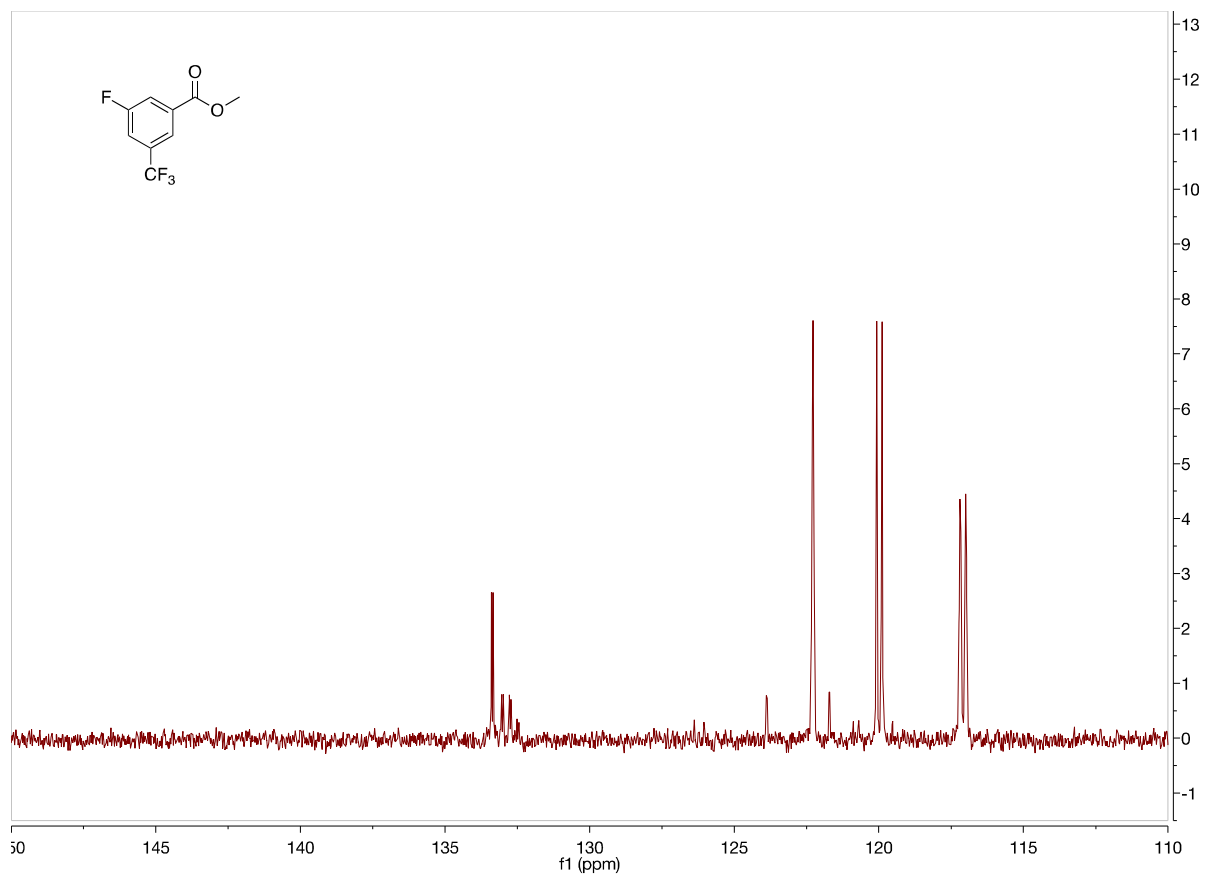


Figure A94. 125 MHz ^{13}C NMR of **3ab'** in CDCl_3 from 150 to 110 ppm

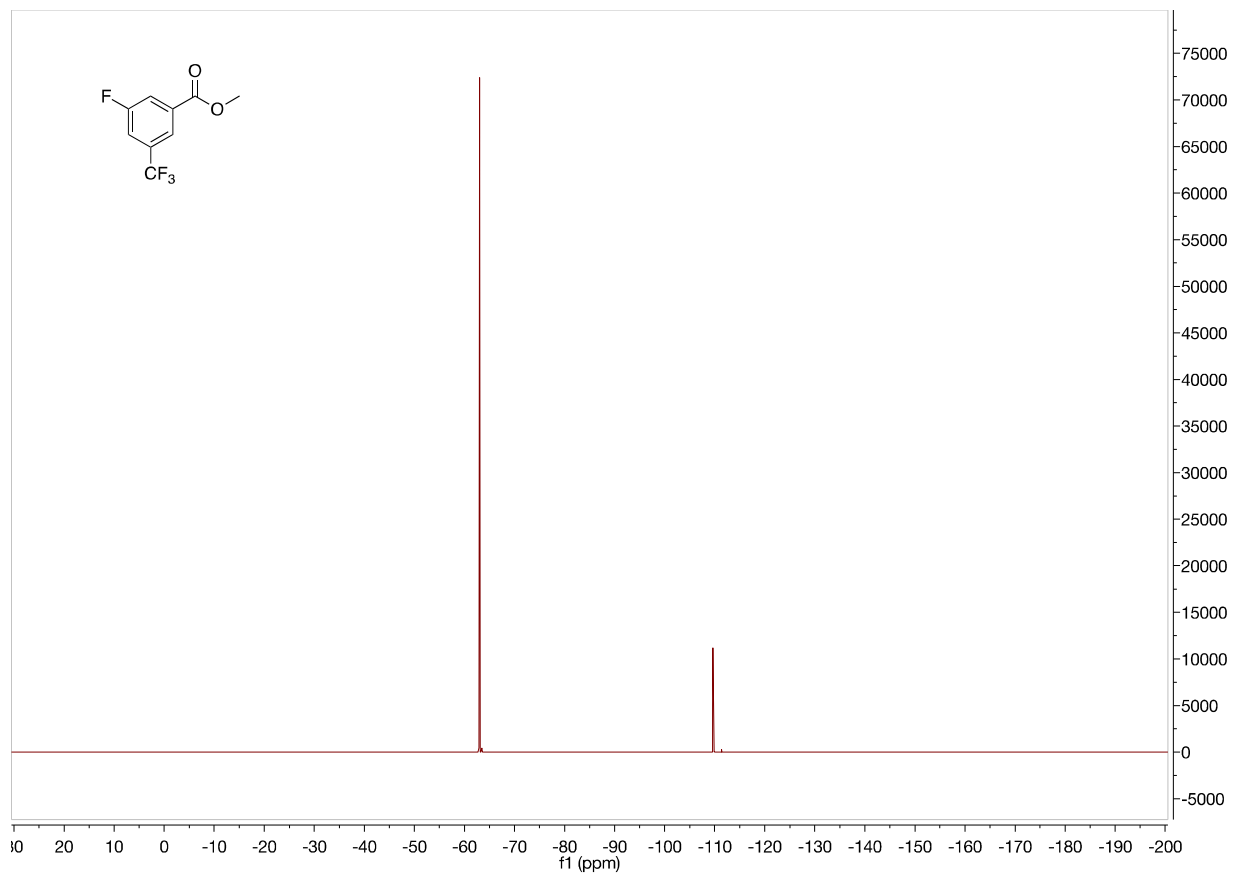


Figure A95. 470 MHz ^{19}F NMR of **3ab'** in CDCl_3

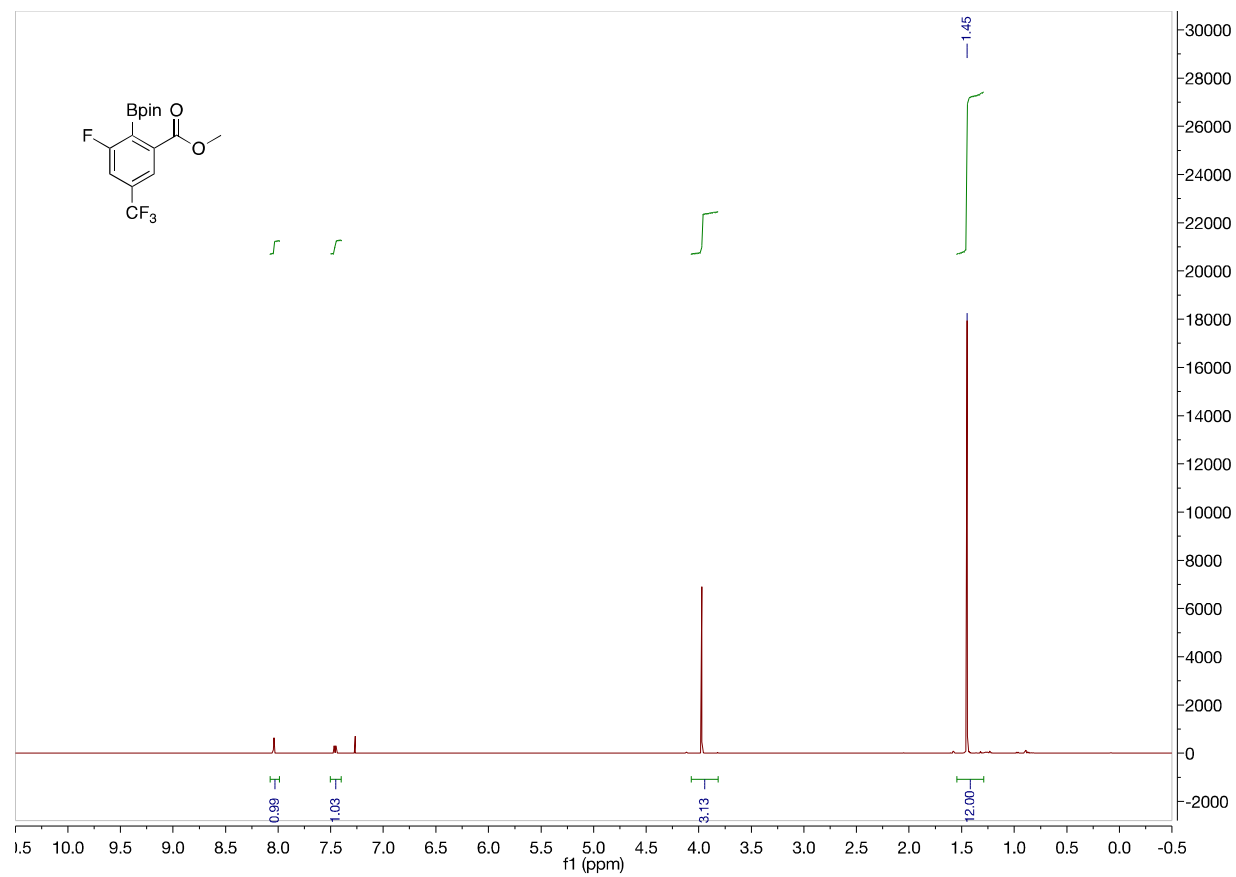


Figure A96. 500 MHz ^1H NMR of **3ab** in CDCl_3

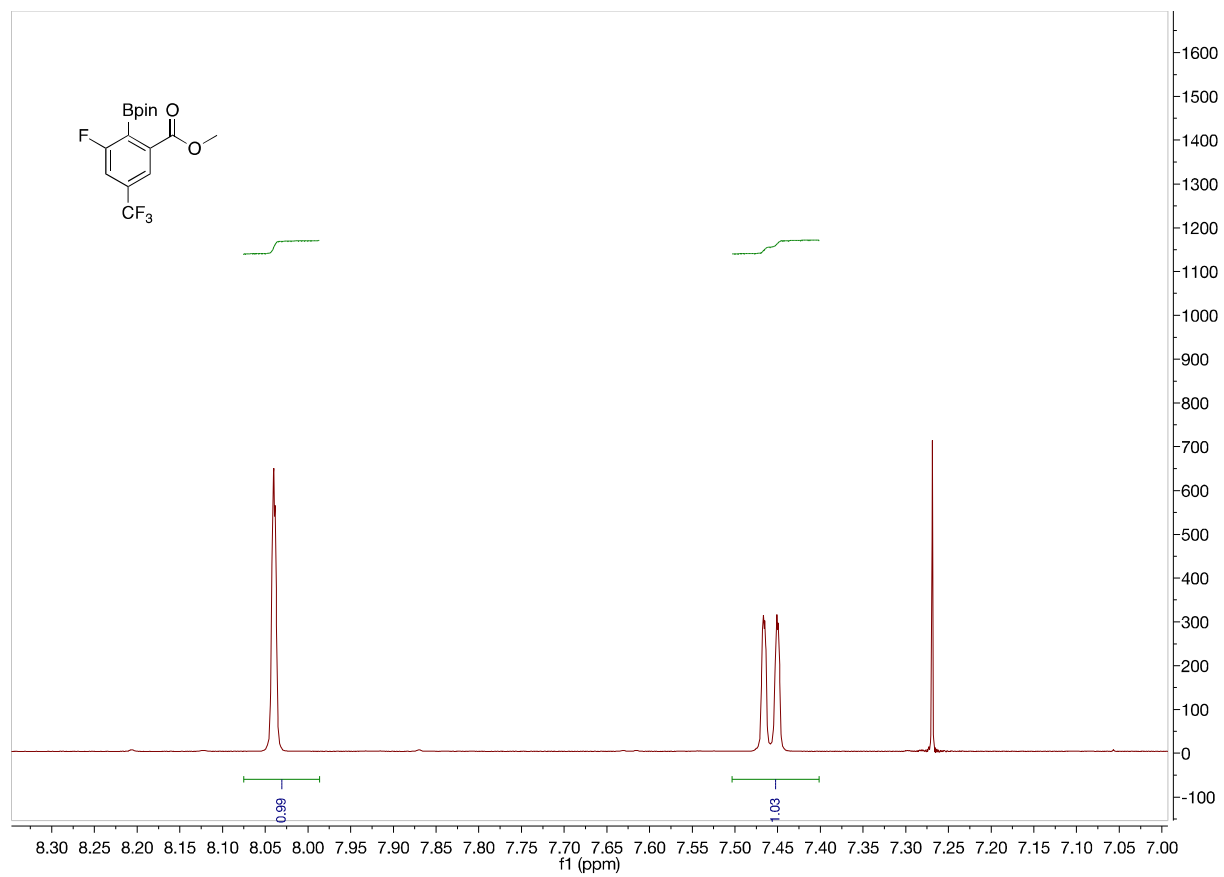


Figure A97. 500 MHz ¹H NMR of **3ab** in CDCl₃ from 8.4 to 7.0 ppm

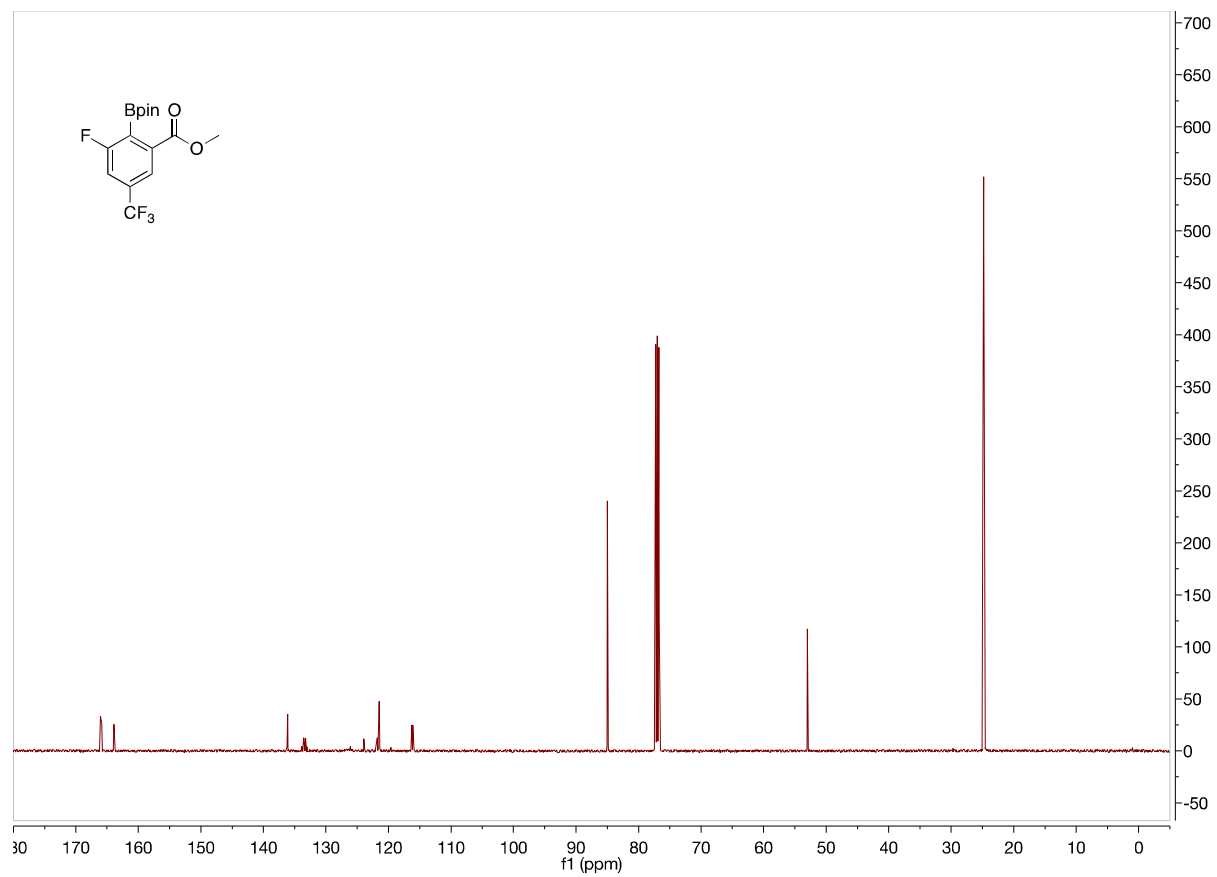


Figure A98. 125 MHz ¹³C NMR of **3ab** in CDCl₃

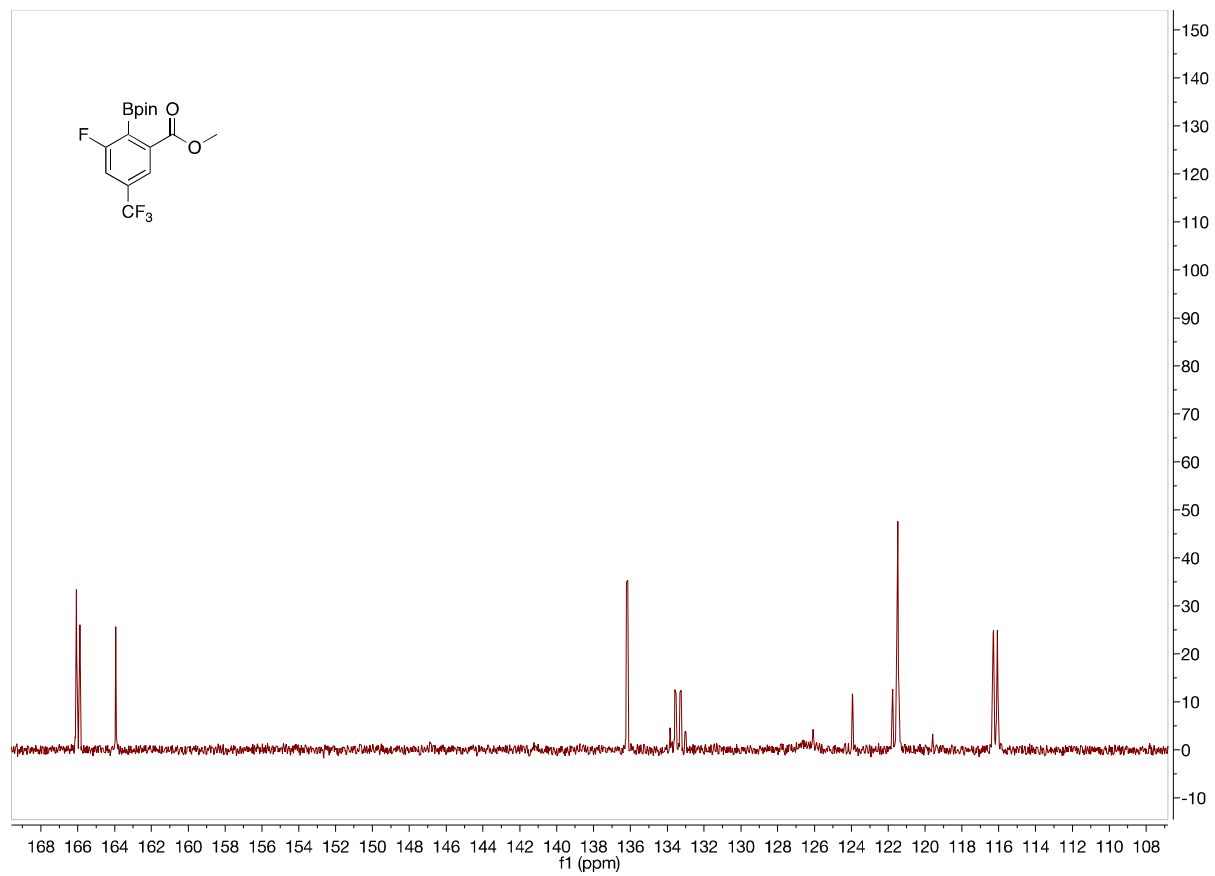


Figure A99. 125 MHz ¹³C NMR of **3ab** in CDCl₃ from 168 to 108 ppm

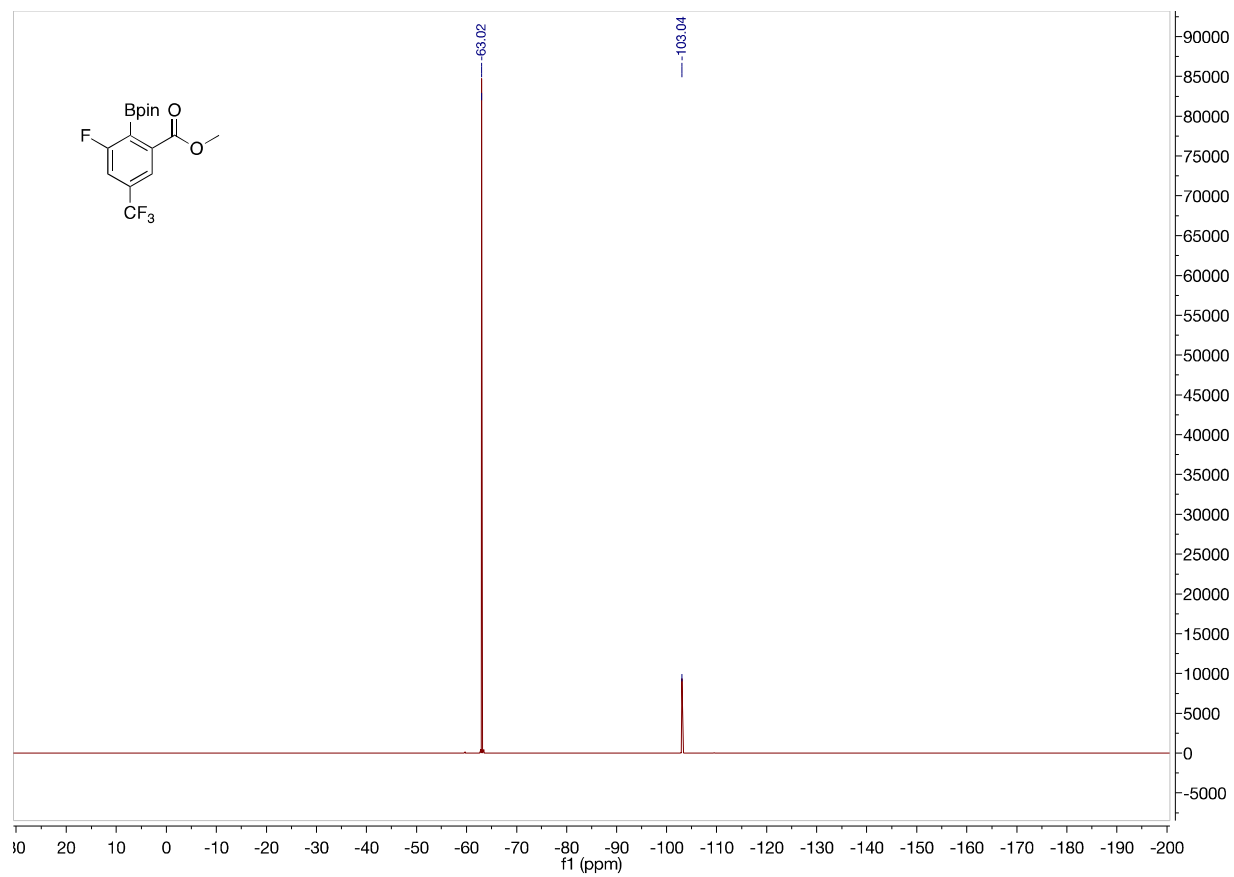


Figure A100. 470 MHz ^{19}F NMR of **3ab** in CDCl_3

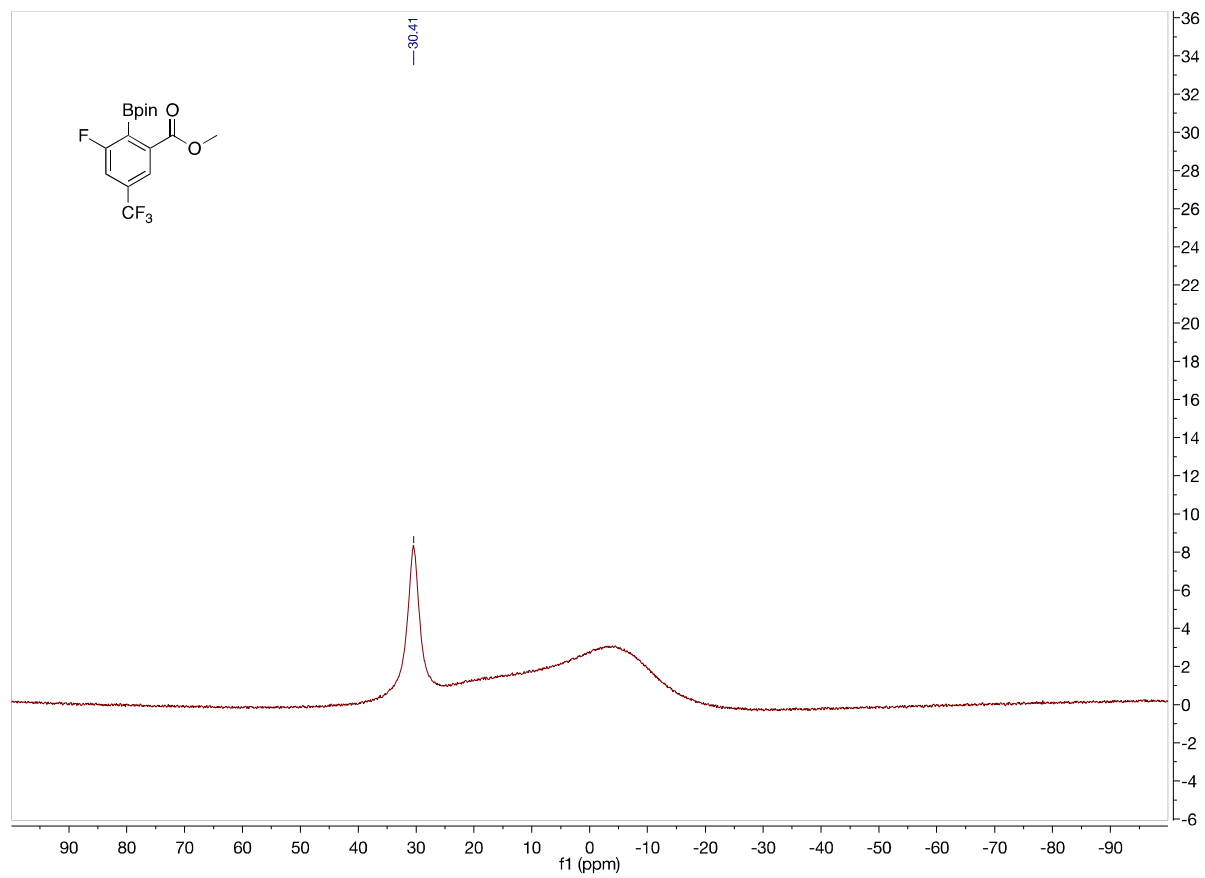


Figure A101. 160 MHz ^{11}B NMR of **3ab** in CDCl_3

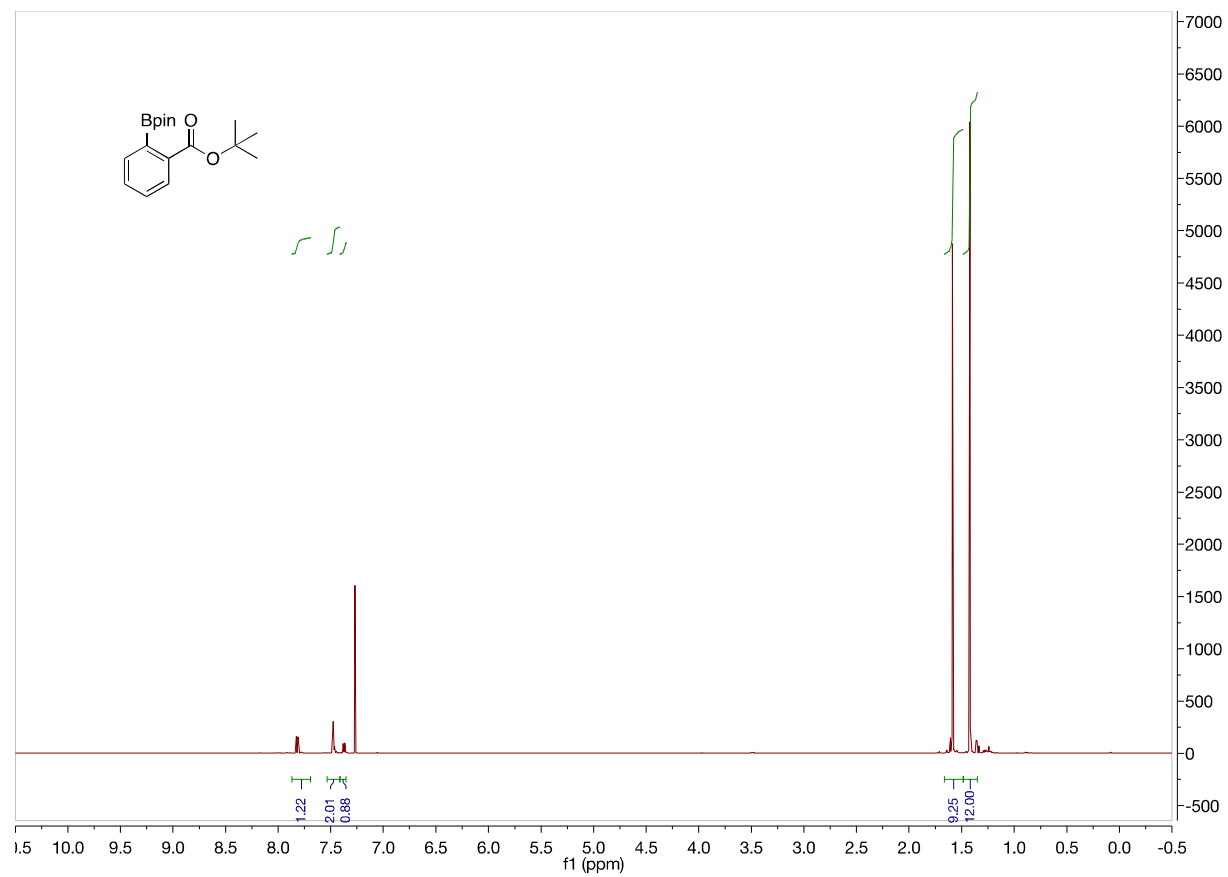


Figure A102. 500 MHz ¹H NMR of 3ac in CDCl₃

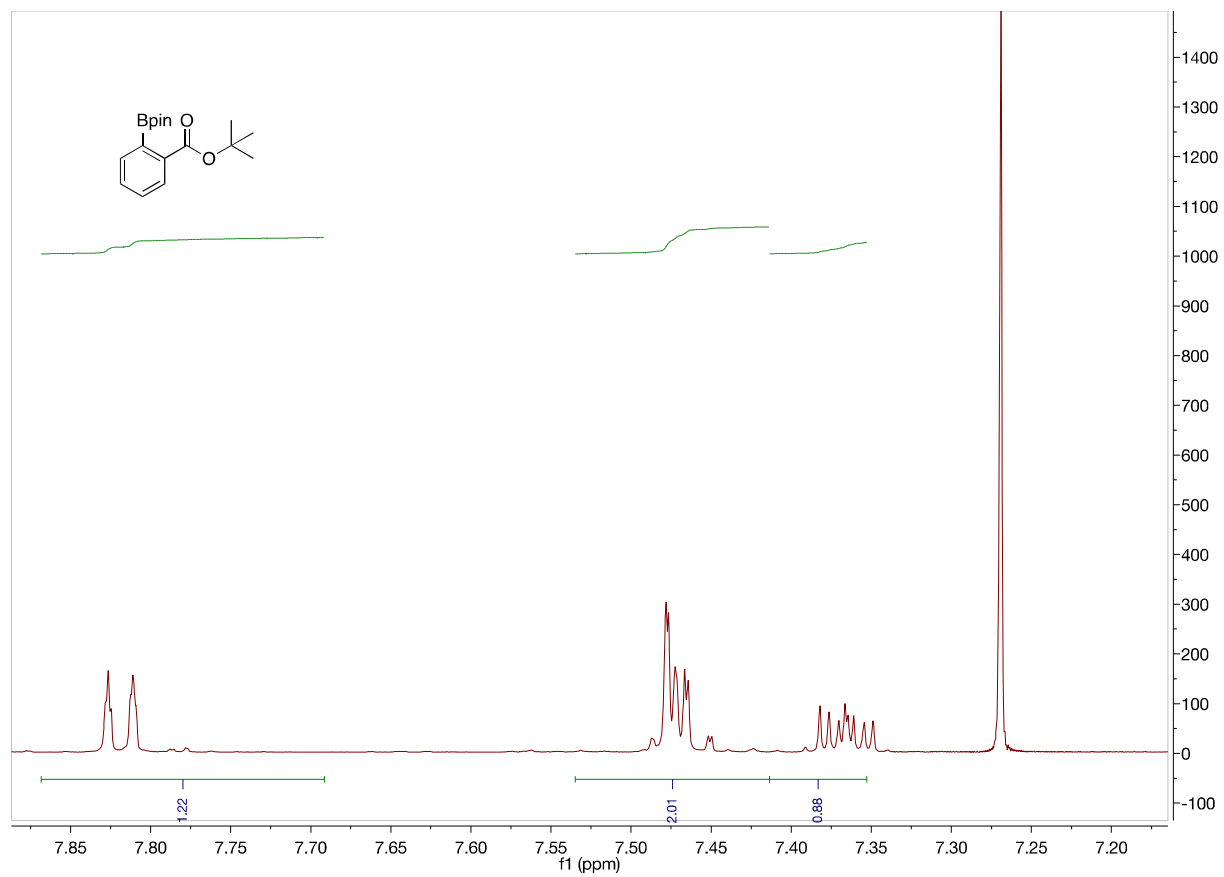


Figure A103. 500 MHz ^1H NMR of **3ac** in CDCl_3 from 7.9 to 7.2 ppm

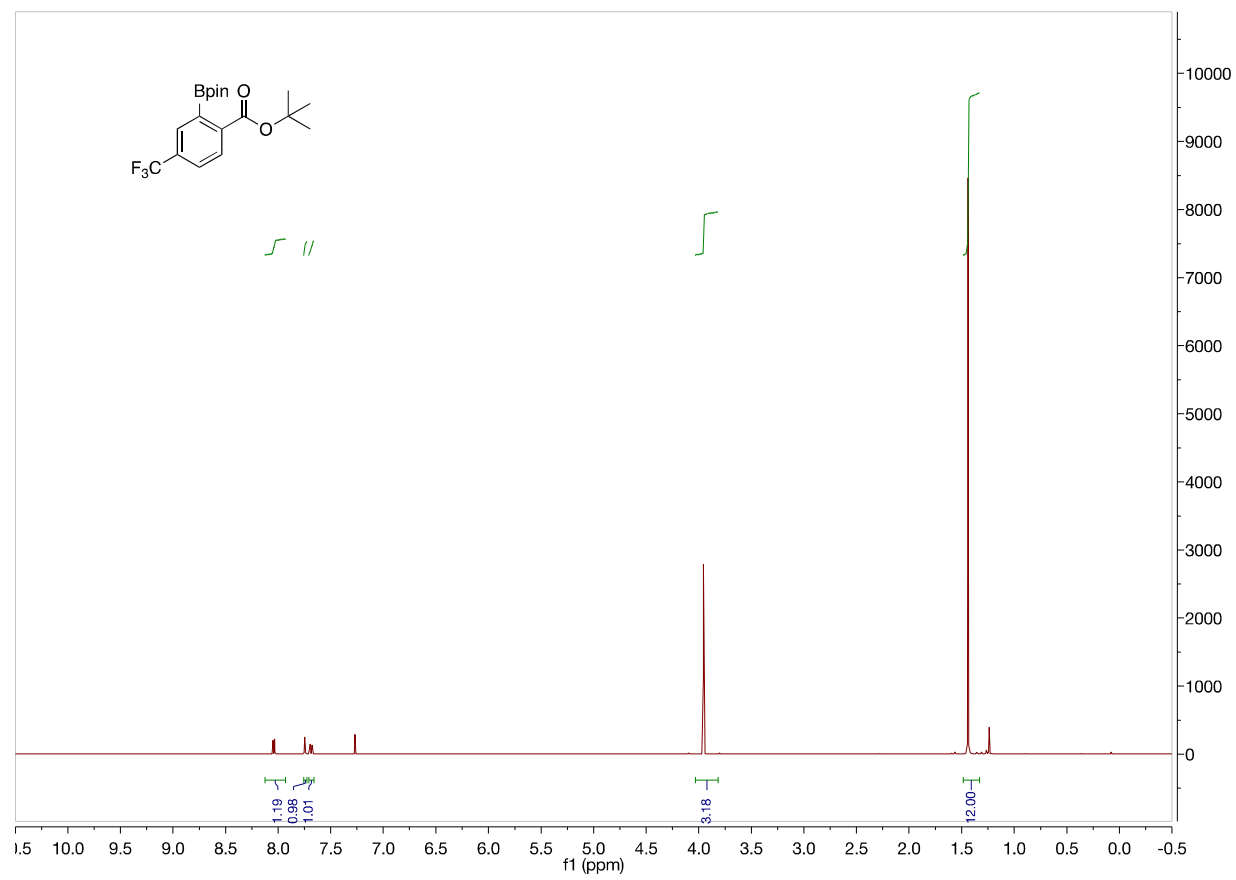


Figure A104. 500 MHz ^1H NMR of **3ad** in CDCl_3

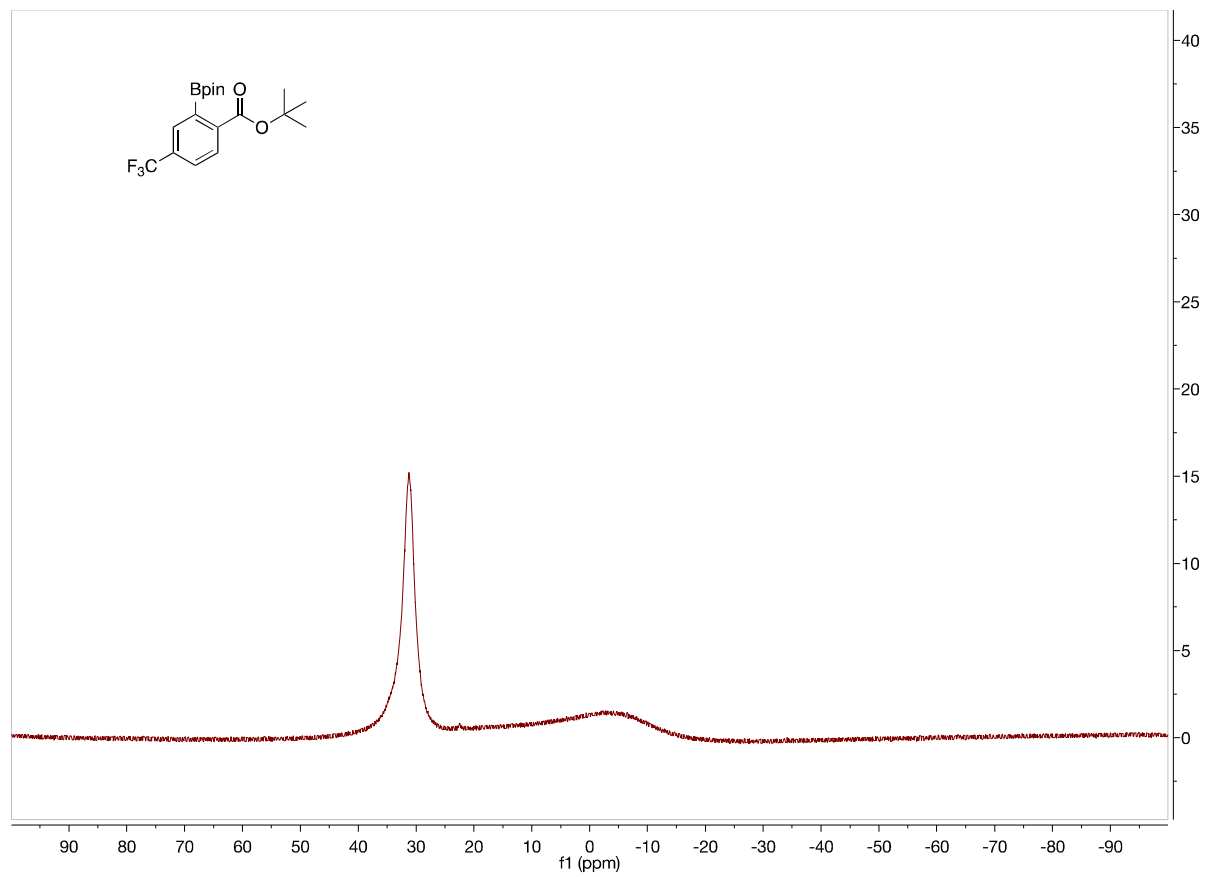


Figure A105. 160 MHz ^{11}B NMR of **3ad** in CDCl_3

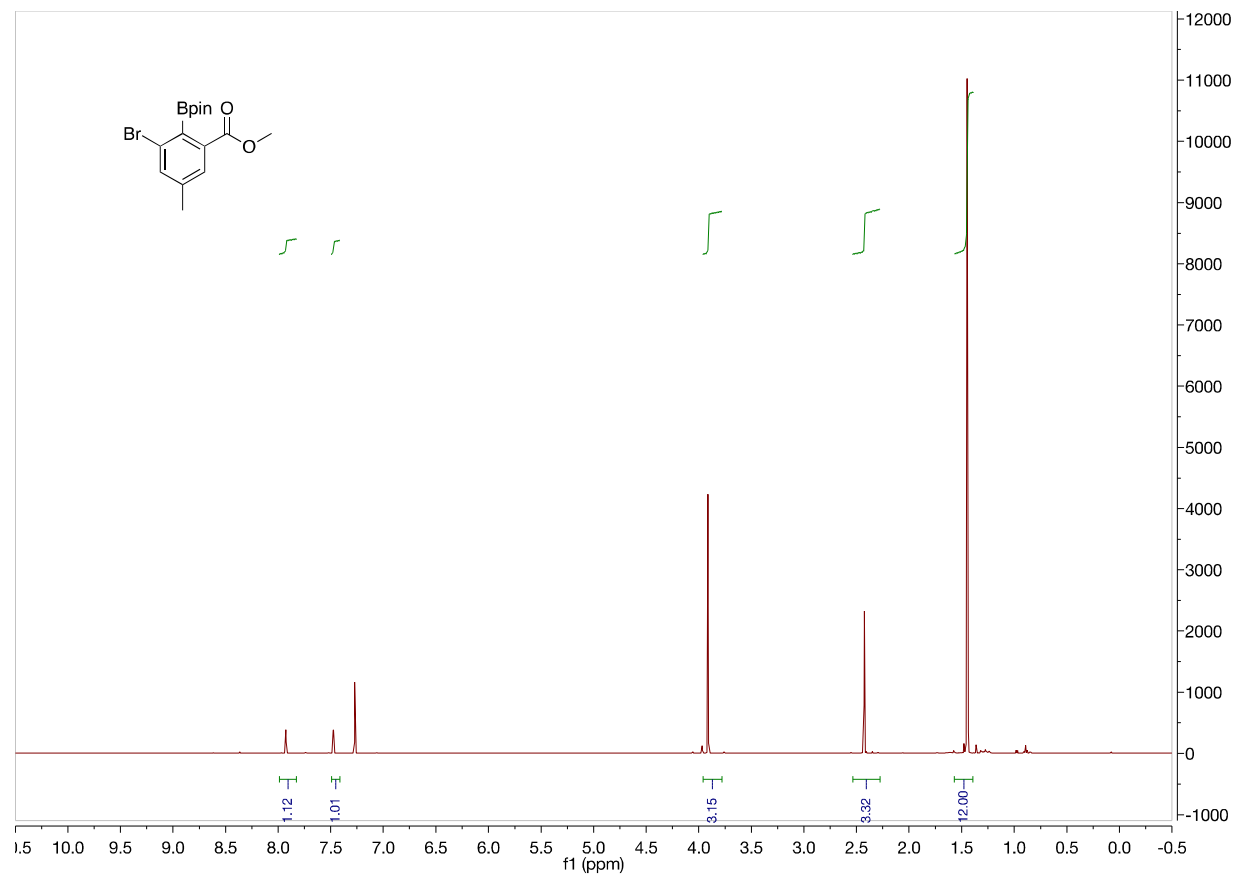


Figure A106. 500 MHz ^1H NMR of **3ae** in CDCl_3

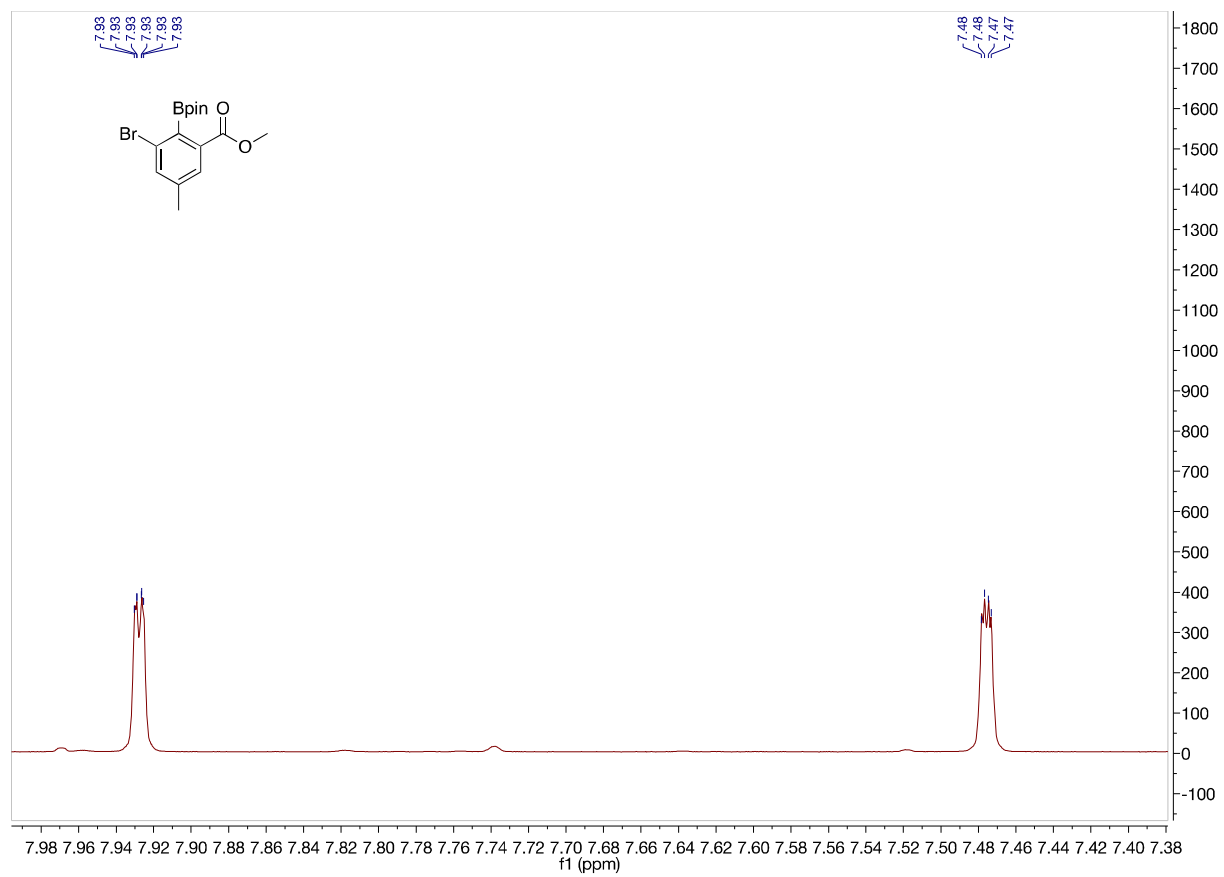


Figure A107. 500 MHz ¹H NMR of **3ae** in CDCl₃ from 8.0 to 7.35 ppm

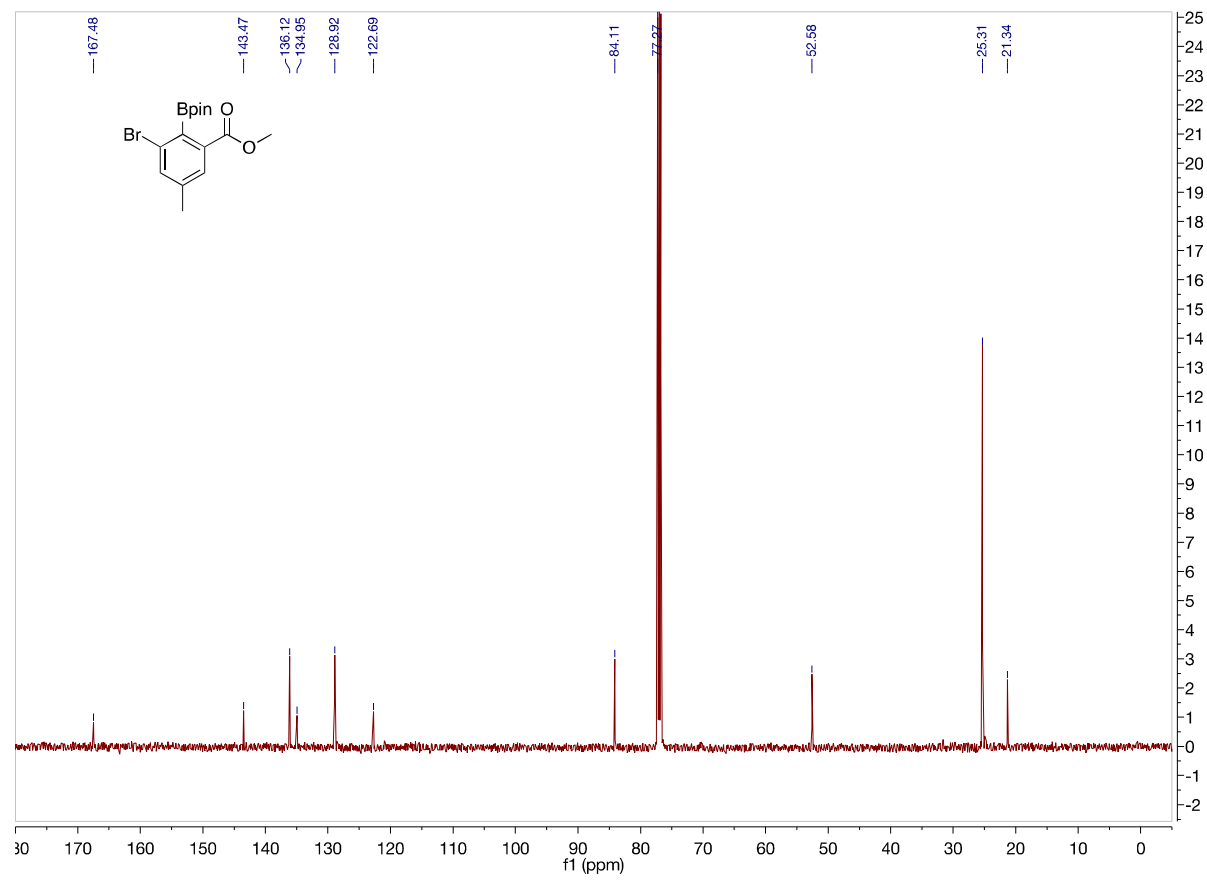


Figure A108. 125 MHz ^{13}C NMR of **3ae** in CDCl_3

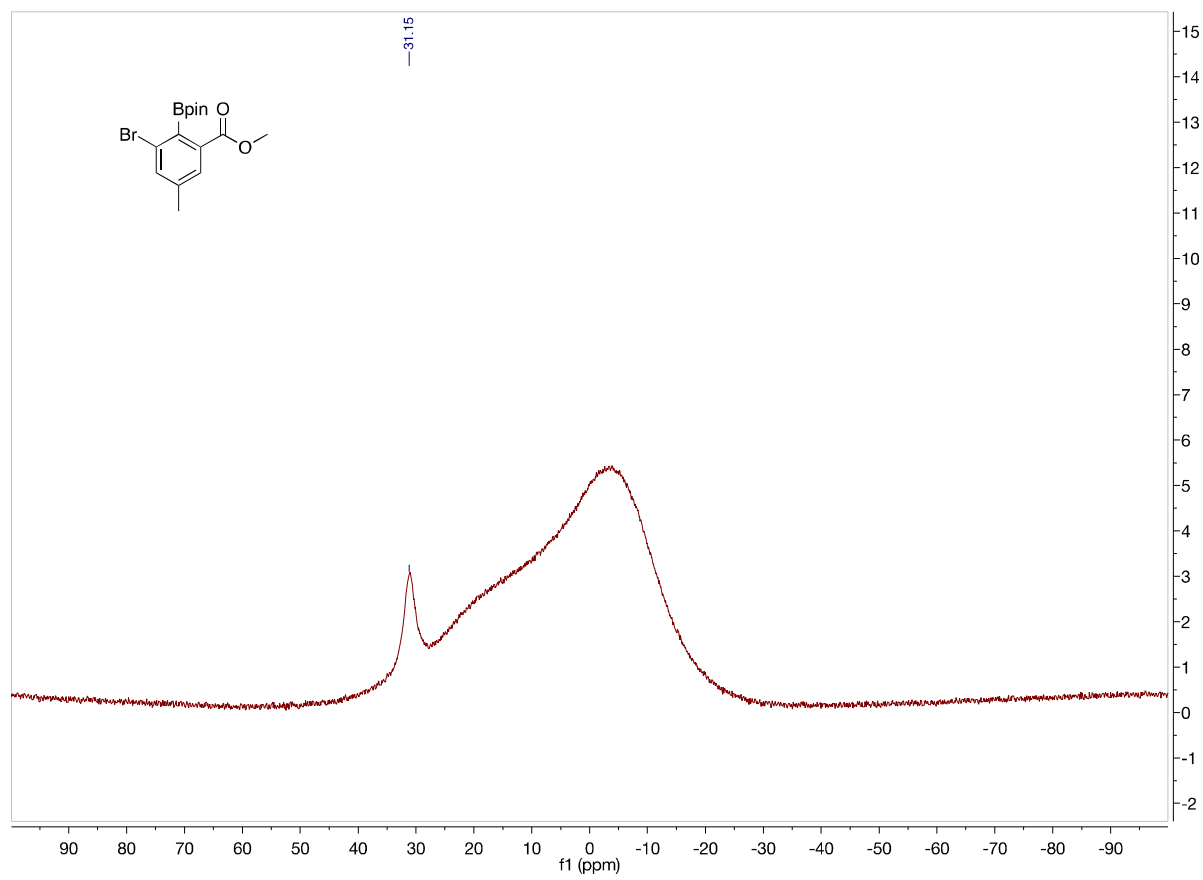


Figure A109. 160 MHz ^{11}B NMR of **3ae** in CDCl_3

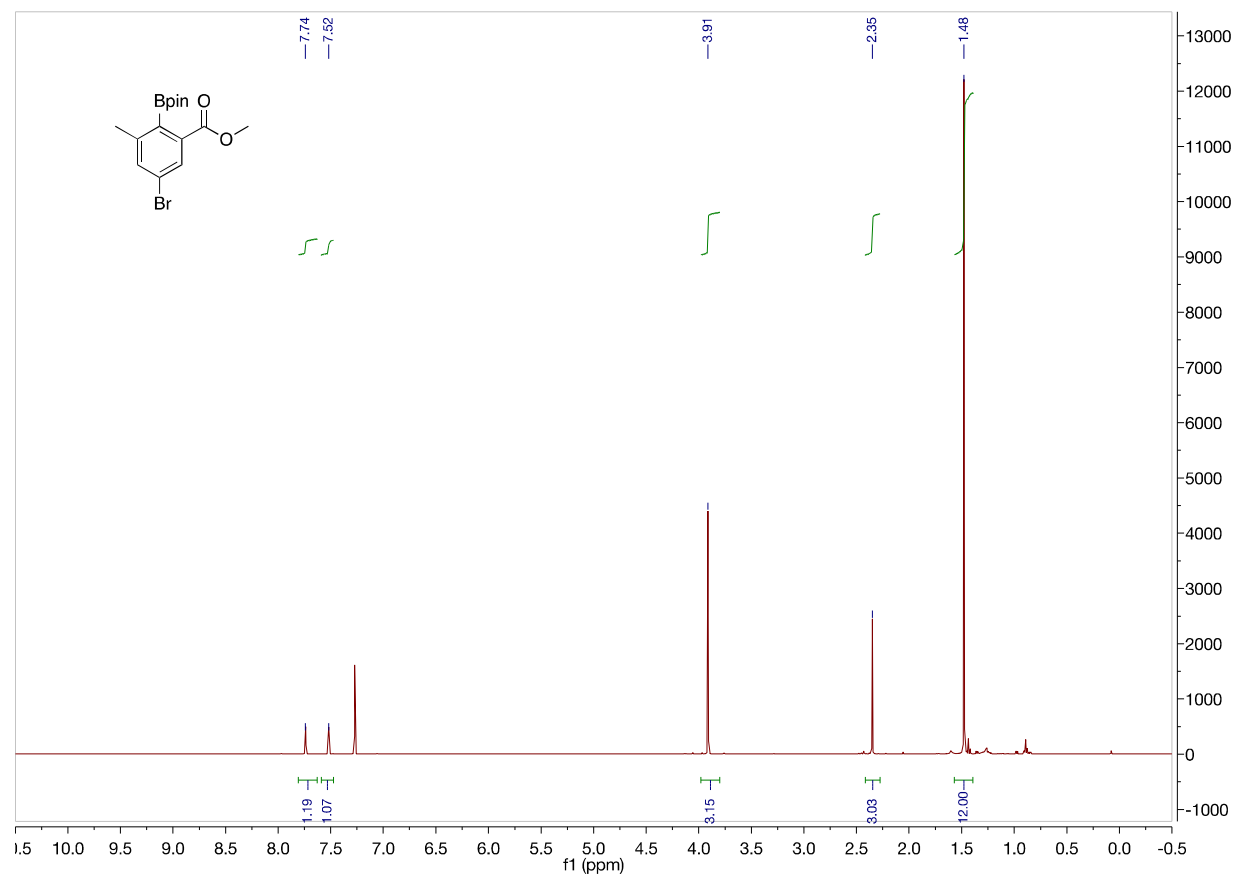


Figure A110. 500 MHz ^1H NMR of **3af** in CDCl_3

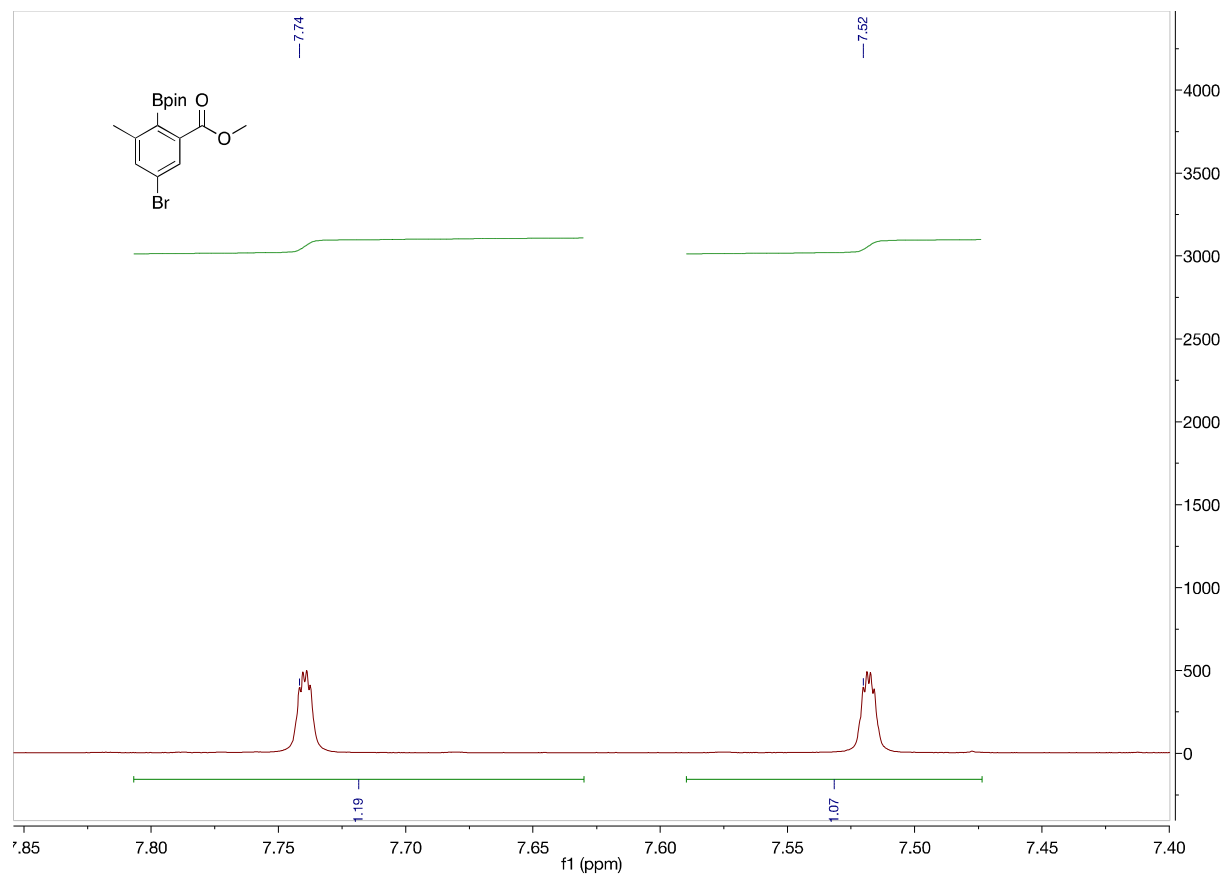


Figure A111. 500 MHz ^1H NMR of **3af** in CDCl_3 from 7.85 to 7.40 ppm

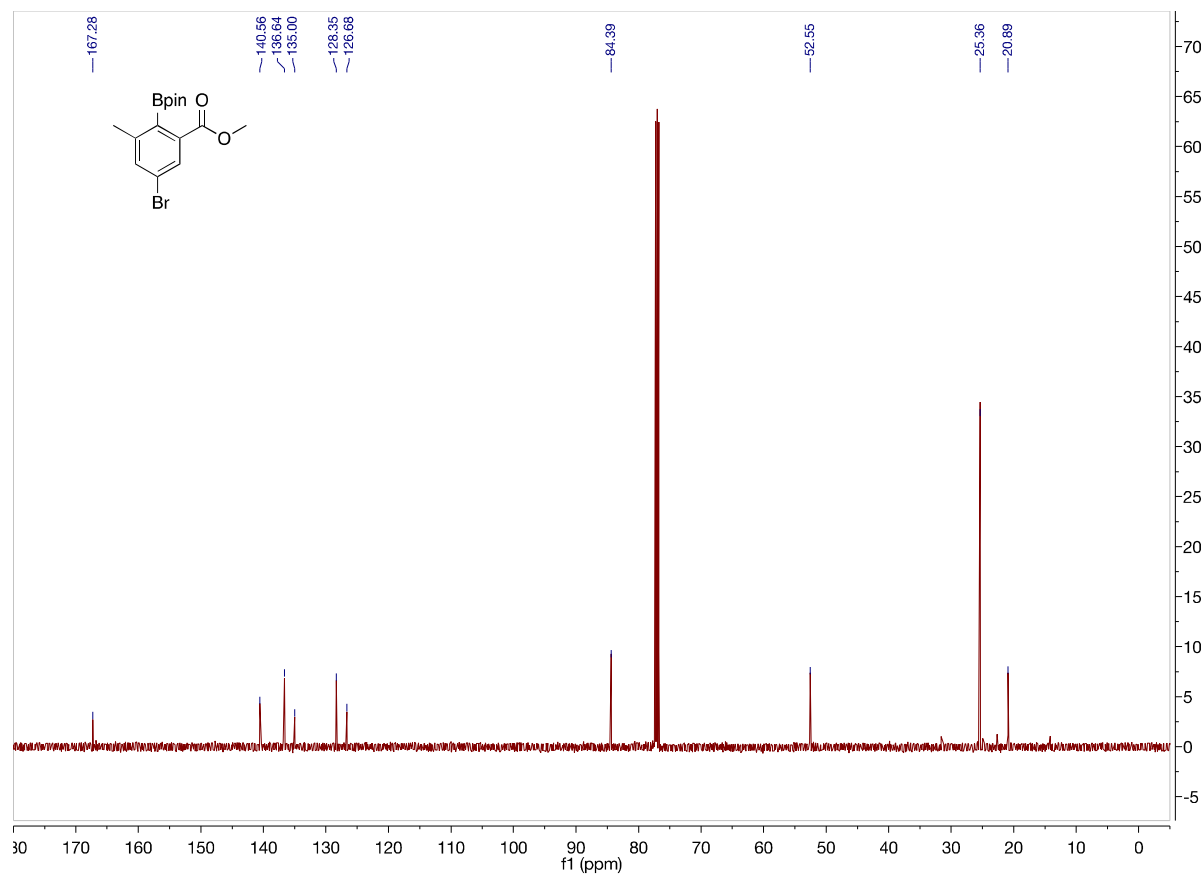


Figure A112. 125 MHz ¹³C NMR of 3af in CDCl₃

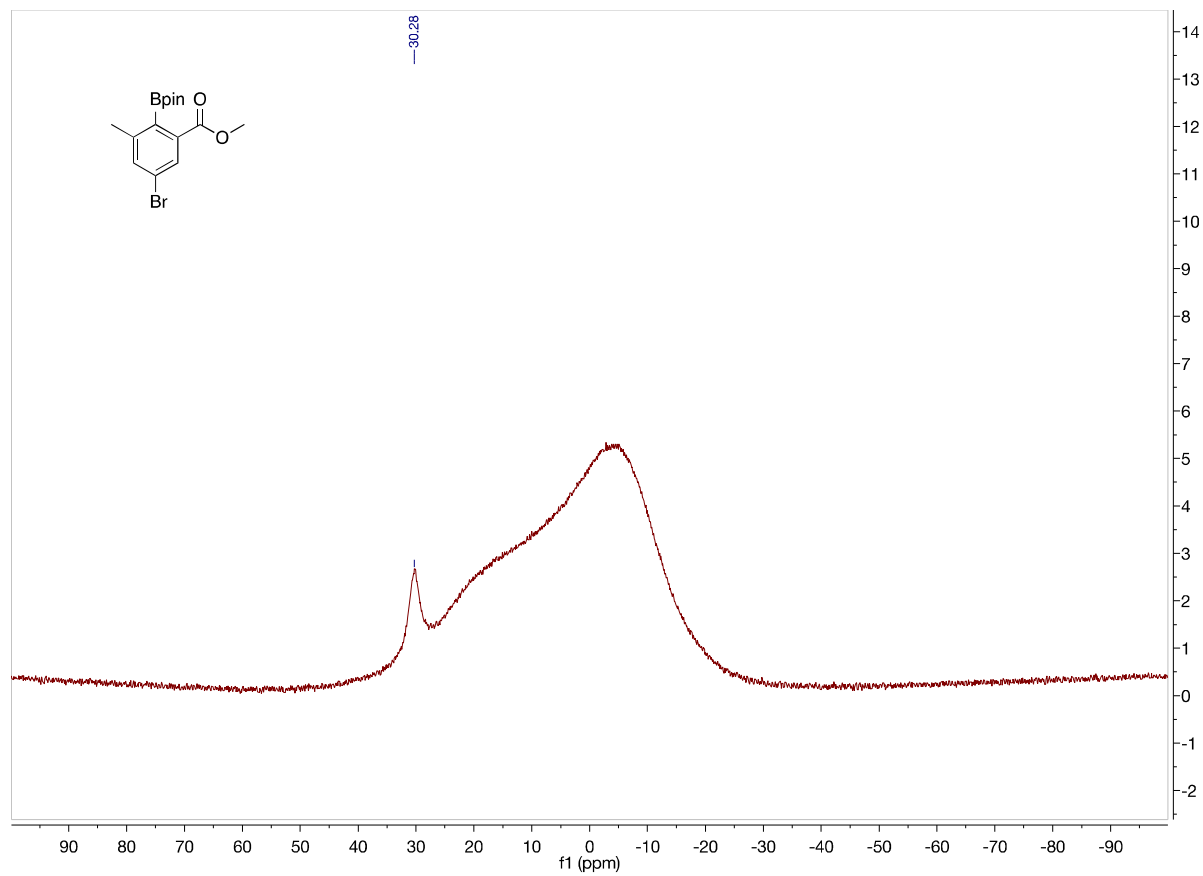


Figure A113. 160 MHz ^{11}B NMR of **3af** in CDCl_3

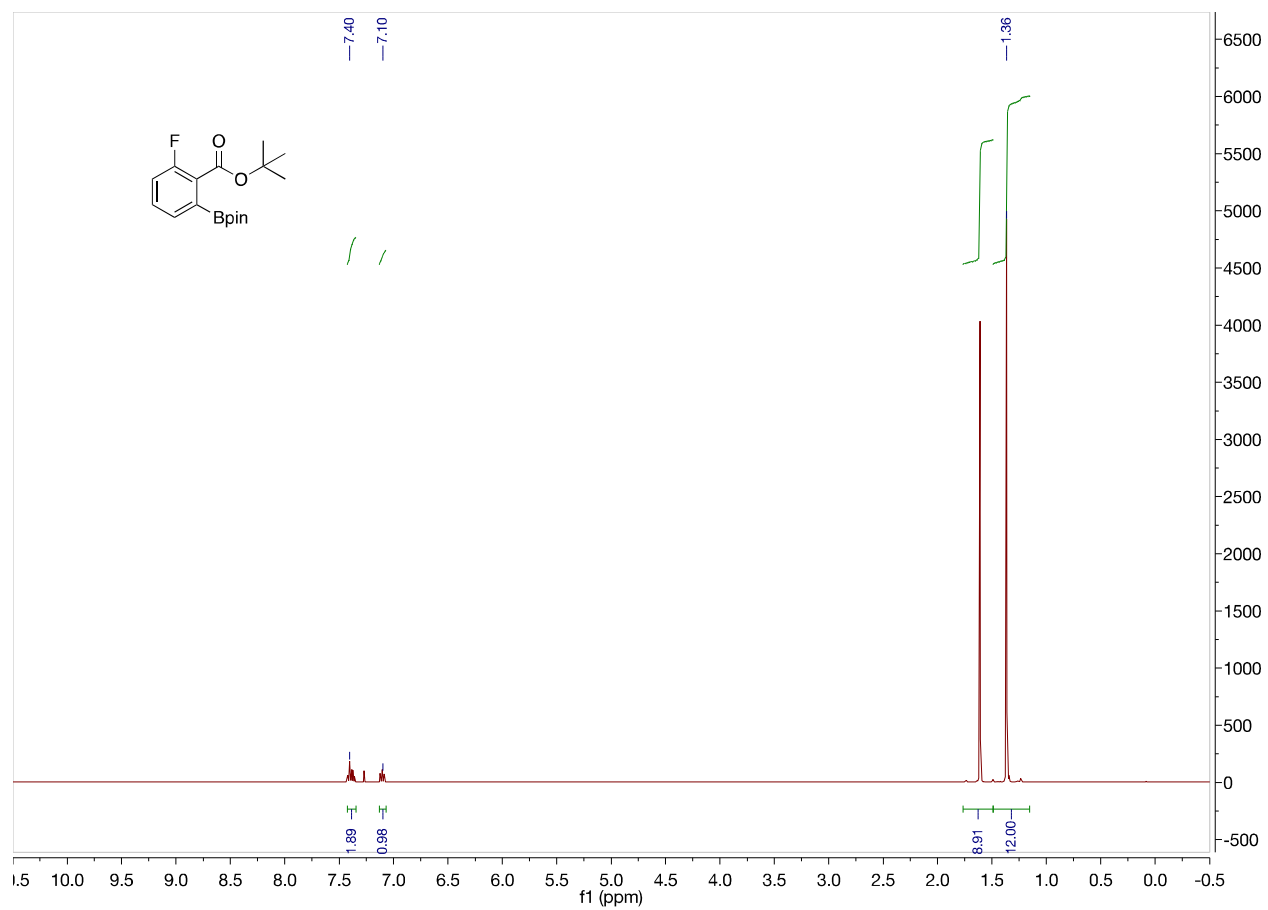


Figure A114. 500 MHz ¹H NMR of **3ah** in CDCl₃

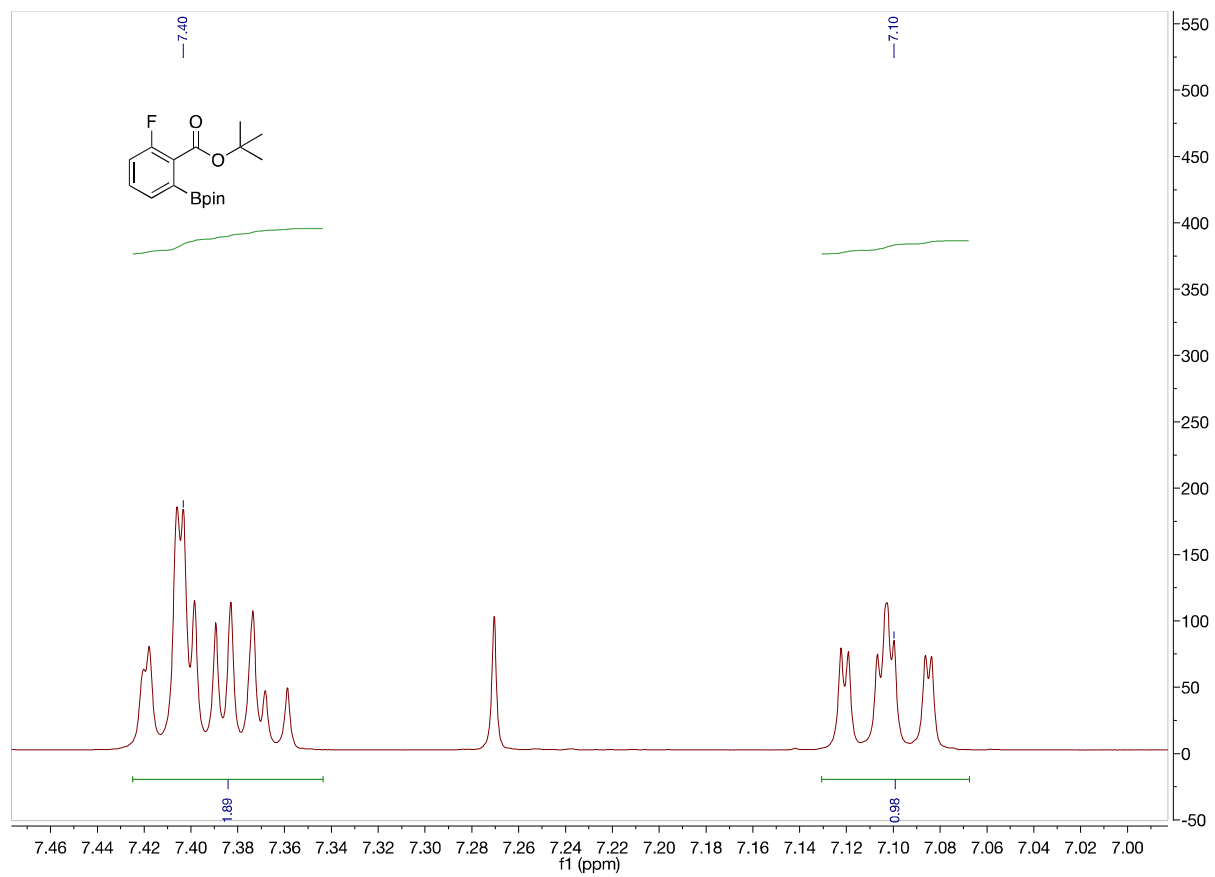


Figure A115. 500 MHz ^1H NMR of **3ah** in CDCl_3 from 7.50 to 7.00 ppm

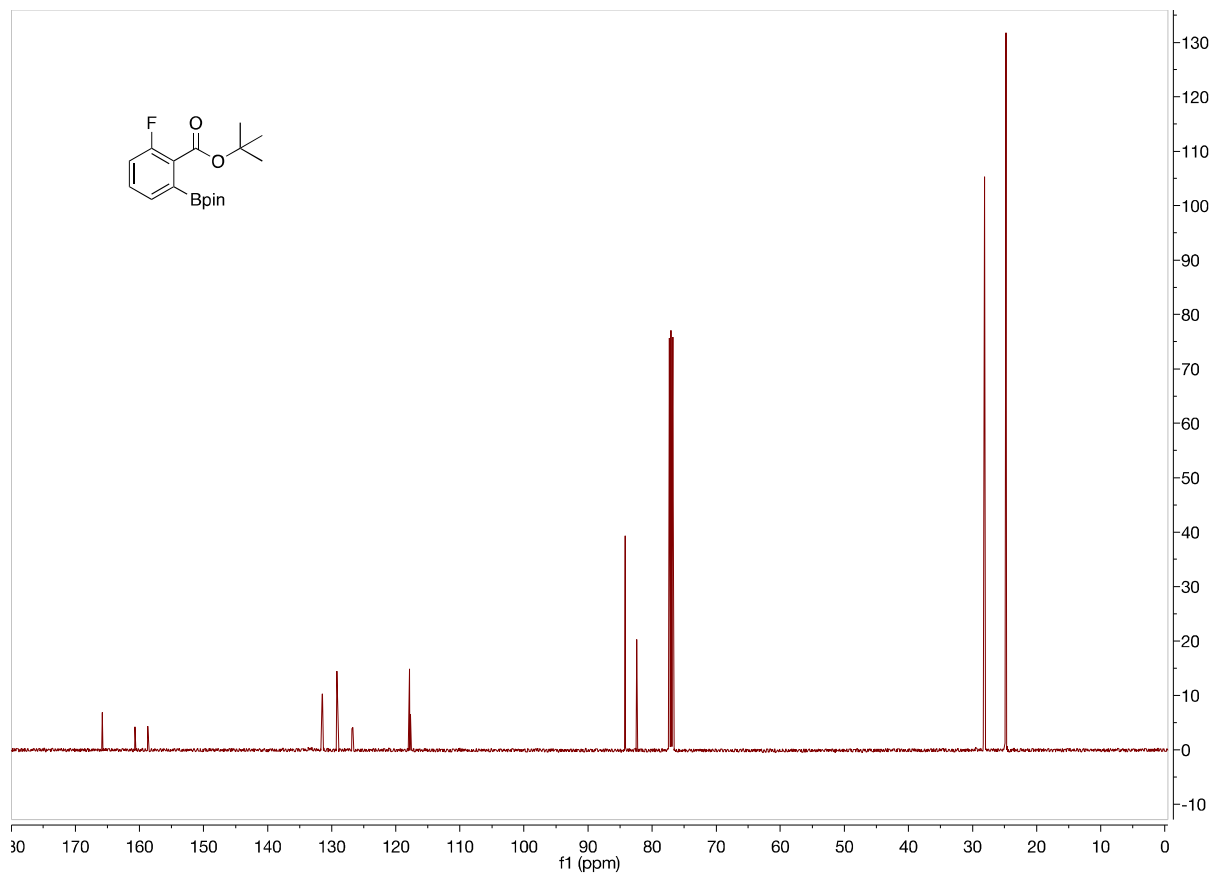


Figure A116. 125 MHz ^{13}C NMR of **3ah** in CDCl_3

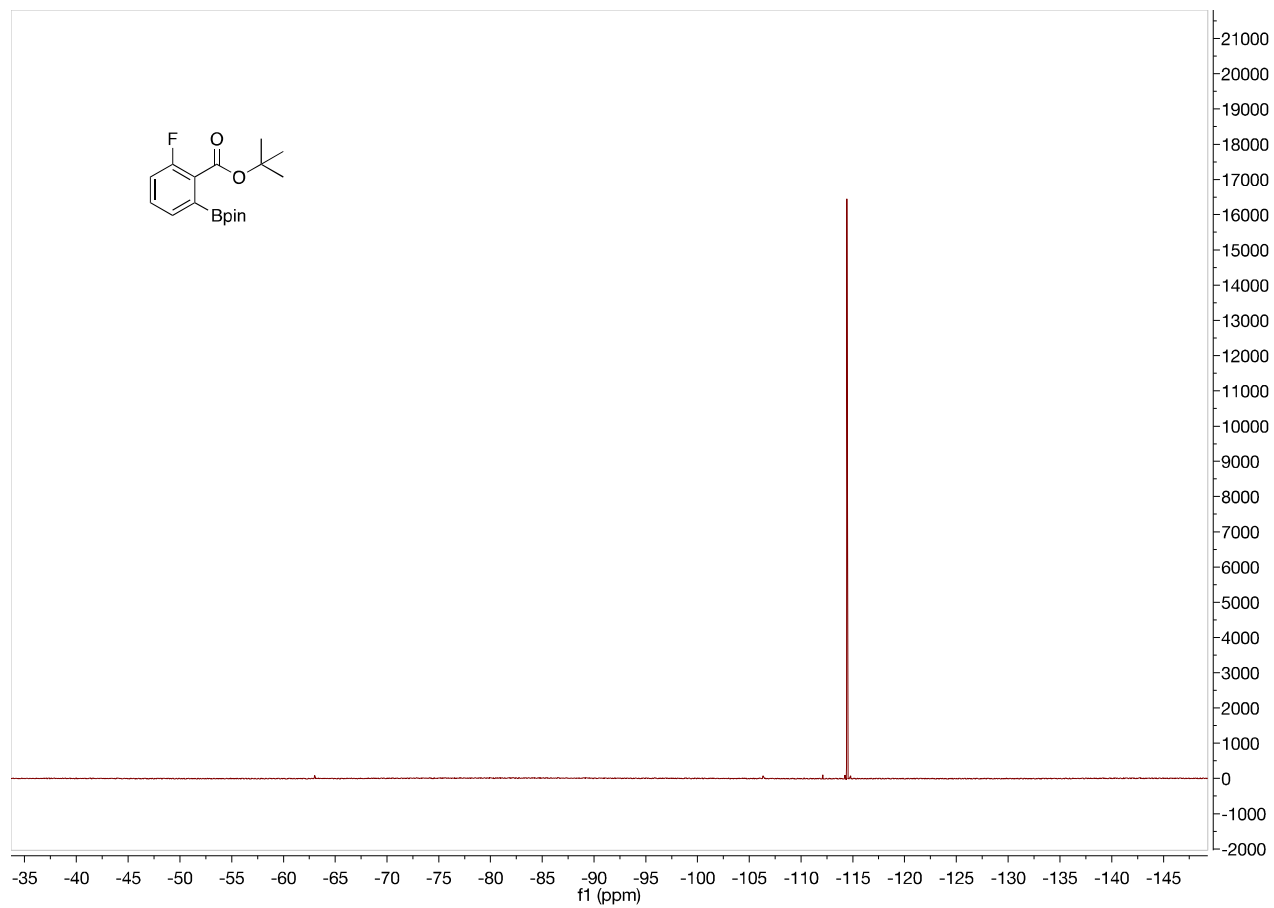


Figure A117. 470 MHz ^{19}F NMR of **3ah** in CDCl_3

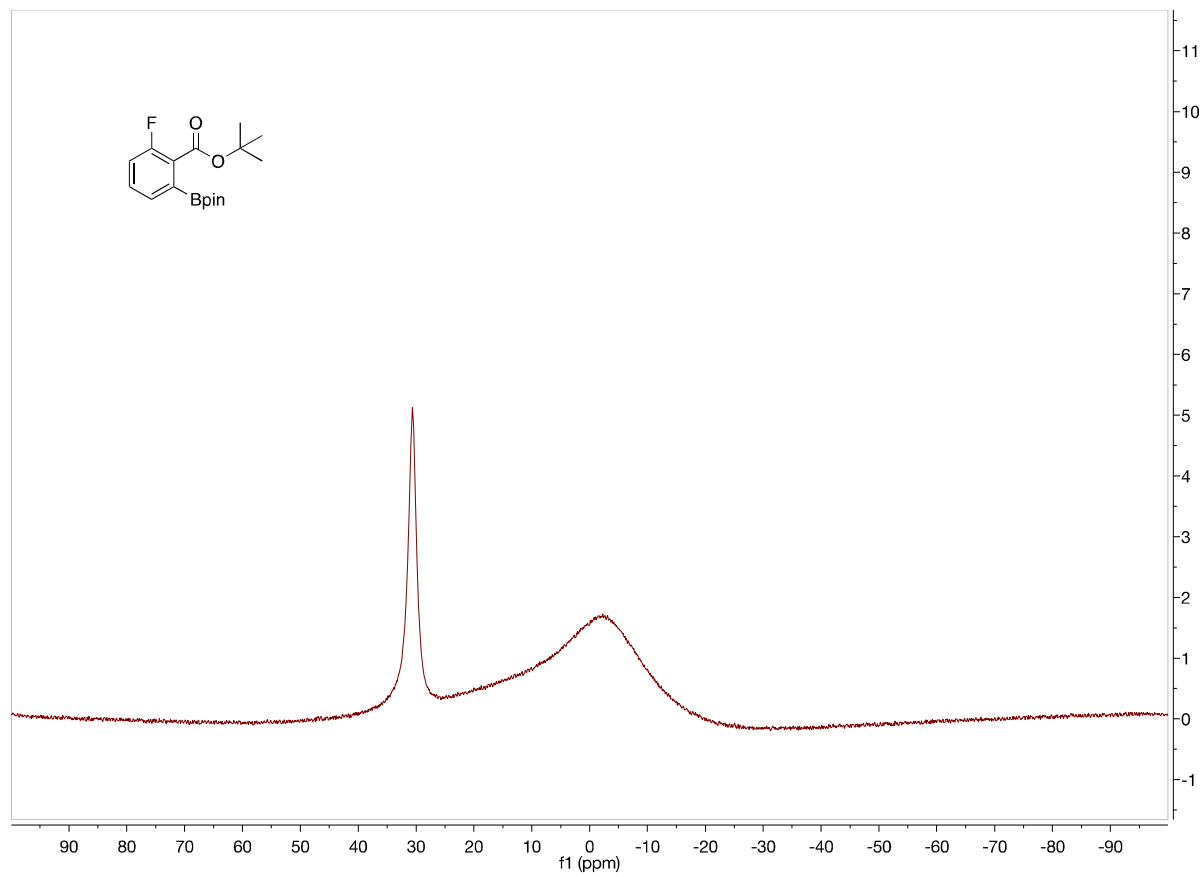


Figure A118. 160 MHz ^{11}B NMR of **3ah** in CDCl_3

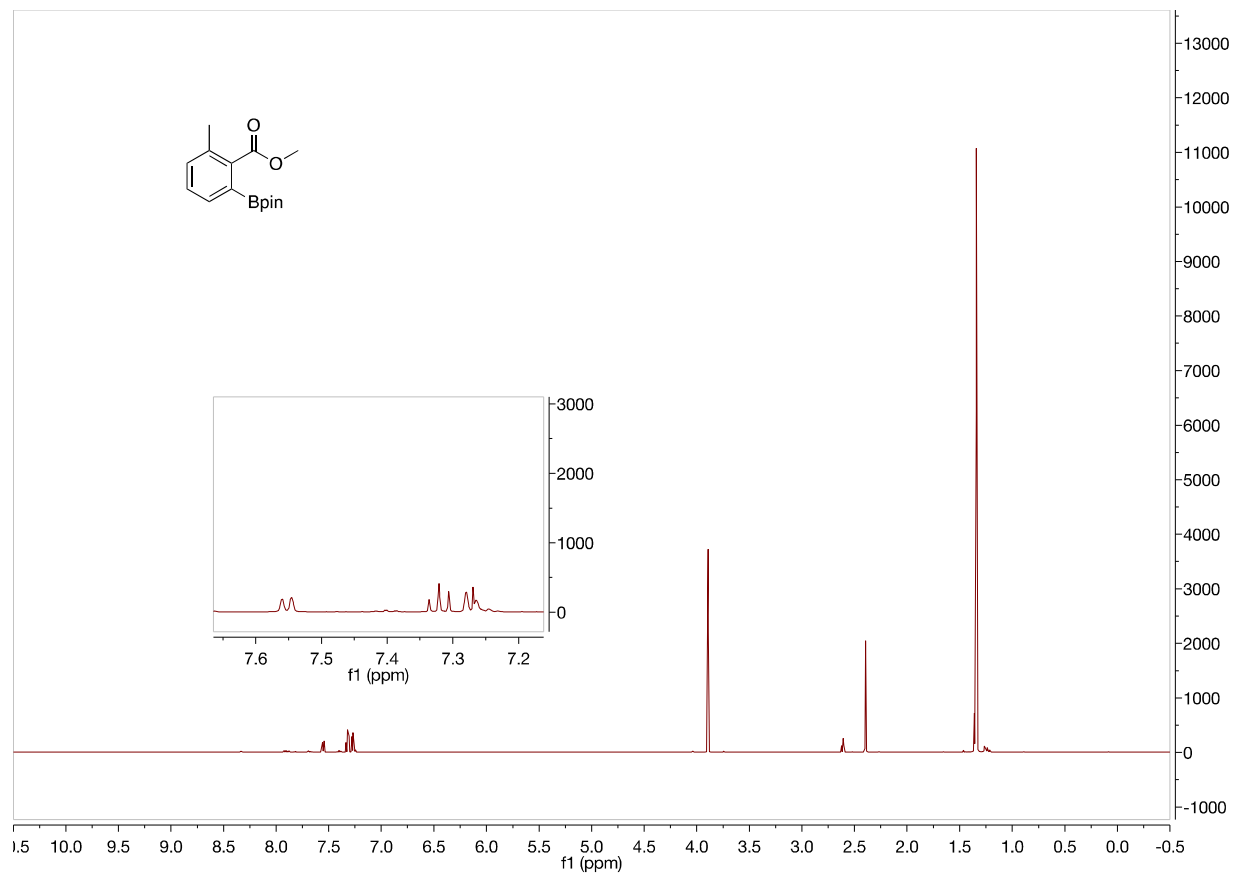


Figure A119. 500 MHz ^1H NMR of **3ai** in CDCl_3

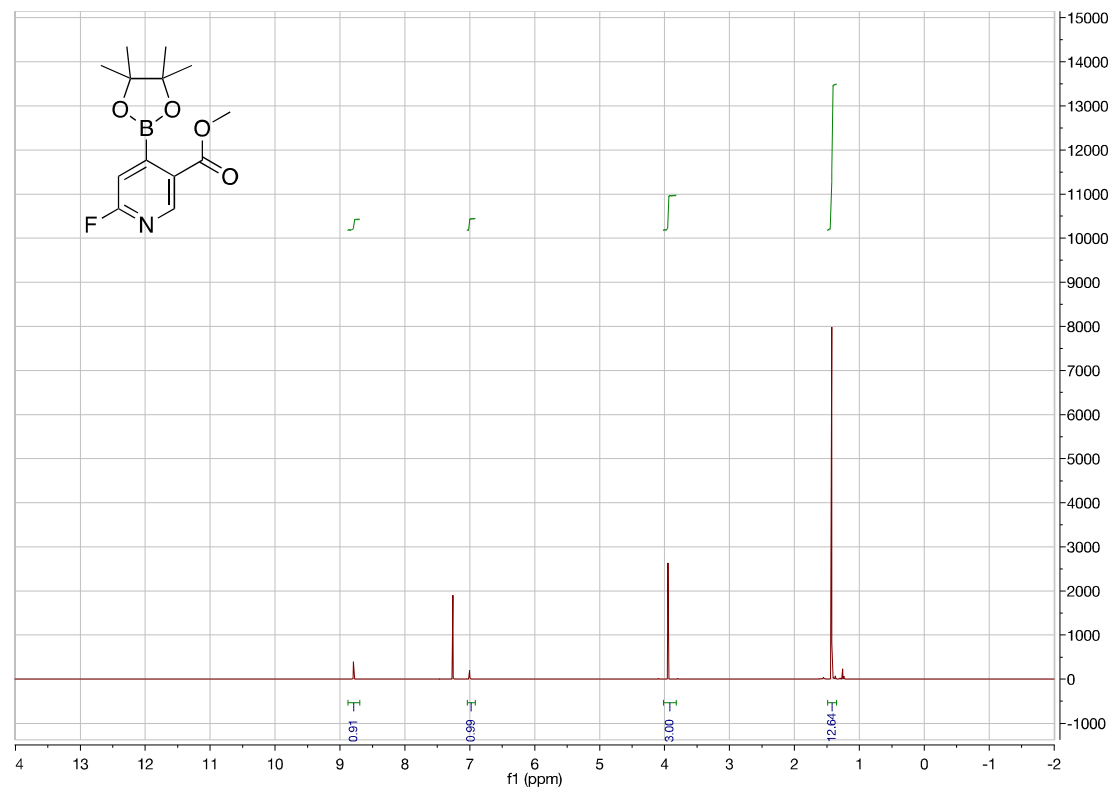


Figure A120. 500 MHz ¹H NMR of **3ao** in CDCl₃

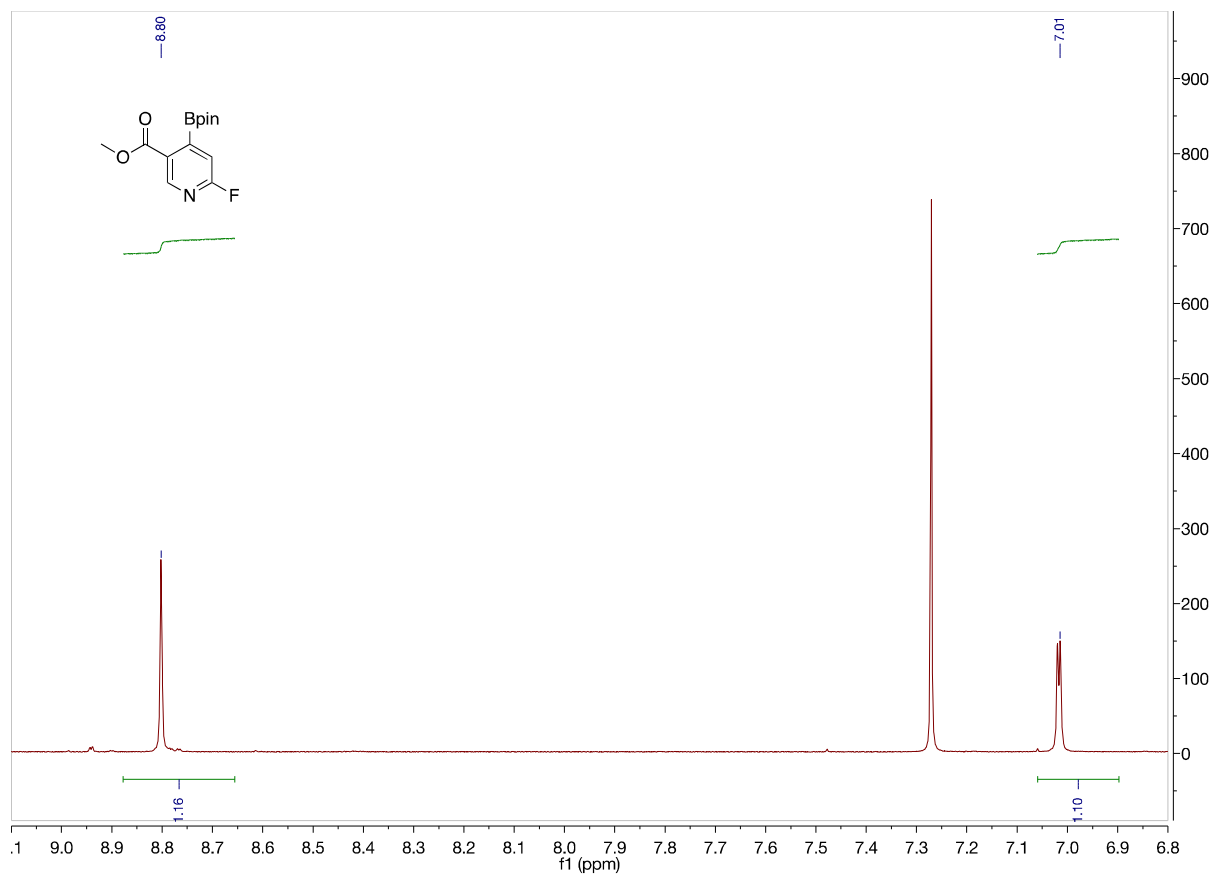


Figure A121. 500 MHz ¹H NMR of **3ao** in CDCl₃ from 9.0 to 6.8 ppm

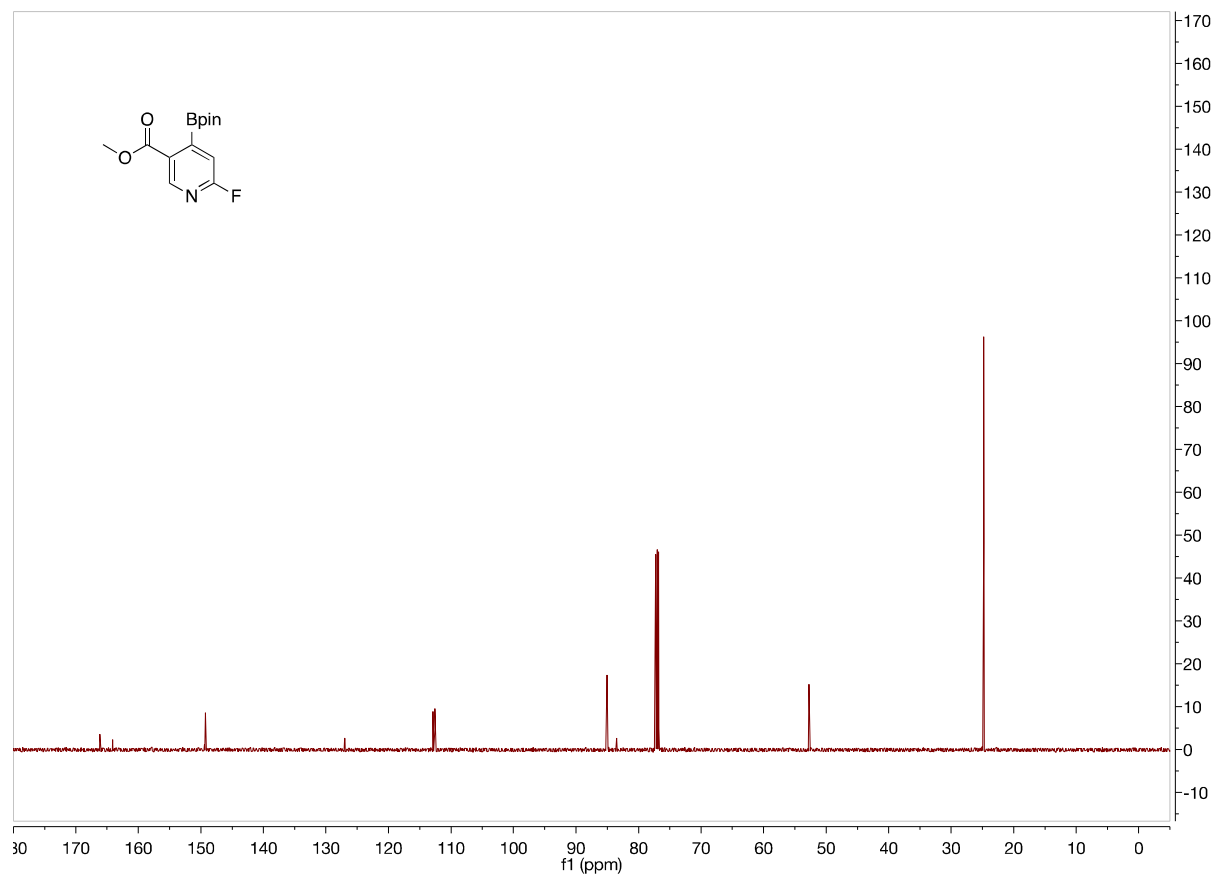


Figure A122. 125 MHz ^{13}C NMR of **3ao** in CDCl_3

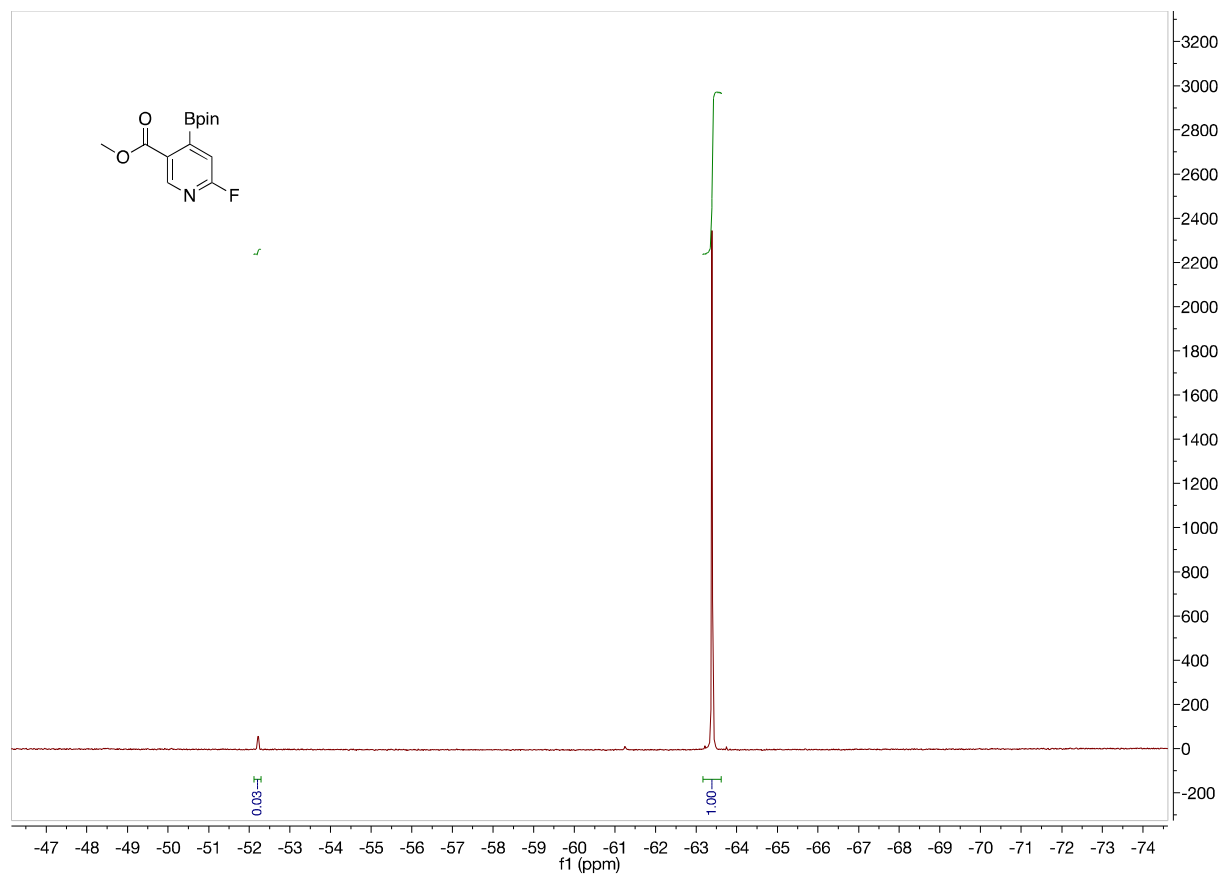


Figure A123. 470 MHz ^{19}F NMR of **3ao** in CDCl_3

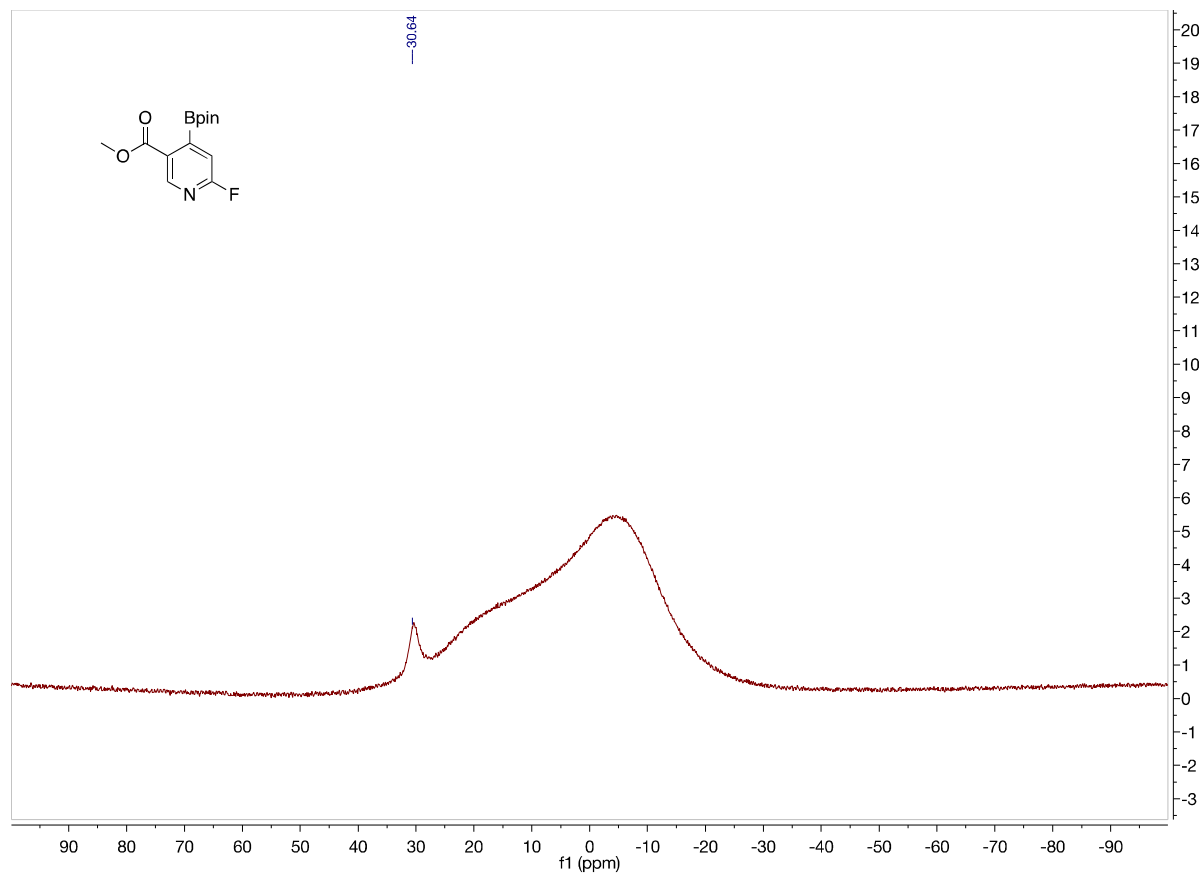


Figure A124. 160 MHz ^{11}B NMR of 3ao in CDCl_3

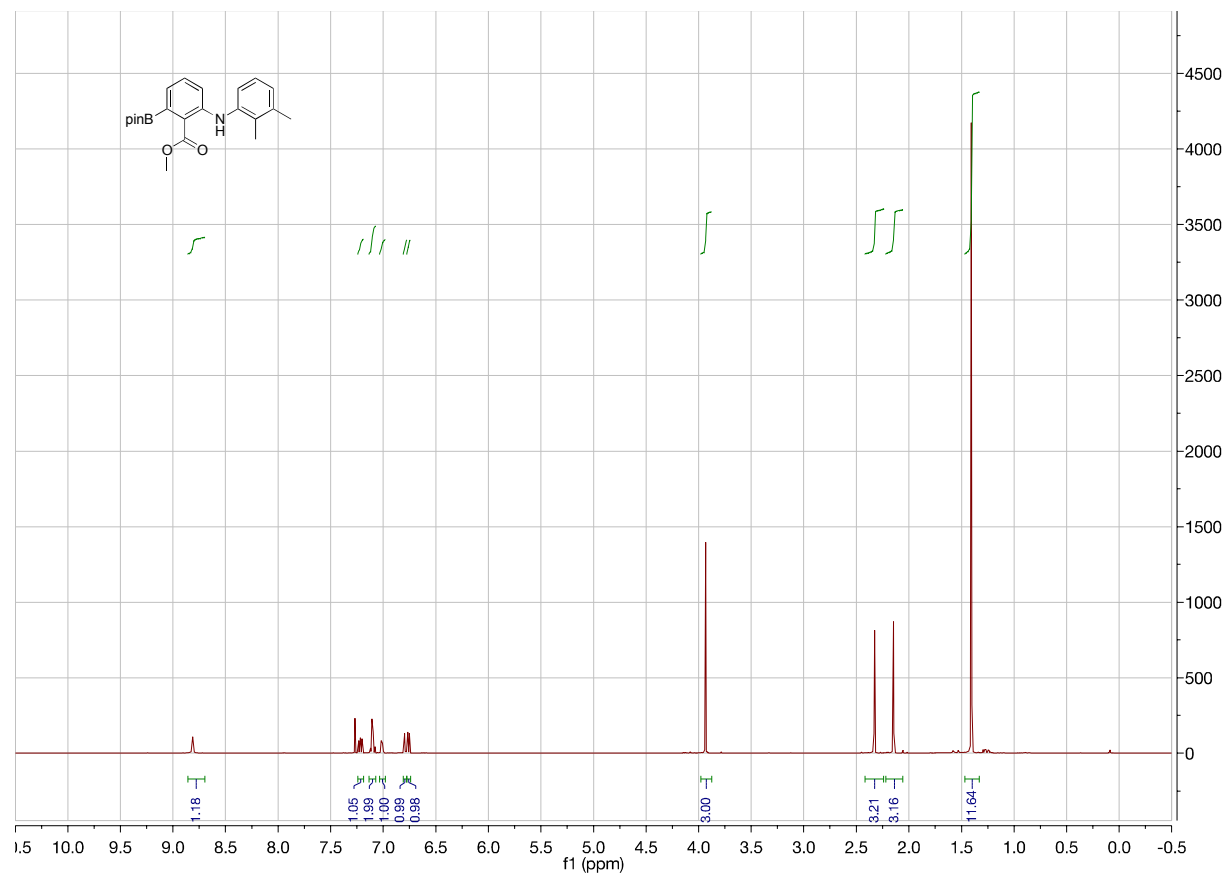


Figure A125. 500 MHz ^1H NMR of **3az** in CDCl_3

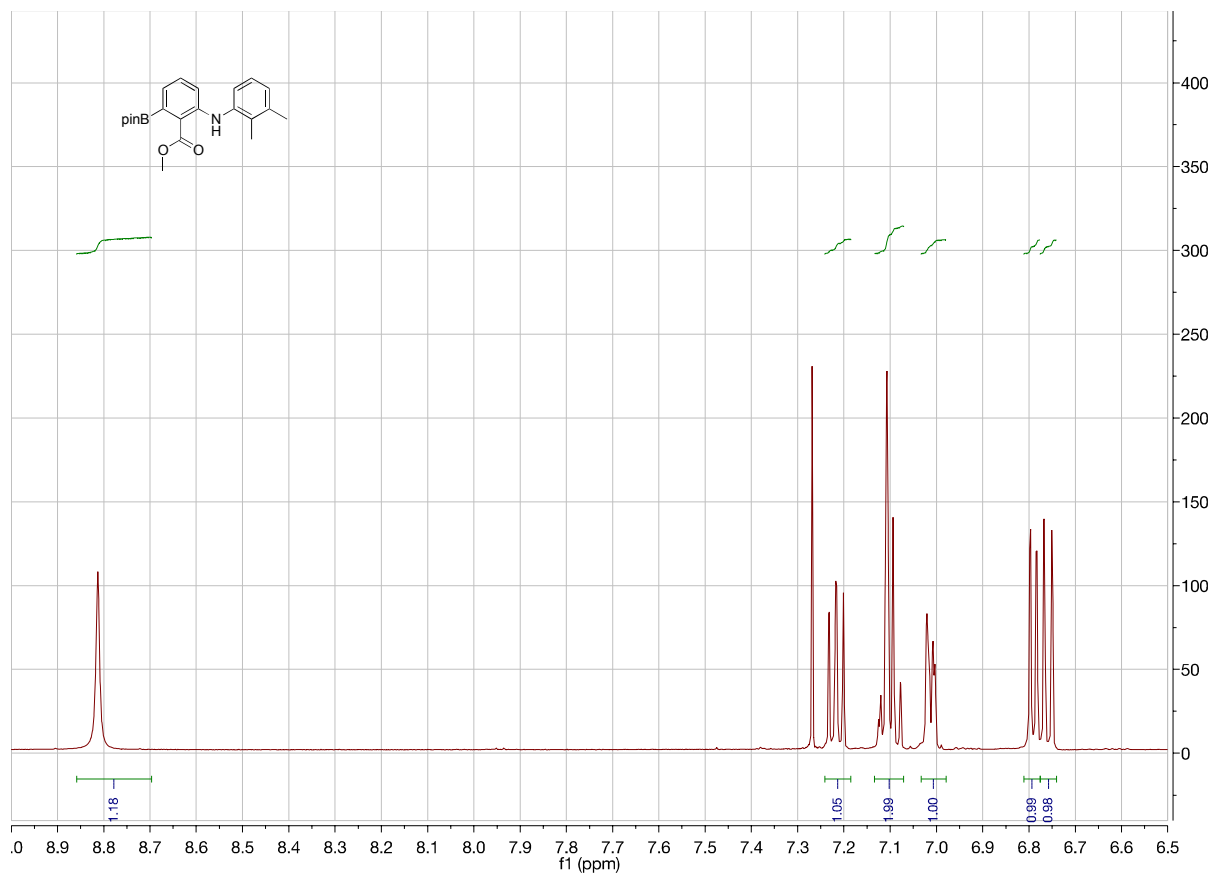


Figure A126. 500 MHz ^1H NMR of **3az** in CDCl_3 from 9.0 to 6.5 ppm

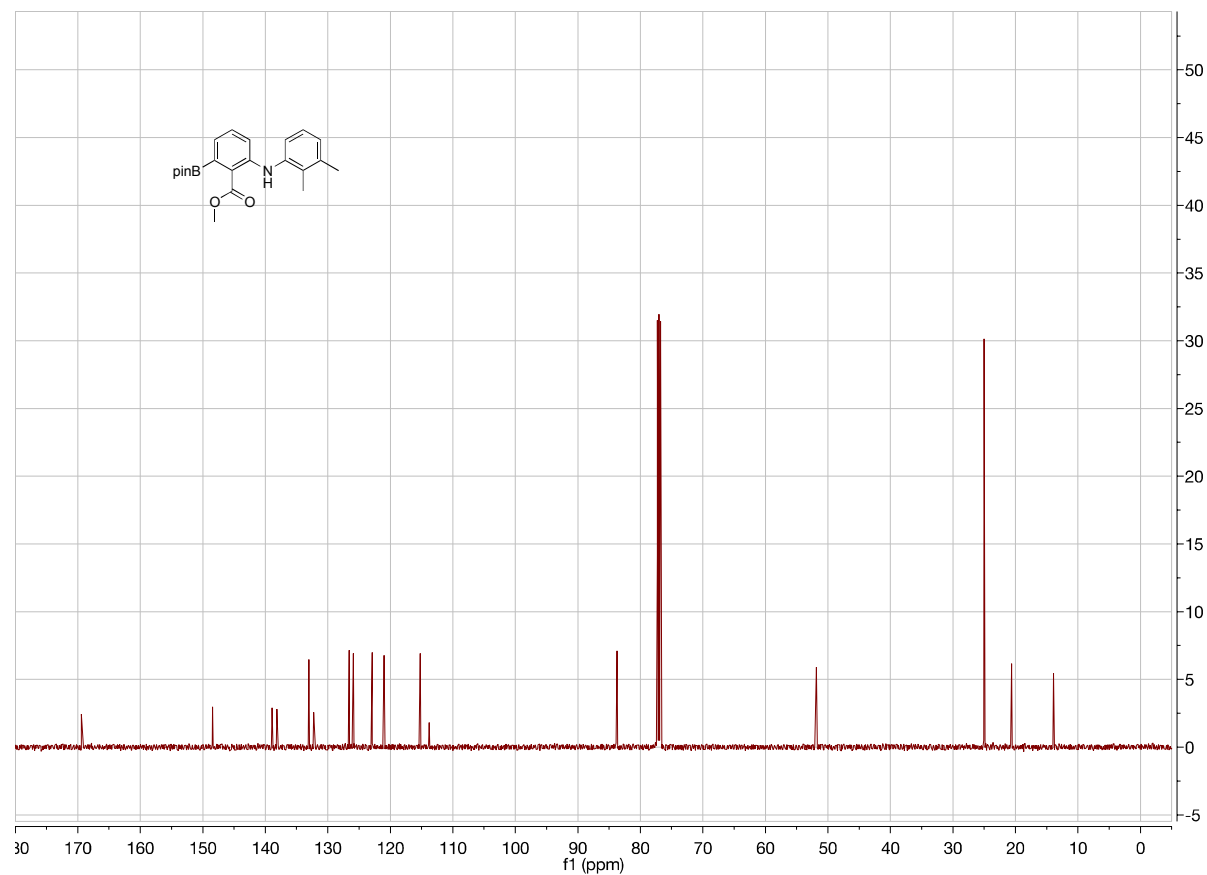
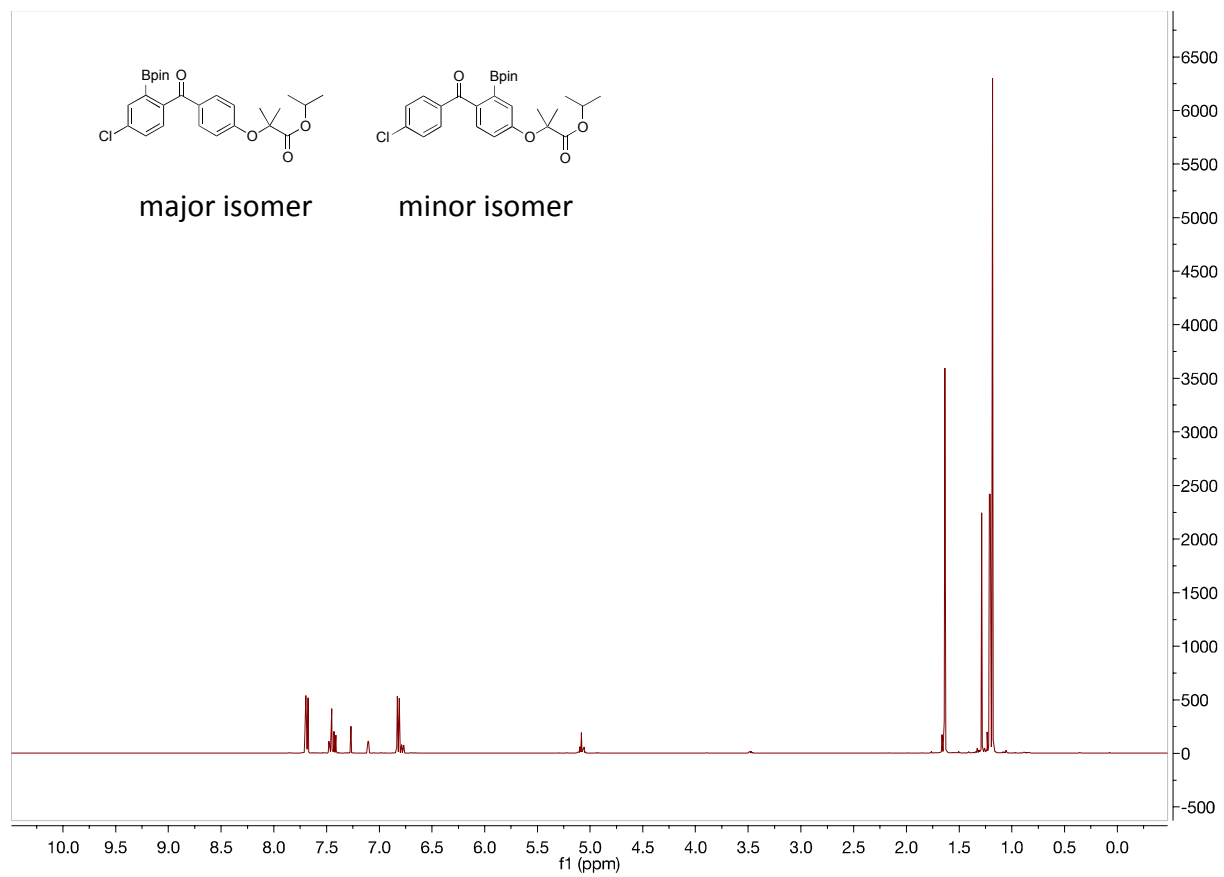


Figure A127. 125 MHz ^{13}C NMR of **3az** in CDCl_3



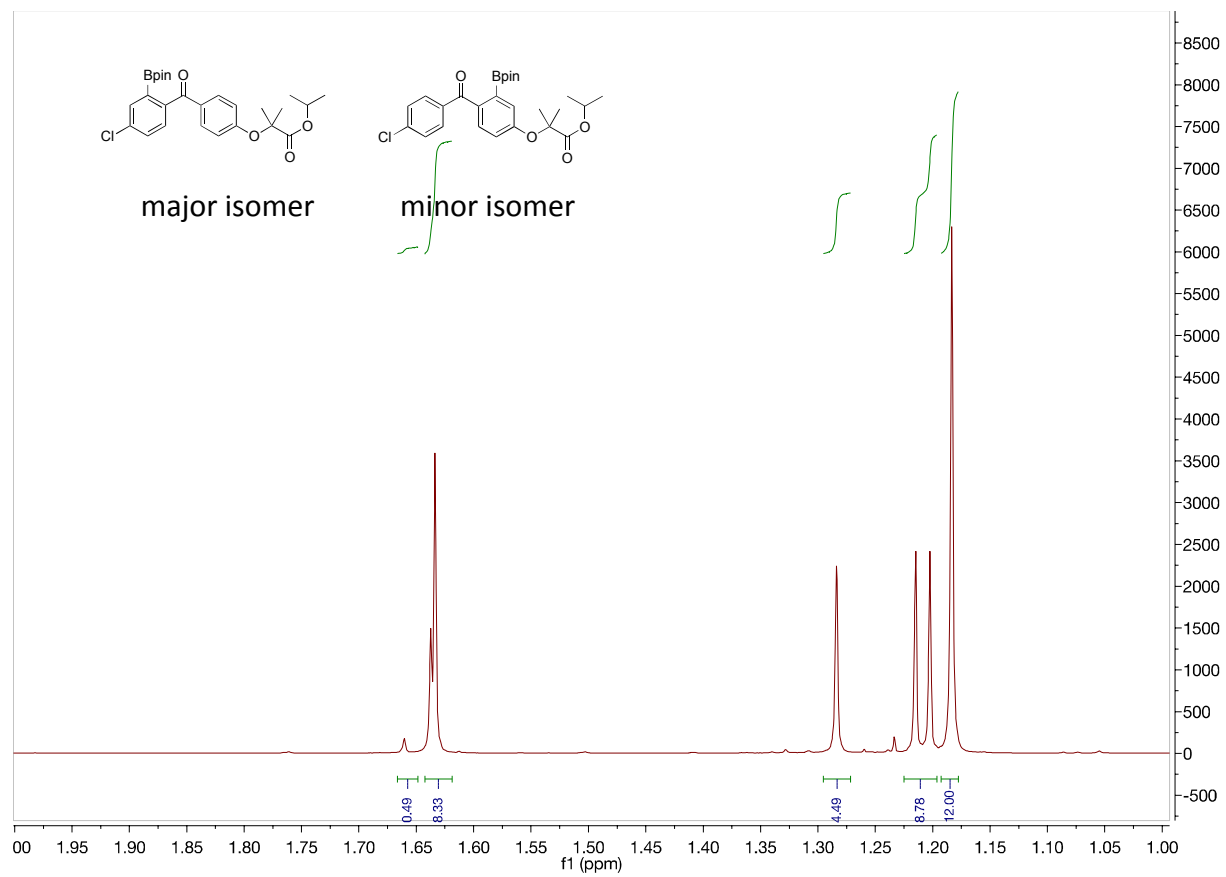


Figure A129. 500 MHz ^1H NMR of **3ba** and **3bb** in CDCl_3 between 2.0ppm and 1.0ppm

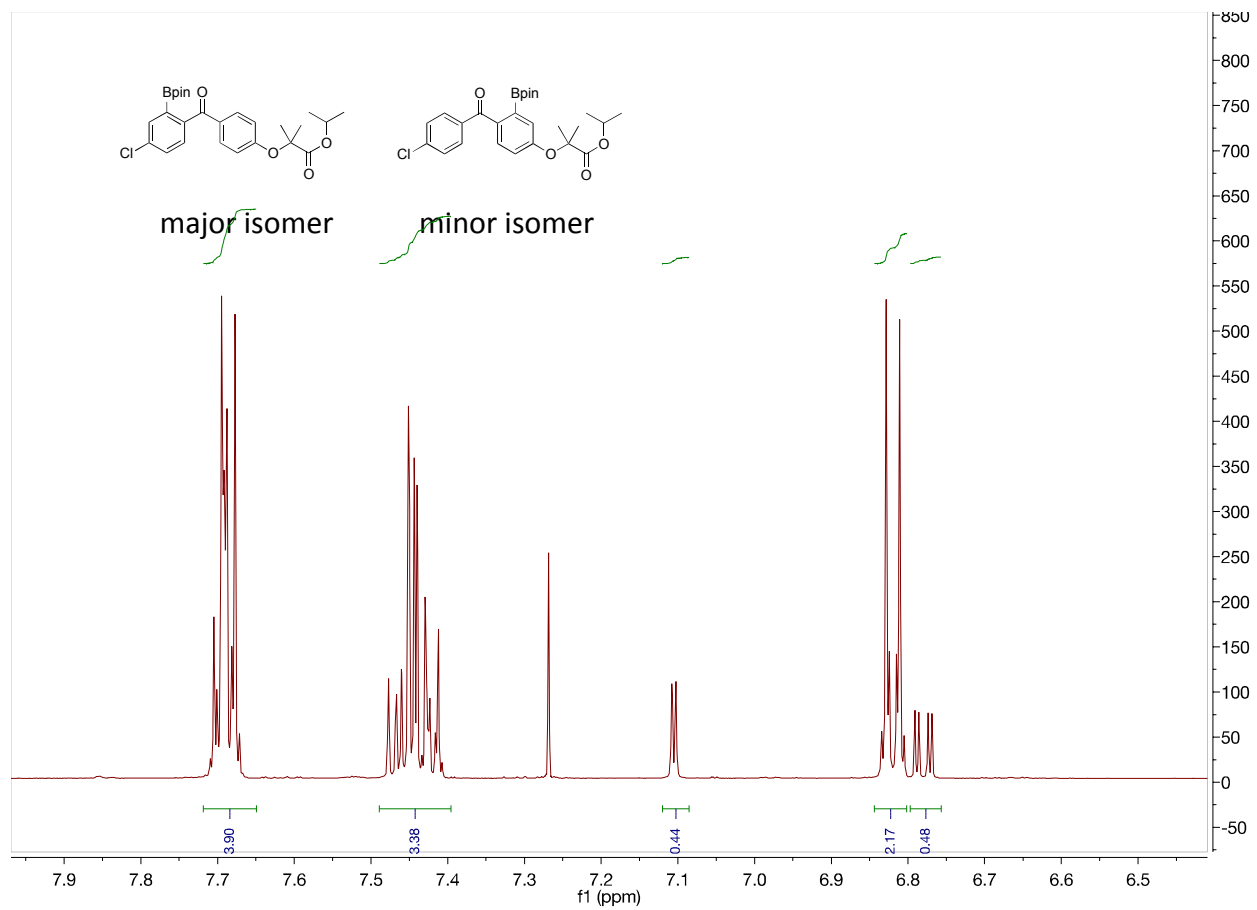


Figure A130. 500 MHz ^1H NMR of **3ba** and **3bb** in CDCl_3 between 8.0ppm and 6.4ppm

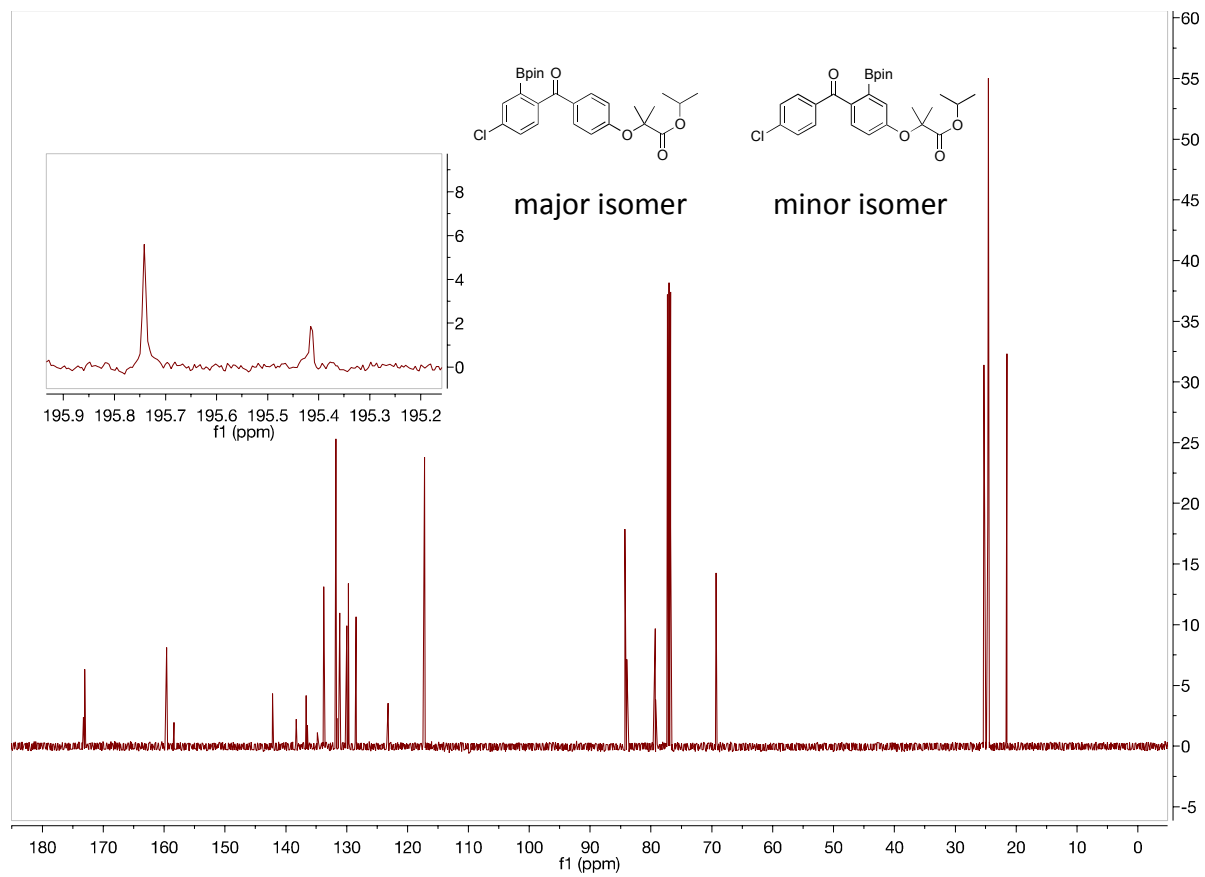


Figure A131. 125 MHz ^{13}C NMR of 3ba and 3bb in CDCl_3

APPENDIX B

Crystal Structure Data

Table B1 Crystal data for compound **2e**

Compound	TMS691
Formula	C ₁₂ H ₂₂ BBrNO ₂
<i>D</i> _{calc.} / g cm ⁻³	1.128
μ /mm ⁻¹	3.075
Formula Weight	303.02
Colour	colourless
Shape	needle
Size/mm ³	1.41×0.14×0.09
<i>T</i> /K	173(2)
Crystal System	monoclinic
Space Group	<i>P</i> 2 ₁ / <i>c</i>
<i>a</i> /Å	8.4980(17)
<i>b</i> /Å	27.935(3)
<i>c</i> /Å	7.5150(9)
α [°]	90
β [°]	90
γ [°]	90
<i>V</i> /Å ³	1784.0(5)
<i>Z</i>	4
<i>Z</i> '	1
Wavelength/Å	1.541838
Radiation type	CuK α
θ _{min} [°]	3.164
θ _{max} [°]	71.638
Measured Refl.	5367
Independent Refl.	1647
Reflections with <i>I</i> > 2(<i>I</i>)	1298
<i>R</i> _{int}	0.0349
Parameters	97
Restraints	1
Largest Peak	0.432
Deepest Hole	-0.282
GooF	1.079
<i>wR</i> ₂ (all data)	0.1594
<i>wR</i> ₂	0.1501
<i>R</i> ₁ (all data)	0.0646
<i>R</i> ₁	0.0535

Table B2 Crystal structure data for **2za**

Compound	MRS218A
CCDC	1826283
Formula	C ₁₆ H ₃₀ BNO ₃
<i>D</i> _{calc.} / g cm ⁻³	1.097
μ /mm ⁻¹	0.578
Formula Weight	295.22
Colour	colourless
Shape	chunk
Size/mm ³	0.30×0.29×0.28
<i>T</i> /K	173(2)
Crystal System	orthorhombic
Flack Parameter	-0.04(8)
Hooft Parameter	-0.04(7)
Space Group	<i>P</i> 2 ₁ 2 ₁ 2 ₁
<i>a</i> /Å	11.80690(10)
<i>b</i> /Å	14.68810(10)
<i>c</i> /Å	30.9318(3)
α [°]	90
β [°]	90
γ [°]	90
<i>V</i> /Å ³	5364.22(8)
<i>Z</i>	12
<i>Z</i> '	3
Wavelength/Å	1.541838
Radiation type	CuK α
θ _{min} [°]	4.007
θ _{max} [°]	72.061
Measured Refl.	32820
Independent Refl.	10453
Reflections Used	9271
<i>R</i> _{int}	0.0451
Parameters	586
Restraints	0
Largest Peak	0.423
Deepest Hole	-0.236
GooF	1.047
<i>wR</i> ₂ (all data)	0.1593
<i>wR</i> ₂	0.1527
<i>R</i> ₁ (all data)	0.0645
<i>R</i> ₁	0.0574

REFERENCES

REFERENCES

- (1) Brown, H. C.; Zweifel, G. *J. Am. Chem. Soc.* **1959**, *81* (1), 247.
- (2) Brown, H. C.; Zweifel, G. *J. Am. Chem. Soc.* **1961**, *83* (2), 486.
- (3) Brown, H. C.; Prasad, J. V. *J. Am. Chem. Soc.* **1986**, *108* (8), 2049.
- (4) Miyaura, N.; Yamada, K.; Suzuki, A. *Tetrahedron Lett.* **1979**, *20* (36), 3437.
- (5) Miyaura, N.; Yanagi, T.; Suzuki, A. *Synth. Commun.* **1981**, *11* (7), 513.
- (6) Lovering, F.; Bikker, J.; Humblet, C. *J. Med. Chem.* **2009**, *52* (21), 6752.
- (7) Lam, P. Y. S.; Clark, C. G.; Saubern, S.; Adams, J.; Winters, M. P.; Chan, D. M. T.; Combs, A. *Tetrahedron Lett.* **1998**, *39* (19), 2941.
- (8) Ainley, A. D.; Challenger, F. *J. Chem. Soc.* **1930**, 2171.
- (9) Murphy, J. M.; Liao, X.; Hartwig, J. F. *J. Am. Chem. Soc.* **2007**, *129* (50), 15434.
- (10) Furuya, T.; Ritter, T. *Org. Lett.* **2009**, *11* (13), 2860.
- (11) Dai, J.-J.; Zhang, W.-M.; Shu, Y.-J.; Sun, Y.-Y.; Xu, J.; Feng, Y.-S.; Xu, H.-J. . **2016**, *52* (41), 6793.
- (12) Chu, L.; Qing, F.-L. *Org. Lett.* **2010**, *12* (21), 5060.
- (13) Senecal, T. D.; Parsons, A. T.; Buchwald, S. L. *J. Org. Chem.* **2011**, *76* (4), 1174.
- (14) Shao, X.; Liu, T.; Lu, L.; Shen, Q. *Org. Lett.* **2014**, *16* (18), 4738.
- (15) Bonet, A.; Odachowski, M.; Leonori, D.; Essafi, S.; Aggarwal, V. K. *Nat. Chem.* **2014**, *6* (7), 584.
- (16) Ishiyama, T.; Murata, M.; Miyaura, N. *J. Org. Chem.* **1995**, *60* (23), 7508.
- (17) Murahashi, S. *J. Am. Chem. Soc.* **1955**, *77* (23), 6403.
- (18) Chatt, J.; Hart, F. A.; Watson, H. R. *J. Chem. Soc.* **1962**, 2537.
- (19) Kleiman, J. P.; Dubeck, M. *J. Am. Chem. Soc.* **1963**, *85* (10), 1544.
- (20) Chatt, J.; Davidson, J. M. *J. Chem. Soc.* **1965**, 843.

- (21) Janowicz, A. H.; Bergman, R. G. *J. Am. Chem. Soc.* **1982**, *104* (1), 352.
- (22) Gustavson, W. A.; Epstein, P. S.; Curtis, M. D. *Organometallics* **1982**, *1* (6), 884.
- (21) Waltz, K. M.; He, X.; Muhoro, C.; Hartwig, J. F. *J. Am. Chem. Soc.* **1995**, *117* (45), 11357.
- (22) Waltz, K. M.; Hartwig, J. F. *Science* **1997**, *277* (5323), 211.
- (23) Iverson, C. N.; Smith, M. R. III *J. Am. Chem. Soc.* **1999**, *121* (33), 7696.
- (24) Cho, J.-Y.; Iverson, C. N.; Smith, M. R. III *J. Am. Chem. Soc.* **2000**, *122* (51), 12868.
- (25) Ishiyama, T.; Takagi, J.; Ishida, K.; Miyaura, N.; Anastasi, N. R.; Hartwig, J. F. *J. Am. Chem. Soc.* **2002**, *124* (3), 390.
- (26) Ishiyama, T.; Takagi, J.; Hartwig, J. F.; Miyaura, N. *Angew. Chem. Int. Ed.* **2002**, *41* (16), 3056.
- (27) Cho, J.-Y.; Tse, M. K.; Holmes, D.; Maleczka, R. E., Jr; Smith, M. R., III *Science* **2002**, *295* (5553), 305.
- (28) Boller, T. M.; Murphy, J. M.; Hapke, M.; Ishiyama, T.; Miyaura, N.; Hartwig, J. F. *J. Am. Chem. Soc.* **2005**, *127* (41), 14263.
- (29) Ghaffari, B.; Vanchura, B. A., 2nd; Chotana, G. A.; Staples, R. J.; Holmes, D.; Maleczka, R. E., Jr; Smith, M. R., III *Organometallics* **2015**, *34* (19), 4732.
- (30) Boebel, T. A.; Hartwig, J. F. *J. Am. Chem. Soc.* **2008**, *130* (24), 7534.
- (31) Preshlock, S. M.; Plattner, D. L.; Maligres, P. E.; Krska, S. W.; Maleczka, R. E., Jr; Smith, M. R., III *Angew. Chem. Int. Ed Engl.* **2013**, *52* (49), 12915.
- (32) Roosen, P. C.; Kallepalli, V. A.; Chattopadhyay, B.; Singleton, D. A.; Maleczka, R. E., Jr; Smith, M. R., III *J. Am. Chem. Soc.* **2012**, *134* (28), 11350.
- (33) Yamamoto, T.; Ishibashi, A.; Suginome, M. *Org. Lett.* **2017**, *19* (4), 886.
- (34) Chattopadhyay, B.; Dannatt, J. E.; Andujar-De Sanctis, I. L.; Gore, K. A.; Maleczka, R. E., Jr; Singleton, D. A.; Smith, M. R., III *J. Am. Chem. Soc.* **2017**.
- (35) Kawamorita, S.; Ohmiya, H.; Hara, K.; Fukuoka, A.; Sawamura, M. *J. Am. Chem. Soc.* **2009**, *131* (14), 5058.

- (36) Su, B.; Zhou, T.-G.; Xu, P.-L.; Shi, Z.-J.; Hartwig, J. F. *Angew. Chem. Int. Ed.* **2017**, *56* (25), 7205.
- (37) Chattopadhyay, B.; Dannatt, J. E.; Andujar-De Sanctis, I. L.; Gore, K. A.; Maleczka, R. E., Jr; Singleton, D. A.; Smith, M. R., III *J. Am. Chem. Soc.* **2017**, *139* (23), 7864.
- (38) Smith, M. R. III; Bisht, R.; Haldar, C.; Pandey, G.; Dannatt, J. E.; Ghaffari, B.; Maleczka, R. E.; Chattopadhyay, B. *ACS Catal.* **2018**, *8* (7), 6216.
- (39) Preshlock, S. M.; Plattner, D. L.; Maligres, P. E.; Krska, S. W.; Maleczka, R. E.; Smith, M. R. III *Angew. Chem. Int. Ed.* **2013**, *52* (49), 12915.
- (40) Kuninobu, Y.; Ida, H.; Nishi, M.; Kanai, M. *Nat. Chem.* **2015**, *7* (9), 712.
- (41) Bisht, R.; Chattopadhyay, B. *Synlett* **2016**, *27* (14), 2043.
- (42) Davis, H. J.; Mihai, M. T.; Phipps, R. J. *J. Am. Chem. Soc.* **2016**, *138* (39), 12759.
- (43) Davis, H. J.; Genov, G. R.; Phipps, R. J. *Angew. Chem. Int. Ed.* **2017**, *56* (43), 13351.
- (44) Mihai, M. T.; Phipps, R. J.; Mkhaliid, I. A.; Barnard, J. H.; Marder, T. B.; Murphy, J. M.; Hartwig, J. F.; Roosen, P. C.; Kallepalli, V. A.; Chattopadhyay, B.; Others. *Synlett* **2017**, *28* (09), 1011.
- (45) Saito, Y.; Segawa, Y.; Itami, K. *J. Am. Chem. Soc.* **2015**, *137* (15), 5193.
- (46) Yang, L.; Semba, K.; Nakao, Y. *Angew. Chem. Int. Ed.* **2017**, *56* (17), 4853.
- (47) Hoque, M. E.; Bisht, R.; Haldar, C.; Chattopadhyay, B. *J. Am. Chem. Soc.* **2017**, *139* (23), 7745.
- (48) Ishiyama, T.; Takagi, J.; Yonekawa, Y.; Hartwig, J. F.; Miyaura, N. *Adv. Synth. Catal.* **2003**, *345* (910), 1103.
- (49) Leonori, D.; Aggarwal, V. K. *Acc. Chem. Res.* **2014**, *47* (10), 3174.
- (50) Kubota, K.; Watanabe, Y.; Hayama, K.; Ito, H. *J. Am. Chem. Soc.* **2016**, *138* (13), 4338.
- (51) Chen, H. Y.; Hartwig, J. F. *Angew. Chem. Int. Ed.* **1999**, *38*, 3391.
- (52) Chen, H.; Schlecht, S.; Semple, T. C.; Hartwig, J. F. *Science* **2000**, *287* (5460), 1995.
- (53) Liskey, C. W.; Hartwig, J. F. *J. Am. Chem. Soc.* **2012**, *134* (30), 12422.

- (54) Palmer, W. N.; Zarate, C.; Chirik, P. J. *J. Am. Chem. Soc.* **2017**, *139* (7), 2589.
- (55) He, J.; Jiang, H.; Takise, R.; Zhu, R.-Y.; Chen, G.; Dai, H.-X.; Dhar, T. G. M.; Shi, J.; Zhang, H.; Cheng, P. T. W.; Yu, J.-Q. *Angew. Chem. Int. Ed Engl.* **2016**, *55* (2), 785.
- (56) He, J.; Shao, Q.; Wu, Q.; Yu, J.-Q. *J. Am. Chem. Soc.* **2017**, *139* (9), 3344.
- (57) Sabatier, P.; Senderens, J. B. *CR Hebd. Seances Acad. Sci* **1897**, *124*, 1358.
- (58) Sabatier, P.; Senderens, J. B. *Compt. rend* **1905**, *140*, 482.
- (59) Voorhees, V.; Adams, R. *J. Am. Chem. Soc.* **1922**, *44* (6), 1397.
- (60) Raney, M. Method of Preparing Catalytic Material. U.S. Patent 1563587 Dec., 1, 1925
- (61) Raney, M. Method of Producing Finely-Divided Nickel. U.S. Patent 1628190 May, 10, 1927
- (62) Beeck, O. *Rev. Mod. Phys.* **1945**, *17* (1), 61.
- (63) Dunworth, W. P.; Nord, F. F. *J. Am. Chem. Soc.* **1952**, *74* (6), 1459.
- (64) Freifelder, M.; Robinson, R. M.; Stone, G. R. *J. Org. Chem.* **1962**, *27* (1), 284.
- (65) Osborn, J. A.; Jardine, F. H.; Young, J. F.; Wilkinson, G. *Journal of the Chemical Society A: Inorganic, Physical, Theoretical* **1966**, 1711.
- (66) Shapley, J. R.; Schrock, R. R.; Osborn, J. A. *J. Am. Chem. Soc.* **1969**, *91* (10), 2816.
- (67) Schrock, R. R.; Osborn, J. A. *J. Am. Chem. Soc.* **1976**, *98* (15), 4450.
- (68) Crabtree, R. H.; Felkin, H.; Morris, G. E. *J. Organomet. Chem.* **1977**, *141* (2), 205.
- (69) Wiesenfeldt, M. P.; Nairoukh, Z.; Li, W.; Glorius, F. *Science* **2017**, *357* (6354), 908.
- (70) Ye, Z.-S.; Chen, M.-W.; Chen, Q.-A.; Shi, L.; Duan, Y.; Zhou, Y.-G. *Angew. Chem. Int. Ed Engl.* **2012**, *51* (40), 10181.
- (71) Duan, Y.; Chen, M.-W.; Ye, Z.-S.; Wang, D.-S.; Chen, Q.-A.; Zhou, Y.-G. *Chemistry* **2011**, *17* (26), 7193.
- (72) Baeza, A.; Pfaltz, A. *Chemistry* **2010**, *16* (7), 2036.
- (73) Wang, D.-S.; Chen, Q.-A.; Li, W.; Yu, C.-B.; Zhou, Y.-G.; Zhang, X. *J. Am. Chem. Soc.* **2010**, *132* (26), 8909.

- (74) Kuwano, R.; Kashiwabara, M.; Ohsumi, M.; Kusano, H. *J. Am. Chem. Soc.* **2008**, *130* (3), 808.
- (75) Ortega, N.; Urban, S.; Beiring, B.; Glorius, F. *Angew. Chem. Int. Ed Engl.* **2012**, *51* (7), 1710.
- (76) Wysocki, J.; Ortega, N.; Glorius, F. *Angew. Chem. Int. Ed Engl.* **2014**, *53* (33), 8751.
- (77) Urban, S.; Beiring, B.; Ortega, N.; Paul, D.; Glorius, F. *J. Am. Chem. Soc.* **2012**, *134* (37), 15241.
- (78) Blum, J.; Amer, I.; Zoran, A.; Sasson, Y. *Tetrahedron Lett.* **1983**, *24* (38), 4139.
- (79) Clark, B. F.; Haller, J. F. Hydrogenation of Chlorovinylboranes. U.S. Patent 3226432, Dec., 28, 1965.
- (80) Woods, W. G.; Bengelsdorf, I. S.; Hunter, D. L. *J. Org. Chem.* **1966**, *31* (9), 2766.
- (81) Morgan, J. B.; Morken, J. P. *J. Am. Chem. Soc.* **2004**, *126* (47), 15338.
- (82) Paptchikhine, A.; Cheruku, P.; Engman, M.; Andersson, P. G. . **2009**, No. 40, 5996.
- (83) Ganić, A.; Pfaltz, A. *Chemistry* **2012**, *18* (22), 6724.
- (84) Molander, G. A.; Ham, J.; Seapy, D. G. *Tetrahedron* **2007**, *63* (3), 768.
- (85) Struble, J. R.; Lee, S. J.; Burke, M. D. *Tetrahedron* **2010**, *66* (26), 4710.
- (86) Iwadate, N.; Suginome, M. *J. Am. Chem. Soc.* **2010**, *132* (8), 2548.
- (87) Kelly, T. A.; Fuchs, V. U.; Perry, C. W.; Snow, R. J. *Tetrahedron* **1993**, *49* (5), 1009.
- (88) Wang, G.; Liu, L.; Wang, H.; Ding, Y.-S.; Zhou, J.; Mao, S.; Li, P. *J. Am. Chem. Soc.* **2017**, *139* (1), 91.
- (89) Kawamorita, S.; Miyazaki, T.; Iwai, T.; Ohmiya, H.; Sawamura, M. *J. Am. Chem. Soc.* **2012**, *134* (31), 12924.
- (90) Varela, A.; Garve, L. K. B.; Leonori, D.; Aggarwal, V. K. *Angew. Chem. Int. Ed.* **2017**, *56* (8), 2127.
- (91) Kubota, K.; Watanabe, Y.; Hayama, K.; Ito, H. *J. Am. Chem. Soc.* **2016**, *138* (13), 4338.

- (92) Yang, C.-T.; Zhang, Z.-Q.; Tajuddin, H.; Wu, C.-C.; Liang, J.; Liu, J.-H.; Fu, Y.; Czyzewska, M.; Steel, P. G.; Marder, T. B.; Liu, L. *Angew. Chem. Int. Ed Engl.* **2012**, *51* (2), 528.
- (93) Liskey, C. W.; Hartwig, J. F. *J. Am. Chem. Soc.* **2012**, *134* (30), 12422.
- (94) Zweifel, G.; Plamondon, J. *J. Org. Chem.* **1970**, *35* (4), 898.
- (95) Kawamorita, S.; Ohmiya, H.; Hara, K.; Fukuoka, A.; Sawamura, M. *J. Am. Chem. Soc.* **2009**, *131* (14), 5058.
- (96) Ishiyama, T.; Isou, H.; Kikuchi, T.; Miyaura, N. *Chem. Commun.* **2010**, *46* (1), 159.
- (97) Itoh, H.; Kikuchi, T.; Ishiyama, T.; Miyaura, N. *Chem. Lett.* **2011**, *40* (9), 1007.
- (98) Ros, A.; Estepa, B.; López-Rodríguez, R.; Álvarez, E.; Fernández, R.; Lassaletta, J. M. *Angew. Chem. Int. Ed Engl.* **2011**, *50* (49), 11724.
- (99) Hale, L. V. A.; McGarry, K. A.; Ringgold, M. A.; Clark, T. B. *Organometallics* **2015**, *34* (1), 51.
- (100) Ghaffari, B.; Preshlock, S. M.; Plattner, D. L.; Staples, R. J.; Maligres, P. E.; Krska, S. W.; Maleczka, R. E., Jr; Smith, M. R., 3rd. *J. Am. Chem. Soc.* **2014**, *136* (41), 14345.
- (101) Wang, G.; Liu, L.; Wang, H.; Ding, Y.-S.; Zhou, J.; Mao, S.; Li, P. *J. Am. Chem. Soc.* **2017**, *139* (1), 91.
- (102) Cho, J.-Y.; Tse, M. K.; Holmes, D.; Maleczka, R. E., Jr; Smith, M. R., 3rd. *Science* **2002**, *295* (5553), 305.
- (103) Boller, T. M.; Murphy, J. M.; Hapke, M.; Ishiyama, T.; Miyaura, N.; Hartwig, J. F. *J. Am. Chem. Soc.* **2005**, *127* (41), 14263.
- (104) Yamazaki, K.; Kawamorita, S.; Ohmiya, H.; Sawamura, M. *Org. Lett.* **2010**, *12* (18), 3978.
- (105) Kawamorita, S.; Murakami, R.; Iwai, T.; Sawamura, M. *J. Am. Chem. Soc.* **2013**, *135* (8), 2947.
- (106) Kawamorita, S.; Ohmiya, H.; Sawamura, M. *J. Org. Chem.* **2010**, *75* (11), 3855.
- (107) Iwai, T.; Harada, T.; Hara, K.; Sawamura, M. *Angew. Chem. Int. Ed.* **2013**, *52* (47), 12322.

- (108) Ros, A.; López-Rodríguez, R.; Estepa, B.; Álvarez, E.; Fernández, R.; Lassaletta, J. *M. J. Am. Chem. Soc.* **2012**, *134* (10), 4573.
- (109) Roering, A. J.; Hale, L. V. A.; Squier, P. A.; Ringgold, M. A.; Wiederspan, E. R.; Clark, T. B. *Org. Lett.* **2012**, *14* (13), 3558.
- (110) Hale, L. V. A.; McGarry, K. A.; Ringgold, M. A.; Clark, T. B. *Organometallics* **2015**, *34* (1), 51.
- (111) Crawford, K. M.; Ramseyer, T. R.; Daley, C. J. A.; Clark, T. B. *Angew. Chem. Int. Ed.* **2014**, *53* (29), 7589.
- (112) Bisht, R.; Chattopadhyay, B. *J. Am. Chem. Soc.* **2016**, *138* (1), 84.
- (113) Preshlock, S. M.; Ghaffari, B.; Maligres, P. E.; Krska, S. W.; Maleczka, R. E.; Smith, M. R. *J. Am. Chem. Soc.* **2013**, *135* (20), 7572.
- (114) Boebel, T. A.; Hartwig, J. F. *J. Am. Chem. Soc.* **2008**, *130* (24), 7534.
- (115) Wang, G.; Xu, L.; Li, P. *J. Am. Chem. Soc.* **2015**, *137* (25), 8058.
- (116) Zhu, J.; Lin, Z.; Marder, T. B. *Inorg. Chem.* **2005**, *44* (25), 9384.
- (117) Preshlock, S. M.; Plattner, D. L.; Maligres, P. E.; Krska, S. W.; Maleczka, R. E., Jr; Smith, M. R., 3rd. *Angew. Chem. Int. Ed Engl.* **2013**, *52* (49), 12915.
- (118) David, L.; Keith, F. *Chem. Lett.* **2010**, *39* (11), 1118.
- (119) Harrison, P.; Morris, J.; Marder, T. B.; Steel, P. G. *Org. Lett.* **2009**, *11* (16), 3586
- (120) Congreve, M. S.; Andrews, S.P.; Mason J. S.; Richardson, C. M.; Brown, G.A. 1,2,4-triazine-4-amine derivatives. International patent WO2011095625 Aug., 11, 2011
- (121) Billingsley, K.; Buchwald, S. L. *J. Am. Chem. Soc.* **2007**, *129* (11), 3358.
- (122) Ishiyama, T.; Takagi, J.; Yonekawa, Y.; Hartwig, J. F.; Miyaura, N. *Adv. Synth. Catal.* **2003**, *345* (910), 1103.
- (123) Colin, S.; Vaysse-Ludot, L.; Lecouvé, J.-P.; Maddaluno, J. *J. Chem. Soc. Perkin 1* **2000**, *24*, 4505.
- (124) Blakemore, P. R.; Burge, M. S. *J. Am. Chem. Soc.* **2007**, *129* (11), 3068.
- (125) Cheng, C.; Hartwig, J. F. *Science* **2014**, *343* (6173), 853.
- (126) Wolan, A.; Zaidlewicz, M. *Org. Biomol. Chem.* **2003**, *1*, 3274

- (127) Kawamorita, S.; Ohmiya, H.; Hara, K.; Fukuoka, A.; Sawamura, M. *J. Am. Chem. Soc.* **2009**, *131*, 5058
- (128) Pramanik, S.; Reddy, R. R.; Ghorai, P. *Organic letters* **2015**, *17* (6), 1393
- (129) Ghaffari, B.; Preshlock, S. M.; Plattner, D. L.; Staples, R. J.; Maligres, P. E.; Krska, S. W.; Maleczka, R. E., Jr; Smith, M. R., 3rd. *J. Am. Chem. Soc.* **2014**, *136* (41), 14345.
- (130) Jayasundara, C. R. K.; Unold, J. M.; Oppenheimer, J.; Smith, M. R., 3rd; Maleczka, R. E., Jr. *Org. Lett.* **2014**, *16* (23), 6072.
- (131) Ishiyama, T.; Isou, H.; Kikuchi, T.; Miyaura, N. *Chem. Commun.* **2010**, *46*, 159
- (132) Van Der Puy, M. *Tetrahedron Lett.* **1987**, *28* (3), 255
- (133) Vijaya Babu, P.; Mukherjee, S.; Gorja, D. R.; Yellanki, S.; Mediseti, R.; Kulkarni, P.; Mukkanti, K.; Pal, M. *RSC Adv.* **2014**, *4* (10), 4878.